UNIVERSIDAD DE GRANADA

UNIVERSIDAD DE GRANADA

Departamento de Farmacología e Instituto de Neurociencias

Facultad de Medicina

PROGRAMA DE DOCTORADO EN BIOMEDICINA

PERIPHERAL SIGMA-1 RECEPTORS: AT THE INTERFACE BETWEEN NOCICEPTOR SENSITIZATION AND IMMUNE CELLS

Tesis doctoral presentada por

MARÍA DEL CARMEN RUIZ CANTERO

Graduada en Bioquímica, para optar al grado de

DOCTOR CON MENCIÓN INTERNACIONAL

Directores: **ENRIQUE JOSÉ COBOS DEL MORAL**

JOSÉ MANUEL BAEYENS CABRERA

Editor: Universidad de Granada. Tesis Doctorales
Autor: Maria del Carmen Ruiz Cantero
ISBN: 978-84-1117-902-7
URI: https://hdl.handle.net/10481/82580

COMPROMISO DE RESPETO DE LOS DERECHOS DE AUTOR

La doctoranda María del Carmen Ruiz Cantero y los directores de la tesis Enrique José Cobos del Moral y José Manuel Baeyens Cabrera:

Garantizamos, al firmar esta tesis doctoral, que el trabajo ha sido realizado por la doctoranda bajo la dirección de los directores de la tesis y hasta donde nuestro conocimiento alcanza, en la realización del trabajo, se han respetado los derechos de otros autores a ser citados, cuando se han utilizado sus resultados o publicaciones.

Granada 24 de abril de 2023

Director/es de la Tesis

Enrique José Cobos del Moral

José Manuel Baeyens Cabrera

Doctoranda

María del Carmen Ruiz Cantero

D. ENRIQUE JOSÉ COBOS DEL MORAL, PROFESOR TITULAR DEL DEPARTAMENTO DE FARMACOLOGÍA E INVESTIGADOR DEL INSTITUTO DE NEUROCIENCIAS DE LA UNIVERSIDAD DE GRANADA

CERTIFICA:

Que el trabajo de investigación titulado, "PERIPHERAL SIGMA-1 RECEPTORS: AT THE INTERFACE BETWEEN NOCICEPTOR SENSITIZATION AND IMMUNE CELLS" ha sido realizado por Dña. María del Carmen Ruiz Cantero para optar al grado de Doctor por la Universidad de Granada, en el Instituto de Neurociencias y el Departamento de Farmacología de la Universidad de Granada, bajo mi dirección.

Y para que conste donde proceda se firma este certificado en Granada a 24 de abril de 2023

Fdo. Enrique José Cobos del Moral

Fdo. María del Carmen Ruiz Cantero

D. JOSÉ MANUEL BAEYENS CABRERA, CATEDRÁTICO DE FARMACOLOGÍA DE LA UNIVERSIDAD DE GRANADA E INVESTIGADOR DEL INSTITUTO DE NEUROCIENCIAS DE LA UNIVERSIDAD DE GRANADA

CERTIFICA:

Que el trabajo de investigación titulado, "PERIPHERAL SIGMA-1 RECEPTORS: AT THE INTERFACE BETWEEN NOCICEPTOR SENSITIZATION AND IMMUNE CELLS" ha sido realizado por Dña. María del Carmen Ruiz Cantero para optar al grado de Doctor por la Universidad de Granada, en el Instituto de Neurociencias y el Departamento de Farmacología de la Universidad de Granada, bajo mi dirección.

Y para que conste donde proceda se firma este certificado en Granada a 24 de abril de 2023

Fdo. José Manuel Baeyens Cabrera

Fdo. María del Carmen Ruiz Cantero

La realización de esta tesis ha sido posible gracias a una beca predoctoral de Formación de Profesorado Universitario (FPU16/03213) del Ministerio de Universidades, y a la financiación de nuestro grupo de investigación por la Junta de Andalucía (grupo CTS-109), la Universidad de Granada (PPJIB2019.11), el Ministerio de Economía y Competitividad (proyecto SAF2016-80540-R y PID2019-108691RB-I00), fondos FEDER, Laboratorios Esteve y Harvard Medical School-Blavatnik Sensory Disorders Research Award.

A Ángel, por sacar lo mejor de mí

A Tere, por cuidarnos a todos tanto

"Me parece haber sido sólo un niño jugando en la orilla del mar, divirtiéndose y buscando una piedra más lisa o una concha más bonita de lo normal, mientras el gran océano de la verdad yacía ante mis ojos con todo por descubrir"

Isaac Newton

Agradecimientos

Aunque este apartado de agradecimientos aparezca como la primera sección de la tesis, realmente he tenido que dejarlo para el final y aún así, durante todo este tiempo, no he encontrado la forma de saber expresar con palabras todo lo que me gustaría. Miro atrás, pienso en toda la gente que de una manera u otra me ha acompañado a lo largo de estos años y todos los momentos vividos, tanto en el laboratorio como fuera de este, y no me resulta nada fácil dar las gracias en tan solo unas páginas a todas estas personas que sin duda han contribuido para que todo esto fuera posible.

En primer lugar me gustaría agradecer la gran labor de mis directores de tesis, Quique y José Manuel. He tenido mucha suerte de haber realizado mi tesis bajo vuestra supervisión, sin duda creo que he tenido a los mejores directores que se podría tener. Gracias por darme la oportunidad de realizar esta Tesis Doctoral, que es tan mía como vuestra, por enseñarme tanto y dedicar todo vuestro esfuerzo para que este trabajo y en general todo el grupo salga adelante.

A Quique, por esta gran idea de proyecto de tesis. No tengo palabras para agradecer todo lo que haces por nosotros. No has sido solo un director de tesis, sino también un amigo. Mil gracias por estar ahí de manera incondicional siempre que te he necesitado, por confiar en mí y por preocuparte de nuestro futuro como si fuera el tuyo.

A José Manuel, por mirar siempre por el bienestar de todos y dar el retoque para que todo roce la perfección. Ha sido un privilegio llegar a tiempo para que pudieras ser uno de mis directores de tesis antes de tu merecida jubilación. Gracias por tu dedicación, paciencia, compromiso constante e implicación en todo, eres un ejemplo a seguir.

A las familias de mis directores; en especial a sus mujeres, Teresa e Isabel y a sus hijos. Gracias por vuestra paciencia mientras Quique y José Manuel dedicaban gran parte de su tiempo en que todo este trabajo saliera lo mejor posible.

A Inma y Ángeles, por apoyarme en cada momento desde que llegué al laboratorio, ser mis confidentes y cuidarme y enseñarme como mis hermanas mayores. Gracias Inma,

y a tu cómplice Antonio, por presentarme a la persona con la que hoy comparto mi vida y en general por hacer que esta fuera mucho mejor, incluso hasta convertirnos en los 'amiguitos' de la playa, donde se que seguiremos compartiendo grande momentos junto a Macarena. Gracias Ángeles porque a pesar de todas las cosas que puedas tener nunca te olvidas de nosotros, y siempre te haces sentir cerca, incluso en Churriana, gracias por ser mi vecina. Nuestra amistad ha ido creciendo como la hiedra y todas las macetas que me diste, que ya cubren todo el muro.

A Rafa, Migue, Gloria y Entrena, por enseñarme y ayudarme en muchos experimentos y en general en todo lo que he necesitado. Gracias por todos los momentos compartidos tanto en el laboratorio como fuera de este. Ha sido un gusto trabajar con vosotros, hacerlo de forma divertida y celebrar los grandes eventos juntos, donde hemos pasado ratos muy agradables. Gracias Rafa por animarme y darme tu visión optimista de esto, y por formar esa gran familia junto a Ángeles y dejarme disfrutar de Manuel y Pedro.

A Paco, por estar siempre pendiente de todas las convocatorias, preocuparte por todo el grupo y mirar por nuestro futuro. Gracias por resolver todas mis dudas y estar siempre dispuesto a ayudarme en todo lo que he necesitado.

A los profesores Eduardo, Javier, Esperanza, Cruzmi, Ahmad, Raquel, Rosa…, por contribuir con sus útiles consejos y conocimientos. Gracias Eduardo y Javier por transmitirme vuestra experiencia en histología y enriquecer así nuestro trabajo.

A Miguel Ángel Huerta, Miriam, Toñi, Diego, Carlos, Mariam, Dani, Ana, Leandro, María, Cristina, Lucía… y al resto de compañeros, también a los que están en Farmacia, a Laura, Enrique, Julio, Guzmán, Mª Elena, Miguel, Chari, Pilar…, y amigos de otros departamentos que no nombro, por compartir cantidad de inquietudes conmigo y ayudarme siempre que os he necesitado. Ha sido un placer compartir con vosotros estos años tanto en el laboratorio, por los pasillos del departamento, en los congresos o en las quedadas. Gracias Miguel Ángel H por estar siempre dispuesto a ayudarme, tener tanta iniciativa y hacer que esta tesis tenga una mayor relevancia clínica.

A Antonio, Vanesa y Paqui, por ayudarme y estar siempre pendiente de lo que he necesitado en el laboratorio. Gracias Antonio por ser la primera persona en recibirme

en el departamento siempre tan amablemente. Gracias Vanesa por darle una tinción rosa a esta tesis.

Al Instituto de Neurociencias, por acogerme en el CIBM, y en especial a Juanmi, Bea y Milagros, con quienes he compartido más de un café, creando hasta el 'club del desayuno', donde hemos pasado muy buenos ratos.

A Elsa y Pilar, por colaborar con nosotros en algunos de los experimentos de esta tesis y complementar con vuestra experiencia nuestro trabajo.

Al equipo de WeLab Barcelona, por las discusiones científicas tan interesantes que hemos tenido sobre el Sigma, especialmente a Enrique, Luz, Jose Miguel, Dani y Manel.

A todos los científicos que he conocido durante los congresos, Sara, María, Meritxell, Iago, Antonio García, Fernando… y con los que no solo he compartido nuestra ciencia sino que hemos disfrutado de ella desde otra perspectiva.

A todos los técnicos del CIC e IBS que tanta ayuda me habéis prestado y de los que he aprendido mucho, en especial a Ana, Sara y Gustavo por su enorme paciencia en el confocal o con los FACS. Además de la unidad de genómica del GENYO, en especial a Adrián, por su ayuda con el análisis genómico.

A mis 'niñas' del pueblo, por ser las amigas de toda la vida. Muchísimas gracias Jeni, Eli, Bar, Bea, Lur, MJ, Auro, María y Mel, por estar ahí siempre en los peores momentos, pero también en tantos buenos ratos compartidos. Siempre tendremos un punto común, El Esparragal, donde hacemos que este pequeño pueblo sea un gran lugar.

A los amigos del instituto, Sofía, María Torres, Antonio, María Caracuel, Victoria, María Aguilera, Agustín, Senda y Javi, porque aunque no nos veamos tanto como quisiéramos, cuando estamos juntos es como si el tiempo no pasara por nosotros.

Aunque se que hay cosas de la ciencia que resultan impactantes, espero que cuando veáis este trabajo entendáis la razón de tener que trabajar con animalitos.

A los amigos de Bioquímica, por demostrarme que la amistad verdadera no depende del tiempo ni la distancia. Aunque cada uno hayamos ido cogiendo caminos diferentes, el Ciclo de Krebs hará que permanezcamos unidos. En especial al 'Aulario Party Rock',

Rocío, Antonio, Nati, Fran, Nieves, Sandra y Laura, por ser el grupo donde nunca falta el apoyo para los innumerables vaciles sufridos. Gracias Rocío por sentarte a mi lado durante toda la carrera y ser participante de mi primer proyecto. Y a los Q-S, Paula, Maite, Rafa, Jose, Patri y Diana, por los viajes compartidos. Gracias Paula y Maite por hacer que sea más divertido comer en la Torre B y convertiros en mis confidentes.

A mis 'compis' de piso, Auro, Ana y María, por todas las vivencias durante la carrera.

Al grupo 'Sabat', por alegrarme cada día de mi estancia en Boston.

Gracias a todos los que me habéis intentado ayudar con el inglés, aunque no haya conseguido progresar y aún sea una de mis grandes retos y tareas pendientes.

A las personas que siempre han estado en mi vida, mi familia, sin vosotros esta etapa no habría sido posible. A mis padres, Manuel y Sierri, por inculcarme la importancia del esfuerzo, constancia y del trabajo bien hecho. Gracias por cuidarme y darme todo lo que he necesitado. Gracias mamá, valiente y trabajadora como la que más, por cuidar de papá y soportar todos los tropiezos que la vida nos va poniendo por el camino. A mis hermanos; Loli, Tere y Jose, por enseñarme y ayudarme tanto. Gracias por animarme y arroparme en tantas ocasiones. Gracias Tere por ser nuestra segunda mamá, y es que gracias a ti todo se sustenta y por eso eres una de las personas a la que dedico esta tesis. A mi cuñada Alicia, has sabido ganarte nuestro cariño a lo largo de estos años. Gracias por darnos junto a mi hermano el mejor fármaco que he probado hasta ahora, mis sobrinos Lucas y Marta, que son la alegría en persona, y es que mientras juego con ellos los problemas no existen. A mi cuñado Jose, por ser mi diseñador cromático y por todas las risas que nos echamos cuando estamos todos juntos, tenéis un hueco muy importante en mi corazón. Al resto de mi familia, especialmente a mi tita Pepi, tita Niña, tita Carmen, tita Manoli, tito Alfonso, tita Rafi, tito Antonio, Che y Eva y sus pequeños Juan José y Martín, así como al resto de primos, por mimarme y cuidarme de una manera tan especial para mí.

A mi nueva familia, Silvia mamá, Jose, Silvia hija y Marcelino, por acogerme como un miembro más de vuestro maravilloso equipo. Gracias por considerarme como si fuera una hija y demostrarnos cada día vuestro apoyo y cariño incondicional.

En general gracias familia, aunque no pueda nombraros a todos, vosotros me demostráis el verdadero sentido de la vida. Espero que cuando veáis este trabajo entendáis lo que he estado haciendo estos años.

Por último, a mi gran amor, Ángel, una de las personas a las que dedico esta tesis por ser la que más la ha sufrido. Llegaste a mi vida con el comienzo de esta tesis, donde ya me hablaban muy bien de ti, y te has convertido en la primera persona que veo al despertar cada mañana. Sé que esto te hace incluso más feliz que a mí. Gracias por tu paciencia, por intentar comprender este trabajo, confiar en mí y ser tan optimista, contigo los problemas siempre son menores. Gracias por escucharme y ayudarme a lo largo de estos años. Gracias por darme la energía que necesito en cada momento, ayudarme a levantarme en cada tropiezo y celebrar cada victoria como si fuese tuya. Gracias por querer compartir conmigo el resto de nuestros días. No tengo dudas de que eres la mejor persona que puedo tener a mi lado y no puedo ser más afortunada por ello. Te quiero mucho y firmaré por ello el 30 de septiembre.

Finalmente y no menos importante, a la financiación y a todas mis pequeñas ratoncillas que habéis hecho posible dar un pasito adelante en el tratamiento del dolor.

Acknowledgements

To Prof. Clifford Woolf, thanks for hosting me in your lab at Boston Children's Hospital/Harvard Medical School and for your kindness and patience during my stay in Boston. It was an honour to do research in such an excellent environment.

To all people from Woolf's lab, in particular to Aakanksha and Jaehoon for being so friendly with me and for teaching and offering me your help with the calcium imaging.

To the rest of the people I met in Boston, thank you very much for making my time away from home easier and much more enjoyable.

INDEX

RESUMEN

RESUMEN

El receptor sigma-1 es una proteína chaperona sensible al Ca^{2+} y regulada por ligandos, con la capacidad de unirse a varios receptores y canales iónicos actuando como una subunidad reguladora (Sánchez-Fernández et al., 2017). Los receptores sigma-1 han sido ampliamente estudiados por sus acciones a nivel del sistema nervioso central y su potencial como diana farmacológica para el tratamiento del dolor (Sánchez-Fernández et al., 2017). De hecho, el antagonista sigma-1 S1RA disminuye la sensibilización central en ensayos preclínicos (Sánchez-Fernández et al., 2017) y ha superado con éxito la fase IIa de ensayos clínicos en pacientes con dolor neuropático, siendo esta su indicación primaria (Bruna et al., 2018). La indicación secundaria del S1RA es la potenciación de la analgesia inducida por fármacos opioides, proceso en el cual el bloqueo de receptores opioides en el sistema nervioso central juega un papel relevante (Sánchez-Fernández et al., 2017). No obstante, nuestro grupo de investigación ha descrito que el receptor sigma-1 se expresa mayoritariamente en las neuronas sensoriales periféricas, situadas en los ganglios de las raíces dorsales (DRG, de sus siglas en inglés "Dorsal Root Ganglia") (Sánchez-Fernández et al., 2017; Montilla-García et al., 2018) y que la inhibición sigma-1 incrementa la analgesia opioide periférica, inducida tanto por fármacos opioides como por péptidos opioides endógenos de origen inmunitario (Sánchez-Fernández et al., 2017; Tejada et al., 2018), lo que muestra el potencial de los receptores sigma-1 periféricos como diana analgésica. Sin embargo, el papel de los receptores sigma-1 en la sensibilización periférica está inexplorado, por lo que nuestro primer objetivo fue evaluar la implicación de los receptores sigma-1 en la sensibilización inducida por sensibilizadores de distintos tipos de neuronas nociceptivas periféricas, e identificar los mecanismos subyacentes implicados.

La sensibilización periférica se produce por algógenos químicos liberados durante el dolor patológico, tales como la prostaglandina E2 (PGE2), el factor de crecimiento nervioso (NGF) y el factor neurotrófico derivado de la glía (GDNF), entre otros, los cuales actúan sobre los nociceptores produciendo hiperalgesia. No todos los sensibilizadores actúan en las mismas poblaciones neuronales. Mientras que la PGE2 y el NGF sensibilizan los nociceptores C peptidérgicos (TRPV1+), el GDNF sensibiliza

nociceptores C no peptidérgicos (IB4+) (Woolf y Ma, 2007). Teniendo en cuenta estos antecedentes, estudiamos si los receptores sigma-1 son capaces de modular la hipersensibilidad inducida por PGE2, NGF y GDNF.

Encontramos que la administración sistémica (subcutánea) o local (intraplantar) de los antagonistas sigma-1 S1RA y BD-1063, en ratones, revirtió la hiperalgesia mecánica (medida mediante el test de presión plantar) inducida por la administración intraplantar de la PGE2 y del NGF, pero no la hipersensibilidad mecánica inducida por el GDNF. El efecto antihiperalgésico de los antagonistas sigma-1 fue abolido por la administración del agonista sigma-1 PRE-084 (indicando la selectividad de dicho efecto), así como por el antagonista opioide periférico naloxona metiodida y el antagonista selectivo opioide μ ciprodime, pero no por el antagonista κ nor-binaltorpimina ni por el antagonista δ naltrindol. Estos resultados indican que el efecto antihiperalgésico de los antagonistas sigma-1 es mediado por la activación de los receptores opioides μ periféricos. Mediante ensayos inmunohistoquímicos, determinamos la presencia de los receptores sigma-1 en todas las neuronas sensoriales periféricas del ratón. También mostramos la presencia del agonista endógeno opioide μ endomorfina-2 (END2) en los nociceptores TRPV1+ pero no en los nociceptores IB4+. Dicha presencia fue confirmada usando el bisturí molecular resiniferatoxina (RTX), que eliminó selectivamente las neuronas TRPV1+ y con ello el marcaje de END2. Además, la administración de un anticuerpo frente a END2 en la pata sensibilizada revirtió el efecto antihiperalgésico inducido por los antagonistas sigma-1, indicando que la acción de este opioide endógeno es esencial para el efecto antihiperalgésico de los antagonistas sigma-1.

Usando proteínas recombinantes, mostramos que el receptor sigma-1 puede unirse tanto al TRPV1 como al receptor opioide μ, y que el antagonismo sigma-1 induce el traslado de los receptores sigma-1 desde el TRPV1 al receptor opioide. Por lo tanto, el receptor sigma-1 podría participar en la comunicación entre el TRPV1 y el receptor opioide μ. La aplicación de PGE2 incrementó el flujo de calcio inducido por la capsaicina, el agonista prototipo TRPV1, en cultivos de neuronas del DRG. Este incremento en el flujo de calcio fue revertido por el S1RA, y de una manera sensible al

antagonista opioide naloxona, lo que concuerda con los efectos opioides inducidos por antagonismo sigma-1 observados en los ensayos *in vivo* comentados anteriormente.

En resumen, estos resultados sugieren que el antagonismo sigma-1 disminuye la sensibilización periférica mediante el incremento del tono opioide endógeno en las neuronas C peptidérgicas, que producen END2, mientras que no altera la sensibilización de los nociceptores C no peptidérgicos.

Nuestro siguiente objetivo fue estudiar el proceso inverso. Es decir, los posibles efectos pronociceptivos de los agonistas sigma-1. El interés de este objetivo radica en la existencia de varios agonistas sigma-1 con interés clínico. A diferencia del PRE-084, el cual es un agonista sigma-1 estándar sin utilidad clínica, el dextrometorfano es un agonista sigma-1 clásico con un uso amplísimo como antitusígeno, y la pridopidina es un agonista selectivo sigma-1 que está actualmente en ensayos clínicos para el tratamiento de la enfermedad de Huntington y la esclerosis lateral amiotrófica (Naia et al., 2021). La administración subcutánea de cualquiera de estos tres productos no produjo ninguna alteración en la respuesta frente a un estímulo mecánico (test de presión plantar) en el ratón, mientras que cuando se administraron a animales inyectados intraplantarmente con una dosis aparentemente ineficaz de PGE2, indujeron una hiperalgesia mecánica robusta. Puesto que la PGE2 es un mediador inflamatorio, exploramos el efecto de los agonistas sigma-1 en una situación que conlleva una inflamación real: un daño tisular inducido por una incisión plantar. A las pocas horas de la incisión (3,5 h) los animales mostraron una disminución aparente del peso apoyado en la pata dañada, valorado mediante el test de distribución de carga dinámica (en inglés “Dynamic Weight Bearing distribution”). Sin embargo, a las 24 horas del daño quirúrgico, los animales mostraron una recuperación total en este parámetro, pese a presentar un edema notable con una infiltración neutrofílica marcada en el sitio de la incisión. En esta situación, los agonistas sigma-1 indujeron una recaída clara de la pérdida de apoyo en la pata operada. Se sabe que los neutrófilos son una de las fuentes principales de PGE2, y de hecho, el efecto proalgésico de los agonistas sigma-1 tras la incisión plantar fue revertido por la administración de un anticuerpo frente al LY6G, el cual inhibió selectivamente el reclutamiento de neutrófilos en la herida quirúrgica. Estos resultados indican que el

efecto pronociceptivo periférico del agonismo sigma-1 depende de la presencia de neutrófilos.

Los efectos de los agonistas sigma-1, tanto en la hiperalgesia inducida por PGE2 como en la incisión plantar, se revirtieron mediante la administración del antagonista sigma-1 BD-1063 en ratones de genotipo salvaje (WT, de sus siglas en inglés "Wild-Type"). Además, los agonistas sigma-1 no produjeron su efecto proalgésico en animales mutantes desprovistos del receptor sigma-1 (KO, de sus siglas en inglés "knockout"). Ambos resultados respaldan la selectividad de los efectos observados.

En cuanto a la población de neuronas sensoriales involucrada en los efectos pronociceptivos de los agonistas sigma-1 en el ratón, encontramos que estos efectos dependen de la acción de los nociceptores TRPV1+, ya que la administración de RTX revirtió completamente el efecto de estos fármacos.

Hasta el momento, solo habíamos demostrado el marcaje del receptor sigma-1 en el DRG del ratón, por lo que también estudiamos la distribución de este receptor en muestras humanas de DRG. Encontramos resultados virtualmente idénticos en ambas especies, con la presencia del receptor sigma-1 en todas las neuronas sensoriales periféricas, por lo que nuestros hallazgos en animales de experimentación podrían tener una repercusión clínica relevante.

En resumen, estos resultados muestran que el receptor sigma-1 está presente en las neuronas del DRG tanto de humanos como de ratón, y que el agonismo de este receptor exacerba el dolor en ratones con una afección inflamatoria. El mecanismo de las acciones pronociceptivas del agonismo sigma-1 implica la potenciación de las acciones de los algógenos químicos liberados por las células inmunitarias, como por ejemplo de la PGE2, los cuales son capaces de sensibilizar a los nociceptores TRPV1+.

La interacción entre el sistema inmunitario y las neuronas sensoriales no es unidireccional. De hecho, se sabe que las neuronas sensoriales participan en el reclutamiento inmunitario tanto a nivel periférico (DRG) como central (médula espinal dorsal), en varias circunstancias de dolor crónico, como puede ser el dolor neuropático. Esto produce un proceso neuroinflamatorio de suma importancia en el desarrollo y mantenimiento del dolor (Austin et al., 2010). De hecho, se ha

demostrado repetidamente, mediante el análisis del transcriptoma del DRG o de la médula espinal dorsal, que la mayoría de los cambios en la expresión génica que ocurren durante el dolor neuropático tras la lesión de un nervio corresponden al proceso de neuroinflamación. Se sabe que el receptor sigma-1 puede participar en la neuroinflamación tras una lesión nerviosa (e.g. Bravo-Caparrós et al., 2020), aunque su papel en este proceso no se ha estudiado de manera exhaustiva. Por lo tanto, nuestro siguiente objetivo fue evaluar, mediante secuenciación masiva del ARN (ARNseq), los cambios transcripcionales inducidos por una misma lesión nerviosa tanto a nivel periférico como en la médula espinal. Para alcanzarlo, hemos evaluado el efecto de la inhibición del receptor sigma-1 (en ratones KO para este receptor) en el trascriptoma del DRG y de la médula espinal dorsal, tras la sección parcial del nervio ciático en el modelo de SNI (de sus siglas en inglés "Spared Nerve Injury").

El SNI indujo una alodinia mecánica (evaluada con el test de von Frey) y al frío (evaluada mediante el test de la acetona) muy robusta. Ambas estuvieron atenuadas en ratones KO sigma-1. Los cambios transcripcionales fueron analizados mediante la secuenciación masiva del ARN (ARN-seq). A nivel del DRG, el SNI indujo alteraciones principalmente en la expresión de tránscritos inmunitarios, incluyendo una amplia variedad de citoquinas y marcadores de células inmunitarias, tales como macrófagos/monocitos y células T, particularmente CD4+. Parte de estos transcritos inmunitarios estaban atenuados en los ratones KO sigma-1. Demostramos, mediante citometría de flujo, que efectivamente estos ratones mutantes tienen una disminución en el reclutamiento de macrófagos/monocitos y, curiosamente, una eliminación total del reclutamiento de células T CD4+ en el DRG tras la lesión nerviosa. Sin embargo, los ratones KO sigma-1 mostraron una respuesta neuroinflamatoria equivalente a la de los ratones WT en la médula espinal dorsal. Además, estos animales mutantes mostraron un reclutamiento inmunitario normal en la pata tras una inflamación experimental (inducida por la administración intraplantar de adyuvante completo de Freund). Por lo tanto, la disminución de la neuroinflamación periférica que encontramos en los ratones KO sigma-1 no se debe a un déficit general del funcionamiento inmunitario. Por último, el tratamiento con maraviroc, un antagonista periférico del CCR5, que inhibe principalmente a las células T CD4+, tuvo un efecto antialodínico frente al

estímulo mecánico aunque no frente al estímulo frio. Por lo tanto, la inhibición inmunitaria por este fármaco no replicó completamente el efecto de la inhibición del receptor sigma-1, que como se ha comentado anteriormente, atenúa ambas formas de hipersensibilidad sensorial.

Nuestros datos indican que los receptores sigma-1 desempeñan un papel fundamental en la comunicación entre las neuronas sensoriales periféricas y el sistema inmunitario tras una lesión nerviosa. Sin embargo, aunque la modulación de la neuroinflamación periférica por los receptores sigma-1 podría explicar la mejoría de la alodinia táctil neuropática observada en ratones KO, difícilmente puede explicar el efecto en la alodinia al frío. Por lo tanto, la inhibición del receptor sigma-1 puede ser potencialmente eficaz para disminuir el dolor neuropático a través de la inhibición de la neuroinflamación periférica y de mecanismos adicionales.

Teniendo en cuenta todo lo comentado anteriormente, las conclusiones globales de esta Tesis Doctoral son las siguientes:

1. Los receptores sigma-1 periféricos son moduladores importantes de la sensibilización de los nociceptores TRPV1+ actuando directamente en el lugar de la lesión dolorosa: mientras que los antagonistas sigma-1 potencian la acción de los opioides endógenos neuronales, reduciendo la hiperalgesia inducida por mediadores inflamatorios, el agonismo sigma-1 tiene un efecto contrario, maximizando la sensibilización periférica inducida por algógenos químicos producidos por las células inmunitarias.
2. Los receptores sigma-1 también son importantes en la interacción entre las neuronas sensoriales periféricas y las células inmunitarias durante el dolor neuropático. La inhibición de los receptores sigma-1 reduce el dolor neuropático, al menos en parte, por la disminución de la respuesta neuroinflamatoria que se produce en el DRG tras una lesión nerviosa.
3. Los antagonistas sigma-1 tienen un potencial analgésico claro en varias circunstancias dolorosas, mientras que el agonismo sigma-1 muestra efectos pronociceptivos que podrían, al menos potencialmente, constituir un efecto secundario en pacientes tratados con agonistas sigma-1.

Bibliografía

Austin, P. J. & Moalem-Taylor, G. (2010). The neuro-immune balance in neuropathic pain: involvement of inflammatory immune cells, immune-like glial cells and cytokines. J. *Neuroimmunol. 229*, 26-50.

Bravo-Caparrós, I., Ruiz-Cantero, M. C., Perazzoli, G., Cronin, S. J. F., Vela, J. M., Hamed, M. F., Penninger, J. M., Baeyens, J. M., Cobos, E. J., & Nieto, F. R. (2020). Sigma-1 receptors control neuropathic pain and macrophage infiltration into the dorsal root ganglion after peripheral nerve injury. *FASEB J. 34*, 5951-5966.

Bruna, J., Videla, S., Argyriou, A. A., Velasco, R., Villoria, J., Santos, C., Nadal, C., Cavaletti, G., Alberti, P., Briani, C., Kalofonos, H. P., Cortinovis, D., Sust, M., Vaque, A., Klein, T., & Plata-Salaman, C. (2018). Efficacy of a Novel Sigma-1 Receptor Antagonist for Oxaliplatin-Induced Neuropathy: A Randomized, Double-Blind, Placebo-Controlled Phase IIa Clinical Trial. *Neurotherapeutics. 15*, 178-189,

Naia, L., Ly, P., Mota, S. I., Lopes, C., Maranga, C., Coelho, P., Gershoni-Emek, N., Ankarcrona, M., Geva, M., Hayden, M. R., & Rego, A. C. (2021). The Sigma-1 Receptor Mediates Pridopidine Rescue of Mitochondrial Function in Huntington Disease Models. *Neurotherapeutics. 18*, 1017-1038.

Montilla-García, Á., Perazzoli, G., Tejada, M. Á., González-Cano, R., Sánchez-Fernández, C., Cobos, E. J., & Baeyens, J. M. (2018). Modality-specific peripheral antinociceptive effects of mu-opioid agonists on heat and mechanical stimuli: Contribution of sigma-1 receptors. *Neuropharmacology 135*, 328-342.

Sánchez-Fernández, C., Entrena, J. M., Baeyens, J. M., & Cobos, E. J. (2017). Sigma-1 Receptor Antagonists: A New Class of Neuromodulatory Analgesics. *Adv. Exp. Med. Biol. 964*, 109-132.

Tejada, M. Á., Montilla-García, Á., González-Cano, R., Bravo-Caparrós, I., Ruiz-Cantero, M. C., Nieto, F. R., & Cobos, E. J. (2018). Targeting immune-driven opioid analgesia by sigma-1 receptors: Opening the door to novel perspectives for the analgesic use of sigma-1 antagonists. *Pharmacol. Res. 131*, 224-230.

Woolf, C. J., & Ma, Q. (2007). Nociceptors—Noxious Stimulus Detectors. *Neuron. 55*, 353-64.

INTRODUCTION

INTRODUCTION

1. PERIPHERAL SENSITIZERS

There are numerous chemical substances that participate in the inflammatory process and that also sensitize sensory neurons. These sensitizers are of a very diverse chemical nature, such as lipid mediators, neurotrophic factors, cytokines, peptides and nucleotides, among others (Basbaum et al., 2009; Ji et al., 2014; Pinho-Ribeiro et al., 2017). Although there is a myriad of these substances, some relevant examples are commented below and are schematically represented (together with some additional sensitizers) in Figure 1. This figure also shows some inhibitory receptors and mechanisms located in the peripheral terminals which might reduce the peripheral sensitization process. These include endogenous opioid peptides, such as β-endorphin (among others), which can be produced by immune cells or keratinocytes (Fell et al., 2014), or even by the sensory neurons itself (Scanlin et al., 2008; Höftberger et al., 2010). In many cases, the presence of these endogenous mechanisms favoring analgesia is not able to compensate the powerful effect of inflammatory mediators, resulting in pain. A more detailed description of the most relevant peripheral sensitizers is given below.

1.1 Lipid mediators

The most commonly used analgesics for inflammatory pain are non-steroidal anti-inflammatory drugs (NSAIDs), which inhibit cyclooxygenase activities (COX), to decrease the production of prostanoids, which include prostaglandins, prostacyclins, and thromboxanes. Prostaglandin E2 (PGE2) is probably the best known inflammatory pain mediator. While PGE2 can be produced by all cell types, immune cells are a primary source of PGE2 production during an inflammatory response (Agard et al., 2013). It activates EP1-EP4 receptors, which are G-protein-coupled receptors located in nociceptors, among other sites. PGE2 sensitizes sensory neurons increasing their response to further stimulation, rather than acting as a direct activator (Kawabata, 2011; Piomelli et al., 2014; Pinho-Ribeiro et al., 2017). The mechanism of its actions

lies in the activation of Protein kinase A (PKA) and Protein kinase A (PKC) downstream of EP4 and EP1, respectively, which sensitize/activate multiple molecules including transient receptor potential vanilloid-1 (TRPV1) channels, among others, leading to hyperalgesia (Kawabata, 2011). When PGE2 is acting on sensory neurons during a prolonged period, it can induce persistent hyperalgesia by activating NFκB signaling in the dorsal root ganglion (DRG) neurons through PKA and PKC pathways (Souza el al., 2015). In addition, PGE2 can also contribute to neurophatic pain (Kawabata, 2011; Pinho-Ribeiro et al., 2017), although to a much lower extent than to inflammatory pain (Bastos et al., 2013).

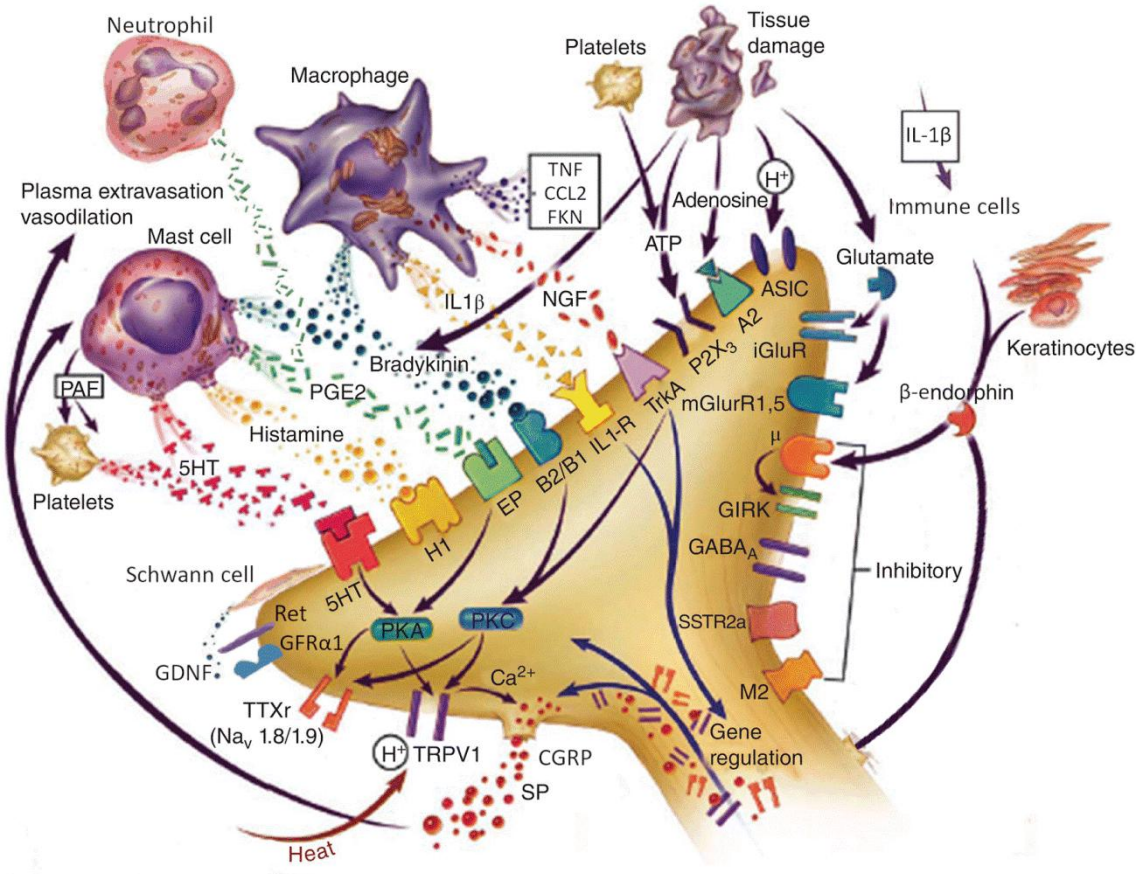

Figure 1. Peripheral sensitizers and their receptors. Inflammation leads to the release of numerous chemicals that act directly or indirectly to alter the sensitivity of peripheral nerve terminals. Some inhibitory receptors which also modulate neuronal excitability are also shown. ASIC, acid-sensing ion channel; CCL2, C-C motif chemokine ligand 2; FNK, fractalkine; GIRK, G-protein-coupled inward rectifying potassium channel; GDNF, glial cell-derived neurotrophic factor; GFRα1, glial cell line derived neurotrophic factor receptor α1; CGRP, calcitonin-gene related peptide; iGluR, ionotropic glutamate receptor; IL-1β, interleukin-1β; mGluR, metabotropic glutamate receptor; NGF, nerve growth factor; PAF, platelet-activating factor; PGE2, prostaglandin E2; PKA, protein kinase A; PKC, protein kinase C; Ret, rearranged during transfection; SSTR2A, somatostatin receptor 2A; TNF, tumour necrosis factor; TrkA, tyrosine kinase receptor A; TTXr, tetrodotoxin-resistant sodium channel; μ, μ-opioid receptor; M_2,

muscarinic receptor; 5HT, serotonin *(Figure taken from Meyer et al., 2006; artwork by Ian Suk from Johns Hopkins University, with modifications).*

Although PGE2 is thought to be the main proalgesic lipid, it should be mentioned that others lipids derived from arachidonic acid, such as leukotrienes are also known pain-mediators. In fact, the injection of LTB_4 induces hyperalgesia in humans by the activation of C- and Aδ-fibers (Pinho-Ribeiro et al., 2017). Also, phospholipids, such as lysophosphatidic acid (LPA), which act directly on nociceptors to increase TRPV1 activity and oxidized polyunsaturated fatty acid derivatives, such as 13-hydroxy-octadecenoic acid (13-HODE) which also activates TRPV1 (Piomelli et al., 2014; Pinho-Ribeiro et al., 2017), might have a relevant role in pain. Therefore, PGE2 and other proalgesic lipids play a key role in the modulation of pain signaling.

1.2 Neurotrophic factors

Tissues highly innervated by nociceptive neurons exhibit increased sensitivity to noxious stimuli, which accounts (at least partially) for the variation in pain sensitivity across different body areas (Pinho-Ribeiro et al., 2017; Magerl et al., 2021). The process of innervation is dynamic and can be influenced by neurotrophic factors, which are upregulated during tissue inflammation and injury. Neurotrophic factors play a crucial role in the restoration of nerve density following injury, but they can also contribute to heightened pain sensitivity (Pinho-Ribeiro et al., 2017), and this was demonstrated for the first time in 1994 by Woolf and coworkers. During inflammation, immune cells, particularly macrophages, produce Nerve Growth Factor (NGF), which activates TrkA receptor in nociceptive neurons. TrKA activation triggers PI3K/Src kinase signaling, leading to the phosphorylation of TRPV1. This process accounts for the fast sensitizing effects of NGF. Moreover, NGF also induces the translocation of TRPV1 from intracellular locations to the plasma membrane, in a process which requires the activation of p38 MAPK in DRG neurons, and that results in the increase in the presence of TRPV1 in the membrane of peripheral terminals in a manner independent of the transcriptional process (Ji et al., 2002). Additionally, the neurotrophic activity of this growth factor, as its name indicates, leads to the growth and sprouting of axon terminals in an inflamed site, further contributing to heightened local pain sensitivity

(Longo et al., 2013; Minnone et al., 2017). NGF also strongly participates on sensitization after nerve injury, as it is a fundamental part of the machinery needed for axon regeneration (Ro et al., 1999; Kwon et al., 2013; Pinho-Ribeiro et al., 2017).

Furthermore, there are other neurotrophic factors that increase their expression after peripheral nerve injury to promote regeneration, including the glial cell-derived neurotrophic factor (GDNF). It has been shown that GDNF is produced by Schwann cells, DRG satellite cells and astrocytes, among others (Nomura et al., 2002). The trophic effects of GDNF depend on receptor complexes formed by one subunit involved in ligand binding, the GDNF family receptor α1 (GFRα1), and another subunit with tyrosine kinase activity involved in transmembrane signaling, named RET (rearranged during transfection). Specifically, GDNF hyperalgesia is mediated by PLCγ, MAPK/ERK, PI3K, CDK5 and Src family kinase signaling (Bogen et al., 2008). Almost half of all RET-expressing nociceptors also express the GFRα1. As distinctive features, the GFRα1/Ret expressing subpopulation of nociceptors also binds the isolectin B4 (IB4) (Alvarez el al., 2012).

1.3 Cytokines

Inflammatory cytokines can be produced by immune cells and play a pivotal role in nociceptor activity and pain sensitization, which has been widely reviewed (Verri et al., 2006; Pinho-Ribeiro et al., 2017). It has been shown that cytokines play a significant role in modulation of pain from diverse etiology, including arthritis, neuropathic pain, and cancer-related pain (Verry et al., 2006; Pinho-Ribeiro et al., 2017). Although there is a wide variety of pro-inflammatory cytokines, interleukin-1β (IL-1β), tumor necrosis factor (TNF), CCL2 (also called MCP1, for Monocyte Chemoattractant Protein-1) and fractalkine, which are mainly related to macrophages/monocytes, should be highlighted.

IL-1β is able to sensitize nociceptive neurons through p38 MAPK phosphorylation of Nav1.8 sodium channels, resulting in an increase of action potencial generation which causes mechanical and thermal hyperalgesia (Binshtok et al., 2008). This interleukin also activates IL-1R1 on nociceptors which increase TRPV1 expression, leading to

heightened sensitivity to thermal stimuli and to the enhanced pain sensitivity during chronic inflammation (Ebbinghaus et al., 2012).

Another known cytokine which produces TRPV1-dependent sensitization is TNF (Jin and Gereau, 2006; Constantin et al., 2008), which also sensitizes TRPA1+ neurons (Fernandes et al., 2011). However, the induction of inflammatory pain *in vivo* by TNF is not only dependent on these TRPs, but also on the production of prostaglandins downstream of the activation of the receptor for TNF (Cunha et al., 2005). Moreover, it is worth mentioning that TNF can also induce a quick modulation of nociceptor sensitivity by phosphorylating Nav1.8 and Nav1.9 sodium channels via p38MAPK, leading to changes in neuronal excitability (Gudes et al., 2015).

Finally, it is worth mentioning that not only immune cells produce cytokines but also neurons can produce some of them. One example is CCL2, which can be produced by sensory neurons after nerve injury and has potent chemotactic activity. It is involved in macrophage recruitment and participates on the neuroinflammatory process during neuropathic pain (Zhu et al., 2014; Kwon et al., 2015; Bravo-Caparrós et al., 2020). This is not the only cytokine which attracts macrophages after nerve injury as this is a complex process which involves other relevant signals such as fractalkine (also known as CX3CL1) (Huang et al., 2014). The role of these two cytokines in the development and maintenance of neuropathic pain is out of any doubt (Zhang et al., 2020, Silva and Malcangio, 2021).

1.4 Peptides

Tissue damaged during inflammation induces the release of several peptides such as bradykinin, which acts on B1-B2-type receptors, which are G-protein-coupled receptors (GPCR) which trigger the activity of PKC and PKA. As for PGE2, bradykinin actions sensitize channels such as TRPV1 or TRPA1 (Choi and Hwang, 2018).

In addition, there are neuropeptides such as the calcitonin-gene related peptide (CGRP) and substance P (SP) which are some of the most potent mediators of vasodilation and tissue edema, which are two of the characteristic events in the inflammation process (Brain et al., 1985). These neuropeptides are primarily released

from sensory nerves and are implicated in pain pathways. The stimulation of sensory neurons with capsaicin, the prototypical TRPV1 agonist produces the release of CGRP and SP, as both often colocalize in the same neurons (Lundberg et al., 1985). The presence of these peptides in specific subsets of nociceptors has led to their being referred to as "peptidergic nociceptors", as opposed to "non-peptidergic nociceptors" that lack of these neuropeptides.

SP signaling promotes nociceptive sensitization across different models of chronic and inflammatory pain. SP preferentially binds to the NK1 receptors, which are GPCR, and triggers the consequent sensory sensitization (Chang et al., 2019). There have been developed antagonists of NK1 receptor, which reached clinical trials. However, they were discontinued because of lack of analgesic efficacy (Hill, 2000). CGRP has a crucial role in pain neurotransmission, but in particular in the development of migraines. It is believed that during migraines, trigeminal afferent nerve fibers release CGRP in the dura mater and subarachnoid space. This activation leads to vasodilation and triggers a series of events including the production of PGE2, nitric oxide, bradykinin, and the degranulation of mast cells in the dura mater, resulting in the release of histamine. All these processes ultimately lead to peripheral and central sensitization (Ferrari et al., 2015). In fact, drugs which block CGRP (galcanezumab) or its receptor (erenumab and the –even more- recent “gepants”) have been recently introduced in the clinical practice for the treatment of migraine, with astonishing results (Chiang et al., 2020). CGRP, as one of the main peptidergic neurotransmitters of nociceptors is also shown in preclinical studies to be relevant for several pain states, in particular those which occur with inflammation and the sensitization of TRPV1 nociceptors (Russell et al., 2014; Powell et al., 2021).

1.5 Nucleotides

Inflammatory responses and tissue damage can also cause the release or leakage of adenosine and its derivatives into the extracellular space, which can subsequently activate nociceptors. Long ago, adenosine was shown to increase hyperalgesia through its A2 receptors (Ledent et al., 1997). Although adenosine can be produced

intracellularly, the main source of adenosine in pathological pain states is adenosine triphosphate (ATP). While ATP is widely recognized as the primary source of energy for cellular metabolism, it was proposed in 1953 that ATP may also have a role in modulating neurotransmission. Numerous studies have supported the potential role of ATP as a peripheral mediator of different pain conditions. The purinergic receptors on sensory nerves primarily responsible for ATP signaling are homomeric P2X3 and heteromeric P2X2/3, which are ligand-gated cation channels able to induce neuronal depolarization. In fact, the ATP analog α,β-methylene ATP, more resistant to hydrolysis than ATP, has been used very often to study the role of purinergic receptors on pain (Krajewski, 2020). It is relevant to note that P2X3 receptors are present in a subset of nociceptors which are devoid of neuropeptides (the non-peptidergic C-nociceptors) (Bradbury et al., 1998; Burnstock, 2000; Woolf and Ma, 2007; Krajewski, 2020). Therefore, some peripheral sensitizers have a strong preference for specific subpopulations of primary afferents and allow the study of the activation/sensitization different subpopulations of nociceptors.

1.6 Others

Among other peripheral sensitizers, it is worth mentioning serotonin (5-HT, 5-hydroxytryptamine), and histamine. While 5-HT is released by activated platelets, and also by activated mast cells, histamine is released by the latter (Pinho-Ribeiro et al., 2017).

Serotonin binds to several 5-HT receptors some of which actives PKA and PKC, leading to the corresponding phoshorilation of receptors and channels (Ohta et al., 2006). In addition, it is known that 5-HT also leads to an upregulation of neuronal acid-sensing ion channels (ASICs), which sense extracellular protons (that are abundant in the inflammatory environment) and increase pain signaling (Qiu et al., 2012).

On the other hand, histamine binds to H1 and H2 receptors on nociceptors to increase the expression of Nav1.8 channels, which in turn cause increased sensitivity to mechanical and thermal stimuli. It not only plays a crucial role in different inflammatory pain conditions (Parada et al., 2001; Massaad et al., 2004; Khalilzadeh et

al., 2018) but also acts as a significant mediator of neuropathic pain induced by peripheral nerve injury (Yue et al., 2014; Pinho-Ribeiro et al., 2017).

2. PERIPHERAL SENSORY NEURONS

Traditionally, somatosensory neurons were classified based on various factors such as their conduction velocity, the size of their cell body, the types of nerve endings, and the specific layers of the spinal cord targeted by their central terminals. According to their conduction velocity sensory neurons can be broadly classified as C-fibers, which are unmyelinated and hence exhibit a slow conduction velocity, Aδ-fibers are lightly myelinated fibers and with an intermediate conduction velocity, and finally, Aβ- and proprioceptive fibers are heavily myelinated and have a higher conduction velocity in comparison to the other sensory fibers (Le Pichon and Chesler, 2014). The size of the soma also varies depending on the type of neuron, as the soma of C-neurons is smaller than the soma of other sensory neurons, while the soma of Aδ-neurons have an intermediate size and the Aβ/proprioceptive neurons have the largest somas among sensory neurons. These features are summarized in Figure 2. Although it is useful to introduce these categories, this broad classification fails to account for the extraordinary molecular and functional diversity of somatosensory neuron subtypes that have emerged in recent years.

The most abundant type of somatosensory neurons corresponds to C-neurons, accounting for over 50% of the total population. They are small in diameter and able to respond to differing combinations of temperatures, pruritogens, tissue damage, chemical irritants, and mechanical stimuli. They can be classified into two broad categories: peptidgergic and non-peptidergic neurons. As previously commented, the former can be distinguished by the expression of CGRP and SP and the latter by the expression of P2X3 and their labelling with IB4, among others markers summarized in Table 1. The presence of these markers reflects the functional characteristics of the neurons, as while peptidergic C-neurons (which express TRPV1) code for heat stimulus, non-peptidergic C-nociceptors code for mechanical stimulation (Cavanaugh et al., 2009; Scherrer et al., 2009; Montilla-García et al., 2018). While in the mouse this distinction is clear since the distribution of some molecular markers show clear differences; in the rat it is not so as there is an obvious colocalization between TRPV1 and IB4 (Woodbury et al., 2004; Cavanaugh et al., 2009; Montilla-García et al., 2018).

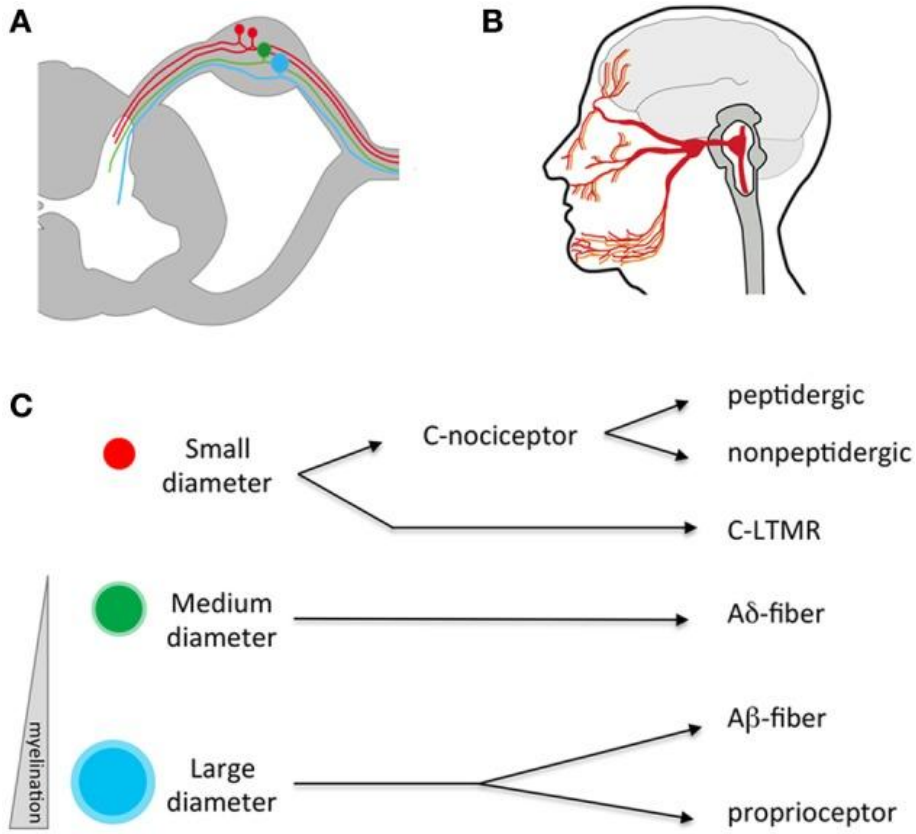

Figure 2. Anatomy of the somatosensory system. (A) Somatosensory neuron cell bodies reside outside the spinal cord in the dorsal root ganglia (DRG). They have a single process that splits, sending an afferent projection to the periphery and an efferent projection to the spinal cord. (B) Somatosensory neurons residing in the trigeminal send processes that innervate peripheral targets through the face, mouth, and dura and central targets in the brainstem. (C) Somatosensory neurons can be divided into three broad categories based on the size of their cell bodies and degree of myelination. Within these broad categories, numerous sub-specializations exist, for example small diameter C fibers are mostly nociceptors while large diameter A neurons respond to low threshold mechanical stimuli. LTMR, low-threshold mechano-receptor *(Figure taken from Le Pichon and Chesler, 2014)*

The distribution of markers across different classes of C-neurons is better summarized in the Venn diagram of Figure 3 (taken from Le Pichon and Chesler, 2014). This clearly exemplifies the complexities of the diverse nature of sensory neurons. Some C-neurons are enriched in TRPs which are responsible of the coding of some specific sensations, as while TRPV1 is activated by heat, TRPA1 and TRPM8 are activated by cold stimuli. These TRPs are not expressed equally in all C-neurons, as TRPV1 is expressed in peptidergic sensory neurons, whereas TRPA1 is expressed in a sub-population of both peptidergic and non-peptidergic C-neurons, (Barabas et al., 2012; Talavera et al., 2020). The distribution of TRPM8 is much less certain, as it is expressed in a subpopulation of small-diameter neurons which do not express TRPV1 and do not bind IB4+, and also in a subpopulation of Aδ-nociceptors (Dhaka et al., 2008;

Takashima et al., 2010). In addition, some TRPs are of high importance for nociceptor sensitization, as commented in the preceding section (see "1. Peripheral Sensitizers"). The recognition of TRPs as a key piece of the physiology of the somatosensory system was manifested with the awarding of "The 2021 Nobel Prize in Physiology or Medicine" to David Julius and Ardem Patapoutian, discoverers of TRPV1 and TRPA1, respectively (Reeh and Fischer, 2022).

Table 1. Some examples of markers for somatosensory cell type in the mouse.

MARKER	SENSORY CELL TYPE
Parvalbumin	Proprioceptors and Aβ neurons
CGRP	Peptidergic C-neurons, sub-population of Aδ-neurons
Substance P	Peptidergic C-neurons
NF200	Myelinated neurons (Aδ-, Aβ-, and proprioceptors)
IB4	Non-peptidergic C-neurons
TRPV1	Peptidergic C-neurons
TRPA1	Sub-populations of peptidergic and non-peptidergic C-nociceptors
TRPM8	Sub-populations of small diameter C-neurons (which do not express TRPV1 and do not bind IB4+) and Aδ-nociceptors
MrgprD	Non-peptidergic C-neurons
MrgprA3	Small diameter C neurons
MrgprB4	Small diameter C neurons
VGlut3	Non-peptidergic C neurons
TH	Non-peptidergic C neurons
TrkB	Aδ-neurons
Npy2r	Aβ-neurons
Chondrolectin	Aβ-neurons
DOR	Sub-populations of non-peptidergic C-neurons and myelinated NF200-positive cells
MOR	Peptidergic C-neurons and Sst+ pruriceptors

Abbreviations: CGRP, calcitonin gene-related peptide; DOR, δ-opioid receptor. NF200, neurofilament heavy chain 200; IB4, isolectin B4; MOR, μ-opioid receptor; MrgprD, Mas-related G-protein-coupled receptor D; MrgprA3, Mas-related G-protein-coupled receptor A3; MrgprB4, Mas-related G-protein-coupled receptor B4; Npy2r, neuropeptide Y receptor type 2; TH, tyrosine hydroxylase; TrkB, tyrosine receptor kinase B; TRPA1, transient receptor potential cation channel subfamily A member 1; TRPV1, transient receptor potential cation channel subfamily V member 1; TRPM8, transient receptor potential cation channel subfamily M member 8; VGluT3, vesicular glutamate transporter type 3; (Table taken from Le Pichon and Chesler, 2014 with slight modification (Basbaum et al., 2009; Cavanaugh et al., 2009; Scherrer et al., 2009; Renthal et al., 2020).

Activation of C fibers often, but not always, results in the sensation of pain, as in addition to nociceptive C-fibers, there are C-fibers that respond to low-threshold mechanical stimuli (C-LTMRs) or to non-painful temperature, and therefore these are non-nociceptive neurons (Dubin and Patapoutian, 2010). In the periphery, it is conventionally thought that C-fibers terminate as free nerve endings in the skin, organs, and bone. However, it has been recently described the existence of specialized cutaneous Schwann cells which are in contact to the supposedly "free" nerve endings and participate on the initiation of sensory transduction (Abdo et al., 2019).

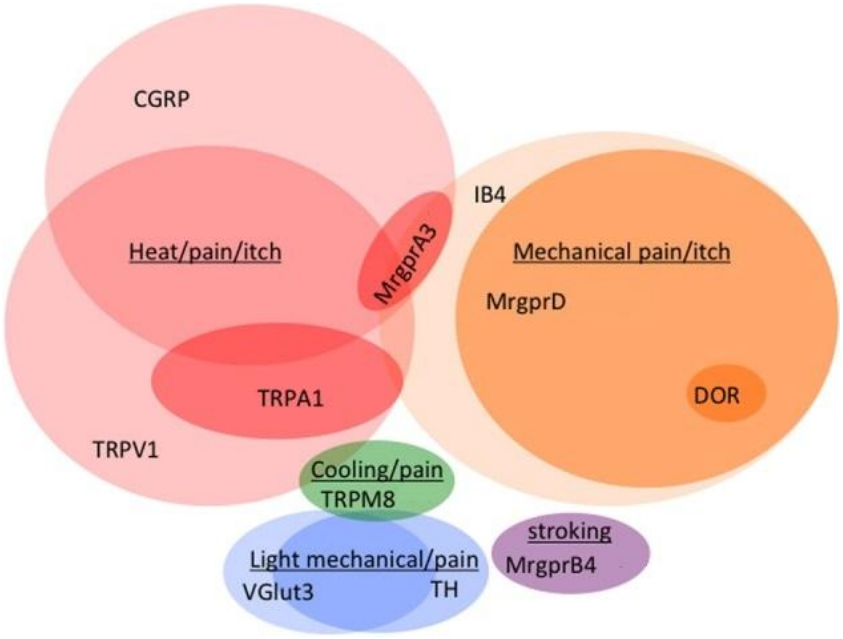

Figure 3. Venn diagram illustrating the distribution of markers across different classes of C fibers in mice (not to scale). Please note that the current evidence indicates that TRPA1 is also present in a subset of non-peptidergic nociceptors *(Figure taken from Le Pichon and Chesler, 2014*).

Aδ-fibers, can be activated by different stimuli such as temperature or pressure, which are typically of higher intensities than the values needed for C-fiber activation. Because of their quicker transmission speed, it is thought these other types of nerve fibers are specialized in detecting intensely localized fast "first pain", rather than the more spatially diffuse slow "second pain" linked to C-fiber nociceptors (Basbaum et al., 2009; Priestley, 2009; Beissner et al., 2010). As commented in the preceding paragraph, a sub-population of Aδ-fibers expresses TRPM8 and code for cold stimulation (McCoy et al., 2011). Aδ-fibers can also become sensitized due to repetitive stimulation or

algogenic chemicals released by tissue damage, thereby playing a critical part in pathological pain (Basbaum et al., 2009). Some markers of this type of neurons have been listed in Table 1, such as NF200 and TrkB (Le Pichon and Chesler, 2014).

Following this classification, the somatosensory neurons with the largest diameter, and fast conduction velocities, are Aβ-neurons, specialized in sensing low-threshold mechanical stimuli, and the Aα-fibers that respond to muscle twitches. Aβ-fibers are low-threshold mechanoreceptors and are further divided into several subclasses that respond to particular types of mechanical stimuli, such as pressure, vibration, and hair deflection. The specialized nerve endings linked to Aβ-fibers, which include Meissner's corpuscles, Pacinian corpuscles, Merkel cells, and the lanceolate nerve endings that envelop hair follicles. Each of them exhibit distinct structural features that likely support the specialized tuning of their associated nerve fibers (Basbaum et al., 2009; Le Pichon and Chesler, 2014), and also include transducers for the coding of mechanical stimulus which do not rely exclusively on neurons (Nikolaev et al., 2020). Some markers of this type of neurons are NF200, Npy2r, chondrolectin and parvalbumin (Table 1).

Nerve endings of proprioceptors also exhibit a high degree of specialization and innervate muscle spindles or Golgi tendon organs, thus are adapted to detect muscle tension and contraction accurately. They can also be labelled with NF200 and parvalbumin (Le Pichon and Chesler, 2014).

At central levels, C- and Aδ-fibers project to the superficial layers of the spinal cord, a region known to be critical for the first stage of the processing of noxious and thermal stimuli (mainly laminae I–II). Not all C neurons project to the exact same site in the superficial dorsal horn of the spinal cord, as whereas peptidergic C-nociceptors project to lamina I and outer lamina II, non-peptidergic C-nociceptors project to inner lamina II. Aδ-fibers typically project to lamina I, although some of these fibers also project to deeper spinal cord layers even to lamina V. Finally, Aβ-fibers project to laminae III–V of the spinal cord. At these locations, peripheral sensory neurons synapse with second order neurons which will connect the spinal cord with several brain nuclei (Figure 4). Proprioceptors also project to deep laminae, similar to Aβ-fibers, although they

synapse to local motor-stretch reflex circuits instead of the ascending sensory circuits (Basbaum et al., 2009; Le Pichon and Chesler, 2014; Kaliyaperumal et al., 2020).

Finally, it is worth mentioning that the classification of the neuronal populations based on their molecular markers commented above is a simplification of the real complexity found in more recent studies. A transcriptional profiling of DRG neurons with single-cell resolution found 9 neuron subtypes: Tac1+/Gpx3+ peptidergic nociceptors, Tac1+/Hpca+ peptidergic nociceptors, Mrgprd+ non-peptidergic nociceptors, Sst+ pruriceptors, Nefh+ A fibers including Aβ-LTMRs and Pvalb+ proprioceptors, Cadps2+ Aδ-LTMRs, Fam19a4+/Th+ C-fiber LTMRs, and a putative cLTMR2 cluster that expresses Fam19a4, but very low levels of Th (Renthal et al., 2020). A database with all expression values found in these neuronal subtypes is publicly available in the following link: https://painseq.shinyapps.io/publish/#

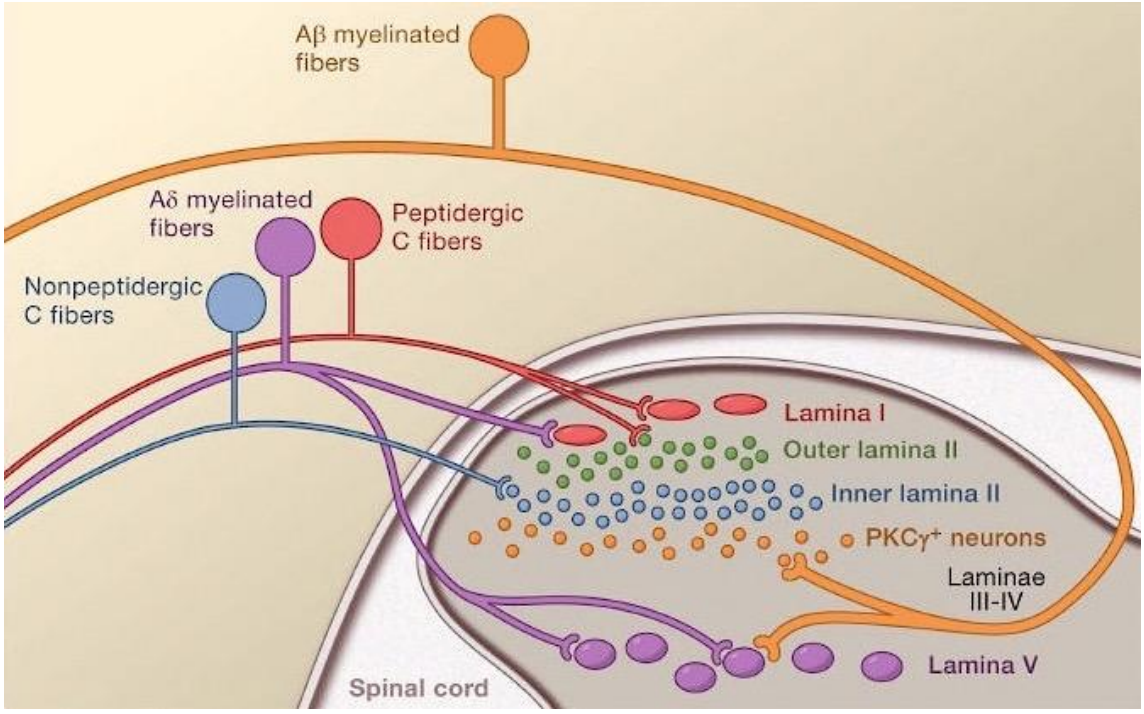

Figure 4. Connections between primary afferent fibers and the spinal cord. There is a very precise laminar organization of the dorsal horn of the spinal cord; subsets of primary afferent fibers target spinal neurons within discrete laminae *(Figure taken from Basbaum et al., 2009)*.

3. SIGMA-1 RECEPTORS AND PAIN

3.1 Historical overview of sigma-1 receptor

Sigma receptors were initially misclassified as a subtype of opioid receptors by Martin and coworkers in 1976. Shortly after, they were found to not bind most opioid drugs, and were defined as different from opioid receptors (Su, 1982). Later, sigma receptors were pharmacologically characterized into two subtypes, which were termed as sigma-1 and sigma-2 receptors (reviewed by Matsumoto et al., 2003; Cobos et al., 2008). The first cloning of the sigma-1 receptor was reported in 1996 from guinea pig liver (Hanner et al., 1996). Subsequently, the receptor was also cloned from several other species, including humans (reviewed in Cobos et al., 2008). All these findings led to the development of sigma-1 knockout mice (Langa et al., 2003) which are undoubtedly powerful tool to improve our knowledge of the biochemical and functional characteristics of the sigma-1 receptor.

Upon cloning the sigma-1 receptor, it was found to be an unique protein, which does not show homology with opioid receptors or with any other known mammalian protein, with over 90% amino acid identity across several species, including rodents and humans (Ruoho et al., 2012). The gen for the human sigma-1 receptor is located in the cromosome 9 band p13 and contains three introns and four exons (Chu and Ruoho, 2016). Although the tridimensional structure of the sigma-1 receptor remained elusive for many years, the crystal structure of the human sigma-1 receptor has recently been elucidated, and a model with three transmembrane domains has been proposed (Chu and Ruoho, 2016; Schmidt et al., 2016). Thus, the sigma-1 receptor is an atypical transmembrane protein of 29-kDa, containing 223 amino acids (Cobos et al., 2008; Su et al., 2010), that has been implicated in various cellular functions and may play a role in both normal and pathological conditions in humans (Hayashi and Su, 2007). There are currently selective ligands for the sigma-1 receptor which are in clinical trials, both agonists such as pridopidine (de Yebenes et al., 2011; Chen et al., 2021) or blarcamesine (Salaciak and Pytka, 2022), with an intended indication for neurodegenerative diseases (de Yebenes et al., 2011; Chen et al., 2021; Salaciak and Pytka, 2022) and the sigma-1 antagonist S1RA with a primary intended indication for

pain treatment (Bruna et al., 2018). The first results on a phase III clinical trial with a sigma-1 ligand were obtained using pridopidine, and were published in 2011 (de Yebenes et al., 2011). Additional clinical trials with pridopidine and blarcamesine are currenty underway (Chen et al., 2021; Salaciak and Pytka, 2022). The sigma-1 antagonist S1RA has only advanced up to now to a phase IIa, and the results were more recently published, in 2018 (Bruna et al., 2018). More details on these compounds and their intended indications are given in the next section.

The sigma-2 receptor has been much less studied, as it was cloned in 2017 (Alon et al., 2017), and there are not published clinical trials with any selective sigma-2 receptor drug yet.

All of these relevant milestones are chronologically indicated on a time scale in Figure 5.

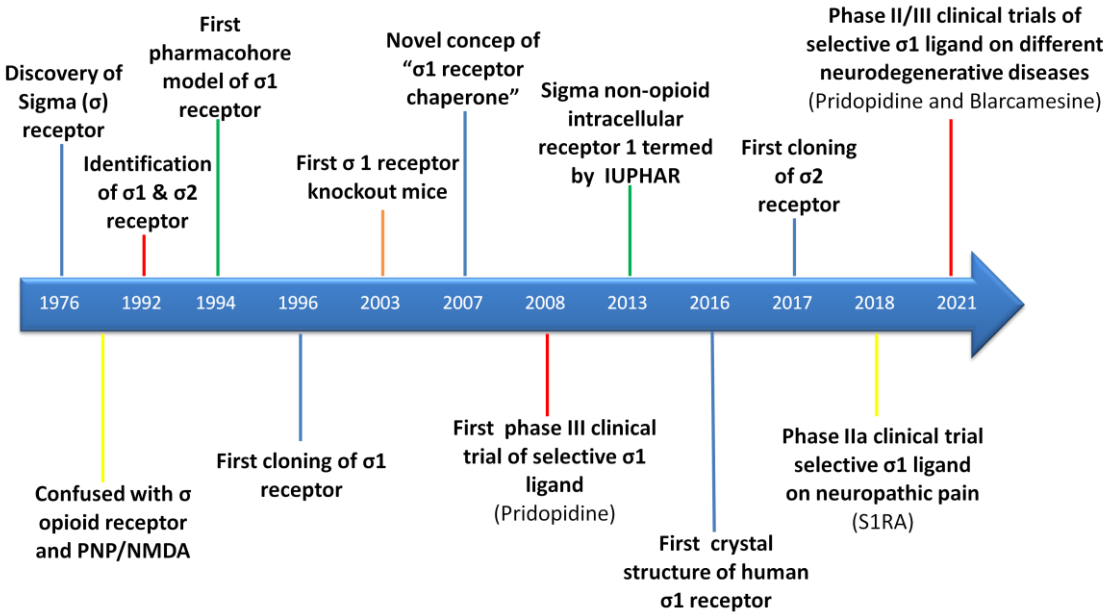

Figure 5. Major milestones in the history of sigma-1 receptors. *Figure modified from Ye et al., 2020.*

A brief overview of the pharmacology, anatomical distribution, subcellular location and chaperoning function of these receptors is provided in the following sections.

3.2 Sigma-1 receptor pharmacology

The activity of the sigma-1 receptor can be modulated by both endogenous and synthetic ligands, and the characteristics of some of them are summarized in Tables 2 and 3.

Among the endogenous ligands there are several neurosteroids such as dehydroepiandrosterone, pregnenolone, progesterone and the natural hallucinogen *N*,*N*-dimethyltryptamine (DMT) (Cobos et al., 2008; Fontanilla et al., 2009; Maurice et al., 2009). However, the status of neurosteroids as authentic endogenous ligands of the sigma-1 receptor is still a matter of debate, given that most of them do not display sufficiently high affinity for the receptor to be qualified as endogenous ligands (Schwarz et al., 1989; Cobos et al., 2008; Zamanillo et al., 2013). A similar statement could be said of DMT, as its affinity for sigma-1 receptor is also poor (as shown in Table 2).

Table 2. Pharmacology of some usual sigma-1 receptor ligands.

Compound	Subtype	Affinity	Function	Other Activities
Putative endogenous ligands				
DHEAS	σ1	+	Agonist	Neurosteroid. $GABA_A$ negative modulator
Pregnenolone sulfate	σ1	+	Agonist	Neurosteroid. NMDA positive/$GABA_A$ negative modulator
Progesterone	σ1	+	Antagonist	Neurosteroid. NMDA negative/$GABA_A$ positive modulator
N,*N*-dimethyltryptamine	σ1	+ or lower	Agonist	Agonist 5-HT2A and 5-HT2A receptors and trace amine-associated receptor 1 (TAAR1)
Benzomorphans				
(+)-Pentazocine	σ1	+++	Agonist	-
(–)-Pentazocine	σ1/σ2	++	Agonist	κ1 agonist, μ1, μ2, ligand, low affinity δ, and κ3 opioid ligand
(+)-SKF-10,047	σ1	+++	Agonist	NMDA receptor ligand
Antipsychotics				
Chlorpromazine	σ1/σ2	++	?	Dopamine D2 antagonist
Haloperidol	σ1/σ2	+++	Antagonist	Dopamine D2 and D3 antagonist; σ2 agonist
Nemonapride	σ1/σ2?	+++	?	Dopamine D2 antagonist
Antidepressants				
Clorgyline	σ1	+++	Agonist?	Irreversible monoamine oxidase A inhibitor

Fluoxetine	σ1	+	Agonist	Selective 5-HT reuptake inhibitor
Fluvoxamine	σ1	+++	Agonist	Selective 5-HT reuptake inhibitor
Imipramine	σ1	++	Agonist	Monoamine reuptake inhibitor
Sertraline	σ1	++	Agonist	Selective 5-HT reuptake inhibitor
Antitussives				
Carbetapentane	σ1/σ2	+++	Agonist	Muscarinic antagonist
Dextromethorphan	σ1	++	Agonist	NMDA receptor allosteric antagonist
Dimemorfan	σ1/σ2	++	Agonist	?
Anticonvulsants				
Phenytoin (DPH)	σ1	Not applicable	Allosteric Modulator	Delayed rectifier K^+ channel blocker; T-type Ca^{2+} current inhibitor; Na^+ current inhibitor
Ropizine	σ1	Not applicable	Allosteric modulator	?
Parkinson's and/or Alzheimer's disease				
Amantadine	?	+	Agonist?	NMDA antagonist, antiviral properties
Donepezil	σ1/σ2?	+++?	Agonist	Cholinesterase inhibitor
Memantine	?	+	Agonist?	NMDA antagonist, antiviral properties
Drugs of abuse				
Cocaine	σ1/σ2	+	Agonist	Monoamine transporters inhibitor, amongst other actions
MDMA	σ1/σ2	+	?	Preferential SERT inhibitor, among other actions
Metamphetamine	σ1/σ2	+	?	Preferential DAT inhibitor, amongs other actions
Other σ drugs				
BD 737	σ1/σ2	+++	Agonist	-
BD 1008	σ1/σ2	+++	Antagonist	σ2 agonist?
BD 1047	σ1	+++	Antagonist	α adrenoceptor ligand
BD 1063	σ1	+++	Antagonist	-
BMY 14802	σ1/σ2	++	Antagonist	5-HT1A agonist
DTG	σ1/σ2	+++	?	σ2 agonist
Eliprodil (SL-82.0715)	σ1/σ2	++	?	NMDA antagonist,α1 adrenoceptor ligand
Haloperidol Metabolite I	σ1	++	Antagonist	-
Haloperidol Metabolite II	σ1/σ2	+++	Irreversible antagonist	Dopamine D2 and D3 ligand
4-IBP	σ1/σ2	+++	Agonist	Dopamine D2 ligand
JO-1784 (Igmesine)	σ1	+++	Agonist	-
Metaphit	σ1/σ2	++	Irreversible antagonist	Acylator of PCP and σ2 binding sites
(+)-MR 200	σ1/σ2	+++	Antagonist	-
MS-377	σ1	+++	Antagonist	-
NE-100	σ1	+++	Antagonist	-
Panamesine (EMD 57445)	σ1/σ2?	+++?	Antagonist	One of its metabolites is a dopaminergic antagonist
(+)-3-PPP	σ1/σ2	++	Agonist	σ2 agonist; NMDA receptor ligand;

				dopaminergic agonist
PRE 084	σ1	+++	Agonist	-
Rimcazole (BW-234U)	σ1/σ2	+	Antagonist	DAT inhibitor
SA4503	σ1	+++	Agonist	-
SR 31742A	?	+++	?	High affinity for C8-C7 sterol isomerase

**Ki or KD values: +++< 50 nM; ++< 500 nM; +< 10 µM. ?: not studied or unclear at the moment. -: no other pharmacological target has been described. σ1: sigma-1 receptor, σ2: sigma-2 receptor (Table taken from Cobos et al., 2008 with slight modifications).*

While sigma-1 receptor is known to not bind most opioid drugs (as previously commented), it exhibits high to moderate affinity towards a diverse range of compounds and some of them are currenly (or have not long ago been) used in therapeutics and with diverse pharmacological uses. These include benzomorphan analgesics such as (-)-pentazocine, antipsychotics such as haloperidol, antidepressants such as fluvoxamine, antitussives such as dextromethorphan, anticonvulsants such as phenytoin, drugs to treat certain neurodegenerative disorders such as donepezil or memantine, and substances of abuse such as cocaine, among others summarized in Table 2 (Cobos et al., 2008; Su et al., 2010). Any of these drugs with known clinical use are selective for sigma-1 receptors, and although this is not to say that sigma-1 receptors do not participate in their therapeutic effects, these drugs were certaintly not intendedly developed because of their affinity for sigma receptors.

Several high-affinity and more selective sigma-1 receptor drugs have been developed and are commonly used to study sigma-1 receptor function in preclinical studies. Among these ligands, listed in table 2 as “Other sigma drugs”, can be found the sigma-1 agonist PRE-084, as well as the sigma-1 antagonists BD-1063, among many others. The development of new sigma-1 receptor ligands is increasing quickly, but so far, there are three drugs which reached clinical trials and deserve a particular attention (see Table 3). As previously commented, pridopidine has already reached phase III clinical trials. This compound is considered to be a selective sigma-1 agonist with a very low affinity for dopamine D2 and D3, adrenergic α2C and serotonin 5-HT1A receptors (Johnston et al., 2018; Grachev et al., 2021). Prodopidine has been tested in patients with Huntington’s disease (Chen et al., 2021) and amyotrophic lateral sclerosis (Jiang

et al., 2022). Blarcamesine (also known as ANAVEX2-73) is also a sigma-1 agonist although with an additional pharmacological component as it is a dual-acting compound with muscarinic antagonistic properties (Villard et al., 2011). Its intended indications are also neurodegenerative diseases which include Alzheimer's disease, Rett syndrome or Parkinson's disease (Salaciak and Pytka, 2022). Finally, the antagonist S1RA (also referred to as MR309 or E-52862) is the compound with a higher described selectivity for sigma-1 receptors, as it has been proved its selectivity on a panel of 170 targets (Romero et al., 2012). This compound has showed efficacy in reducing chemotherapy-induced neuropathic pain with a good safety and tolerability profiles in a phase IIa clinical trial (Bruna et al., 2018; Bruna and Velasco, 2018). Due to the importance of the use of S1RA for the experiments of this Doctoral Thesis, the clinical trials using this compound will be more deeply detailed in "3.10 Clinical trials with the selective sigma-1 antagonist S1RA".

Table 3. Sigma-1 receptor ligands in clinical trials with theirs intended indications.

Compound	**Subtype Selectivity**	**Affinity for σ1 Site***	**Function on σ1 Site**	**Other Activities**	**intended indications**
Pridopidine	σ1	++	Agonist	-	Huntington's disease and amyotrophic lateral sclerosis
Blarcamesine (ANAVEX2-73)	σ1	+++	Agonist	Muscarinic antagonist	Alzheimer's disease, Rett syndrome and Parkinson's disease
S1RA (also MR309 or E-52862)	σ1	+++	Antagonist	-	Neuropathic pain

**Ki values from Agha and McCurdy, 2021: +++< 50 nM; ++< 500 nM; +< 10 µM. -: no other pharmacological target has been described. σ1: sigma-1 receptor. See text for references.*

3.3 Anatomical distribution, subcellular location and chaperoning function of sigma-1 receptors

Sigma-1 receptors have been found in several very different anatomical regions, which include the heart, liver, placenta, thymus, lung, kidney, stomach, skeletal muscle, and pancreas (Aishwarya et al., 2021). However, these receptors have been mostly studied within the nervous system, and particularly in the central nervous system. Sigma-1 receptors are located in areas important for pain neurotransmission including both the spinal cord dorsal horn and supraspinal sites, such as rostroventral medulla, periaqueductal gray matter and locus coeruleus (Roh et al., 2011; Sánchez-Fernández et al., 2013; Zamanillo et al., 2013). We found more recently that the expression of sigma-1 receptor is much higher in the DRG than in any area of the central nervous system tested (Sánchez-Fernández et al., 2014). In fact sigma-1 receptors are expressed in every single peripheral sensory neuron in the mouse (Montilla-García et al., 2018; Bravo-Caparrós et al., 2020; Shin et al., 2022), and also in Schwann cells (Palacios et al., 2004). The anatomical location of sigma-1 receptors suggests that these receptors may play a crucial role in sensory neurotransmission at the peripheral nervous system.

At the subcellular level, the sigma-1 receptor is located in multiple cell membranes, including microsomal, mitochondrial, nuclear, and plasma membranes (Cobos et al., 2007). These receptor proteins are particularly enriched in the endoplasmic reticulum (ER) lipid rafts (Figure 6), where they interact with mitochondria at the mitochondria-associated ER membrane domain (MAM) (Hayashi and Su, 2007). Sigma-1 receptor is currently considered to be a chaperone protein, which interacts with several protein partners (Hayashi and Su, 2007). The interaction of sigma-1 receptors found at MAM with inositol 1,4,5-trisphosphate (IP_3) receptors results in an enhancement of Ca^{+2} signaling from the ER to the mitochondria (Sánchez-Fernández et al., 2017).

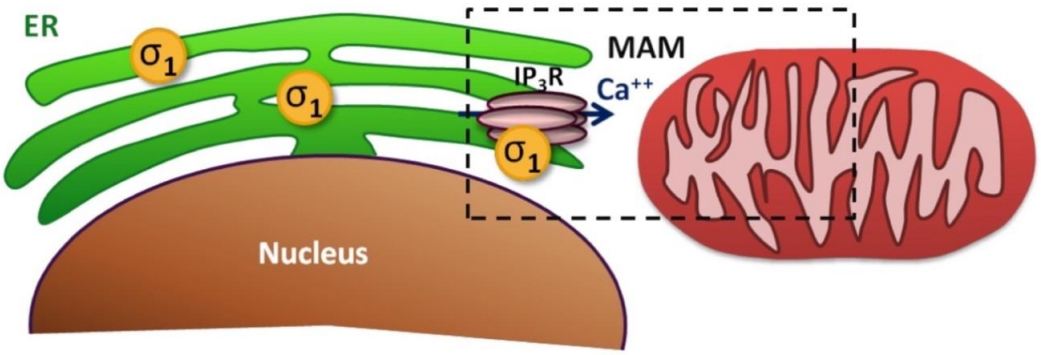

Figure 6. Subcellular location of sigma-1 receptors (σ1). σ1 are located at mitochondrion-associated endoplasmic reticulum (ER) membranes (MAM). The Ca^{2+} influx from the ER to mitochondria is potentiated by σ1 *(Figure taken from Sánchez-Fernández, 2014).*

In situations of cellular stress, sigma-1 receptors are activated and translocated to other areas of the cell, particularly to areas close to the plasma membrane and maybe to the plasma membrane itself, where they physically interact with several membrane proteins (Kourrich et al., 2012; Sánchez-Fernández et al., 2017), modifying their biological function (Su et al., 2016) (Figure 7). The interaction between sigma-1 receptor and their protein targets is Ca^{2+}-dependent (Rodríguez-Muñoz et al., 2015a), and this suggests that sigma-1 receptor act as an intracellular Ca^{2+} sensor to modulate neuronal physiology. In fact, Ca^{2+} is an endogenous molecule that triggers the activity of the sigma-1 receptor, and thus it might be the endogenous ligand that has been sought for so many years. The chaperone domain of sigma-1 receptor is located at the C-terminus (residues 112–223) and allows it to bind to several protein targets to modify their functions (Ortega-Roldán et al., 2013). Therefore, sigma-1 receptors are far from the classification of a physiological receptor, and taking into account all the characteristics commented here, it would fall into the definition of a Ca^{2+}-sensitive and ligand-operated chaperone.

The number of the discovered protein targets of the sigma-1 receptor is increasing (Figure 7). The protein targets of sigma-1 receptor are of different molecular nature, such as G-protein-coupled receptors (GPCRs) and ion channels. The GPCRs include dopamine receptors D1 and D2, serotonin receptors 1A and 2A (Rodríguez-Muñoz et al., 2015a), cannabinoid receptor 1 (Sánchez-Blázquez et al., 2014) and μ-opioid receptors (Kim et al., 2010; Rodríguez-Muñoz et al., 2015a; Rodríguez-Muñoz et al., 2015b). Among the ion channels that interact with sigma-1 receptor are transient

receptor potential (TRP) channels, such as TRPA1, TRPM8 and TRPV1 (Cortés-Montero et al., 2019; Ortíz-Rentería et al., 2018), voltage-dependent K^+ channels (Kv1.2, Kv1.3, Kv1.4 and Kv1.5) (Kourrich et al., 2012; Kourrich et al., 2013), L-type voltage-dependent Ca^{2+} channels (Tchedre et al., 2008), voltage-gated sodium channels (Nav1.5) (Balasuriya et al., 2012), acid-sensing ion channels of the 1a subtype, gamma-aminobutyric acid type A receptors (Su et al., 2010; Kourrich et al., 2012), and *N*-methyl-D-aspartate receptors (NMDARs) (Rodríguez-Muñoz et al., 2015a; Rodríguez-Muñoz et al., 2015b).

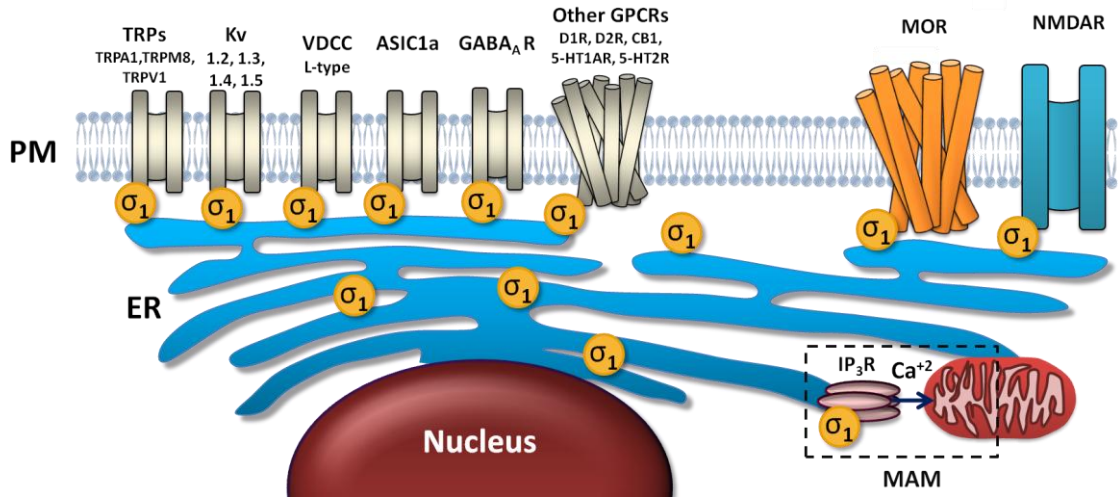

Figure 7. Sigma-1 receptors (σ1) located in the endoplasmic reticulum (ER) can modulate several receptors and channels in the plasma membrane (PM). The two best known protein targets of σ1 are the μ-opioid receptor (MOR) and the *N*-methyl-*D*-aspartate receptor (NMDAR), and they are represented at a larger scale for clarity. Other protein partners of σ1 at the PM, represented from left to right in the figure, include transient receptor potential channels (TRPs, which include TRPV1, TRPA1 and TRPM8), voltage-gated K^+ channels (Kv1.2, 1.3, 1.4, 1.5), L-type voltage-dependent calcium channels (VDCC), acid-sensing ion channels of the 1a subtype (ASIC1a), $GABA_A$ receptors ($GABA_AR$), and other G-protein-coupled receptors (GPCRs) such as dopamine (D1 and D2) receptors, cannabinoid receptor 1 (CB1R) and serotonin receptors 1A (5-HT1AR) and 2A (5-HT2AR) *(Figure taken from Sánchez-Fernández et al., 2017 with slight modifications).*

Interestingly, some of the protein targets of sigma-1 receptors have the ability to interact also between themselves, functioning in a synchronized manner. A known example is the modulation of μ-opioid receptors, which can be regulated by complex interactions involving the sigma-1 receptor and NMDAR, and one additional protein termed histidine triad nucleotide-binding protein 1 (HINT1) which is able to bind μ-opioid receptors and NMDAR (Rodríguez-Muñoz et al., 2015a; Rodríguez-Muñoz et al.,

2015b). The process of μ-opioid receptor modulation based on these interactions is summarized in Figure 8. In the resting state, the μ-opioid receptor, sigma-1 receptor, NMDAR and HINT1 form a macromolecular complex. The activation of the μ-opioid receptor by an opioid agonist leads the phosphorylation of NMDARs by the protein kinase C γ (PKCγ). This event results in the dissociation of NMDARs from the μ-opioid receptor-HINT1 complex, thereby increasing the activity of NMDARs and allowing more Ca^{2+} ions to permeate into the cytosol. The increase in intracellular Ca^{2+} levels triggers the activation of the Ca^{+2}-calmodulin (CaM) complex, which enhances the activity of calmodulin-dependent kinase II (CaMKII). CaMKII then acts on the μ-opioid receptor, reducing its activity. Moreover, the increase in Ca^{2+} levels leads to the binding of sigma-1 receptors to NMDARs, which shields them from the inhibitory effect of CaM. This results in the enhancement of NMDAR activity and subsequently a decrease in the activity of the μ-opioid receptor. However, in the presence of a sigma-1 antagonist, the sigma-1 receptor remains bound to the μ-opioid receptor and aids in the transfer of HINT1 to NMDARs. Without the protective effect of sigma-1 receptors against the binding of CaM, NMDAR activity decreases (reviewed in Rodríguez-Muñoz 2015a and b). In other words, the sigma-1 receptor is able to take place of CaM from the binding to the NMDAR, increasing its activity, and consequently decreasing μ-opioid receptor signaling. However, sigma-1 antagonism produces the opposite effect, facilitating the binding of CaM to the NMDA receptor and increasing opioid analgesia.

Functionally, as it will be more extensively described later, sigma-1 antagonism increases opioid antinociception. Interestingly, this does not only occur at central levels but it is also produced peripherally (reviewed by Sánchez-Fernández et al., 2017). It should be noted that NMDAR is mostly expressed by central neurons (Hansen et al., 2017). Therefore, there might be a peripheral counterpart of this interaction in sensory neurons where μ-opioid receptors would interact with a different cation channel. Candidates could be among TRP channels or P2X receptors, as they are mostly expressed in primary afferents (Chen et al., 1995; Levine and Alessandri-Haber, 2007). As commented earlier (see “1. Peripheral sensitizers”), these channels can be activated or sensitized by the action of several peripheral inflammatory (or neuroinflammatory) mediators, and are important for the peripheral sensitization process and hence for

chronic pain development. Importantly, there are no previous studies focused on the role of sigma-1 receptors on peripheral sensitization.

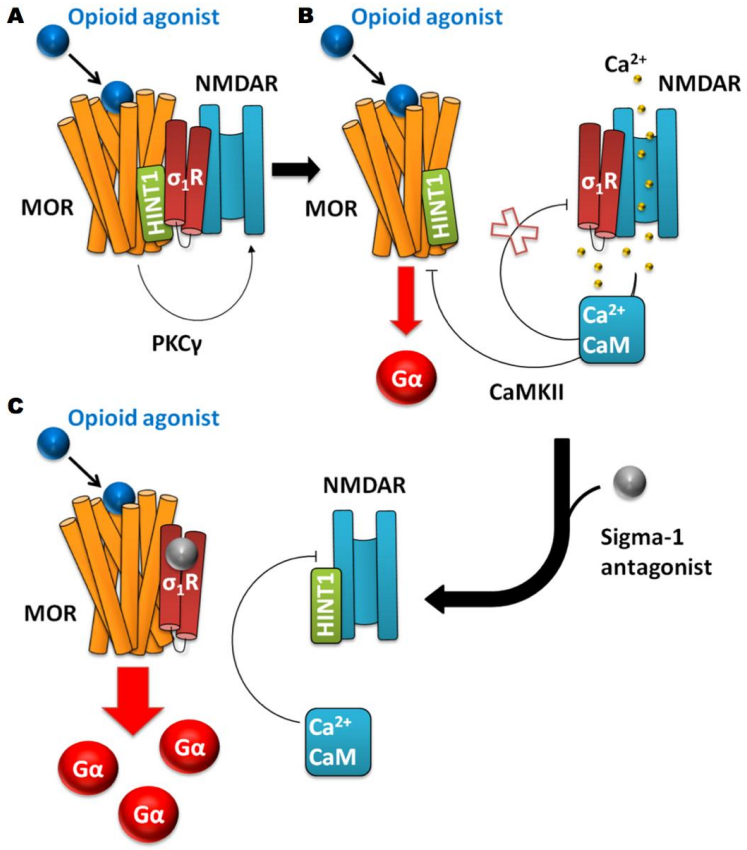

Figure 8. Schematic representation of the interaction between sigma-1 receptor (σ1R), μ-opioid receptor (MOR), NMDA receptor (NMDAR) and histidine triad nucleotide-binding protein 1 (HINT1). (A) MOR activation by an agonist leads to the activation of NMDARs through protein kinase C γ (PKCγ). (B) NMDAR activation promotes Ca^{+2} influx and facilitates the interaction of σ1R with NMDARs, which impedes the inhibitory action of Ca^{+2}-calmodulin (CaM) on NMDARs. Ca^{+2}-CaM impacts negatively on MOR signaling by the activation of calmodulin-dependent kinase II (CaMKII). (C) Sigma-1 antagonists stabilize the association of σ1R to MOR, and promote the transfer of HINT1 to NMDARs. When NMDARs do not bind σ1Rs, they increase their susceptibility to the inhibitory effect of Ca^{+2}-CaM. As result their inhibitory influence on MOR signaling is reduced *(Figure taken from Sánchez-Fernández et al., 2017)*.

3.4 Sigma-1 receptors as a one-of-a-kind type of drug target and the need for novel analgesics

As previously described, the sigma-1 receptor is a Ca^{2+}-sensing chaperone (Hayashi and Su, 2007). Currently, to the best of our knowledge there is no drug on the market, for any therapeutic indication, that directly modulates a chaperone activity. Therefore,

sigma-1 receptors are not only a novel but also a one-of-a-kind type of drug target. This peculiarity of sigma-1 receptors has attracted considerable attention from pharmacologists around the world during recent decades.

The sigma-1 receptor interactome includes many protein targets, some of them mentioned above. Once sigma-1 receptors interact with their proteins partners, they act as a regulatory subunit and have a profound impact on neurotransmission (Kourrich et al., 2012; Sánchez-Fernández et al., 2017). Taking into account the mechanism of action of these pharmacological receptors, it is not surprising that sigma-1 ligands have been proposed as therapeutic tools for the treatment of several pathologies affecting the nervous system, including depression and anxiety (Kulkarni and Dhir, 2009), memory and learning disorders (Maurice and Goguadze, 2017), and pain (Merlos et al., 2017; Sánchez-Fernández et al., 2017). In this chapter of the Introduction section, we will focus on the detailed examination of specific aspects of the role of sigma-1 receptors in pathological pain.

Approximately 20% of individuals in developed countries suffer from chronic pain (Sá et al., 2019), and this proportion rises to 30% when only the adult population is considered (Johannes et al., 2010). Therefore, it is not an exaggeration to say that millions of people suffer from chronic pain, making this issue a major public health concern (Goldberg and McGee, 2011; Pina et al., 2017). Conventional analgesics such as opioids, nonsteroidal anti-inflammatory drugs, and gabapentinoids show limited analgesic efficacy in many chronic pain conditions, or significant side effects that strongly limit their use (Yaksh et al., 2015; Phillips et al., 2017; Mathieson et al., 2020). The development of analgesics to modulate new pharmacological targets, and therefore with truly novel mechanisms of action, is rare (Kissin, 2010; Mao et al., 2011), and among the few exceptions is the selective sigma-1 antagonist S1RA. This new molecular entity is a first-in-class compound that has already shown encouraging results in preclinical studies of relevant pain models and promising results in clinical trials, as described below.

Recent years have seen intense preclinical research on the mechanisms of chronic pain. The importance of the interactions between sensory neurons and non-neuronal cells in the production and maintenance of pain has been firmly established, in

particular regarding the role of the immune cells that accumulate in an inflamed area after injury, as well as the neuroinflammatory processes that occur both in the peripheral and central nervous system in several chronic pain pathologies (Ji et al., 2018; Carroll, 2004). It is thus possible that to optimize pharmacological approaches to pain treatment, it will be necessary to modulate not only the neurotransmission processes from an exclusively neuronal perspective, but also the complex interactions between neurons and other cell types. As described here, the sigma-1 receptor plays an important role in these processes. Our aims here are to review the generalities of the chemical communication between non-neuronal cells and neurons in the generation of chronic pain, and to summarize the scientific evidence that links the actions of sigma-1 receptors with these processes.

3.5 Neuroimmune interactions in an injured peripheral tissue: the sigma-1 receptor modulates immune-driven opioid analgesia

Neuroimmune interactions in an injured (inflamed) tissue play a vital role in the induction and maintenance of pain, as previously commented (see “1. Peripheral sensitizers”). Recruitment of immune cells to the target tissue occurs shortly after peripheral tissue damage. The predominant immune cells at the inflamed site change over time in a coordinated fashion. In general terms, neutrophils are the predominant immune cells during acute inflammation, macrophages play a more relevant role in later stages, and lymphocytes increase their numbers and functions during chronification of the inflammatory process (without, however, diminishing the relevance of the actions of other immune cells) (Carroll, 2004; Ghasemlou et al., 2015; Moro-García et al., 2018). All of these immune cells produce a wide variety of pro-inflammatory cytokines, including tumor necrosis factor (TNF), IL-1β, IL-6, IL17A, as well as lipid mediators including arachidonic acid derivatives such as PGE2, 5,6-epoxyeicosatrienoic and 5-hydroxyeicosatetraenoic acid (Pinho-Ribeiro et al., 2017; Ji et al., 2014). Several of these cytokines are produced only by specific immune cell types (Pinho-Ribeiro et al., 2017). The release of these substances (along with others) plays a key role in coordinating the inflammatory response as a whole, not only in terms of the actions of immune cells, but also in terms of vascular and other processes

(Kolls et al., 2004; Tanaka et al., 2014; Yao et al., 2019; Wagner et al., 2010). In addition, immune cells, particularly macrophages, also release NGF, whose actions are important to restore the density of nerve endings in the injured area (Brown et al., 1991; Takano et al., 2017). The peripheral terminals of nociceptive neurons express receptors not only for NGF, but also for the cytokines and lipid mediators mentioned above. In response to these factors released by immune cells, nociceptors become sensitized, responding with greater intensity to sensory stimuli and promoting pain (Tejada et al., 2018; Ji et al., 2014; Pinho-Ribeiro et al., 2017). Therefore, sensory neurons act as sensors for chemicals of immune origin, and consequently as sensors for the presence of immune cells in the injured area.

It is important to note that neutrophils, macrophages or lymphocytes are known to produce endogenous opioid peptides, such as β-endorphin, enkephalins, dynorphins or endomorphins, which bind to the μ, κ and δ opioid receptors with different preferences (Tejada et al., 2018). In fact, immune cells are the main source of endogenous opioids during inflammation (Przewlocki et al., 1992; Rittner et al., 2001). However, the production of these analgesic molecules is not able to counteract the effects of the multitude of pro-algesic factors that are released during inflammation. As early as the 1st century BC, Celsus had described pain as one of the cardinal signs of inflammation. As it is well known, pain usually tends to subside with the resolution of inflammation and the consequent cessation of immune response in the affected tissue, which highlights the importance of the immune system in neuronal sensitization at the inflamed site.

Sigma-1 receptors, as noted in the section 3.3, are able to bind opioid receptors acting as a regulatory subunit. The earliest evidence for the modulation of opioid effects by sigma-1 receptors is from 1993, when Chien and Pasternak showed that haloperidol, a dopamine antagonist used clinically as an antipsychotic but which also has high affinity for sigma-1 receptors (Cobos et al., 2008), was able to greatly increase the antinociceptive effects of the μ opioid agonist morphine (Chien and Pasternak, 1993). Later studies showed that not only haloperidol, but also more selective sigma-1 antagonists such as BD-1063 or S1RA, were able to increase opioid analgesia induced by morphine and other μ-opioids in clinical use, such as oxycodone or fentanyl

(Sánchez-Fernández et al., 2013; Sánchez-Fernández et al., 2014). Sigma-1 antagonism was also shown to enhance the antinociceptive effect induced by κ agonists such as U50,488H or naloxone benzoylhydrazone, as well as the effect induced by the δ agonist [D-Pen^2, D-Pen^5] enkephalin. The multiple drug combinations of sigma-1 antagonists and opioid agonists used in these studies were reviewed previously (Sánchez-Fernández et al., 2017). Therefore, the effect initially described for the combination of haloperidol and morphine can be considered extensive to other more selective sigma-1 antagonists, as well as to other opioid drugs with different selectivity for the three main opioid receptor subtypes.

We proposed that sigma-1 antagonism could also potentiate opioid analgesia induced by endogenous opioid peptides, and not only that produced by opioid drugs. Sigma-1 antagonism produces antihyperalgesic effects during inflammation both in the rat (Parenti et al., 2014a; Parenti et al., 2014b) and in the mouse (Tejada et al., 2014; Gris et al., 2014). In a recent study we showed that when inflammatory hypersensitivity was fully established in mice, pharmacological blockade of sigma-1 receptors by BD-1063 or S1RA produced a peripherally-mediated opioid antihyperalgesic effect (reversible by the peripheral opioid antagonist naloxone methiodide) in the inflamed paw, without inducing analgesia in other areas without inflammation. This antihyperalgesic effect was dependent on the presence of immune cells (macrophages or neutrophils) in the inflamed site (Tejada et al., 2017), which (as noted above) are the main source of endogenous opioid peptides during inflammation. Therefore, the pharmacological blockade of sigma-1 receptors induces opioid analgesia selectively in the painful area, maximizing the analgesic potential of immune cells that naturally accumulate in the inflamed site. These results are summarized in Table 4. It is important to note that even though sigma-1 antagonism induces (indirect) opioid effects, this does not mean that its effects are completely equivalent to the administration of an opioid drug. In fact, sigma-1 antagonism lacks the limiting side effects that characterize opioid drugs, such as constipation, and also lacks the reinforcing properties of opioids, at least in rodents (Vidal-Torres et al., 2013; Sánchez-Fernández et al., 2013; Sánchez-Fernández et al., 2014). The latter characteristic is

particularly relevant in light of the opioid epidemic currently causing great concern in some parts of the world, particularly in the USA (Lyden and Binswanger, 2019).

It is worth to mention that up to now it has not been explored wether sigma-1 receptors are able to modulate pain hypersensitivity resulting from stimulation with specific peripheral sensitizers (i.e. in the absence of such complex inflammatory environment enriched on immune cells – and hence without the presence of endogenous opioid peptides from immune origin). Taking into account that sigma-1 receptors can bind and modulate some important pieces of the peripheral sensitization process, such as TRP channels (see section 3.3), which are known to be present in discrete neuronal populations (see section 2), it could be interesting to test the role of sigma-1 receptors on the sensitization induced by several different algogenic chemicals which would affect specific neuronal subtypes.

3.6 The role of sigma-1 receptors in peripheral neuroinflammation

Schwann cells are the most abundant glial cells in the peripheral nervous system. When a nerve is injured, Schwann cells acquire a repairing phenotype, gaining proliferation capacity and releasing several factors that stimulate the injured axons. These factors include neurotrophins such as GDNF (glial-derived neurotrophic factor), BDNF (brain-derived neurotrophic factor) and NGF, which promote growth and regeneration in the damaged axons, although they also sensitize sensory neurons and therefore promote the development of neuropathic pain (Scholz and Woolf, 2007; Wei et al., 2019). These neurotrophins are not the only pronociceptive factors produced by repair Schwann cells: these cells are also able to release ATP, which interacts with purinergic receptors in sensory axons to induce neuronal depolarization (Wei et al., 2019). Eventually, Schwann cells produce several pro-inflammatory cytokines (including TNF, IL-6 and IL-1) after nerve damage, which (as discussed in the previous section) contribute to the sensitization of peripheral sensory neurons and to the recruitment of immune cells. The macrophages, T-cells and mast cells recruited through this mechanism consequently increase the levels of pro-inflammatory cytokines to reinforce sensitization in the nociceptive axons (Scholz and Woolf, 2007;

Wei et al., 2019). Thus the action of Schwann cells plays a highly relevant role in the generation of neuropathic pain.

In intact nerves, Schwann cells strongly express sigma-1 receptors (Palacios et al., 2004; Shen et al., 2017), and their expression is maintained when the nerve is damaged and Schwann cells proliferate (Shen et al., 2017). The number of these cells increases after partial section of the sciatic nerve in rats, resulting in a local increase in the density of sigma-1 receptors at the neuroma. These reactions made it possible for the sigma-1 radioligand [^{18}F]FTC-146 to detect the site of peripheral nerve damage when it was used as a probe in positron emission tomography and magnetic resonance imaging (PET/MRI) studies (Shen et al., 2017). Sigma-1 receptors at the site of nerve damage may play an important functional role, since the administration of FTC-146 at the neuroma site was shown to reduce sensory hypersensitivity (Shen et al., 2017). However, more studies are needed to clarify whether the action of this sigma-1 ligand in neuropathic pain occurs at the Schwann cell level or at the neuronal level. It would also be interesting to determine whether the administration of sigma-1 ligands is able to alter the proliferation of Schwann cells or the immune cells that are recruited to the injured site, or to alter the levels of pronociceptive factors at the site of nerve damage.

During chronic pain, peripheral neuroinflammation also occurs at the level of the DRG, where the bodies of the peripheral sensory neurons are located. Most studies on this process have focused on the effects seen after peripheral nerve injury. Satellite cells, which surround the bodies of peripheral sensory neurons, are among the first glial cells to be activated after nerve injury. One of the factors that produces the activation of satellite cells is ATP released from the neuronal soma by the nociceptive activity induced by nerve injury (Ji et al., 2016). After nerve damage, mainly neurons but also active satellite cells produce BDNF, which contributes to both axonal regeneration and nociceptive sensitization (Zhu et al., 2012; Sikandar et al., 2018). Active satellite cells produce TNF, which, in turn, participates in the increased excitability of sensory neurons (Ji et al., 2016). In addition to the production of TNF, active satellite cells release specific proteases that cleave the chemokine fractalkine from the plasma membrane of the bodies of sensory neurons, converting it to its active soluble form (Souza et al., 2013). As previously noted in the section 1.3, fractalkine is one of the

most important signals for macrophage invasion of the DRG, along with chemokine CCL2, which is released by damaged neurons (Scholz and Woolf, 2007). Macrophages are arrayed in a characteristic distribution in the DRG, surrounding the bodies of damaged neurons, and therefore establishing very close contact with them (Vega-Avelaira et al., 2009). Macrophages release pro-inflammatory cytokines such as IL-6 (among others), which sensitize the sensory neurons with which they make contact as well as neighboring neurons. These neighboring cells, despite not being damaged by nerve injury, are sensitized by the local pro-inflammatory environment of the DRG (Scholz and Woolf, 2007). T-cells, attracted by macrophages to DRG (Raoof et al., 2018), also contribute to DRG neuroinflammation, and are of great importance in neuropathic pain development (Cobos et al., 2018). In contrast, neutrophils do not appear to be recruited to the DRG after nerve injury (Bravo-Caparrós et al., 2020), except when inflammation in the nerve is particularly prominent after injury (Scholz and Woolf, 2007).

The role of sigma-1 receptors in the DRG during neuropathic pain has been explored in recent studies. The DRG contains a much higher density of sigma-1 receptors than several central areas important in pain processing, such as the dorsal spinal cord, basolateral amygdala, periaqueductal gray, and rostroventral medulla (Sánchez-Fernández et al., 2014). Although the first study to describe the location of sigma-1 receptors in the rat DRG reported their presence in both neurons and satellite cells (Bangaru et al., 2013), later studies in mice and rats showed that sigma-1 receptors exhibited a specific neuronal distribution (Mavlyutov et al., 2016; Montilla-García et al., 2018; Bravo-Caparrós et al., 2020; Shin et al., 2020). After damage to the peripheral nerve, sigma-1 receptors of the neuronal soma from damaged neurons are activated (purportedly due to the increase in intracellular Ca^{2+} induced by the injury) and translocate from intracellular locations to areas close to the plasma membrane (Bravo-Caparrós et al., 2020, Shin et al., 2022). It is interesting to note that injured neurons with translocated sigma-1 receptors are mainly the same cells that show concentrated macrophages surrounding the neuronal body. It is thus possible that sigma-1 receptors play a relevant role in neuron–macrophage communication in this context (Bravo-Caparrós et al., 2020). In this connection, sigma-1 receptor knockout mice showed a

marked decrease in CCL2 production at the DRG, with a consequent reduction in macrophage infiltration in this peripheral nervous tissue (Bravo-Caparrós et al., 2020). The decrease in macrophages in these mutant sigma-1 receptor knockout mice was accompanied by a decrease in IL-6 content in the injured DRG (Bravo-Caparrós et al., 2020), and therefore resulted in a less pro-inflammatory environment. Sigma-1 receptor knockout mice show decreased neuropathic sensory hypersensitivity (Bravo-Caparrós et al., 2019 and 2020), as did wild-type rats in which viral vectors administered into DRG at the time of nerve injury were used to induce a sustained decrease in sigma-1 receptor expression in peripheral sensory neurons (Shin et al., 2022). It is likely that (as seen in sigma-1 knockout mice) pain amelioration was supported by the prevention of peripheral neuroinflammation in wild-type animals treated with viral vectors.

A further finding relevant to peripheral neuroinflammation is that chronic systemic treatment with S1RA, before neuroinflammation was fully established, reduced the increase in BDNF levels in the DRG during the development of experimental osteoarthritis in the knee (Carcolé et al., 2019a). Although BDNF in the DRG is produced by both sensory neurons and satellite cells (Sikandar et al., 2018), taking into account that sigma-1 receptors are apparently not present in the latter, it is likely that the decrease in the levels of this neurotrophin in response to S1RA treatment is due to direct sigma-1 receptor inhibition on peripheral neurons. However, given the intense communication between neurons and satellite cells, it cannot be ruled out that the decrease in neuronal activity induced by S1RA indirectly affects the activation of satellite cells and hence the levels of BDNF produced by these glial cells. More studies are needed to clarify this particular aspect of the effect of sigma-1 receptors on the peripheral neuroinflammatory responses.

Studies that explored the role of sigma-1 receptors in peripheral neuroinflammation are summarized in Table 4.

In summary, although additional studies are still needed to fully understand the influence of sigma-1 receptors in the activity of different types of glial and immune cells during peripheral neuroinflammation induced by chronic pain, the scientific evidence to date indicates that these receptors play a relevant role in this process.

Table 4. Summary of studies that describe the cellular location of sigma-1 receptors and their role in neuroimmune interactions and neuroinflammation in different pain models. This Table 4 does not show studies focused on the distribution of sigma-1 receptors in the absence of any disease state.

Type of pain	Pain model	Species	Sex	Tissue	Sigma-1 receptor expression	Sigma-1 ligand/KO	Route	Effect on neuroimmune interaction or neuroinflammation	Effect on pain	References
Inflammatory pain	Carrageenan i.pl.	Mouse	Female	Hindpaw	-	BD1063/ S1RA*	s.c. and i.pl.	↑ effect of endogenous opioid peptides from immune cells	↓ mechanical and heat hyperalgesia	Tejada et al., 2017
		Rat	Male	Spinal cord	-	BD-1047	i.t.	↓ D-serine y serine racemase in astrocytes	-	Choi et al., 2018b
	Zymosan i.pl.	Rat	Male	Spinal cord	Neurons	BD-1047	p.o.	↓ microgliosis ↓ IL-1β	-	Jeong et al., 2015
Peripheral neuropathic pain	Spared nerve injury	Rat	Male	Sciatic nerve	Schwann cells	FTC-146*	Injection at the neuroma site	-	↓ mechanical allodynia	Shen et al., 2017
		Mouse	Female	Dorsal root ganglion	Neurons	KO	-	↓macrophage infiltration ↓ CCL2 and IL-6	↓ cold and mechanical allodynia	Bravo-Caparrós et al., 2019 and 2020)
		Mouse	Male and female	-	-	S1RA*	s.c.	↑ effect of endogenous opioid peptides from unknown sources	↓ mechanical and heat hypersensitivity	Bravo-Caparrós et al., 2019
		Rat	Male	Dorsal root ganglion	Neurons	Inhibition of expression by viral vector	Micro-injection into the dorsal root ganglion	-	↓ mechanical, heat and cold hypersensitivity	Shin et al., 2020

(Table 4. Contd….)

Type of pain	Pain model	Species	Sex	Tissue	Sigma-1 receptor expression	Sigma-1 ligand/KO	Route	Effect on neuroimmune interaction or neuroinflammation	Effect on pain	References
Peripheral neuropathic pain	Spinal nerve ligation	Rat	Male	Dorsal root ganglion	Neurons	-	-	-	-	Bangaru et al., 2013
	Chronic constriction injury	Mouse	Male	Spinal cord	Astrocytes	BD-1047	i.t.	↓ astrocytosis	↓ mechanical allodynia	Moon et al., 2014
					Astrocytes	BD-1047	i.t.	↓ D-serine in astrocytes	↓ mechanical allodynia	Moon et al., 2015
					-	BD-1047	i.t.	Effects opposite to astrocyte activation	↓ mechanical allodynia	Choi et al., 2017
Central neuropathic pain	Spinal cord contusion	Mouse	Female	Spinal cord	-	KO		↓ TNF and IL-1β	↓ mechanical and heat hypersensitivity	Castany et al., 2018
					-	S1RA	i.p.	↓ TNF and IL-1β	↓ mechanical and heat hypersensitivity	Castany et al., 2019
	Spinal cord hemisection	Mouse	Male	Spinal cord	Astrocytes	BD-1047	i.t.	↓ astrocytosis ↓ Cx43	↓ mechanical allodynia	Choi et al., 2016

(Table 4. Contd….)

Type of pain	Pain model	Species	Sex	Tissue	Sigma-1 receptor expression	Sigma-1 ligand/KO	Route	Effect on neuroimmune interaction or neuroinflammation	Effect on pain	References
Osteoarthritis	Intra-articular monoiodoacetate	Mouse	Male	Dorsal root ganglion	-	S1RA	i.p.	↓ BDNF	↓ mechanical allodynia	Carcolé et al., 2019a
				Spinal cord	-	S1RA	i.p.	↓ microgliosis ↓ TNF and IL-1β	↓ mechanical allodynia	Carcolé et al., 2019a
				Medial prefrontal cortex	-	S1RA	i.p.	↓ microgliosis	↓ mechanical allodynia ↓ cognitive deficits ↓ depressive-like behaviors	Carcolé et al., 2019b
Cancer pain	Injection of cancer cells into the tibia	Rat	Female	Spinal cord	-	BD-1047	i.t.	↓ microgliosis ↓TNF	↓ mechanical allodynia	Zhu et al., 2015
Pain induced by chemical algogens	Formalin i.pl.	Mouse	Male	Spinal cord	Astrocytes	BD-1047	i.t.	↓ activation of astrocytic aromatase	↓ nociceptive responses	Choi et al., 2018a
	NMDA i.t.	Mouse	Male	Spinal cord	-	PRE-084	i.t.	↑ astrocyte activation	↑ nociceptive responses	Choi et al., 2017

*BDNF: brain-derived neurotrophic factor, IL: interleukin, i.pl.: intraplantar, i.t.: intrathecal, i.p.: intraperitoneal, KO: knockout, NMDA: N-methyl-D-aspartic acid, p.o.: oral administration, s.c.: subcutaneous, TNF: tumor necrosis factor. *Indicates that acute drug treatments were performed when pain behavior was fully developed.*

3.7 Role of sigma-1 receptors in central neuroinflammation

There are two glial cell types whose role is decisive in the events that take place in the spinal cord dorsal horn during chronic pain: microglia and astrocytes. Microglia are immune cells of the central nervous system equivalent to peripheral macrophages. CCL2 and ATP produced by the central terminals of peripheral sensory neurons play a key role in microglial activation (Scholz and Woolf, 2007, Ji et al., 2016). In addition, active microglia are able to cleave fractalkine from the neuronal membrane through enzymatic actions, which in turn reinforces the activity of these immune cells (Clark et al., 2014). The activation of microglia by nociceptive stimulation leads to their proliferation in the spinal cord dorsal horn, which, as in their peripheral counterparts, contributes greatly to the production of pro-inflammatory cytokines such as TNF, IL1-β and IL-6, and hence to the increased activity of central neurons to facilitate the central transmission of pain signals (Scholz and Woolf, 2007; Pinho-Ribeiro et al., 2017). Furthermore, these pro-inflammatory cytokines, together with factors released by the central terminals of peripheral sensory neurons (such as ATP), promote astrocyte activation (Ji et al., 2016).

Astrocytes constitute networks interconnected by gap junctions, which contain hemichannels formed by connexins, e.g. connexin 43 (Cx43). The union of two hemichannels, one from each astrocyte, forms a complete channel. These channels allow a rapid exchange of ions and metabolites between astrocytes that constitute the network (Xing et al., 2019). When astrocytes are activated by the signals described in the preceding paragraph, they become hypertrophic, and Cx43 moves to places other than the gap junctions between astrocytes, which allows ATP and D-serine to leak into the extracellular environment (Ji et al., 2018, Xing et al., 2019). D-serine is synthesized by an inducible racemase in the astrocyte. While ATP activates neuronal purinergic receptors, D-serine acts as a co-agonist (at the glycine-binding site) of NMDA receptors at central synapses (Xing et al., 2019). Together, the activity of microglia and astrocytes contributes to the sensitization of central nociceptive pathways. Microglia activate earlier than astrocytes during chronic pain, and therefore it is hypothesized that while microglia are particularly relevant in early stages of pathological pain, astrocytes play a more important role in its maintenance (Yan et al., 2017). However, astrocytes can be

activated in response to brief (minutes) nociceptive stimuli by enhancing aromatase activity, which produces 17β-estradiol (O'Brien et al., 2015; Choi et al., 2018a). This product has a neuroprotective effect (Azcoitia et al., 2003), although it also exerts pronociceptive actions (O'Brien et al., 2015).

While the evidence for the location of sigma-1 receptors in peripheral sensory neurons is clear, some immunohistochemical studies have shown an exclusively neuronal location of this receptor in the dorsal horn (Alonso et al., 2000; Jeong et al., 2015), while others have detected this receptor in astrocytes but not in neurons (Moon et al., 2014; Choi et al., 2016). Therefore, there is no consensus on the exact location of sigma-1 receptors in the dorsal horn. The disparate findings may be due to the specificity of the antibodies used, as well as to the different staining procedures. More studies are needed to clarify the exact location of sigma-1 receptors in the spinal cord. Although the precise location of these receptors in the dorsal horn is not clear, the results of studies aimed at determining their role in central neuroinflammation are highly consistent, as will be described below.

A decrease in microgliosis in the spinal cord dorsal horn was seen after the preemptive administration (before pain and neuroinflammation were established) of a single dose of the sigma-1 antagonist BD-1047 in a model of acute inflammation in rats (Jeong et al., 2015), and after repeated treatment with sigma-1 antagonists (BD-1047 or S1RA) in the early stages of development of chronic pain in models of osteoarthritis in mice (Carcolé et al., 2019a), and bone cancer pain in rats (Zhu et al., 2015). The decrease in microgliosis induced by sigma-1 antagonism was accompanied by a decrease in pro-inflammatory cytokines of microglial origin, such as TNF or IL-1β (Carcolé et al., 2019a; Jeong et al., 2015). In a mouse model of central neuropathic pain (spinal cord contusion), a marked decrease was seen in the levels of these pro-inflammatory cytokines in sigma-1 receptor knockout mice or in wild-type mice after S1RA treatment (Castany et al., 2018; Castany et al., 2019). In all these studies, the decrease in microglial activity or in pro-inflammatory cytokines in the dorsal horn induced by sigma-1 receptor inhibition was accompanied by a decrease in sensory hypersensitivity.

The repeated early administration of the sigma-1 receptor antagonist BD-1047 also prevented astrocytosis in the spinal cord dorsal horn in several pathological pain models. These include carrageenan inflammation in rats (Choi et al., 2018b), peripheral neuropathic pain induced by mechanical injury to the sciatic nerve in mice (Moon et al., 2014), and a mouse model of central neuropathic pain (spinal cord hemisection) (Choi et al., 2016). In addition, sigma-1 receptor inhibition decreased the expression of serine racemase, with a consequent decrease in D-serine production (Moon et al., 2015), and connexin Cx43 expression (Choi et al., 2016), which may affect the release of chemical algogens by astrocytes at central synapses. In all these studies, a decrease in sensory hypersensitivity was seen in the different pain models, indicating that the decrease in astrocyte activity by sigma-1 antagonism had functional repercussions. As noted above, D-serine acts as a co-agonist for NMDA receptors. Therefore, pain relief mediated by the inhibition of astrocyte activity by sigma-1 antagonism can be explained by a decrease in glutamatergic activity in the dorsal horn. In this connection, the intrathecal administration of the sigma-1 agonist PRE-084 was reported to increase the pronociceptive effects of NMDA, and this process was reversed by inhibitors of astrocyte activity (Choi et al., 2017); these findings support the modulation of astrocyte-mediated glutamatergic pronociceptive effects by sigma-1 receptors. Finally, as an example of the role of sigma-1 receptors in the rapid pronociceptive effects of astrocytes, it was reported that intraplantar formalin triggered increased astrocyte aromatase activity within minutes of injection, and that this process was inhibited by sigma-1 antagonism (Choi et al., 2018a).

Studies that explored the role of sigma-1 receptors in central neuroinflammation are summarized in Table 4.

It is important to note that all central processes in these chronic pain models (except those induced by direct injury to the spinal cord) are triggered by an initial peripheral nociceptive activity. As previously discussed, CCL2 from peripheral sensory neurons plays an important role in microglial recruitment, and the activity of these immune cells is in turn important for the activation of astroglia. Given that the inhibition of sigma-1 receptors reduces the production of this chemokine in the DRG (Bravo-Caparrós et al., 2020), it cannot be ruled out that at least part of the central effects of

sigma-1 receptor inhibition described in this section are influenced by peripheral sigma-1 receptors. Even studies in which sigma-1 antagonists were administered intrathecally (see Table 4) may be influenced by peripheral actions of the drugs tested, given that in this type of experimental procedure the injected solution reaches the DRG (Tan et al., 2015).

Taken together, these results suggest that sigma-1 receptors play a highly relevant role in central neuroinflammation by modulating the activity of microglia and astrocytes in the spinal cord dorsal horn.

In addition to neuroinflammation in the spinal cord, it is known that during chronic pain, microglial activity increases in supraspinal areas, both in rodents (Blaszczyk et al., 2018; Carcolé et al., 2019b) and humans (Loggia et al., 2015). Although the role of supraspinal neuroinflammation in pain is much less well studied than at the spinal cord level, it is believed to increase nociceptive transmission and pain perception (Fiore and Austin, 2016). Administration of the sigma-1 antagonist S1RA to animals with experimental osteoarthritis was reported to decrease microglial proliferation in the medial prefrontal cortex (Carcolé et al., 2019b), which is relevant for emotional processing (Gusnard et al., 2001; Etkin et al., 2011), cognitive function (Phelps et al., 2004), and the modulation of pain perception (Apkarian et al., 2005). Interestingly, sigma-1 antagonism not only decreased sensory hypersensitivity, but also improved cognitive deficits and depressive-like behaviors in these animals (Carcolé et al., 2019b). This research is summarized in Table 4. The results to date indicate that sigma-1 antagonism, possibly due to supraspinal modulation of the neuroinflammatory response, not only decreases simple reflex behaviors based on stimulus-response results indicative of sensory hypersensitivity (González-Cano et al., 2020), but is also able to alter deeper aspects of the pain experience.

3.8 Is prevention better than cure?

As described in the preceding sections, the studies showing that sigma-1 antagonism decreased peripheral and central neuroinflammation used a preemptive approach in which drug treatment was started before pain and neuroinflammation were fully

established. Moreover, in the knockout mice used in these studies, the sigma-1 gene was constitutively inactivated, and therefore sigma-1 receptors were not expressed during pain induction. When viral vectors were used to decrease sigma-1 receptor expression during neuropathic pain, they were administered at the time of the nerve injury (see Table 4 for references). However, it has been shown that repeated administration of the selective sigma-1 antagonist S1RA was also able to induce ameliorative effects when sensory hypersensitivity was fully established in models of osteoarthritis (Carcolé et al., 2019a) and neuropathic pain of different etiologies (Bura et al., 2013; Gris et al., 2016; Paniagua et al., 2017). It is thus likely that this later treatment with a sigma-1 antagonist would also be able to decrease markers of neuroinflammation, although this remains to be tested.

It is important to note that the acute systemic administration of S1RA also ameliorated sensory hypersensitivity when chronic pain was fully established in a model of osteoarthritis (Carcolé et al., 2019a) and several types of neuropathic pain (Nieto et al., 2012; Romero et al., 2012; Gris et al., 2016; Paniagua et al., 2017; Bravo-Caparrós et al., 2019, Paniagua et al., 2019). If the prevention or reversion of neuroinflammation were the only mechanism by which sigma-1 receptor inhibition decreased pain behavior in these pain models, acute sigma-1 antagonism would not be expected to produce a robust effect once neuroinflammation was fully developed. We recently reported, as summarized in Table 5, that the ameliorative effect of the acute systemic administration of S1RA on neuropathic pain was reversed by the peripheral opioid antagonist naloxone methiodide (Bravo-Caparrós et al., 2019). Considering the abundance of immune cells in the peripheral nervous system during neuropathic pain (and other types of chronic pain), and that immune cells produce endogenous opioids (Tejada et al., 2018), it seems reasonable to posit that the inhibition of sigma-1 receptors enhances immune-driven opioid analgesia during neuropathic pain, in consonance with the findings discussed in section 2 of the “Material and Methods, Results and Discussion” of this Thesis regarding inflammatory pain. In summary, it is clear that sigma-1 antagonism can be beneficial even when chronic pain states are fully developed.

3.9 Does the modulation of neuroinflammation by sigma-1 receptors differ between sexes?

Traditionally, in preclinical research and particularly in neurosciences, the use of female animals has been almost completely avoided (Beery and Zucker et al., 2011). This is particularly relevant for pain research, since a large part of chronic pain disorders are, in general terms, more prevalent in women than in men (Greenspan et al., 2007). Therefore the need to study pain processing in both sexes is clear. Furthermore, it was recently found that the role of neuroinflammation in pain may be different between animals of each sex (at least in mice). Specifically, it is thought that microglia play a more relevant role in neuropathic pain in male animals than in females, whereas T-cells play a more relevant role in females than in males (Sorge et al., 2015). Regarding the research articles reviewed here, although more studies used male than female animals (see Table 4) and no formal comparison between males and females was reported in any individual study, sigma-1 receptor inhibition appears to curtail neuroinflammatory processes in both sexes.

Some previous studies evaluated the effect of sigma-1 receptor inhibition on pain modulation in animals of both sexes. Specifically, sigma-1 receptor knockout mice of both sexes showed equivalent losses of sensitivity to capsaicin-induced mechanical allodynia (a behavioral model of central sensitization) (Entrena et al., 2009). It was further reported that there were no differences between sexes, either in mutant animals or in wild-type mice treated with S1RA, in hypersensitivity to a mechanical, heat or cold stimulus in a model of peripheral neuropathic pain (Bravo-Caparrós et al., 2019). Therefore, at present there is no evidence to suggest the existence of sex-dependent differences in pain modulation by sigma-1 receptors. It should be noted that although sexual dimorphism can be expressed as a difference in pain sensitivity, this is not always the case given that mechanistic differences between sexes have been observed despite the fact that sensitivity to the painful stimulus was identical in males and females (González-Cano et al., 2020). Therefore, it cannot be ruled out that there may be as yet unidentified parameters of sexual dimorphism in the role of sigma-1 receptors as modulators of the communication between sensory neurons and immune or glial cells.

3.10 Clinical trials with the selective sigma-1 antagonist S1RA

S1RA is a selective sigma-1 receptor antagonist developed by Esteve Pharmaceuticals S.A. in collaboration with several research groups, including our own group. As discussed in previous sections, antagonism of sigma-1 receptors by S1RA (and by other sigma-1 ligands) induces ameliorative effects on pain in animal models of inflammation, central and peripheral neuropathy, osteoarthritis, and cancer. At least some of these effects can be attributed to the potentiation of immune-driven opioid analgesia, the modulation of central and peripheral neuroinflammatory responses, or both mechanisms.

Three independent phase I clinical trials involving a total of 174 individuals showed S1RA to have a good safety profile in healthy people (Abadías et al., 2013). In addition, S1RA has been tested in a phase IIa clinical trial for the treatment of neuropathic pain induced by oxaliplatin (Bruna et al., 2018), a widely used antineoplastic which induces the development of peripheral neuropathy in a high percentage of patients (Sisignano et al., 2014). In this study, patients received preemptive treatment with S1RA, which was given during the first 5 days of each chemotherapy cycle (Bruna et al., 2018). S1RA decreased hypersensitivity to a cold stimulus, as well as the percentage of patients who experienced severe chronic neuropathy. However, although the results are undoubtedly promising, the number of participants was small (62 patients treated with S1RA) (Bruna et al., 2018). Therefore, more studies are needed to more thoroughly evaluate the analgesic potential of S1RA in oxaliplatin-induced neuropathic pain.

Preclinical studies have shown that S1RA is able to inhibit the development of peripheral neuropathy induced not only by oxaliplatin (Gris et al., 2016), but also by the antineoplastic drugs paclitaxel (Nieto et al., 2012; Nieto et al., 2014), cisplatin and vincristine (Paniagua et al., 2019). However, the modulation of neuroinflammatory processes by sigma-1 receptors in neuropathic pain induced by these antineoplastics has not been studied to date. Neuroinflammation during this particular type of neuropathy does not appear to be as robust as that produced after traumatic nerve damage, and the mechanisms appear to not be fully overlapping between the different chemotherapeutics employed. For instance, microgliosis seems to predominate in paclitaxel-induced neuropathic pain, whereas astrocytosis appears to be more relevant

in oxaliplatin-induced neuropathy (Sisignano et al., 2014). Therefore, additional studies are needed to determine the mechanism by which S1RA inhibits neuropathic pain induced by antineoplastic drugs.

A final consideration is that given the safety profile of S1RA in clinical trials, and the robust ameliorative effects of this drug in animal models of pain of different etiology, further clinical trials in patients with other types of painful disorders (in addition to chemotherapy-induced neuropathic pain) appear to be fully warranted.

Therefore, we have summarized the current scientific evidence that the inhibition of sigma-1 receptors increases the peripheral opioid analgesia induced by immune cells, and decreases peripheral and central neuroinflammation in several models of pathological pain. Although the original research reviewed here was carried out in a variety of pain models covering very specific aspects of the overall process, the findings, when taken together, support the conclusion that sigma-1 receptors play a key role in the communication between neurons and non-neuronal cells at several key steps in painful neurotransmission (see Figure 9). In light of the relevance of the interactions between sensory neurons and non-neuronal cells in chronic pain, sigma-1 antagonists may constitute a new class of analgesics with an unprecedented mechanism of action. We look forward to new preclinical and clinical studies focused on exploring the therapeutic possibilities of these intriguing receptors.

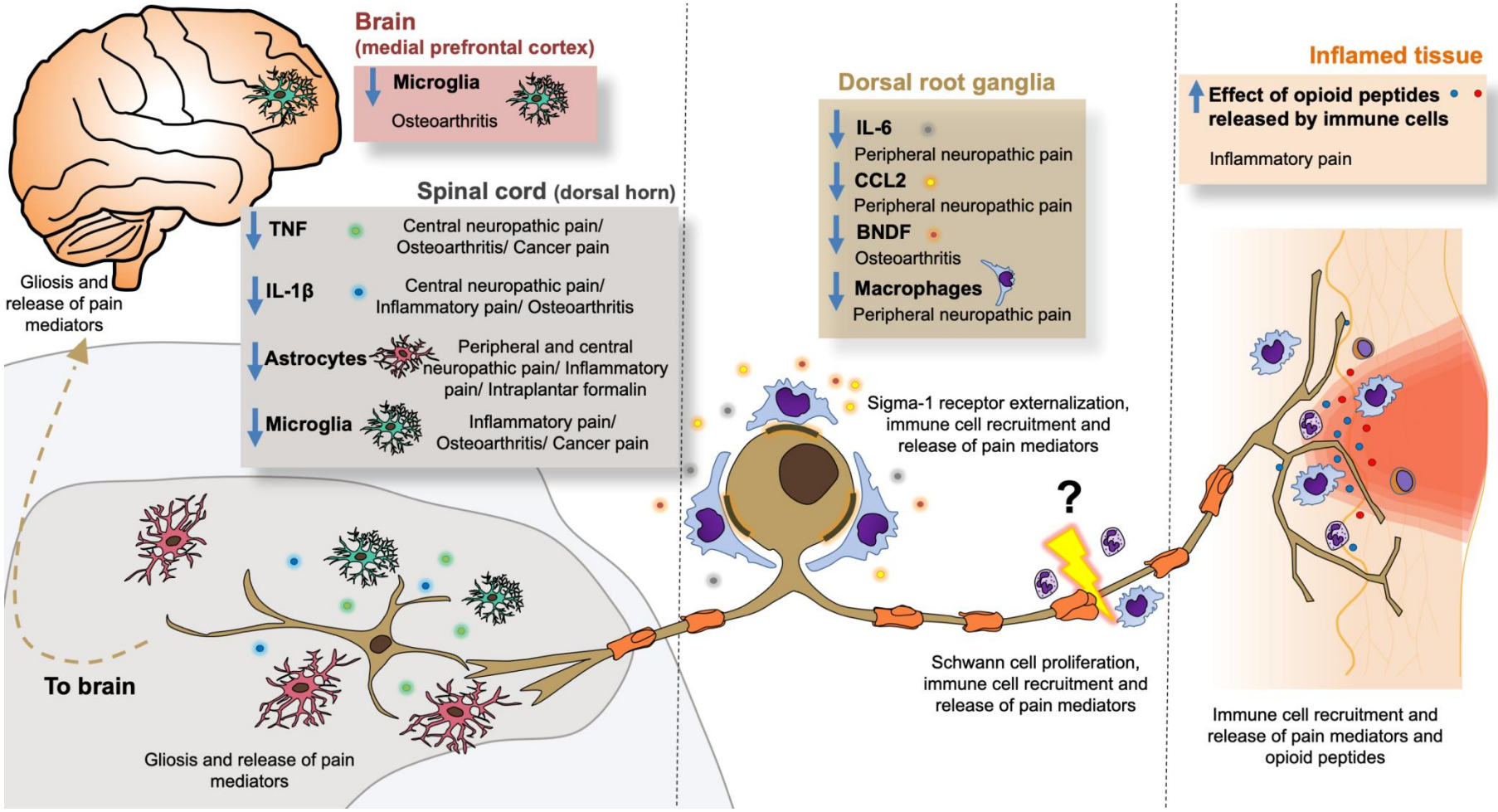

Figure 9. Effect of sigma-1 receptor inhibition on neuroimmune and neuroglial interactions in pain. Neurons and non-neuronal cells interact through chemical signals at several steps of nociceptive transmission. The colored boxes summarize the effects of sigma-1 receptor inhibition and the preclinical pain models in which they have been described. The effect of sigma-1 receptor inhibition in Schwann cells is unknown (although these cells express this receptor), and this gap in our knowledge is indicated with a question mark. See references in the text and in Table 5 for further information.

RATIONALE AND GOALS

RATIONALE AND GOALS

There is significant preclinical evidence suggesting that sigma-1 receptor plays a prominent role in pathological pain of diverse etiology. This is supported by studies which show the reduction of pain-like behaviors in sigma-1 receptor KO mice or in WT treated with sigma-1 antagonists (reviewed in Sanchez-Fernández et al., 2017; Ruiz-Cantero et al., 2021). Neuropathic pain is the primary intended indication of the selective sigma-1 receptor antagonist S1RA, which has been successfully tested in a phase IIa clinical trial on chemotherapy-induced neuropathic pain (Bruna et al., 2018), after phase I studies which demonstrated its safety and tolerability in healthy people (Abadias et al., 2013). The secondary intended indication of S1RA is the enhancement of opioid analgesia (Vela et al., 2015), as there is overwhelming preclinical evidence for the increase of the antinociceptive effect induced by several clinically relevant opioid drugs (such as morphine) by sigma-1 antagonism (reviewed in Sánchez-Fernández et al., 2017).

Although the effects of sigma-1 receptors have been classically attributed to their central actions (Merlos et al., 2017; Sánchez-Fernández et al., 2017), our research group found not long ago that peripheral sigma-1 receptors might also play an important role on pain modulation. We showed that peripheral sigma-1 antagonism is able to enhance the antinociceptive effects of opioid drugs (Sánchez-Fernández et al., 2013 and 2014), and the antihyperalgesic effects of endogenous opioid peptides from immune cells recruited to an inflamed site (Tejada et al., 2017). In addition, sigma-1 receptor inhibition is able to decrease peripheral neuroinflammation in the DRG after nerve injury (Bravo-Caparrós et al., 2020), which is an important process in neuropathic pain development (Cobos et al., 2018).

For this PhD Thesis project, we focused on advancing the knowledge of the role of sigma-1 receptors in peripheral sensitization. Immune cells do not only produce endogenous opioid peptides, as mentioned above, but they also produce (along with other cell types) a variety of algogenic chemicals which promote sensitization of the peripheral terminals of the nociceptors. However, it is unknown whether sigma-1 receptors are able to modulate sensory hypersensitivity resulting from these substances. We initially studied the potential ameliorative effects of sigma-1

antagonism on peripheral sensitization induced by local administration of several algogenic chemicals which act on different populations of nociceptors. Then, we aimed to study the reverse process, that is, the potential pronociceptive effects of sigma-1 agonists after injection of algogenic chemicals and also during inflammation produced by a surgical incision, which involves the recruitment of immune cells to the injured site and the consequent release of inflammatory mediators. Finally, and also in line with the study of the interaction between sigma-1 receptors and immune cells in pain sensitization, we compared the effect of sigma-1 inhibition (in sigma-1 receptor KO mice) in the transcriptomic changes which occur in the DRG and in the dorsal spinal cord after nerve injury, with a particular focus on the study of the impact of sigma-1 receptors on peripheral and central neuroinflammation.

The detailed rationale and specific goals of each of these parts of this PhD Thesis are described below.

1. Sigma-1 receptor curtails endogenous opioid analgesia during sensitization of TRPV1 nociceptors

The sigma-1 receptor is a ligand-operated chaperone which, in response to the increase in the intracellular Ca^{2+} concentration, physically interacts with several different receptors and channels (Su et al., 2016). N-methyl-D-aspartate receptors (NMDAR) are major protein targets of sigma-1 receptor (Sánchez-Fernández et al., 2017) and sigma-1 antagonism decreases NMDAR activity in the spinal cord to inhibit central sensitization and ameliorate neuropathic pain (Zamanillo et al., 2013). Sigma-1 receptor participates in the crosstalk between the μ-opioid receptor and NMDAR to modulate opioid analgesia at the CNS. Ca^{2+}-activated calmodulin (CaM), as summarized in Figure 8 (pag 33), is a negative regulator of NMDAR and sigma-1 receptor competes with CaM for the binding to NMDAR; therefore, the binding of sigma-1 receptor to NMDAR reduces CaM-induced NMDAR inhibition, which decreases μ-opioid receptor actions. In the presence of a sigma-1 antagonist, sigma-1 receptors dissociate from NMDAR and transfer to μ-opioid receptor, allowing CaM to bind NMDAR, and enhancing μ-opioid receptor activity (Rodríguez-Muñoz et al., 2015a and b). Modulation of μ-opioid receptor-mediated analgesia by sigma-1 receptor has been classically attributed to actions in the CNS (Mei and Pasternak, 2007); however, we

more recently reported that sigma-1 antagonism also enhances peripheral antinociception induced by opioid drugs, including not only opioid analgesics such as morphine and fentanyl, but also the peripheral μ-opioid receptor agonist loperamide, used clinically as an antidiarrheal drug (Sánchez-Fernández et al., 2013 and 2014). In fact, sigma-1 antagonism is even able to induce peripheral antihyperalgesic effects by the potentiation of endogenous opioid peptides derived from immune cells in peripheral inflamed tissue (Tejada et al., 2017).

Transient receptor potential vanilloid-1 (TRPV1) is another more recently identified protein target of sigma-1 receptors (Ortíz-Rentería et al., 2018; Cortés-Montero et al., 2019). In adult mice, TRPV1 receptors are mostly concentrated in peptidergic C-nociceptors, which can express neuropeptides such as calcitonin gene-related peptide (CGRP) or substance P (Priestley, 2009; Renthal et al., 2020), and play an important role in peripheral sensitization in response to algogenic ligands such as prostaglandin E2 (PGE2) (Moriyama et al., 2005) and nerve growth factor (NGF) (Zhang et al., 2005). Non-peptidergic C-nociceptors do not express TRPV1 but can be labelled with Isolectin B4 (IB4), and sensitized by other factors, such as glial cell line-derived neurotrophic factor (GDNF) (Alvarez et al., 2012). These peripheral sensitizers are produced in a variety of pathological pain states and play a pivotal role in pain generation (Ji et al., 2016; Kotliarova and Sidorova, 2021). Although the role of sigma-1 receptor in peripheral mechanisms of nociception are much less studied than at central levels, we reported that these receptors are expressed at a much higher density in DRG than in the dorsal spinal cord or several pain-related supraspinal areas in the mouse (Sánchez-Fernández et al., 2014). Therefore, we hypothesized that sigma-1 receptors may play a significant role in peripherally-mediated nociceptive sensitization. This hypothesis has not been tested previously.

Taken all this into account, our **first goal** was to test whether sigma-1 antagonists ameliorate the hyperalgesia induced by peripheral sensitizers of TRPV1+ and IB4+ nociceptors, and to identify the mechanisms underlying this action. As we found that the antihyperalgesic effect of sigma-1 antagonists on sensitizers of TRPV1+ nociceptors involves activation of the endogenous opioid system, we sought to determine the endogenous opioid peptide involved and its cellular source, and also tested whether

there might be crosstalk between μ-opioid receptor and TRPV1 with the participation of sigma-1 receptors, similar to the one described for NMDAR in the CNS.

2. Sigma-1 receptor agonism exacerbates immune-driven nociception: role of TRPV1+ nociceptors

Not only sigma-1 antagonists may have therapeutic utility. For instance, sigma-1 agonists have antitussive properties (Kamei, 1998). Dextromethorphan, a classic sigma-1 agonist (Cobos et al., 2008), was approved by the FDA in 1958 as an over-the-counter antitussive drug, and it is still widely used (Nguyen et al., 2016). This drug has a variety of pharmacological activities in addition to sigma-1 agonism, including NMDA antagonism (Nguyen et al., 2016), and it is believed to preferentially act centrally to suppress cough (Canning, 2009). There are other more selective sigma-1 agonists, such as PRE-084 or pridopidine (among others). PRE-084 is widely used in preclinical research as a prototypic sigma-1 agonist (Cobos et al., 2008; Motawe et al., 2020), whereas pridopidine is currently being tested in clinical trials for central neurodegenerative diseases, specifically for Huntington's disease (Chen et al., 2021) and amyotrophic lateral sclerosis (ALS) (Jiang et al., 2022).

Early studies showed that sigma-1 antagonism enhances opioid antinociception at central levels (e.g. Mei and Pasternak, 2001). Later studies found that sigma-1 antagonism decreases central sensitization to ameliorate chronic pain (Merlos et al., 2017; Sánchez-Fernández et al., 2017; Ruiz-Cantero et al., 2021). On the other hand, the systemic administration of sigma-1 agonists enhances mechanical hypersensitivity induced by capsaicin (a behavioral model of central sensitization), suggesting that sigma-1 agonism might potentiate central pain pathways after priming of the nociceptive system (Entrena et al., 2016). In agreement with this idea, it is known that the central (intrathecal) administration of sigma-1 agonists induces sensory hypersensitivity (e.g. Roh et al., 2008 and 2011). In spite of that, we reported that sigma-1 receptors are expressed at a much higher density in the DRG than in the dorsal spinal cord or several pain-related supraspinal areas in the mouse (Sánchez-Fernández et al., 2014), as pointed out above. In fact, sigma-1 receptors are located in every single peripheral sensory neuron in this animal species (Montilla-García et al., 2018; Bravo-Caparrós et al., 2020; Shin et al., 2022); however, it is unknown whether these

receptors have a similar distribution in human tissue. Therefore, our **second goal** was to study the expression of sigma-1 receptors on DRG tissue from human patients.

As stated in the previous section, peripheral TRPV1+ neurons can be sensitized by algogenic chemicals such as PGE2. This peripheral sensitizer is a major algogenic chemical robustly released during the inflammatory process, such as that produced after tissue injury (among other pain states which involve inflammation) (Buvanendran et al., 2006). PGE2 can be produced by all cell types of the body, but epithelia, fibroblasts, and infiltrating inflammatory cells represent the major sources of this compound (Kalinski, 2012). In the course of the experiments performed to meet the first goal of this Thesis (see the previous section), we found that sigma-1 antagonism decreased sensitization of TRPV1+ nociceptors. Therefore, we hypothesized that sigma-1 agonism may exacerbates nociception through TRPV1+ neurons (opposite to the sigma-1 antagonists), a hypothesis which is unexplored. Taking into account these antecedents, the **third goal** of this PhD Thesis was to test whether sigma-1 agonism enhances PGE2-induced hyperalgesia and pain during inflammation following plantar incision in mice, and to determine the involvement of TRPV1+ nociceptors and that of infiltration by immune inflammatory cells that release PGE2 on the effects observed. The relevance of this research lies in the fact that, as noted above, several drugs marketed for clinical use or currently tested in clinical trials are sigma-1 agonists and a possible side effect of these drugs might be to exacerbate pain in patients who suffer from it at the same time as the pathology for which sigma-1 agonists are indicated (e.g. cough or neurodegenerative diseases).

3. Sigma-1 receptors control peripheral neuroinflammation after nerve injury: a transcriptomic study

The previous goals of this PhD Thesis project focused on the study of the role of sigma-1 receptors in the modulation of the peripheral pronociceptive effects induced by algogenic chemicals, which can be produced by immune cells. However, the interaction of immune cells-sensory neurons is not a one-way street, as sensory neurons also reciprocally interact with immune cells and participate in their recruitment to trigger neuroinflammation, which is critically important for the development of chronic pain. It is well known that injured peripheral sensory neurons

can produce some chemokines, such as CCL2, to recruit macrophages cells into the DRG, and that T cells, attracted by macrophages to DRG (Raoof et al., 2018), also contribute to peripheral neuroinflammation (Cobos et al., 2018). This process favors an inflammatory environment, with the production of pro-inflammatory cytokines and neurotrophins, which plays a pivotal role on chronic pain development (Ji et al., 2016). Neuroinflammation is not restricted to the DRG, as during chronic pain there is a robust inflammatory response in the dorsal horn of the spinal cord, in which participates microglia and astrocytes. The factors released by the central terminals of injured neurons (e.g. ATP and CCL2) activate microglia, which are the central counterparts of peripheral macrophages. Active microglia proliferate, and similar to peripheral macrophages, contributes to the production of a pro-inflammatory environment which increase the activity of central neurons to promote pain signals (Scholz and Woolf, 2007; Pinho-Ribeiro et al., 2017). Furthermore, microglial-derived factors together with substances released by the central terminals of peripheral sensory neurons, promote astrocyte activation, which in turn increase the neurotransmission of central synapses (Ji et al., 2016).

The evidence for the role of sigma-1 receptors in neuroinflammation during chronic pain is sparsely explored, as each previously published research article covered a very specific aspect of the neuroinflammatory response and not in comparable pain models. We recently found that sigma-1 receptor KO mice showed a decrease in macrophage/monocyte infiltration into the DRG (Bravo-Caparrós et al., 2020). Other studies on peripheral neuropathic pain showed that sigma-1 receptor inhibition decreased astrocytosis in the dorsal spinal cord (Moon et al., 2014 and 2015). In addition, a decrease in spinal microgliosis by sigma-1 receptor inhibition was seen in cancer pain (Zhu et al., 2015), osteoarthritis (Carcolé et al., 2019) and during paw inflammation induced by zimosan (Jeong et al., 2015), although to our knowledge there are no previous reports exploring a possible attenuation of microgliosis during peripheral neuropathic pain by sigma-1 receptor inhibition. The study of the impact of sigma-1 receptor inhibition on the neuroinflammatory process as a whole, both at peripheral (DRG) and central (dorsal spinal cord) levels and in a single pain model,

would be useful to improve our understanding of the role of sigma-1 receptors in the pathophysiology of chronic pain with a global perspective.

In light of these antecedents, our **fourth goal** was to compare genome-wide transcriptomic changes (by RNA-Seq) after peripheral nerve injury in the DRG and the dorsal spinal cord in WT and sigma-1 receptor KO mice. We aimed to obtain a comprehensive picture of the effect of sigma-1 inhibition in all complex processes that occur at both locations in a comparable manner. As a model of nerve injury, we used the SNI (Spared Nerve Injury) model, which consists on the transection of the tibial and common peroneal branches of the sciatic nerve, and it is known to induce sensory hypersensitivity to several stimulus which is accompanied by a marked DRG and dorsal spinal cord neuroinflammation (Costigan et al., 2009; Cobos et al., 2018).

MATERIAL AND METHODS, RESULTS AND DISCUSSION

1. SIGMA-1 RECEPTOR CURTAILS ENDOGENOUS OPIOID ANALGESIA DURING SENSITIZATION OF TRPV1 NOCICEPTORS

1.1 Material and methods

1.1.1 Experimental animals

Most experiments were done in female CD-1 mice (Charles River, Barcelona, Spain), weighing 25-30 g. Animals were housed in colony cages (10 mice per cage), in a temperature-controlled room (22 ± 2 °C) with an automatic 12-h light/dark cycle (08:00–20:00 h). An igloo and a plastic tunnel were placed in each housing cage for environmental enrichment. Some experiments were performed on male mice from the same strain. It is known that male mice are more aggressive to other mice than female animals (Edwards, 1968), and that the stress induced by fights with the alpha male can induce opioid analgesia (Miczek et al., 1982). We considered that this behaviour of male mice might be a confounder in our experiments in the context on the modulation of endogenous opioid analgesia by sigma-1 receptors. Therefore, we performed most experiments in female animals. However, we also tested male mice in some key experiments (see the Results section) to explore a possible sexual dimorphism in sigma-1-mediated modulation of hyperalgesia induced by peripheral sensitizers. Animals were fed a standard laboratory diet and tap water ad libitum until the beginning of the experiments. The behavioural experiments were done during the light phase (from 9:00 a.m. to 3:00 p.m.). The mice were randomized to treatment groups, testing each day a balanced number of animals from several experimental groups, and female mice were also tested randomly throughout the estrous cycle. Mice were handled in accordance with international standards (European Communities Council directive 2010/63), and the experimental protocols were approved by regional (Junta de Andalucía) and Institutional (Research Ethics Committee of the University of Granada) authorities. To decrease the number of animals in this study, we used the same mice for behavioural studies, FACS analysis and immunostaining, when possible. Animal studies are reported in compliance with the ARRIVE guidelines and with the recommendations made by the British Journal of Pharmacology (Lilley et al., 2020).

1.1.2 Peripheral sensitizers, drugs and *in vivo* antibodies

The peripheral sensitizers, PGE2, NGF and GDNF, were injected intraplantarly (i.pl.) into the right hind paw in a volume of 20 µL, using a 1710 TLL Hamilton microsyringe (Teknokroma, Barcelona, Spain) with a 301/2-gauge needle. PGE2 (Tocris Cookson Ltd., Bristol, United Kingdom) and NGF (Sigma-Aldrich, Madrid, Spain) were dissolved in sterile physiological saline (0.9% NaCl), and GDNF (Preprotech, London, United Kingdom) was dissolved in 0.1% bovine serum albumin (Sigma-Aldrich) in sterile physiological saline. Stock PGE2, NGF or GDNF solutions were stored at -20 ºC and further dilutions were performed to obtain the appropriate final concentrations for the different experiments, right before administration. PGE2 (0.5 nmol), NGF (1 µg) and GDNF (40 ng) were i.pl. injected at 10 min, 3 hours and 20 min before the behavioural evaluation, respectively. These doses and times after administration were selected from their dose-response effects and time-courses (Figure 1A-F).

We used three sigma-1 receptor ligands: S1RA (E-52862.HCl; 4-[2-[[5-methyl-1-(2-naphthalenyl)-1H-pyrazol-3-yl]oxy]ethyl] morpholine) (DC Chemicals, Shanghai, China) and BD-1063 (1-[2-(3,4-dichlorophenyl)ethyl]-4-methylpiperazine dihydrochloride) (Tocris Cookson Ltd.) were used as two selective sigma-1 antagonists, and PRE-084 (2-[4-morpholinethyl]1-phenylcyclohexanecarboxylate hydrochloride) (Tocris Cookson Ltd.) was used as a selective sigma-1 agonist (Cobos et al., 2008). In addition, we used several opioid receptor ligands. These include the prototypic µ-opioid agonist morphine hydrochloride (General Directorate of Pharmacy and Drugs, Spanish Ministry of Health), the centrally-penetrant opioid antagonist naloxone hydrochloride and its quaternary derivative naloxone methiodide (both from Sigma-Aldrich), which was used as a peripherally restricted opioid antagonist. Finally, the µ antagonist cyprodime, the κ antagonist nor-binaltorphimine and the δ antagonist naltrindole (all from Tocris Cookson Ltd.) were used as selective antagonists for the three major opioid receptor subtypes. All drugs were dissolved in sterile physiological saline. To study the effect of systemic treatments, drugs were injected subcutaneously (s.c.) into the interscapular zone in a volume of 5 mL kg-1. When the effect of the association of two drugs was tested, each drug was injected into a different area of the interscapular zone. To test for the effects of local treatments, drugs or their solvents were administered i.pl. in a

volume of 20 µL. The sigma-1 antagonists or morphine were administered 30 min before the behavioural evaluation. The sigma-1 agonist PRE-084 or the opioid antagonists were injected 5 min before the sigma-1 antagonists or morphine (35 min before the behavioural evaluation).

The dose of PRE-084 used (32 mg kg-1, s.c.), was selected based on our previous studies (Entrena et al., 2009; Montilla-García et al., 2018; Bravo-Caparrós et al., 2019), as well as the doses of naloxone (1 mg kg-1, s.c.) and naloxone methiodide (2 mg kg-1, s.c.) (Sánchez-Fernández et al., 2014; Tejada et al., 2017; Montilla-García et al., 2018). The doses of cyprodime (10-15 mg kg-1, s.c.) used to reverse the effects of the sigma-1 antagonists were selected based on the reversion of the antihyperalgesic effect of the prototypic µ opioid agonist morphine (see "Results" for details), and are in a range similar to the ones used in previous studies (Hutcheson et al., 1999). Nor-binaltorphimine (10 mg kg-1, s.c.) and naltrindole (5 mg kg-1, s.c.) have been repeatedly reported to reverse opioid effects at the same doses used in our study or lower (Hutcheson et al., 1999; Baamonde et al., 2005).

To block the effects of the endogenous opioid peptides (EOPs), 20 µL of a solution containing 3-E7 monoclonal antibody (MAB5276, Millipore), which recognizes the pan-opioid sequence Tyr–Gly–Gly–Phe at the N-terminus of most EOPs (Rittner et al., 2001) was administered i.pl. at a dose of 1 µg. The i.pl. administration of this antibody has been previously shown to abolish the effects of sigma-1 antagonism on carrageenan-induced hyperalgesia (Tejada et al., 2017). As other EOPs, such as endomorphin-2 (END2) (Alexander et al., 2021), lack of this consensus sequence we used the i.pl. administration (1 µg) of an specific antibody (G-044-11, Phoenix Pharmaceuticals) to block its effects *in vivo*. When these antibodies and the sigma-1 antagonists were associated i.pl., they were dissolved in the same solution and injected together to avoid paw lesions due to multiple injections in the same paw.

1.1.3 *In vivo* ablation of TRPV1-expressing nociceptors

We used resiniferatoxin (RTX, Tocris Cookson Ltd) as a "molecular scalpel" to selectively ablate TRPV1-expressing neurons. RTX was dissolved in vehicle (10% Tween

80 and 10% ethanol in physiological saline). Animals received two doses of RTX via i.p., two consecutive days (25 µg kg-1 each dose). This total dose (50 µg kg-1) has been previously reported to ablate all peripheral TRPV1+ neurons (Hsieh et al., 2008; Montilla-García et al., 2017 and 2018; González-Cano et al., 2020), but we divided it in two doses to minimize distress. The control group received a double injection with an equal volume of vehicle. To minimize suffering, all procedures were done under isoflurane anesthesia in oxygen (IsoVet®, B. Braun, Barcelona, Spain). The initial isoflurane dose was 4% for the induction of general anesthesia, during 5 min. Then, RTX (or its solvent) was injected and anesthesia was maintained during 10 min with isoflurane 2%. The efficacy of the treatment was determined by immunohistochemical assays of L4 DRG (see "Results" for details). Animals were placed in their home cages for 5 days after the first i.p. injection before behavioral testing and sample collection.

1.1.4 Assessment of hyperalgesia

The animals were placed in the experimental room for a 1 h acclimation period before starting the experiments. For the assessment of either mechanical or thermal hyperalgesia, the mice were gently pincer grasped between the thumb and index fingers by the skin above the interscapular area, and submitted to the sensory stimulation. All mice were used in only one experimental procedure (mechanical or thermal stimulation). The experimenters who evaluated the behavioural responses were blinded to the treatment group of each experimental animal.

Mechanical hypersensitivity was assessed with the paw pressure test following a previously described protocol (Menéndez et al., 2005; Tejada et al., 2017) with slight modifications. After the appropriate time after drug administration, mechanical stimulation was applied to the right hindpaw with an Analgesimeter (Model 37215, Ugo-Basile, Varese, Italy). A blunt cone-shaped paw-presser was applied at a constant intensity of 100 g to the dorsal surface of the hindpaw until the animal showed a struggle response. The struggle latency was measured with a chronometer. The test was done three times with a 1-min interval between stimulations, and the mean value of the three trials was recorded as the animal's struggle latency.

Thermal hypersensitivity was assessed with the unilateral hot plate test following a previously described protocol (Menéndez et al., 2002; Montilla-García et al., 2018), with slight modifications. After the appropriate time after drug administration, the plantar side of the stimulated hindpaw was placed on the surface of a thermal analgesimeter (Model PE34, Series 8, IITC Life Science Inc., Los Angeles, USA) previously set at 42 ± 1 ºC until the animal showed a paw withdrawal response. The latency in seconds from paw stimulation to the behavioural response was measured with a digital chronometer. The test was done three times with a 1-min interval between stimulations, and the mean value of the three trials was recorded as the animal's paw withdrawal latency. Only a clear unilateral withdrawal of the paw was recorded as response. We avoided simultaneous heat stimulation in both hind paws by placing the plantar side of the tested hind paw on the hot plate while the other hind paw was placed on filter paper (off the hot plate) during observations (see Supplementary Video 2 in (Montilla-García et al., 2018)).

1.1.5 Immunohistochemistry

Mice were anesthetized with 4% isoflurane (in oxygen) and perfused transcardially with 0.9% saline solution followed by 4% paraformaldehyde (Sigma-Aldrich). The L4 DRGs were dissected and post-fixed for 1 h in the same paraformaldehyde solution. Embedding procedure differed depending on the staining to be performed, as not all antibodies used showed optimal results in all embedding media. Samples for sigma-1 receptor or CGRP immunostaining were dehydrated and embedded in paraffin. Tissue sections 5 µm thick were cut with a sliding microtome, mounted on microscope slides (Sigma-Aldrich), deparaffinized in xylol (Panreac Quimica, Castellar del Vàlles, Spain) and rehydrated before antigen retrieval (steam heating for 22 min with 1% citrate buffer, pH 8). Samples for END2 staining were incubated for 48 h in 30% sucrose (Sigma-Aldrich) at 4ºC to be embedded in O.C.T Tissue-Tek medium (Sakura Finetek, Barcelona, Spain), and frozen and stored at -80º C until their immunohistochemical study. Sections of DRG 15 µm thick were cut with a cryostat and thaw-mounted onto Superfrost Plus microscope slides (Thermo Fisher Scientific).

Tissue sections were incubated for 1 h in blocking solution with 5% normal goat or donkey serum, depending on the experiment, 0.3% Triton X-100, and 0.1% Tween 20 in Tris buffer solution. Then, the slides were incubated with the primary antibodies in blocking solution. The primary antibodies used were: mouse anti-sigma-1 receptor (1:200, sc-137075, Santa Cruz Biotechnology), rabbit anti-PGP9.5 (1:400, AB1761, Millipore), rabbit anti-CGRP (1:800, T-4032, BMA Biomedicals), goat anti-TRPV1 (1:100, sc-12498, Santa Cruz Biotechnology), and rabbit anti-END2 (15 µg mL-1, G-044-11, Phoenix Pharmaceuticals). Incubation with the primary antibodies for sigma-1 receptor, PGP9.5, CGRP and TRPV1 lasted for 1 h at room temperature (RT), whereas incubation with the primary antibody for END2 lasted overnight at 4°C. When stainings for END2 were performed, sections were incubated with the anti-END2 antibody overnight, and the next day, after washing three times for 10 min, the samples were incubated with the anti-TRPV1 antibody for 1 h. After incubation with the primary antibodies, sections were washed again three times for 10 min and incubated with the appropriate secondary antibodies: Alexa Fluor-488 goat anti-mouse (A-11029, Thermo Fisher Scientific), Alexa Fluor-594 goat anti-rabbit (A-11012, Thermo Fisher Scientific), Alexa Fluor-647 donkey anti-mouse (A-31571, Thermo Fisher Scientific), Alexa Fluor-488 donkey anti-mouse (A-21202, Thermo Fisher Scientific), Alexa Fluor-488 donkey anti-goat (A11055) or Alexa Fluor-647 donkey anti-rabbit (A-31573, Thermo Fisher Scientific) (all 1:500). We also stained tissue sections with Bandeiraea simplicifolia lectin I, isolectin B4 (IB4) conjugated with Dylight-594 (1:100, DL-1207, Vector Laboratories). Finally, slides were washed three times for 10 min before the mounting procedure and they were coverslipped with ProLong Gold Antifade mounting medium (Thermo Fisher Scientific). Images were acquired with a confocal laser-scanning microscope (Model A1, Nikon Instruments Europe BV, Amsterdam, Netherlands).

To illustrate the overlap between different markers, we performed Venn diagrams. To construct these diagrams, an experimenter blinded to the treatments counted the neurons stained in 4 DRG slices per animal. There was a minimum separation between slices of 15 µm. The values from 5 different animals were averaged to construct the Venn diagrams.

The immunohistochemistry procedures used in the present study comply with the recommendations made by the British Journal of Pharmacology (Alexander et al., 2018).

1.1.6 Fluorescence-activated cell sorting (FACS) analysis

We used plantar tissue from mice i.pl. injected with 20 µL of a solution containing PGE2 (0.5 nmol), GDNF (40 ng) or NGF (1 µg). Samples were collected at 10 min, 20 min and 3 hours after the injection of PGE2, GDNF or NGF, respectively. As a positive control for neurotrophil recruitment, we used samples from mice i.pl. treated with λ-carrageenan (50 µL, 1% wt vol-1 in saline; Sigma-Aldrich) 3 hours before sample collection (Tejada et al., 2017). Mice were killed by cervical dislocation and plantar tissue was dissected and digested with collagenase IV (1 mg mL-1, LS004188, Worthington, Lakewood, NJ, USA) and DNAse I (0.1%, LS002007, Worthington) for 1 h at 37°C with agitation. Samples were filtered (pore size 70 µm) and the rat anti-CD32/16 antibody (1:100, 20 min, 553141; Biolegend, San Diego, CA) was used to block Fc-γRII (CD32) and Fc-γRIII (CD16) binding to IgG. Cells were incubated with antibodies recognizing the hematopoietic cell marker CD45 (1:200, 103108, clone 30-F11, BiolegendBioLegend), the myeloid marker CD11b (1:100, 101227, BioLegend), and the neutrophil-specific marker Ly6G (1:100, 127617, BioLegend), together with a viability dye (1:1000, 65-0865-14; Thermo Fisher Scientific), for 30 min on ice. The population of neutrophils (CD45+ CD11b+ Ly6G+ cells) was determined in cells labelled with the viability dye. Before and after incubation with the antibodies, the cells were washed three times in 2% fetal bovine serum (FBS)/PBS (FACS buffer). Cells were fixed with 2% paraformaldehyde for 20 min, and on the next day samples were assayed with a BD FACSCanto II flow cytometer (BD Biosciences, San Jose, CA, USA). Compensation beads were used as compensation controls, and fluorescence minus one (FMO) controls were included to determine the level of nonspecific staining and autofluorescence associated with different cell subsets. All data were analyzed with FlowJo 2.0 software (Treestar, Ashland, OR, USA).

1.1.7 Recombinant protein expression

The coding region of the full-length murine sigma-1 receptor (AF004927) and the C-terminal (Ct) regions of μ-opioid receptor (AB047546: residues 286-398) and TRPV1 (NP_542437; residues 680–839) were amplified by reverse transcription polymerase chain reaction (RT-PCR) using total RNA isolated from the mouse brain as the template.

Specific primers containing an upstream Sgf I restriction site and a downstream Pme I restriction site were used, as described previously (Rodríguez-Muñoz et al., 2015b). The PCR products were cloned downstream of the glutathione S-transferase (GST)/HaloTag® coding sequence (Flexi® Vector, Promega, Spain) and the tobacco etch virus (TEV) protease site, and when sequenced, the proteins were identical to the GenBank™ sequences. The vector was introduced into the Escherichia coli BL21 (KRX L3002, Promega), and clones were selected on solid medium containing ampicillin. After 3 h of induction at RT, in the presence of 1 mM isopropyl β-D-1-thiogalactopyranoside (IPTG) and 0.1% Rhamnose, the cells were collected by centrifugation and maintained at −80 °C. The fusion proteins were purified under native conditions on GStrap FF columns (17-5130-01; GE Healthcare, Spain) or with HaloLink Resin (G1915; Promega). When necessary, the fusion proteins retained were cleaved on the column with ProTEV protease (V605A; Promega) and further purification was achieved by high-resolution ion exchange (780-0001Enrich Q; BioRad, Spain). Sequences were confirmed by automated capillary sequencing. Recombinant calmodulin (CaM, 208694) was purchased at Merck Millipore (Spain).

1.1.8 *In vitro* interactions between recombinant proteins: pull-down of recombinant proteins and the effect of drugs on sigma-1 receptor/TRPV1/μ-opioid receptor Ct interactions

Having demonstrated that the sigma-1 receptor do not bind to GST (Z02039; GenScript Co., USA) (Cortés-Montero et al., 2019), we assessed the association of GST-free sigma-1 receptors with the GST-tagged TRPV1 Ct or μ-opioid receptor Ct sequences. The C-terminal domains of TRPV1 (100 nM) and μ-opioid receptor (200 nM) were immobilized through covalent attachment to N-Hydroxysuccinimide (NHS)-activated

Sepharose 4 fast flow (4FF, 17-0906-01; GE) according to the manufacturer's instructions. Recombinant sigma-1 receptor (200 nM) was then incubated with either NHS-blocked Sepharose 4FF (negative control) or with the immobilized TRPV1/μ-opioid receptor sequence in 200 μL of a buffer containing 50 mM Tris–HCl (pH 7.5), 0.2 % 3-[(3-cholamidopropyl) dimethylammonio]-1-propanesulfonate (CHAPS) and 3 mM CaCl2. The samples were mixed by rotation for 30 min at RT, and the sigma-1 receptors bound to TRPV1/μ-opioid receptor-Sepharose 4FF were recovered by centrifugation and washed three times. To study whether the drugs used provoked changes in the TRPV1/μ-opioid receptor-sigma-1 receptor association, the agarose-attached TRPV1–sigma-1 receptor complexes were incubated for a further 30 min at RT with rotation in the presence of the drugs and with or without the other receptor (μ-opioid receptor or TRPV1) in a final reaction volume of 300 μL of 50 mM Tris–HCl (pH 7.5), 3 mM CaCl2 and 0.2 % CHAPS. In some experiments, we added CaM (200 nM) after the incubation of TRPV1–sigma-1 receptor complexes with the drugs and the respective washes and the mix were incubated for a further 30 min at RT with rotation. Agarose pellets containing the bound proteins were obtained by centrifugation, and they were washed thrice in the presence of 3 mM CaCl2 and then solubilized in 2× Laemmli buffer, analyzing the sigma-1 receptor/CaM content in Western blots. The compounds studied were S1RA and BD1063 (10 nM) and were dissolved in aqueous solution.

The sigma-1 receptor/CaM bound to the Sepharose-TRPV1/μ-opioid receptor sequences were resolved with Sodium dodecyl sulfate–polyacrylamide gel electrophoresis (SDS-PAGE) in 4–12% Bis–Tris gels (NP0341; Invitrogen, Fisher Scientific, Spain), with 2-(N-morpholino) ethanesulfonic acid SDS (MES SDS) as the running buffer (NP0002; Invitrogen). The proteins were transferred onto 0.2 μm Polyvinylidene difluoride (PVDF) membranes (162-0176; BioRad) and probed overnight at 6°C with primary antibodies diluted in Tris-buffered saline (pH 7.7) (TBS) + 0.05% Tween 20 (TTBS): anti-sigma-1 receptor (42-3300, Thermo Fisher Scientific), anti-CaM (05-173, Millipore). All primary antibodies were detected using the appropriate horseradish-peroxidase-conjugated secondary antibodies.

The blot areas containing the corresponding sizes of the cloned target proteins were selected for image capture and analysis. The Western blot images were visualized by

chemiluminescence (170-5061; BioRad) and recorded on an ImageQuant™ LAS 500 (GE). For each blot, the area containing the target cloned protein was typically selected. The device automatically captures the selected area and the associated software automatically calculated the optimal exposure time to provide the strongest possible signal from which the rest of the signals could be accurately quantified. For each group of immunosignals derived from the same cloned protein, the area of the strongest signal was used to determine the average optical density of the pixels within the object area mm-2 of all the signals (AlphaEase FC software). The gray values of the means were then normalized within the 8 bit/256 gray levels [(256 − computed value)/computed value].

The Western blotting procedures used in the present study comply with the recommendations made by the British Journal of Pharmacology (Alexander et al., 2018).

1.1.9 Calcium imaging

Thoracic and lumbar DRGs were dissected and transferred into 10% FBS and 1% penicillin–streptomycin supplemented DMEM 1x (10-013-CV; Thermo Fisher Scientific) at 4ºC. DRGs were then digested in 5 mg mL-1 collagenase and 1mg mL-1 Dispase II (Roche, Indianapolis, IN) and then triturated using fire-polished glass Pasteur pipettes of decreasing sizes in the presence of DNAse I inhibitor (50 U) using standard procedures (Wainger et al., 2015). Cells were centrifuged through 10% BSA (Sigma-Aldrich) and resuspended in 1 mL Neurobasal (Sigma-Aldrich) containing B27 supplement (Invitrogen), penicillin and streptomycin, 2 ng mL-1 GDNF, 10 µM arabinocytidine (all from Sigma-Aldrich). Cells were plated on poly-D-lysine (500 ug mL-1) and laminin (5 mg mL-1) coated 35 mm tissue culture dishes at 5000–8000 per dish, 5% carbon dioxide, at 37°C.

After 48 h, neurons were incubated for 50 min with 4 µg mL-1 Fura2-AM (Invitrogen) at RT. Cell were washed out with standard extracellular solution (SES) (Boston BioProducts) and images were acquired on a Nikon Eclipse Ti microscope (Nikon,

Melville, NY) with standard 340- and 380-nm filters controlled by a Ludl Mac6000 shutter using Nikon Elements software. Images were taken every 3 s.

Cells were incubated in SES for 2 min. Then, a first exposure to a low concentration (0.05 µM) of the TRPV1 agonist capsaicin was made for 30 s. Cells were incubated with PGE2 (10 µM) for 7.5 min (from 11:30 to 19:00 min), and submitted to a second application of the same low concentration of capsaicin (0.05 µM) at the end of PGE2 incubation (from 18:30 to 19:00 min). When the effects of S1RA (10 µM) were tested, it was added to the solution 3 minutes before PGE2 application, and remained in the medium for the whole duration of PGE2 incubation (from 8:30 to 19:00 min). This concentration of S1RA is approximately the same than the plasma concentration of neuropathic patients treated with the sigma-1 receptor antagonist (Abadias et al., 2013; Bruna et al., 2018). In the experiments where naloxone (1 µM) was used to reverse the effect of S1RA, the opioid antagonist was added to the medium 1 min before S1RA application (from 7:30 to 19:00 min). A high concentration of capsaicin (1 µM) was applied at 24 min for 30 s, to determine all capsaicin-sensitive neurons. Finally cells were exposed to KCl (80 mM) for 10 sec at 29:30 min, as a positive control to determine the total number of viable neurons at the end of the experiment. After the application of each compound, cells were washed appropriately.

PGE2-induced sensitization was defined as the increase in F340/380 obtained with the low dose of capsacin during the application of PGE2 minus the value obtained in the first application of capsaicin. We selected plates with at least 6 neurons which responded to both capsaicin (1 µM) and KCl and had a stable signal during the total exposure time.

1.1.10 Data and Statistical Analysis

Studies were designed to generate groups of equal size. Statistical analysis was undertaken only for studies where each group size was at least n=5. Most statistical analysis was carried out with one-way analysis of variance (ANOVA), followed by a Bonferroni post-hoc test. We examined whether data were normally distributed (Shapiro-Wilk test) and the homogeneity of variances (Brown-Forsythe test) before the

ANOVA was performed. The post-hoc test was run only if F achieved the necessary level of statistical significance ($P < 0.05$) and data fulfilled the assumptions of the ANOVA. In some experiments, the original data were log-transformed to meet the ANOVA assumptions. Results from Western blot assays were analyzed using a Kruskal–Wallis test, which is suitable for nonparametric data, followed by a Student–Newman–Keuls post-hoc test. The signals from the Western blot were expressed as the change relative to the assay-matched controls, which were assigned an arbitrary value of 1. Statistical analyses were performed with the SigmaPlot 14.5 program. The differences between values were considered significant when the P value was below 0.05. Sample sizes for experiments were estimated based on our previous studies (Wainger et al., 2015; Tejada et al., 2017; Cortés-Montero et al., 2019). The declared group size is the number of independent values, and that statistical analysis was done using these independent values. The data and statistical analysis comply with the recommendations on experimental design and analysis in pharmacology (Curtis et al., 2022).

1.2 Results

1.2.1 Involvement of TRPV1+ nociceptors in the hyperalgesia induced by PGE2, NGF and GDNF

We first studied the distribution of several neuronal markers in the DRG from intact female mice. Specifically, we stained for sigma-1 receptor, CGRP, TRPV1, and IB4. sigma-1 receptor stained numerous cells with neuronal morphology (Figure 2A); in fact, the double labelling of sigma-1 receptor with the pan-neuronal marker PGP9.5 showed that sigma-1 receptors were present in most, if not all, DRG neurons (PGP9.5+ cells) (Figure 3). CGRP+ cells accounted for 28% of sigma-1 receptor+-neurons (Figure 2A and B). Double labelling of CGRP and TRPV1 showed that both neuronal populations markedly overlap, as most CGRP+ neurons express TRPV1, and most TRPV1+ neurons express this neuropeptide (Figure 2C and D). On the other hand, staining for TRPV1 and IB4 showed minimal overlap among DRG neurons, and each

population constituted about one-third of sigma-1 receptor+ cells (see top panels of Figure 4A for representative images, and Figure 4B). Treatment with RTX virtually abolished TRPV1 labelling, but IB4 staining was still readily detectable (Figure 4A, bottom panels). In fact, the proportion of IB4+ neurons over the remaining sigma-1 receptor+ cells was even increased, since when TRPV1+ population is ablated, the remaining IB4 neurons represent a higher percentage considering the surviving neurons as the 100% (compare Figure 4B and C). These results confirm the specificity of the ablation of TRPV1+ neurons by RTX.

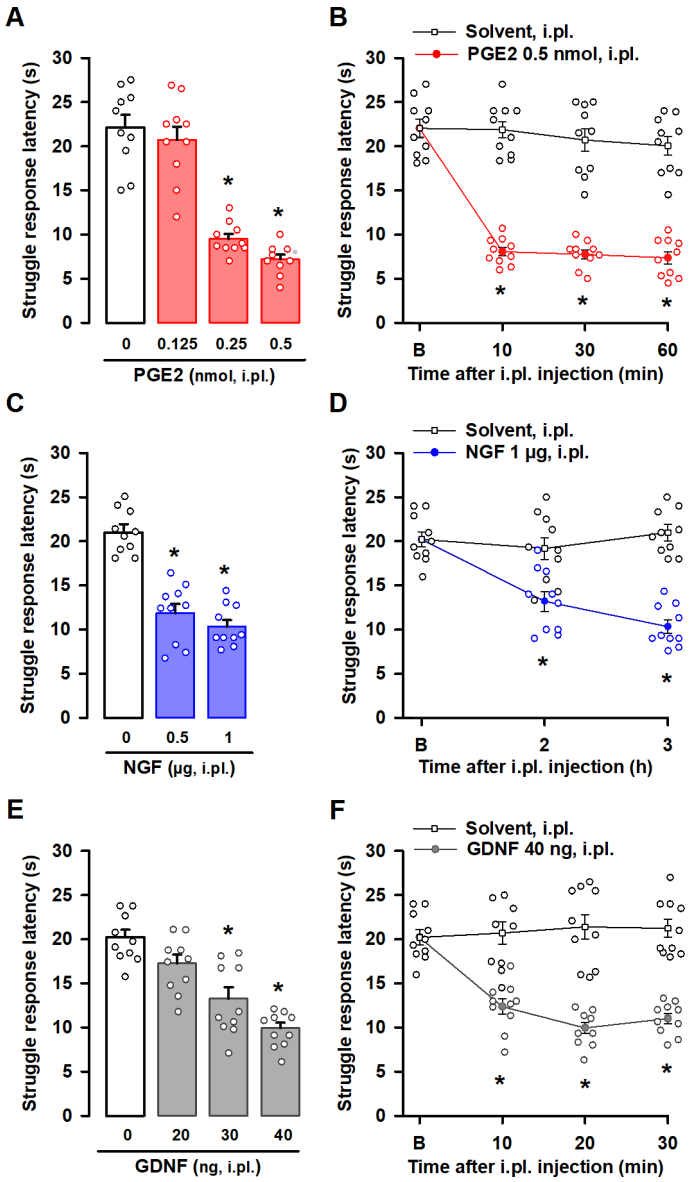

Figure 1. Dose-response and time course of the effects induced by PGE2, NGF or GDNF on the behavioural responses to mechanical stimulus. The results represent the latency to struggle response evoked by a mechanical stimulus of 100 g in mice intraplantarly (i.pl.) injected with the peripheral sensitizers and evaluated under different conditions: (A) administration of several doses of PGE2 (0.125-0.5 nmol) or its solvent and evaluation 10 min after administration, (B) time course of the effect induced by PGE2 0.5 nmol or its solvent, (C) administration of several doses of NGF (0.5-1 µg) or its solvent and evaluation 3 h after administration, (D) time course of the effect induced by NGF 1 µg or its solvent, (E) administration of several doses of GDNF (20-40 ng) or its solvent and evaluation 20 min after administration, (F) time course of the effect induced by GDNF 40 ng or its solvent. Each bar or point and vertical line represent the mean ± SEM of the values obtained in 10 animals. (A, C, E) Statistically significant differences between the values obtained in control non-sensitized animals (white bars) and the other experimental groups: $*P < 0.05$ (one-way ANOVA followed by Bonferroni test), and (B, D, F) between the animals treated with the peripheral sensitizers and their solvents at the same time after treatment: $*P < 0.05$ (two-way ANOVA followed by Bonferroni test). Data shown in A and B were log-transformed to meet the ANOVA assumptions.

We next aimed to study the effects of the *in vivo* ablation of TRPV1-expressing neurons by RTX on the behavioural responses to sensory stimulation after the administration of several peripheral sensitizers, as well as in non-sensitized animals. PGE2 and NGF induced a marked decrease in paw withdrawal latency to a contact heat stimulus (42 ± 1 ºC) in comparison to saline-injected mice, denoting development of heat hyperalgesia (Figure 4D and E). RTX increased the response latency in non-sensitized animals as well as in mice sensitized with PGE2 or NGF (Figure 4D and E). We also tested the effect of GDNF on heat sensitivity. In our experimental conditions, this neurotrophin (in contradistinction to the other peripheral sensitizers tested) was unable to induce heat hyperalgesia (Figure 4F).

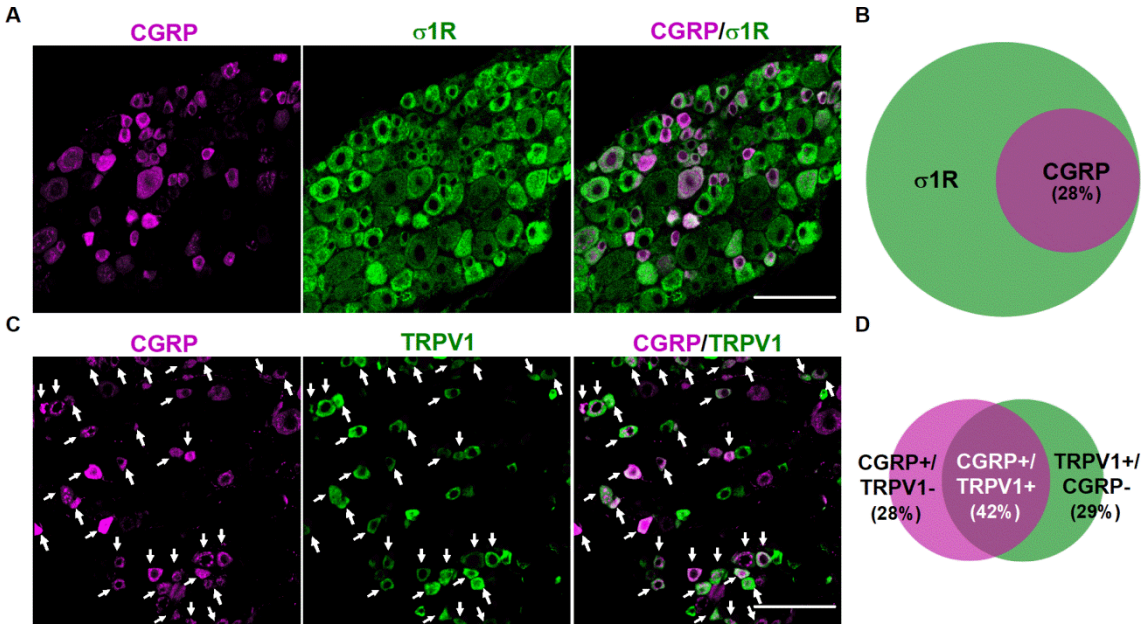

Figure 2. Double labelling of CGRP in combination with the sigma-1 receptor (σ1R) and TRPV1. Immunostaining was performed in the L4 dorsal root ganglion (DRG) from female mice. (A) Representative images from the double labelling of CGPR (magenta) and σ1R (green). Scale bar 50 µm. (B) Venn diagram showing the overlap between CGRP+ and σ1R+ neurons. (C) Representative images from the double labelling of CGPR (magenta) and TRPV1 (green). White arrows indicate co-localization of CGRP and TRPV1 markers. Scale bar 50 µm. (D) Venn diagram displaying the percentage of CGRP+, TRPV1+ and CGRP+/TRPV1+ neurons among the total number of neurons labelled with any of these markers. Samples from 5 mice were used to construct the Venn diagrams.

PGE2 and NGF also induced mechanical hyperalgesia, decreasing the struggle latency to paw pressure in comparison to saline-injected mice (Figure 4G and H). RTX treatment did not affect the responses to mechanical stimulation in non-sensitized animals but abolished PGE2- and NGF-induced mechanical hypersensitivity (Figure 4G

and H). Therefore, while TRPV1-expressing neurons are dispensable for mechanical nociceptive pain, they are essential for the mechanical hyperalgesia induced by these two chemical algogens. GDNF also induced significant mechanical hypersensitivity, which remained in spite of the ablation of TRPV1+ neurons by RTX treatment (Figure 4I). Therefore, although mechanical hypersensitivity can be triggered by PGE2, NGF and GDNF, only that from PGE2 and NGF is dependent on TRPV1+ nociceptors.

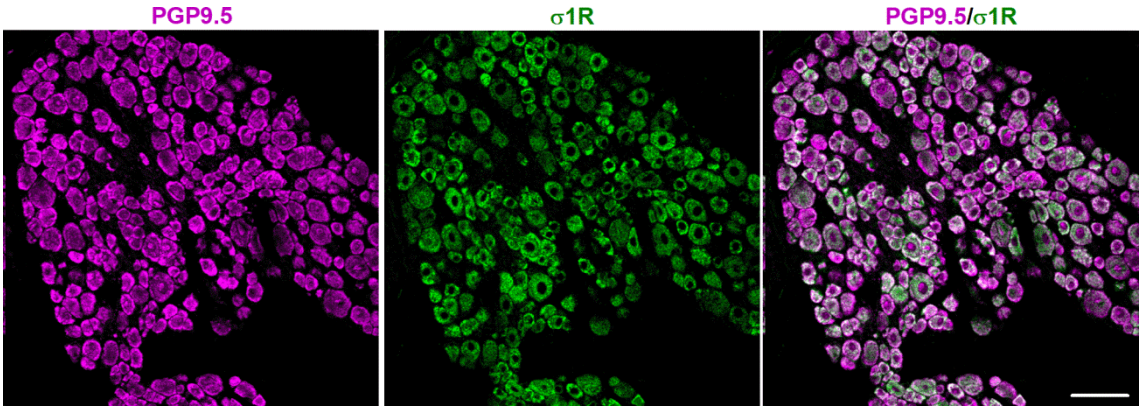

Figure 3. The sigma-1 receptor (σ1R) is present in all dorsal root ganglion (DRG) neurons. Representative images from the double labelling of the pan-neuronal marker PGP9.5 (magenta) and σ1R (green) in the L4 DRG from Naïve mice. Scale bar 100 µm.

1.2.2 The antihyperalgesic effects of sigma-1 antagonism and the peripheral opioid system

As all three peripheral sensitizers induced mechanical hyperalgesia, we first tested the effects of sigma-1 antagonists on this sensory modality, in female animals. The systemic (subcutaneous, s.c.) administration of the sigma-1 antagonists S1RA and BD-1063 did not modify the struggle latency to mechanical stimulation in non-sensitized animals (Figure 5), but induced a dose-dependent increase in the response latency in PGE2- or NGF-treated mice, reaching values similar to control animals (i.e. a full antihyperalgesic effect) at the highest dose tested (Figure 6A and B). However, neither S1RA nor BD-1063, at doses that fully reversed hyperalgesia induced by PGE2 or NGF, were able to induce any effect on GDNF-induced mechanical hyperalgesia (Figure 6C). The s.c. administration of the sigma-1 agonist PRE-084 did not alter the struggle response to mechanical stimulation in non-sensitized animals (Figure 5), but reversed the effect of both S1RA and BD-1063 on PGE2-induced hyperalgesia (Figure 6D and E,

respectively). These results support the selectivity of the effects induced by the sigma-1 antagonists on the receptor. Mirroring the results in female mice, S1RA induced a full antihyperalgesic effect to the mechanical stimulus in male mice sensitized with PGE2, and this effect was reversed by PRE-084 (Figure 7A). In addition, S1RA was unable to induce any effect on GDNF-induced mechanical hyperalgesia in male mice (Figure 7B). These results suggest that the overall effect of sigma-1 antagonism on peripheral sensitization is preserved in both sexes in the mouse.

The ameliorative effects induced by S1RA or BD-1063 on PGE2-induced hyperalgesia in female mice were also reversed not only by the opioid antagonist naloxone but also by its peripherally-restricted analog naloxone methiodide (Figure 6D and E). Similarly, the effects induced by S1RA on PGE2-induced hyperalgesia in male mice were also fully reversed by naloxone methiodide (Figure 7A). These results suggest the involvement of the peripheral opioid system in the effects induced by sigma-1 antagonism in mice from both sexes. To identify which opioid receptor subtype was participating in the antihyperalgesic effects induced by S1RA and BD-1063 in female mice, we used antagonists with selectivity for the opioid receptor subtypes. The antihyperalgesic effect induced by the sigma-1 antagonists was abolished by the μ-opioid antagonist cyprodime, but not the δ-opioid antagonist naltrindole or the κ-opioid antagonist nor-binaltorphimine (Figure 6D and E). We also tested the effects of S1RA and BD-1063 on NGF-induced hyperalgesia, with equivalent results (i.e. the effects of the sigma-1 antagonists were reversed by PRE-084, naloxone, naloxone methiodide and cyprodime, but not by naltrindole or nor-binaltorphimine) (Figure 6F and G). These results suggest that the effect of systemically-administered sigma-1 antagonists on PGE2- and NGF-induced hyperalgesia involves the activation of peripheral μ-opioid receptor, but not other opioid receptor subtypes. The s.c. administration of S1RA and BD-1063 also induced robust antihyperalgesic effects to a heat stimulus in mice sensitized with PGE2 and NGF, and these were reversed by both the sigma-1 agonist PRE-084 and the peripheral opioid antagonist Nx-M (Figure 8), mirroring the peripheral opioid effects induced by sigma-1 antagonism on mechanical hyperalgesia induced by these sensitizers of TRPV1+ neurons.

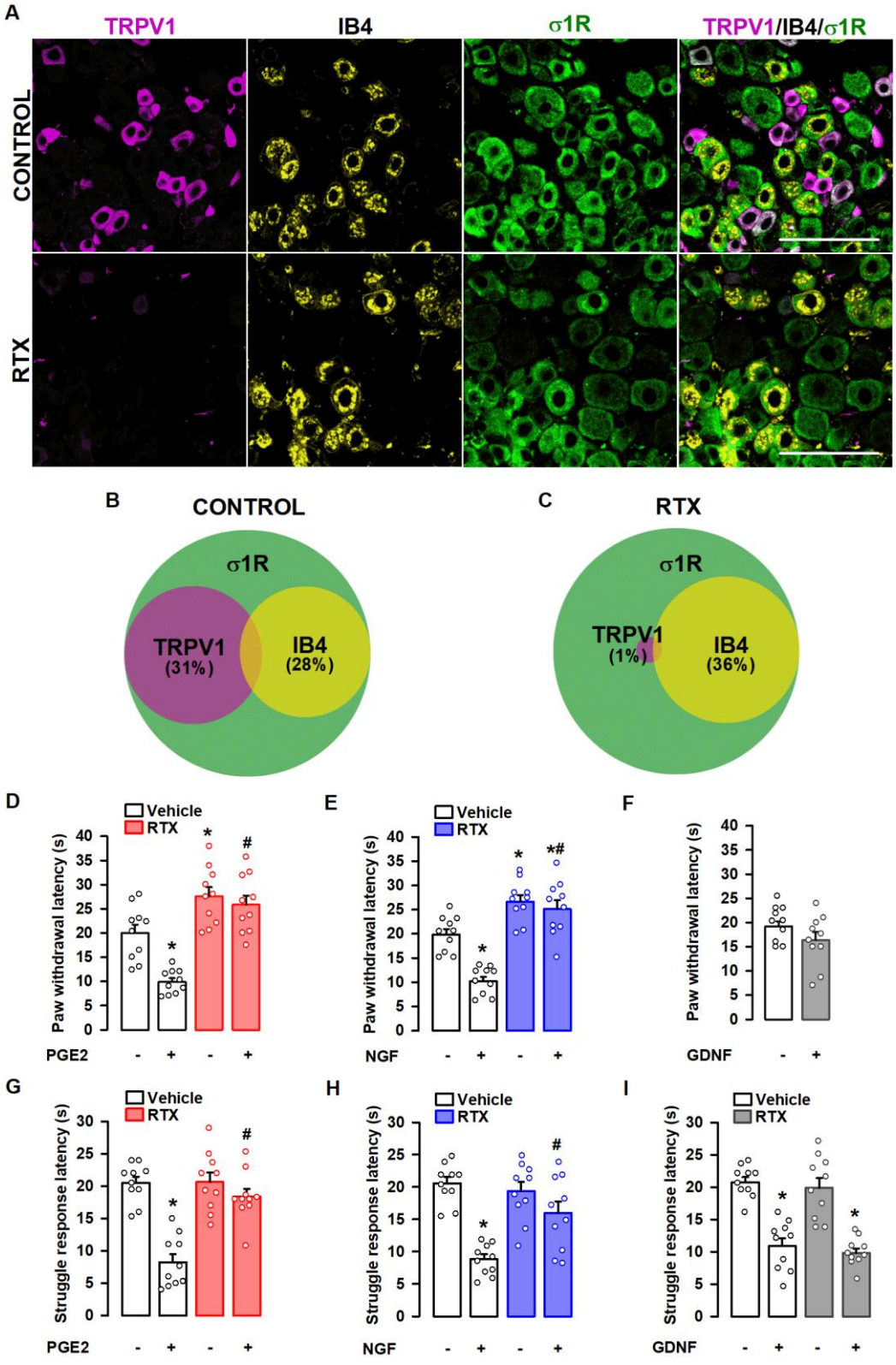

Figure 4. Effect of the ablation of TRPV1-expressing neurons on mechanical hyperalgesia induced by PGE2, NGF and GDNF. Female mice were treated intraperitoneally (i.p.) with resiniferatoxin (RTX, 25 µg/kg for two consecutive days) or its vehicle five days before obtaining samples or performing the behavioural experiments. (A) Triple labelling of TRPV1 (magenta), isolectin B4 (IB4, yellow) and sigma-1 receptor (σ1R, green) in the L4 dorsal root ganglion (DRG). Top panels: samples from vehicle-treated mice (control). Bottom panels: samples from mice treated with resiniferatoxin (RTX). Scale bar, 100 µm. (B and C) Venn diagrams showing the overlap between TRPV1+, IB4+ and σ1R+ neurons in samples from

control mice (B) and from mice treated with RTX (C). Samples from 5 mice per group were used to construct the Venn diagrams. (D-I) The behavioural results represent the latency to paw withdrawal evoked by a heat stimulus of 42 ± 1 ºC (D, E and F), and the latency to struggle response evoked by a mechanical stimulus of 100 g (G, H and I) in mice treated intraplantarly (i.pl.) with PGE2 (0.5 nmol) (D and G), NGF (1 µg) (E and H), GDNF (40 ng) (F and I) or their solvents. Values are the mean ± SEM (10 animals per group). Statistically significant differences between the values obtained in control non-sensitized animals and mice treated with the peripheral sensitizers: **P*<0.05, and between the values obtained in animals sensitized with PGE2 or NGF, and administered with RTX or its vehicle: #P < 0.05 (one-way ANOVA followed by Bonferroni test). Data shown in H and I were log-transformed to meet the ANOVA assumptions.

We also tested the effects of PRE-084 and the opioid antagonists on the antihyperalgesic effect induced by morphine in female mice, the prototypic opioid agonist. Systemic (s.c.) administration of morphine induced a dose-dependent antihyperalgesic effect in animals sensitized with PGE2 and tested with the mechanical stimulus (Figure 9A). The antihyperalgesic effect of morphine was not modified by the sigma-1 agonist PRE-084 (Figure 9B) (at the same dose that reverses the antihyperalgesic effect induced by the sigma-1 antagonists). The antihyperalgesic effect of morphine was fully reversed by the opioid antagonist naloxone and its quaternary derivative naloxone methiodide (Figure 9B), indicating that these effects were mediated peripherally. Morphine effects were also dose-dependently and fully reversed by cyprodime (at the same dose used to reverse the effect of sigma-1 antagonists), but not by naltrindole or nor-binaltorphimine (Figure 9B).

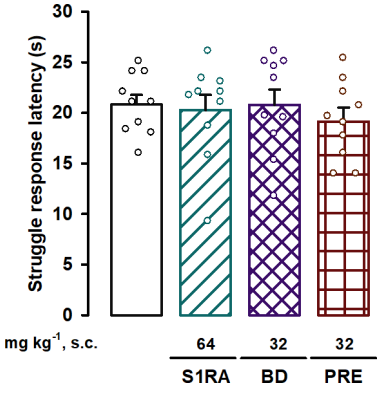

Figure 5. Absence of effects of S1RA, BD-1063 (BD) and PRE-084 (PRE) in mice without sensitization. The results represent the latency to struggle response evoked by a mechanical stimulus of 100 g in mice administered subcutaneously (s.c.) with S1RA, BD and PRE or saline. Each bar and vertical line represent the mean ± SEM of the values obtained in 10 animals. No significant differences between the values obtained in control saline-treated animals (white bar) and animals administered with S1RA, BD or PRE were found (one-way ANOVA followed by Bonferroni test).

We also tested the effect of morphine on GDNF-induced hyperalgesia in female mice. This opioid also induced a dose-dependent antihyperalgesic effect (Figure 9C), which was reversed by naloxone but not by PRE-084 (Figure 9D). In contrast to the results on

PGE2-induced hyperalgesia, naloxone methiodide did not modify the antihyperalgesic effect of morphine after sensitization with GDNF (Figure 9D), pointing to central actions of morphine as responsible for this antihyperalgesic effect. These results highlight the differences of opioid effects depending on the peripheral sensitizer used, which might be related to the different neuronal populations sensitized by each algogen.

In summary, both the systemic administration of sigma-1 antagonists and morphine induced antihyperalgesic effects which are mediated by peripheral μ-opioid receptor activation, in animals sensitized with PGE2 or NGF. However, the opioid mediated antihyperalgesic effects of sigma-1 antagonism were absent on GDNF-induced hypersensitivity. Moreover, morphine's antihyperalgesic effect on GDNF-induced hyperalgesia, does not depend on peripheral opioid receptors.

1.2.3 Sigma-1 antagonism and endogenous opioid peptides

We hypothesized that sigma-1 antagonists might induce peripheral opioid effects at the peripheral terminal sensitized site, where the animals receive sensory stimulation. The i.pl. administration of the sigma-1 antagonists S1RA or BD-1063 dose-dependently fully reversed mechanical hyperalgesia induced by either PGE2 (Figure 10A) or NGF (Figure 10B) in female mice, without altering the response latency of non-sensitized animals (Figure 11).

To neutralize the actions of endogenous opioid peptides at the sensitized site, we i.pl. administered a monoclonal antibody, 3-E7, which recognizes the pan-opioid sequence Tyr–Gly–Gly–Phe at the N-terminus of most opioid peptides (see Methods). The i.pl. administration of 3-E7 did not modify the antihyperalgesic effect of S1RA or BD-1063 on the mechanical hyperalgesia induced by either PGE2 (Figure 10C) or NGF (Figure 10D), suggesting that opioid peptides containing the target sequence of the 3-E7 do not mediate the effect observed. The administration of this antibody did not alter the response latency of non-sensitized animals (Figure 11).

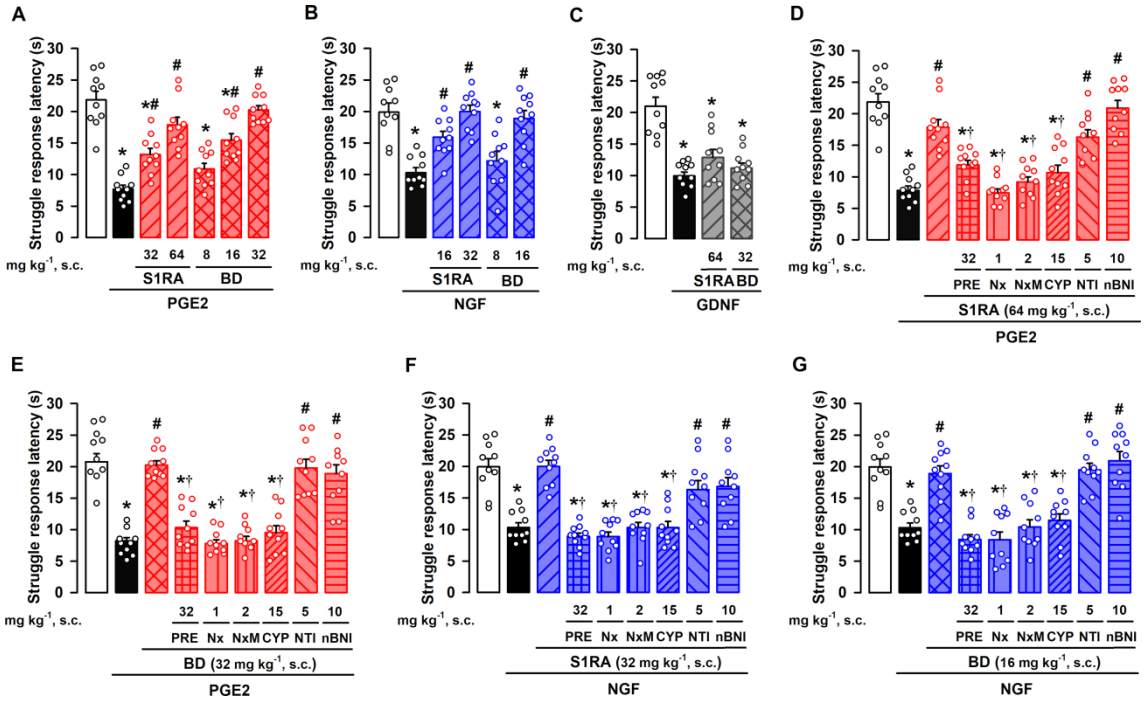

Figure 6. Effects of the systemic administration of the sigma-1 antagonists S1RA and BD-1063 (BD) on mechanical hyperalgesia induced by PGE2, NGF or GDNF. The results represent the latency to struggle response evoked by a mechanical stimulus of 100 g in female mice administered subcutaneosly (s.c.) with S1RA, BD or saline, and intraplantarly (i.pl.) with (A) PGE2 (0.5 nmol), (B) NGF (1 µg), (C) GDNF (40 ng) or their solvents. Animals treated with S1RA or BD or their solvent also received the s.c. administration of PRE-084 (PRE), naloxone (Nx), naloxone methiodide (NxM), cyprodime (CYP), naltrindole (NTI), nor-binaltorphimine (nBNI), or saline, and were tested on mechanical hyperalgesia induced by PGE2 (D and E) and NGF (F and G). Values are the mean ± SEM (10 animals per group). Statistically significant differences between the values obtained in control non-sensitized animals (white bars) and the other experimental groups: $*P < 0.05$, between the values obtained in PGE2-, NGF- or GDNF-treated animals administered with S1RA, BD or their solvent: $\#P < 0.05$, and between PGE2- or NGF-treated animals administered with S1RA or BD alone or their association with PRE, Nx, NxM or CYP: $\dagger P < 0.05$ (one-way ANOVA followed by Bonferroni test). Data shown in C and E were log-transformed to meet the ANOVA assumptions.

Taking into account that the antihyperalgesic effect of sigma-1 antagonism appeared to be mediated exclusively by peripheral µ-opioid receptor activation (as described in the preceding section), that endomorphins have a high affinity and selectivity for µ-opioid receptors, and that these endogenous opioid peptides differ from most opioid peptides in their N-terminal sequence (Horvath, 2000; Machelska, 2011) (and therefore are not susceptible to the neutralizing effects of 3-E7), they are candidates for the antihyperalgesic effects induced by sigma-1 antagonists. Supporting this, i.pl. administration of a monoclonal antibody against endomorphin-2 did not alter the response latency of non-sensitized animals (Figure 11), but fully reversed the local

antihyperalgesic effect of both S1RA and BD-1063 after sensitization with either PGE2 (Figure 10E) or NGF (Figure 10F).

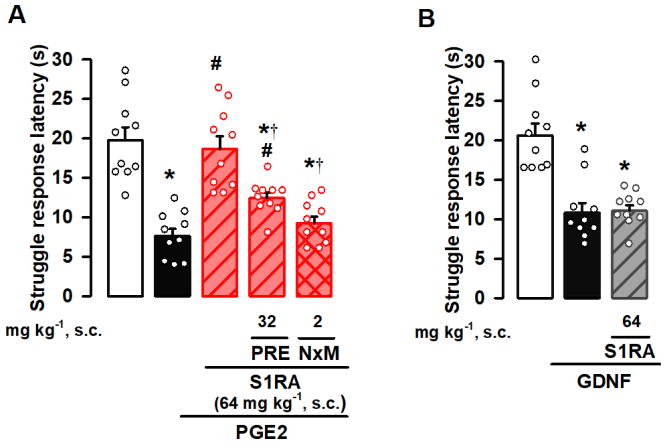

Figure 7. Effects of the systemic administration of the sigma-1 antagonist S1RA on mechanical hyperalgesia induced by PGE2 or GDNF in male mice. The results represent the latency to struggle response evoked by a mechanical stimulus of 100 g in male mice administered subcutaneously (s.c.) with S1RA or saline, and intraplantarly (i.pl.) with the peripheral sensitizers or their solvents. (A) Animals treated with S1RA also received the s.c. administration of PRE-084 (PRE), naloxone methiodide (NxM) or saline, and were tested on mechanical hyperalgesia induced by PGE2. (B) Animals treated with S1RA were tested on mechanical hyperalgesia induced by GDNF. Each bar and vertical line represent the mean ± SEM of the values obtained in 10 animals. Statistically significant differences between the values obtained in control non-sensitized animals (white bars) and the other experimental groups: *P < 0.05, between the values obtained in PGE2-treated animals administered with S1RA or their solvent: #P < 0.05, and between PGE2-treated animals administered with S1RA alone or their association with PRE or NxM: †P < 0.05 (one-way ANOVA followed by Bonferroni test). Data shown in A and B were log-transformed to meet the ANOVA assumptions.

We then aimed to identify the source of the endomorphin-2 responsible for the antihyperalgesic effects induced by sigma-1 antagonism, and tested immune cells and peripheral sensory neurons as possible sources of this endogenous opioid peptide.

We first tested in female mice whether the i.pl. administration of the peripheral sensitizers recruited immune cells to the injected site. We used samples from mice administered with carrageenan, a pro-inflammatory agent, as a positive control. Although we found a prominent increase in immune cells (stained with the pan-hematopoietic cell marker CD45) in paw tissue after carrageenan injection, we did not find any accumulation of these cells after the injection of PGE2, NGF or GDNF (Figure 12A and B). As neutrophils are known to be early recruited to the inflamed site (Rittner et al., 2001), we also tested for possible increases of this specific immune cell population. We found prominent neutrophil (CD45+CD11b+Ly6G+ cells) recruitment in

paw tissue after carrageenan injection, but we did not find any accumulation of these immune cells after the injection of any of the algogenic compound tested (Figure 12C and D). Therefore, it is unlike that immune cells would constitute the cells harboring the endogenous opioid peptides responsible of the peripheral opioid effects induced by sigma-1 antagonism against PGE2- and NGF-induced hyperalgesia.

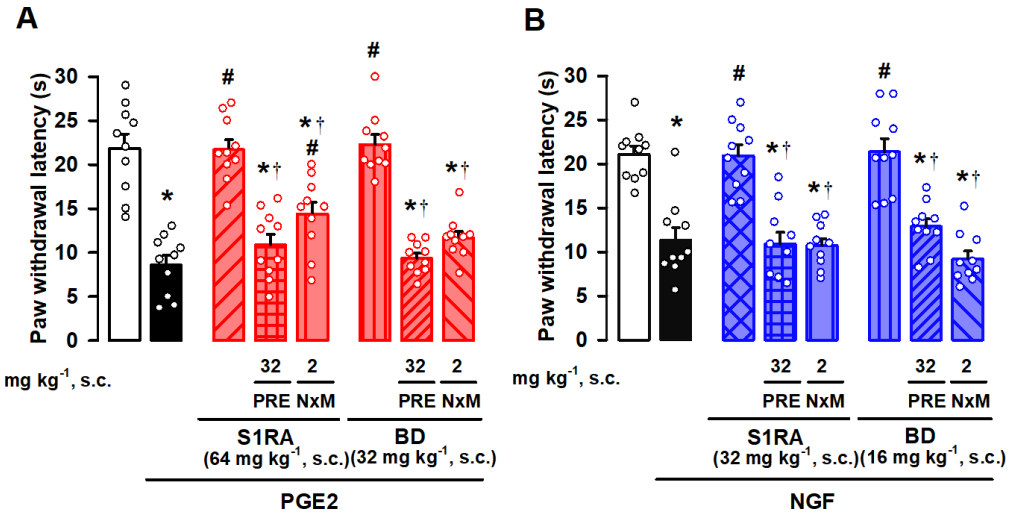

Figure 8. Effects of the systemic administration of the sigma-1 antagonists S1RA and BD-1063 (BD) on heat hyperalgesia induced by PGE2 or NGF. The results represent the latency to paw withdrawal evoked by a heat stimulus of 42 ± 1 ºC in mice administered subcutaneosly (s.c.) with S1RA, BD or saline, and intraplantarly (i.pl.) with (A) PGE2 (0.5 nmol), (B) NGF (1 µg) or their solvents. Animals treated with S1RA or BD or their solvent also received the s.c. administration of PRE-084 (PRE), naloxone methiodide (NxM) or saline, and were tested on heat hyperalgesia induced by the peripheral sensitizers. Values are the mean ± SEM (10 animals per group). Statistically significant differences between the values obtained in control non-sensitized animals (white bars) and the other experimental groups: **P* < 0.05, between the values obtained in PGE2-, or NGF-treated animals administered with S1RA, BD or their solvent: #*P* < 0.05, and between PGE2- or NGF-treated animals administered with S1RA or BD alone or their association with PRE or NxM: †*P* < 0.05 (one-way ANOVA followed by Bonferroni test).

We then tested whether endomorphin-2 was present in peripheral sensory neurons from female mice. Using the same antibody which administered *in vivo* was able to abolish the antihyperalgesic effects of sigma-1 antagonists, we found endomorphin-2 immunoreactivity in DRG samples, and interestingly, the majority of this labelling was found in TRPV1+ nociceptors, with a virtual absence of endomorphin-2 staining on IB4+ neurons (see left panels of Figure 13A, and Figure 13B). A few additional larger cells with neuronal morphology (TRPV1-/IB4- cells) were also found to be endomorphin-2+ (see left panels of Figure 13A and Figure 14 for representative images of high and low magnification, respectively). As a proof of the specificity of the

expression of endomorphin-2 by TRPV1+ nociceptors, we performed immunostaining experiments after RTX administration. Treatment with this toxin completely ablated TRPV1 staining and most of endomorphin-2 immunoreactivity (Figure 13C), which remained only in some larger neurons, whereas IB4 labelling was globally preserved (see right panels of Figure 13A and Figure 14), and in fact constituted most of the labelled (CGRP+, IB4+ or TRPV1+) neurons after the ablation of TRPV1+ nociceptors (Figure 13C). These results suggest that most of the neurons which express endomorphin-2 correspond to peptidergic (TRPV1+) nociceptors. This pattern for the expression of endomorphin-2 agrees with the naloxone-sensitive effect of sigma-1 antagonists on hyperalgesia induced by sensitizers of TRPV1+ nociceptors, such as PGE2 or NGF.

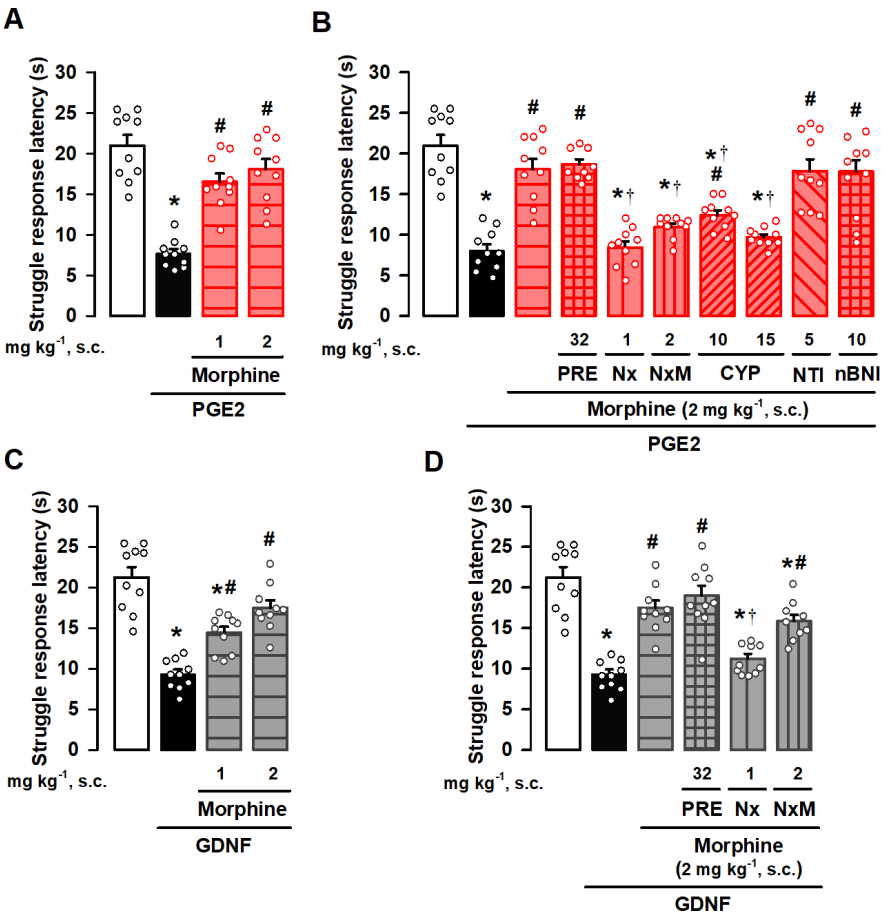

Figure 9. Effects of the systemic administration of morphine on mechanical hyperalgesia induced by PGE2 or GDNF. The results represent the latency to struggle response evoked by a mechanical stimulus of 100 g in mice administered subcutaneously (s.c.) with morphine or saline, and intraplantarly (i.pl.) with the peripheral sensitizers or their solvents. (A) Dose-response effect of morphine on mechanical hyperalgesia induced by PGE2 (0.5 nmol). (B) Animals treated with morphine also received the s.c. administration of PRE-084 (PRE), naloxone (Nx), naloxone methiodide (NxM), cyprodime (CYP), naltrindole (NTI), nor-binaltorphimine (nBNI), or saline, and were tested on mechanical hyperalgesia

induced by PGE2. (C) Dose-response effect of morphine on mechanical hyperalgesia induced by GDNF (40 ng). (D) Animals treated with morphine also received the s.c. administration of PRE, Nx or NxM, and were tested on mechanical hyperalgesia induced by GDNF. Each bar and vertical line represent the mean ± SEM of the values obtained in 10 animals. Statistically significant differences between the values obtained in control non-sensitized animals (white bars) and the other experimental groups: $*P < 0.05$, between the values obtained in PGE2- or GDNF-treated animals administered with morphine or their solvent: $\#P < 0.05$, and between PGE2- or GDNF-treated animals administered with morphine alone or their association with PRE, Nx, NxM or CYP: $\dagger P < 0.05$ (one-way ANOVA followed by Bonferroni test). Data shown in A, B and C were log-transformed to meet the ANOVA assumptions.

1.2.4 Sigma-1 receptor: a link between TRPV1 and μ-opioid receptor

As previously commented, the modulation of μ-opioid receptor antinociception by sigma-1 receptor at the CNS involves the participation of NMDARs (see the Introduction section). Taking into account that the opioid-dependent antihyperalgesic effect of sigma-1 antagonism appears to involve peptidergic (TRPV1+) nociceptors, we hypothesized that the central NMDAR mechanism might have a peripheral analog based on interactions of TRPV1, sigma-1 receptors and μ-opioid receptors.

Using recombinant proteins, we found that sigma-1 receptor and CaM each strongly interact with the C-terminal segment of TRPV1 in the presence of calcium (see lanes one and seven in Figure 15A). However, when sigma-1 receptor and CaM are present together, sigma-1 receptor binds to TRPV1 and this does not allow CaM to bind the C-terminal domain of TRPV1 (Figure 15A, lane six). This CaM binding site is important for TRPV1 desensitization (Numazaki et al., 2003). The presence of either S1RA or BD-1063 hinders the interaction between sigma-1 receptor and TRPV1 (Figure 15A, lanes two and four), allowing CaM to bind to the TRPV1 channel (Figure 15A, lanes three and five). We also examined the influence of μ-opioid receptor on the interaction between sigma-1 receptor and TRPV1 and found that the presence of the C-terminus of μ-opioid receptor, which contains the binding site for sigma-1 receptors (Rodríguez-Muñoz et al., 2015a and b) enhanced the dissociation of sigma-1 receptors from the C-terminal domain of TRPV1 that is induced by S1RA (Figure 15B). In the presence of S1RA, the interaction between sigma-1 receptor and the C-terminal domain of μ-opioid receptor is markedly increased, in spite of the presence of the C-terminus of TRPV1 (Figure 15C). In other words, sigma-1 antagonism promotes the transfer of sigma-1 receptors from the C-terminal domain of TRPV1 to the C-terminus of μ-opioid receptor, and this facilitates the binding of CaM to the C-terminus of TRPV1.

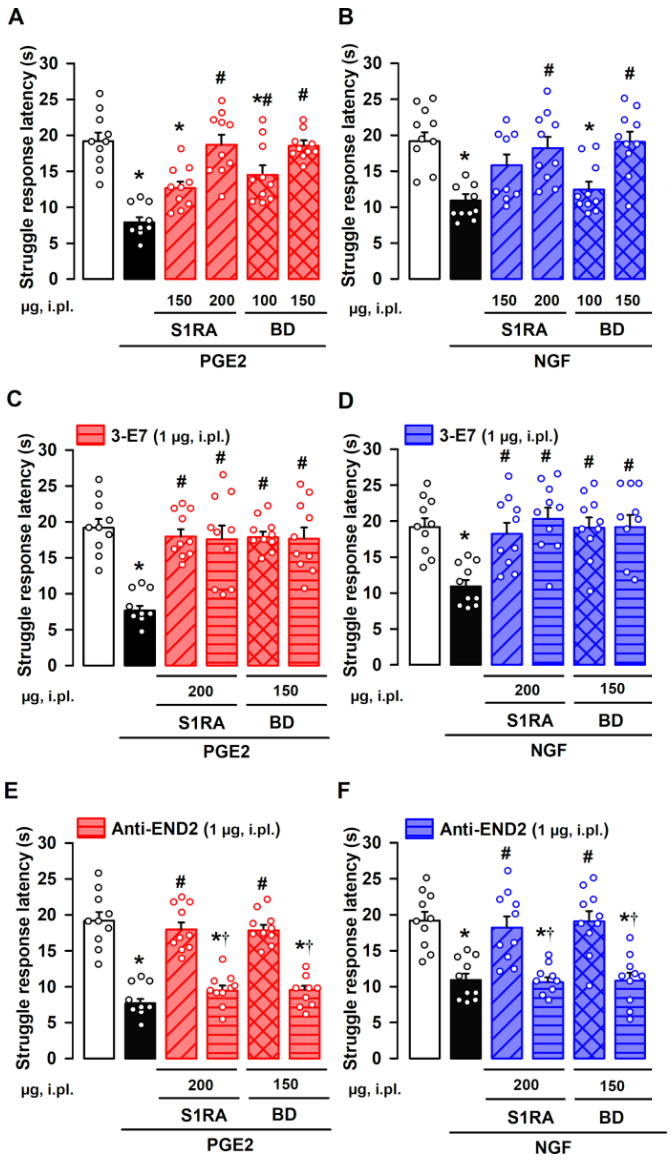

Figure 10. Effects of the local administration of the σ1 antagonists S1RA and BD-1063 (BD) on mechanical hyperalgesia induced by PGE2 or NGF. The results represent the latency to struggle response evoked by a mechanical stimulus of 100 g in female mice administered intraplantarly (i.pl.) with S1RA, BD or saline, and with (A, C and E) PGE2 (0.5 nmol), (B, D and F) NGF (1 μg) or their solvent. Animals i.pl. treated with S1RA or BD were also coadministered with antibodies for endogenous opioid peptides: 3-E7 (C and D) and anti-endomorphin-2 (anti-END2) (E and F), and tested on mechanical hyperalgesia induced by PGE2 (C and E) and NGF (D and F). Values are the mean ± SEM (10 animals per group). Statistically significant differences between the values obtained in control non-sensitized animals (white bars) and the other experimental groups: **P* < 0.05, between the values obtained in PGE2- or NGF-treated animals administered with S1RA, BD or their solvent: #*P* < 0.05, and between PGE2- or NGF-treated animals administered with S1RA or BD alone or coadministered with the anti-END2 antibody: †*P* < 0.05 (one-way ANOVA followed by Bonferroni test). Data shown in C were log-transformed to meet the ANOVA assumptions.

Our results indicate that sigma-1 receptors are a key player in the crosstalk between μ-opioid receptor and TRPV1.

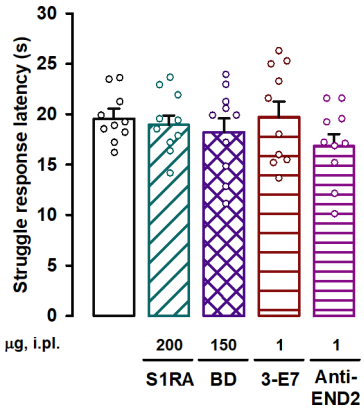

Figure 11. Absence of effects induced by the local administration of S1RA, BD-1063 (BD) and the antibodies 3-E7 and anti-endomorphin2 (anti-END2), in mice without sensitization. The results represent the latency to struggle response evoked by a mechanical stimulus of 100 g in mice administered intraplantarly (i.pl.) with S1RA, BD and the antibodies 3-E7 and anti-END2 or saline. Each bar and vertical line represent the mean ± SEM of the values obtained in 10 animals. No significant differences between the values obtained in control saline-treated animals (white bar) and animals administered with S1RA, BD, 3-E7 or anti-END2 were found (one-way ANOVA followed by Bonferroni test).

We then explored the functional consequences of the interactions between sigma-1 receptors, TRPV1 and opioid receptors for nociceptor sensitization. We performed calcium-imaging experiments on cultured capsaicin-sensitive DRG neurons from adult female mice, sensitized with PGE2. The application of a low concentration of capsaicin (0.05 μM) produced a hardly measurable increase in intracellular calcium concentration. However, after application of PGE2, these neurons showed a robust increase in intracellular calcium in response to the same low concentration of capsaicin (see Figure 15D for a representative recording), indicating the sensitization of TRPV1+ nociceptors by this algogen. We then measured the effect of S1RA on the PGE2-induced sensitization, and found that application of the sigma-1 antagonist greatly decreased the peak amplitude of PGE2-sensitized neurons responses to capsaicin (Figure 15E). This effect was reversed by the opioid antagonist naloxone (Figure 15E), which indicates that S1RA acts through opioid activation to reverse TRPV1+ neuron sensitization.

1.3 Discussion

TRPV1+ nociceptors can be sensitized by PGE2 and NGF, and express the endogenous μ-opioid receptor agonist endomorphin-2. We show that sigma-1 receptors are also expressed by these neurons and participate in the crosstalk between TRPV1 and μ-opioid receptor, tonically limiting the antihyperalgesic effect of the endogenous opioid peptide.

Most CGRP+ DRG neurons express TRPV1 and vice versa, as shown here and in previous studies (Priestley, 2009). On the other hand, TRPV1+ and IB4+ neurons constitute separate cellular populations (peptidergic and non-peptidergic C-nociceptors, respectively) with only occasional overlap, as shown in the current and previous studies using several mouse strains (Zwick et al., 2002; Woodbury et al., 2004; Sheehan et al., 2019). The *in vivo* ablation of peptidergic (TRPV1+) C neurons by RTX increased the response latency to heat stimulus in non-sensitized animals and in mice sensitized with PGE2 or NGF, in agreement with the known role of TRPV1+ neurons in

the coding of heat nociception or hypersensitivity (Cavanaugh et al., 2009). We also show that RTX-sensitive neurons are dispensable for mechanical nociceptive pain, in agreement with previous studies (Zhang et al., 2013; Montilla-García et al., 2018), but they are essential for the mechanical hyperalgesia induced by PGE2 or NGF. These latter results can be explained by the fact that both algogenic compounds induce mechanosensitivity in those nociceptors which are normally mechanically insensitive (Emery et al., 2016; Prato et al., 2017), and this might be dependent on a phenotypic switch of peptidergic C-nociceptors (Prato et al., 2017).

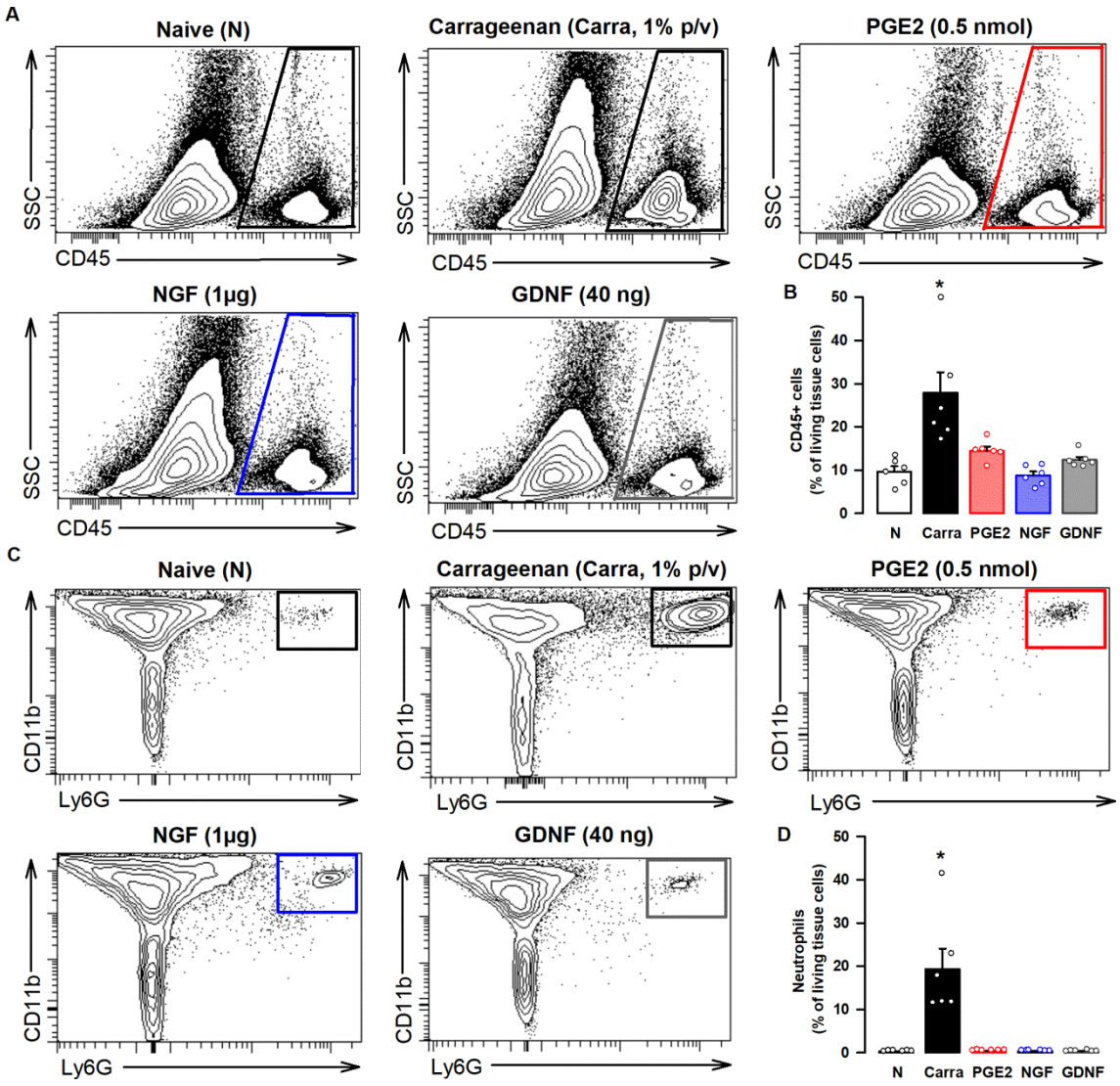

Figure 12. The *in vivo* treatment with PGE2, NGF or GDNF do not produce significant immune cell recruitment at the injection site. (A) Representative side scatter (SSC) vs CD45 plots showing that cells from hematopoietic lineage (CD45+ cells) do not increase in the paw from female mice after intraplantar (i.pl.) administration of PGE2 (0.5 nmol), NGF (1 µg) or GDNF (40 ng), in comparison to naïve (N) mice, whereas this cell population highly increases after the i.pl. administration of a solution containing 1 %

carrageenan (carra). Gating for CD45+ cells is shown as a trapezoid in the right side of each FACS diagram. (B) Quantification of CD45+ cells with respect to the number of living cells in the paw from naïve mice and after the i.pl. treatments. (C) Representative FACS diagrams, gated from CD45+ cells, showing that neutrophils (CD11b+Ly6G+ cells) highly increase in the paw from female mice after the i.pl. administration of carra but not after the injection of any of the three peripheral sensitizers tested. Gating for neutrophil quantification is shown as a square in the right corner of each FACS diagram. (D) Quantification of neutrophils with respect to the number of living cells in the paw from naïve mice and after the i.pl. treatments. (B and D) Values are the mean ± SEM (6 animals per group). Statistically significant differences between naïve and carrageenan-treated animals: *P < 0.05. There were no significant differences between naïve animals and those treated with PGE2, NGF and GDNF (one-way ANOVA followed by Bonferroni test). Data shown in B and D were log-transformed to meet the ANOVA assumptions.

The systemic administration of the sigma-1 antagonists S1RA and BD-1063 reversed mechanical and heat hyperalgesia induced by PGE2 and NGF. Interestingly, the opioid antagonist naloxone and its peripherally restricted analog naloxone methiodide abolished the effects of not only morphine, used as a reference opioid analgesic, but also those of the sigma-1 antagonists, indicating that these effects were opioid in nature and mediated peripherally. These peripheral opioid-dependent effects induced by sigma-1 antagonism are seen in mice from both sexes. In addition, the antihyperalgesic effects of sigma-1 antagonists and morphine to the mechanical stimulus involved the activation of μ-opioid receptor, but not other opioid receptor subtypes, as they were fully reversed by cyprodime, but not by naltrindole or nor-binaltorphimine (at doses known to inhibit μ, δ and κ opioid responses, respectively) (Hutcheson et al., 1999; Baamonde et al., 2005). Although it seems evident to attribute the effect of morphine to direct actions on μ-opioid receptor (Matthes et al., 1996), S1RA or BD-1063 lack any affinity for μ-opioid receptor (Sánchez-Fernández et al., 2013). Since sigma-1 antagonism is known to potentiate opioid analgesia (Sánchez-Fernández et al., 2017), we hypothesized that the peripheral opioid-like effects of sigma-1 antagonists on PGE2- and NGF-induced hyperalgesia might be the result of the potentiation of endogenous opioid peptides released at the sensitized site. The local administration of sigma-1 antagonists abolished PGE2- and NGF-induced mechanical hyperalgesia, and this was not reversed by the administration of 3-E7, a monoclonal antibody which recognizes the N-terminus of most endogenous opioid peptides. However, the antihyperalgesic effects of sigma-1 antagonists were reversed by an antibody against endomorphin-2, which lacks the consensus N-terminus of other opioid peptides and, in agreement with the previously commented μ-opioid selectivity

of the effects induced by sigma-1 antagonists, is a selective μ-opioid agonist (Horvath, 2000; Machelska, 2011).

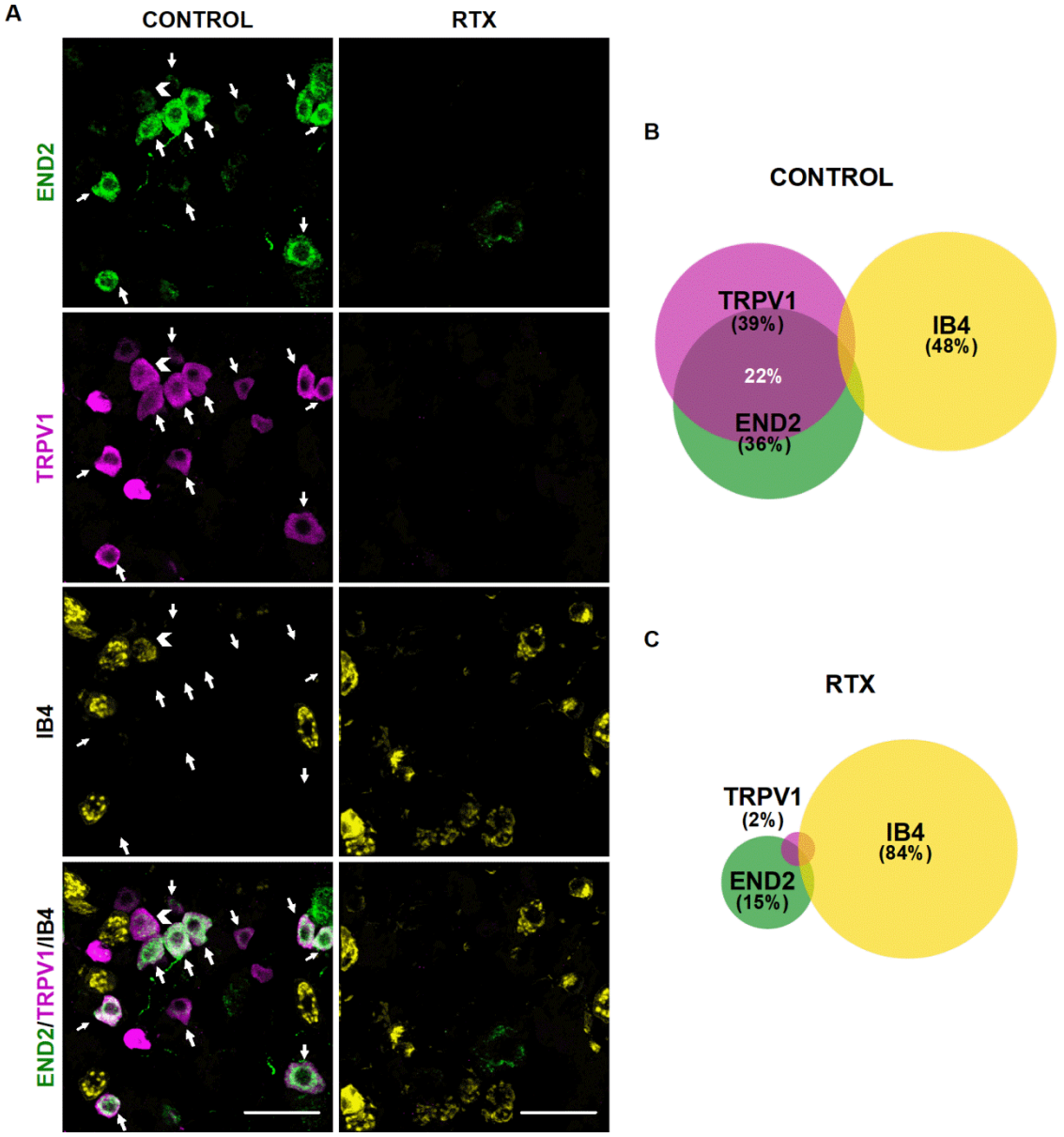

Figure 13. Endomorphin-2 (END2) is present in TRPV1+ but not in IB4+ neurons. (A) Triple labelling of endomorphin-2 (END2, green), TRPV1 (magenta) and isolectin B4 (IB4, yellow) in L4 DRG from female mice. Left panels: samples from solvent-treated mice (control). Right panels: samples from mice treated with resiniferatoxin (RTX). White arrows indicate co-localization of END2 and TRPV1 markers. White arrowhead indicates co-localization of TRPV1 and IB4 markers. Scale bar 50 μm. (B and C) Venn diagrams displaying the percentage of TRPV1+, IB4+ and END2+ neurons among the total number of neurons labelled with any of these markers in samples from control mice (B) and from mice treated with RTX (C). Samples from 5 mice per group were used to construct the Venn diagrams.

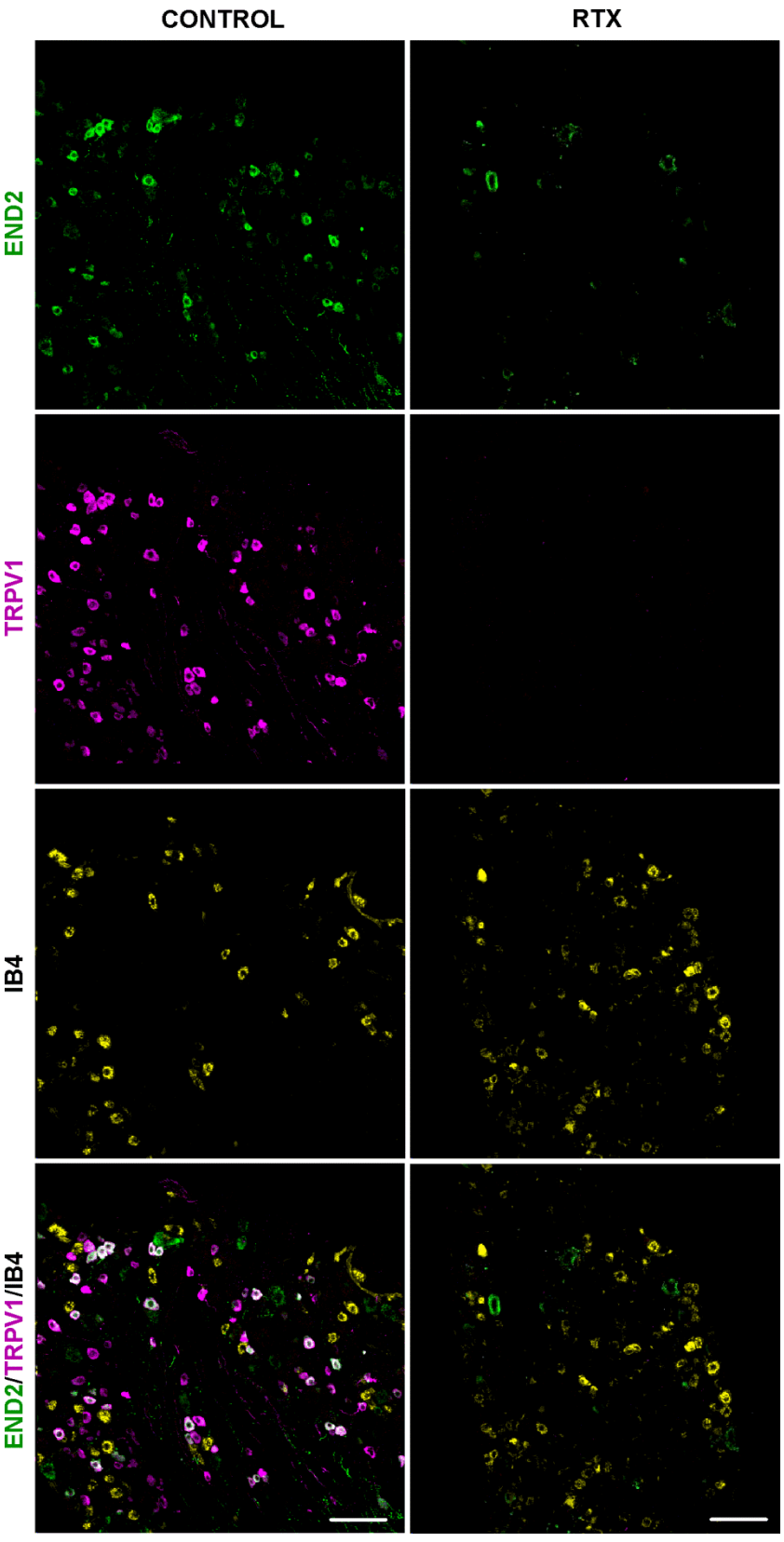

Figure 14. Endomorphin-2 (END2) is present in TRPV1+ but not in IB4+ neurons. Representative low magnification images from triple labelling of endomorphin-2 (green), TRPV1 (magenta) and IB4 (yellow) in the L4 dorsal root ganglion (DRG). Left panels: samples from solvent-treated mice (control). Right panels: samples from mice treated with resiniferatoxin (RTX). Scale bar 100 µm.

Immune cells can produce endomorphins (Mousa et al., 2002; Labuz et al., 2006), and we recently described that sigma-1 antagonism enhances the opioid analgesia induced by opioid peptides released by immune cells during inflammation (Tejada et al., 2017).

We show here that PGE2 or NGF did not recruit immune cells which might account for the antihyperalgesic effect of sigma-1 antagonists. However, we found endomorphin-2 immunoreactivity in mouse DRG neurons, in agreement with previous studies in the rat which show that endomorphin-2 (but not endomorphin-1) is produced by peripheral sensory neurons (Sanderson et al., 2004; Fichna et al., 2007; Scanlin et al., 2008). Importantly, we show that endomorphin-2 is mostly expressed by peptidergic (TRPV1+) nociceptors, a result which also agrees with the previously described distribution of this endogenous opioid peptide in the rat DRG, as it was shown to colocalize with substance P and CGRP (Sanderson et al., 2004). Therefore, the sensory neurons required for PGE2- and NGF-induced hyperalgesia are the same neuronal subtype which expresses endomorphin-2. In spite of the well-known analgesic actions of endomorphin-2 (Fichna et al., 2007), the production of this endogenous opioid peptide by TRPV1+ nociceptors seems not enough to counterbalance sensitization by PGE2 or NGF, except when potentiated by sigma-1 antagonists. Our results might be explained by the contribution of an autocrine mechanism, in the peripheral terminal of the nociceptor, in the antihyperalgesic effect of sigma-1 antagonism.

The modulation of μ-opioid receptor-mediated analgesia by sigma-1 receptor in the CNS relies on the binding of sigma-1 receptor to NMDAR, physically preventing the binding of CaM to NMDAR, and hence reducing the inhibition of channel activity. sigma-1 antagonism dissociates sigma-1 receptors from NMDAR and transfer them to μ-opioid receptor. In this situation, CaM gains access to NMDARs to curtail channel activity and consequently enhancing μ-opioid receptor actions (Rodríguez-Muñoz et al., 2015a and b). TRPV1 is another protein partner of sigma-1 receptors (Ortíz-Rentería et al., 2018; Cortés-Montero et al., 2019), and similar to NMDARs, it is a Ca2+ channel regulated by CaM, and binding of CaM to the C-terminus of TRPV1 promotes the desensitization of the channel (Numazaki et al., 2003). We showed here that sigma-1 antagonism promotes the transfer of sigma-1 receptors from the C-terminal domain of TRPV1 to the C-terminus of μ-opioid receptor, and this facilitates the binding of CaM to the C-terminus of TRPV1. Therefore, we show for the first time that the mechanism for the modulation of opioid analgesia by sigma-1 receptors based on the crosstalk between NMDARs and μ-opioid receptor, have an analog on peptidergic

C neurons which uses TRPV1 instead of NMDARs. TRPV1 has multiple known protein partners able to alter channel function (Zhao and Tsang, 2016). It may be worth testing in future studies whether sigma-1 receptor influence other components of the interactome of TRPV1 in addition to CaM binding.

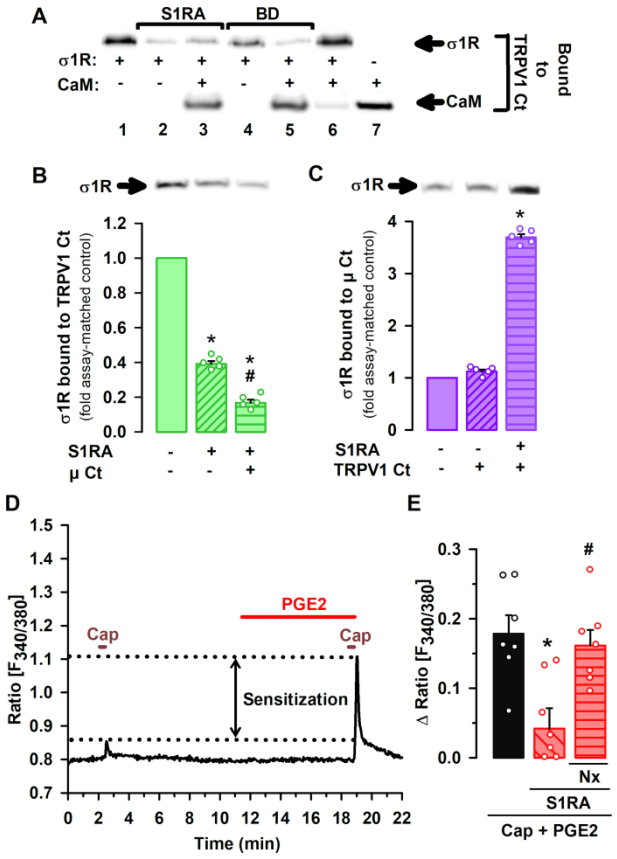

Figure 15. **Influence of sigma-1 antagonism on the interaction of the sigma-1 receptor (σ1R) with TRPV1 and μ-opioid receptors (μ), and the effect on PGE2-induced sensitization of TRPV1 neurons.** (A-C) Experiments were performed in the presence of $CaCl_2$. Blots shown are representative of three experiments. Gels were cropped to show bands under investigation only and full-length gels are provided in Figure 16A-C. (A) Effect of S1RA and BD-1063 (BD) on the *in vitro* interaction of the σ1 receptor (σ1R) and calmodulin (CaM) with the C-terminus (Ct) of TRPV1. σ1R and CaM were incubated with TRPV1 Ct immobilized in N-hydroxysuccinimide (NHS)-activated Sepharose. The bands represent σ1R and CaM that remained bound to the TRPV1 Ct after incubation with the σ1 antagonists or their solvent. (B) Immobilized TRPV1 Ct was incubated with σ1R with and without μ Ct. The blots represent σ1R that remained bound to the TRPV1 Ct after incubation with S1RA or its solvent. (C) Immobilized μ Ct was incubated with σ1R with and without TRPV1 Ct. The blots represent σ1R that remained bound to the μ Ct after incubation with S1RA or its solvent. (B and C) The signals from the blots were expressed as the change relative to the controls, which were assigned an arbitrary value of 1. Values are the mean ± SEM (5 determinations per group). Statistically significant differences between the values obtained in the control (solid bars) and the other experimental groups (striped bars): $*P < 0.05$, and between the values of the group incubated with S1RA alone or with μ Ct: $\#P < 0.05$ (Kruskal–Wallis test followed by Student–Newman–Keuls test). (D) Representative calcium imaging recording (ratio F340/380) of a cultured mouse DRG neuron treated with 0.05 μM capsaicin (Cap) before and after treatment with PGE2. Sensitization of calcium flux by PGE2 is shown between dotted lines. (E) Mean response amplitudes for the increase in the ratio F340/380 in response to capsaicin in cultured neurons from

female mice, sensitized with PGE2 and incubated with S1RA, naloxone (Nx) or their solvents. Values are the mean ± SEM of the values found in 7 different culture dishes, each obtained from a different mouse. Statistically significant differences between the capsaicin response in PGE2-sensitized neurons incubated with S1RA or its solvent: **P* < 0.05, and between the responses from sensitized neurons treated with S1RA alone or associated with Nx: #*P* < 0.05 (one-way ANOVA followed by Bonferroni test).

PGE2 increased calcium flux induced by capsaicin, the prototype TRPV1 agonist (Wainger et al., 2015), and this was fully reversed by S1RA, and in a naloxone-sensitive manner. It is known that endomorphin-2 is released by DRG neurons in response to intracellular calcium increases (Scanlin et al., 2008), and this might account for the naloxone-sensitive effect of S1RA that we recorded. Altogether, our data and previous literature show that sensitization of TRPV1 results in enhanced Ca2+ influx, which promotes the release of endogenous opioid peptides (endomorphin-2) with the potential to induce analgesia through μ-opioid receptor activation. However, this analgesia through neuronally-derived endogenous opioids might be curtailed by the binding of sigma-1 receptor to TRPV1 (Figure 17A). Sigma-1 receptor antagonists trigger the transfer of sigma-1 receptors from the TRPV1 to the μ-opioid receptor, decreasing Ca2+ flux and enhancing the action of endomorphin-2 to induce opioid analgesia in the sensitized peripheral terminal, in the absence of an exogenous opioid drug (Figure 17B). Although extracellular calcium influx through TRPV1 after capsaicin activation is the expected primary responsible for the increase in intracellular calcium we observed, other channels in the plasma membrane and in intracellular locations can also be activated after TRPV1 stimulation and participate in calcium flux (Shah et al., 2020; DuBreuil et al., 2021). Therefore, the modulation of TRPV1 by sigma-1 receptors may merit further study using electrophysiological recordings as a more direct approach to study channel functioning.

TRPV1 are relevant for both pain and itch (Roberson et al., 2013). As sigma-1 antagonism decreases sensitization of TRPV1+ neurons, it could be hypothesized that these drugs might induce antipruritogenic effects in addition to the antihyperalgesic effects showed here. This possibility will be addressed in future studies.

We also tested the effects of sigma-1 antagonism on the hyperalgesia induced by a different peripheral sensitizer: GDNF. This algogenic compound induced RTX-insensitive mechanical hyperalgesia without inducing significant heat hypersensitivity.

The cellular targets of GDNF are non-peptidergic C-nociceptors (IB4+ neurons) (Alvarez et al., 2012), a neuronal population resistant to RTX (Zhang et al., 2013; Montilla-García et al., 2018) that although relevant for mechanical hypersensitivity, is dispensable for heat sensitivity (Cavanaugh et al., 2009), which explains the behavioural effects observed. We also show that sigma-1 antagonism was absolutely devoid of effect on GDNF-induced hyperalgesia in either female or male mice. It is relevant to note that IB4+ neurons do not express endomorphin-2. In addition, similar to PGE2 or NGF, GDNF failed to recruit immune cells at the site of injection that could harbor endogenous opioid peptides to be potentiated by sigma-1 antagonism. Therefore, our results suggest that sigma-1 antagonism needs from the presence of an opioid agonist susceptible of being potentiated to relieve hyperalgesia from peripheral sensitization, and point to the specificity in the modulation of the sensitization of TRPV1 neurons because of their content on endomorphin-2.

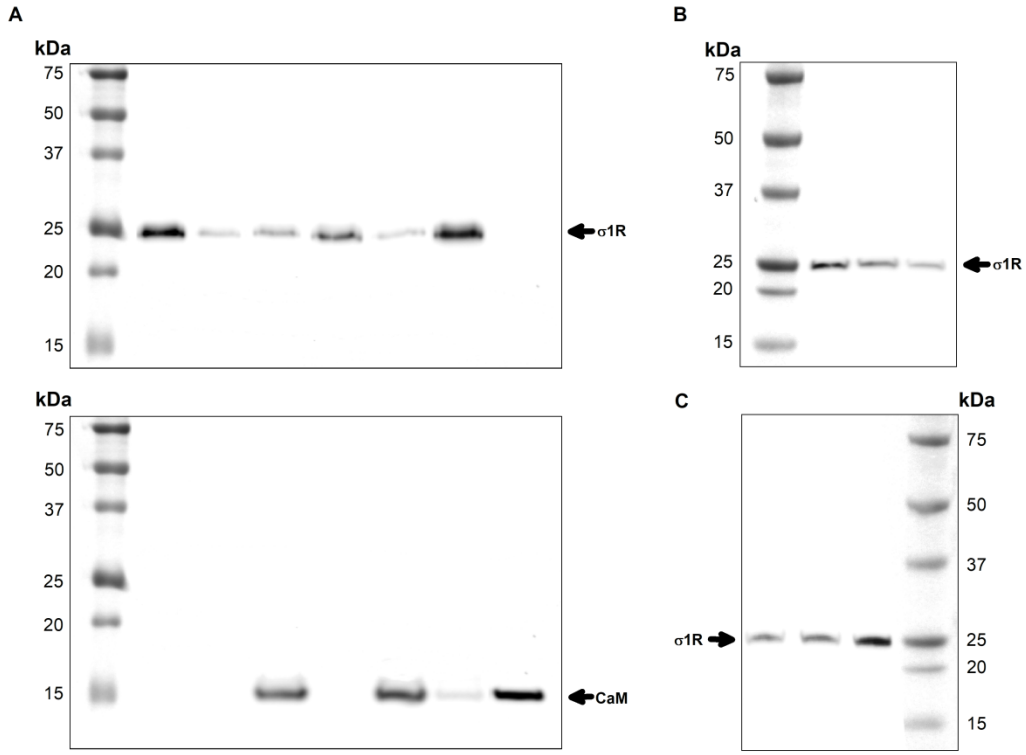

Figure 16. Full-length gels used for Figure 15. (A) Upper image: chemiluminescent visualization of sigma-1 receptor. Lower image: detection of calmodulin (CaM), which was blotted on the same membrane as above subsequent to sigma-1 receptor staining. These images correspond to the cropped gel showed in Figure 15A. (B) Full-length gel used for Figure 15B, and (C) full-length gel used for Figure 15C.

TRPV1+ nociceptors constitute a relatively small population of neurons in the mouse, but most human nociceptors express TRPV1 (Middleton et al., 2021). Therefore, it would be expected that the effects of sigma-1 antagonism on peripheral sensitization, which appear to be restricted to TRPV1+ neurons in the mouse, would be broader in humans.

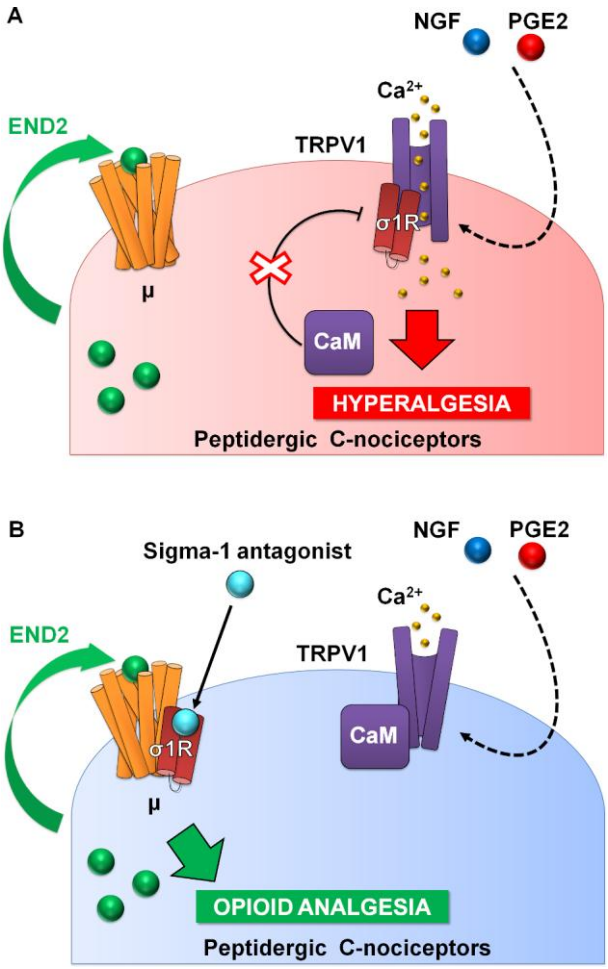

Figure 17. Proposed mechanism of action for the effects of sigma-1 antagonism on hyperalgesia induced by sensitization of TRPV1+ neurons. (A) Sensitization by algogenic chemicals (such as PGE2 and NGF) favors Ca^{2+} influx through TRPV1. In response to Ca^{2+}, sigma-1 receptor (σ1R) binds to TRPV1 preventing calmodulin (CaM) binding (and therefore preventing desensitization of the channel). TRPV1+ neurons produce the endogenous opioid peptide endomorphin-2 (END2), whose effects are not sufficient to relieve hyperalgesia. (B) σ1 antagonists transfer σ1R from TRPV1 to μ opioid receptor (μ) , and this facilitates the interaction of CaM to the desensitization site of TRPV1 and the enhancement of the effects of END2, producing opioid-mediated antihyperalgesic effects during nociceptor sensitization.

In summary, sigma-1 receptors limit peripheral opioid analgesia during sensitization of peptidergic C nociceptors. Sigma-1 antagonists are able to harness neuronally-derived endogenous opioids to reduce hyperalgesia at the pain site, by promoting TRPV1

desensitization and increasing μ-opioid receptor activity. The modulation of the endogenous opioid analgesia by sigma-1 receptors might have potential clinical application for pain treatment.

2. SIGMA-1 RECEPTOR AGONISM EXACERBATES IMMUNE-DRIVEN NOCICEPTION: ROLE OF TRPV1+ NOCICEPTORS

2.1 Material and methods

2.1.1 Experimental animals

Experiments were done in wild-type (WT) female CD-1 mice (Charles River, Barcelona, Spain) and sigma-1 knockout (KO) mice (Animal Experimentation Unit - CIC UGR, Granada, Spain), weighing 25-30 g (8 to 11 weeks old). Knockout mice were generated on a CD-1 background as previously described (Entrena et al., 2009). Animals were housed in colony cages (10 mice per cage), in a temperature-controlled room (22 ± 2 °C) with an automatic 12-h light/dark cycle (08:00–20:00 h). An igloo and a plastic tunnel were placed in each housing cage for environmental enrichment. Animals were fed a standard laboratory diet and tap water ad libitum until the beginning of the experiments. The behavioral experiments were done during the light phase (from 9:00 a.m. to 3:00 p.m.). The mice were randomized to treatment groups, testing each day a balanced number of animals from several experimental groups, and they were also tested randomly throughout the estrous cycle. Mice were handled in accordance with international standards (European Communities Council directive 2010/63), and the experimental protocols were approved by regional (Junta de Andalucía) and Institutional (Research Ethics Committee of the University of Granada) authorities. To decrease the number of animals in this study, we used the same mice for behavioral studies, hematoxylin-eosin staining and immunostaining, when possible.

2.1.2 Administration of PGE2, drugs, and antibodies for *in vivo* use

The peripheral sensitizer PGE2 (Tocris Cookson Ltd., Bristol, United Kingdom) was injected intraplantarly (i.pl.) into the right hind paw in a volume of 20 µL, using a 1710 TLL Hamilton microsyringe (Teknokroma, Barcelona, Spain) with a 301/2-gauge needle. It was dissolved in sterile physiological saline (0.9% NaCl), the stock solution was stored at -20 ºC and further dilutions were performed to obtain the appropriate final concentrations for the different experiments, right before administration. PGE2 was

i.pl. injected at 10 min before the behavioral evaluation based on our previous study (Ruiz-Cantero et al., 2023).

We used five sigma-1 receptor ligands. PRE-084 (2-[4-morpholinethyl]1-phenylcyclohexanecarboxylate hydrochloride), pridopidine (both from Tocris Cookson Ltd.) and dextromethorphan hydrobromide monohydrate (Sigma-Aldrich, Madrid, Spain) were used as sigma-1 agonists. BD-1063 (1-[2-(3,4-dichlorophenyl)ethyl]-4-methylpiperazine dihydrochloride) (Tocris) and S1RA (4-[2-[[5-methyl-1-(2-naphthalenyl)-1H-pyrazol-3-yl]oxy]ethyl] morpholine) (DC Chemicals, Shanghai, China) were used as selective sigma-1 antagonists (Cobos et al., 2008; Romero et al., 2012; Chen et al., 2021; Jiang et al., 2022).

To block TRPV1 actions, ruthenium red (RR) (Tocris), an antagonist of TRP channels (Nasser et al., 2015), was administered i.pl. at a dose of 32 µg. This dose was selected from the dose-response of its antihyperalgesic effects with PGE2 0.5 nmol, i.pl. (Figure 1).

All drugs were dissolved in sterile physiological saline. To study the effect of systemic treatments, drugs were injected subcutaneously (s.c.) into the interscapular zone in a volume of 5 mL/kg. When the effect of the association of two drugs was tested, each drug was injected into a different area of the interscapular zone. To test for the effects of local treatments, drugs or their solvents were administered i.pl. in a volume of 20 µL. The sigma-1 agonists and RR were administered 30 min before the behavioral evaluation. The sigma-1 antagonists BD-1063 or S1RA were injected 5 min before the sigma-1 agonists (35 min before the behavioral evaluation).

The doses of BD-1063 (32 mg/kg, s.c. or 150 µg, i.pl.) and S1RA (200 µg, i.pl.) used, were selected based on our previous study (Ruiz-Cantero et al., 2023).

An anti-Ly6G antibody (BE0075-1; Bio X Cell, Lebanon, NH, USA) was administered intraperitoneally (10 µg/0.2 ml) to inhibit neutrophil infiltration (Tejada et al., 2017). The administration of a nonreactive isotype antibody (BE0089, Bio X Cell) was used as a control.

2.1.3 Superficial plantar incision procedure

As we intended to determine whether sigma-1 agonism exacerbated nociceptive behaviors, we chose a superficial plantar incision as the model, as the lesion is not severe and therefore potentially sensitive for detecting possible increases in pain-like behaviors. The procedure for a superficial plantar incision was adapted from previous studies (Xu and Brennan, 2009; Lu et al., 2022), as has been described that weight bearing asymmetry is recovered as soon as 24h after surgical injury in mice (Lu et al., 2022). Mice were anesthetized with 4% isoflurane (IsoVet®, B. Braun, Barcelona, Spain) in oxygen. During the surgical procedure, anesthesia was maintained with 2.5% isoflurane delivered via a nose cone. The left hindpaw was prepared for the surgery with 10% povidone-iodine. Then, a 5 mm longitudinal incision was made with a single stroke of a number 11 blade through the skin of the hindpaw. The skin was opposed with two single sutures using supramid 5/0 non-absorbable polyamide multifilament thread on a TB15-CT 19 mm needle. The sham surgery comprised anesthesia and the antiseptic preparation of the hindpaw, but no incision was performed.

2.1.4 Fluorescence-activated cell sorting (FACS) analysis

Samples containing the incision and the surrounding tissue (0.6 x 0.2 mm) were collected at 3.5 and 24 h after the plantar incision. Mice were killed by cervical dislocation and plantar tissue was dissected and digested with collagenase IV (1 mg mL-1, LS004188, Worthington, Lakewood, NJ, USA) and DNAse I (0.1%, LS002007, Worthington) for 1 h at 37°C with agitation. Samples were mechanically crushed over a 70 µm filter, then were filtered again in a tube with cell strainer cap (pore size 35 µm) and the rat anti-CD32/16 antibody (1:100, 20 min, Biolegend, San Diego, CA) was used to block Fc-γRII (CD32) and Fc-γRIII (CD16) binding to IgG. Cells were incubated with antibodies recognizing the hematopoietic cell marker CD45 (1:200, clone 30-F11, BioLegend), the myeloid marker CD11b (1:100, BioLegend), and the neutrophil-specific marker Ly6G (1:100, BioLegend), together with a viability dye (1:1000, 65-0865-14; Thermo Fisher Scientific, Massachusetts, USA), for 30 min on ice. The population of neutrophils was determined by using the following markers: CD45+ CD11b+ Ly6G+

cells, and the population of macrophages/monocytes was determined by using the following markers: CD45+ CD11b+ Ly6G-. Before and after incubation with the antibodies, the cells were washed three times in 2% fetal bovine serum (FBS)/PBS (FACS buffer). Cells were fixed with 2% paraformaldehyde for 20 min, and on the next day samples were assayed with a BD FACSCanto II flow cytometer (BD Biosciences, San Jose, CA, USA). Compensation beads were used as compensation controls, and fluorescence minus one (FMO) controls were included to determine the level of nonspecific staining and autofluorescence associated with different cell subsets. All data were analyzed with FlowJo 2.0 software (Treestar, Ashland, OR, USA).

2.1.5 Histology

The paws were dissected and fixed with paraformaldehyde (Sigma-Aldrich) for 24 h at room temperature. Then, they were decalcified in Osteosoft solution (Sigma-Aldrich) at room temperature for 5 days. Next, samples were dehydrated with 70% alcohol, embedded in paraffin and sectioned transversally. Tissue sections (5 µm) were obtained from the mid-plantar region, between the two sutures (see above), and stained with hematoxylin and eosin, according to a previously described method (Montilla-García et al., 2017). Images were acquired with a Nikon Eclipse 50i microscope equipped with a DS-Ri1 camera.

2.1.6 *In vivo* ablation of TRPV1-expressing nociceptors

We used resiniferatoxin (RTX, Tocris Cookson Ltd) as a "molecular scalpel" to selectively ablate TRPV1-expressing neurons. RTX was dissolved in vehicle (10% Tween 80 and 10% ethanol in physiological saline). Animals received two doses of RTX via i.p., two consecutive days (25 µg/kg each dose). We divided it in two doses to minimize distress following a previously described protocol (Ruiz-Cantero et al., 2023). The control group received a double injection with an equal volume of vehicle. To minimize suffering, all procedures were done under isoflurane anesthesia in oxygen. The initial isoflurane dose was 4% for the induction of general anesthesia, during 5 min. Then, RTX (or its solvent) was injected and anesthesia was maintained during 10 min with

isoflurane 2%. The efficacy of the treatment was determined by immunohistochemical assays of L4 DRG (see “Results” for details). Animals were placed in their home cages for 5 days after the first i.p. injection before behavioral testing and sample collection.

2.1.7 Immunohistochemistry

Mice were anesthetized with 4% isoflurane (in oxygen) and perfused transcardially with 0.9% saline solution followed by 4% paraformaldehyde (Sigma-Aldrich). The L4 DRGs were dissected and post-fixed for 1 h in the same paraformaldehyde solution. Samples were dehydrated and embedded in paraffin.

Samples of human lumbar DRGs, embedded in paraffin between 12 and 24 h after the individual's death, were purchased from Tissue Solutions (Glasgow, Scotland).

Tissue sections 5 µm thick were cut with a sliding microtome, mounted on microscope slides (Sigma-Aldrich), deparaffinized in xylol (Panreac Quimica, Castellar del Vàlles, Spain) and rehydrated before antigen retrieval (steam heating for 22 min with 1% citrate buffer, pH 8).

Tissue sections were incubated for 1 h in blocking solution with 5% normal donkey or goat serum, depending on the experiment, 0.3% Triton X-100, and 0.1% Tween 20 in Tris buffer solution. Then, the slides were incubated with the primary antibodies in blocking solution for 1 h at room temperature (RT). The primary antibodies used were: rabbit anti-PGP9.5 (1:400, AB1761, Millipore, MA, USA), mouse anti-sigma-1 receptor (1:200, sc-137075, Santa Cruz Biotechnology) and goat anti-TRPV1 (1:100, sc-12498; Santa Cruz Biotechnology, Heidelberg, Germany). After incubation with the primary antibody, sections were washed again three times for 10 min and incubated with the appropriate secondary antibodies: Alexa Fluor-488 donkey anti-goat (A11055), Alexa Fluor-488 goat anti-mouse (A-11029), Alexa Fluor-594 goat anti-rabbit (A-11012) (all 1:500, from Thermo Fisher Scientific). In some experiments, to test the specificity of the sigma-1 receptor antibody used, we performed the staining procedure omitting the primary antibody. We also stained tissue sections with Bandeiraea simplicifolia lectin I, isolectin B4 (IB4) conjugated with Dylight-594 (1:100, DL-1207; Vector

Laboratories Ltd., Peterborough, United Kingdom). Slides were incubated for 5 min with Hoechst 33342 for nucleic acid staining (1:1000, Life Technologies, Carlsbad, CA, USA), and washed three times before the mounting procedure. Finally, slides were coverslipped with ProLong Gold Antifade mounting medium (Thermo Fisher Scientific). Images were acquired with a confocal laser-scanning microscope (Model A1, Nikon Instruments Europe BV, Amsterdam, Netherlands).

2.1.8 Behavioral tests

The animals were placed in the experimental room for a 1 h acclimation period before starting the experiments. All mice were used in only one experimental procedure (mechanical stimulation or dynamic weight bearing). The experimenters who evaluated the behavioral responses were blinded to the treatment group of each experimental animal.

2.1.8.1 Assessment of mechanical hyperalgesia

Mechanical hypersensitivity was assessed with the paw pressure test following a previously described protocol (Ruiz-Cantero et al., 2023). After the appropriate time after drug administration, mechanical stimulation was applied to the right hindpaw with an Analgesimeter (Model 37215, Ugo-Basile, Varese, Italy). Briefly, the mice were gently pincer grasped between the thumb and index fingers by the skin above the interscapular area. A blunt cone-shaped paw-presser was applied at a constant intensity of 100 g to the dorsal surface of the hindpaw until the animal showed a struggle response. The struggle latency was measured with a chronometer. The test was done three times with a 1-min interval between stimulations, and the mean value of the three trials was recorded as the animal's struggle latency.

2.1.8.2 Assessment of changes on hindpaw weight bearing distribution in freely moving mice

The behavioral effects of paw incision were evaluated using a dynamic weight bearing device (Bioseb, Boulogne, France), where we assessed changes in the weight borne in each limb in freely moving animals, as described previously (Cobos et al., 2012), with modifications. Each mouse was individually placed in a transparent plexiglass evaluation cage (11 cm wide × 11 cm long × 22 cm high) with a floor provided with pressure sensors. Mice were allowed to move freely for 5 min while a camera recorded each movement. The video recording and the paw pressure prints obtained by the instrumented floor were synchronized and analysed by the provided software (BIO-ADWB2-v2.2.6, Bioseb). Pressure prints were manually corrected and validated by an observer blinded to the treatments using the images seen in the video recording as a reference. Frames in which the reading of the paw pressure was not stable because of excessive movement of the animal, were automatically discarded by the software from analysis. Frames in which it was not possible to match a pressure print to a specific part of the mouse (i.e. when it was not evident if a pressure print was made by a paw or a different part of the mouse, such as the tail) were manually discarded by the observer.

After the baseline recording was registered, the mice were anesthetized and a plantar incision was made. To evaluate the time course of the weight bearing alterations after plantar incision, mice were evaluated at 3.5, 24 and 48 h after the procedure. The sigma-1 agonists were administered 24 h after the plantar incision, and their effects were tested at 30 min, 60 min and 24 h after drug injection. Reversal of the effect of sigma-1 agonists by BD-1063, S1RA or by sigma-1 knockout were always tested 30 min after the administration of the sigma-1 agonists. All results were expressed as the ratio between the weight borne by the injured and the non-injured limb.

2.1.9 Data analysis

The data were analyzed with the SigmaPlot 12.0 program (Systat Software Inc., San Jose, CA, USA). Most statistical analysis was carried out with one-way analysis of

variance (ANOVA). Two-way repeated-measures ANOVA were used for the analysis of the time courses of weight bearing differences after plantar incision. The Student–Newman–Keuls post-test was used in all cases. The differences between means were considered significant when the P value was below 0.05.

2.2 Results

2.2.1 Comparison of PGE2-induced mechanical hyperalgesia in wild-type and sigma-1 knockout mice

We first explored the effects of the peripheral sensitizer PGE2 on the struggle response to mechanical stimulation in WT and sigma-1 KO mice. We intraplantarly administered PGE2 or its solvent (saline), and tested the behavioral response 10 min after the injection. Both WT and sigma-1 KO mice i.pl. treated with saline showed a similar (non-significantly different) latency to respond to the mechanical stimulation (21.67 ± 1.01 in WT vs 21.30 ± 1.22 in sigma-1 KO mice). We found that PGE2 (0.125 – 0.5 nmol) induced a similar dose-dependent decrease in the latency to respond (i.e. mechanical hyperalgesia) in animals from both genotypes (Figure 2). The administration of the lower dose of PGE2 (0.125 nmol) showed no difference in the response latency in comparison to solvent-treated animals from either genotype (Figure 2). The lack of efficacy of this low dose of PGE2 to show sensitization was not because the evaluation time was too short, because we evaluated WT mice at 30 or 60 min after PGE2 administration and we did not detect any significant variation in the response to the mechanical stimulation in comparison to solvent-treated animals (Figure 3). In contrast, a higher dose of 0.5 nmol PGE2 induced a pronounced and sustained hyperalgesia from 10 min to at least 60 min post-administration, reaching values of struggle response latency of approximately 8 seconds (Figure 3).

2.2.2 The systemic administration of sigma-1 agonists enhances PGE2-induced mechanical hyperalgesia without altering normal mechanical sensitivity

We studied the effects of the systemic administration of sigma-1 agonists in animals treated with a low dose of i.pl. PGE2 (0.125 nmol), which as noted above does not induce sensitization to the mechanical stimulation. The s.c. administration of the nonselective sigma-1 agonist dextromethorphan (8-16 mg/kg) induced a dose-dependent decrease in the struggle response latency of PGE2-injected mice, reaching an averaged value of response latency below 10 seconds with the highest dose tested (Figure 4A). This latency value was similar to that yielded after sensitization with PGE2 0.5 nmol, a much higher dose of the peripheral sensitizer (compare Figs. 2 and 3). The effect of the antitussive drug was replicated by the s.c. administration of the prototypical sigma-1 agonist PRE-084 (8-32 mg/kg) and also by the selective sigma-1 agonist pridopidine (0.125-0.25 mg/kg), which also dose-dependently decreased the response latency of mice injected with a low dose of PGE2 (Figure 4A).

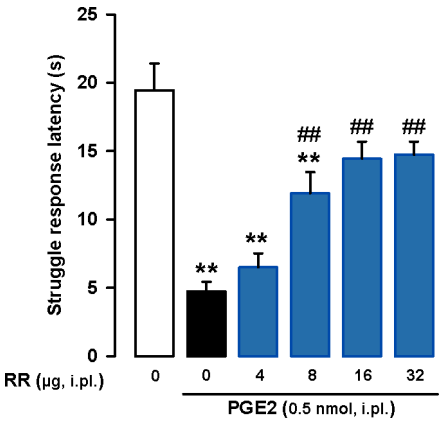

Figure 1. Effects of the local administration of the TRP antagonist ruthenium red on PGE2-induced mechanical hyperalgesia. The results represent the latency to struggle response evoked by a mechanical stimulus of 100 g in mice administered intraplantarly (i.pl.) with PGE2 (0.5 nmol) and with ruthenium red (RR, 4-32 µg). Each bar and vertical line represent the mean ± SEM of the values obtained in 8-11 animals. Statistically significant differences between the values obtained in control non-sensitized animals (white bar) and the other experimental groups: **P < 0.01, and between the values obtained in PGE2-treated animals administered with RR or its solvent: ##P < 0.01 (one-way ANOVA followed by Student-Newman-Keuls test).

Importantly, when we administered the sigma-1 agonists to non-sensitized mice, at a dose high enough to markedly potentiate PGE2-induced mechanical hyperalgesia (dextromethorphan 16 mg/kg, PRE-084 32 mg/kg, and pridopidine 0.25 mg/kg), we did not find any change in the struggle latency to mechanical stimulation (Figure 4B).

These results indicate that systemic sigma-1 agonism is unable to induce sensitization to the mechanical stimulus per se, but it is able to enhance the PGE2-induced mechanical hyperalgesia.

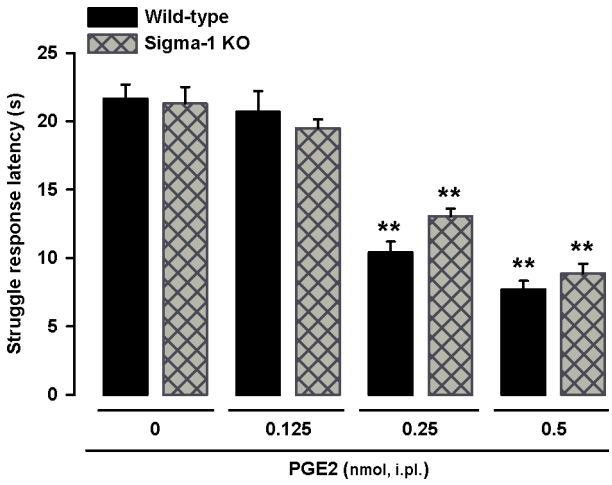

Figure 2. Effects induced by PGE2 on the behavioral responses to mechanical stimulus in wild-type and sigma-1 knockout mice. The results represent the latency to struggle response evoked by a mechanical stimulus of 100 g in wild-type (WT) or sigma-1 knockout (KO) mice intraplantarly (i.pl.) injected with several doses of PGE2 (0.125-0.5 nmol) or its solvent. Each bar and vertical line represent the mean ± SEM of the values obtained in 8-11 animals. Statistically significant differences between the values obtained in control non-sensitized animals and the other experimental groups: **P < 0.01. No significant differences were found between WT and KO values at any dose of PGE2 tested (two-way ANOVA followed by Student-Newman-Keuls test).

2.2.3 Hindpaw weight bearing asymmetry in response to plantar incision: effects of the systemic administration of sigma-1 agonists and dependence on neutrophil infiltration

As PGE2 is an inflammatory mediator, we next aimed to explore the effects of sigma-1 agonists on a more translational model which involves inflammation. Since inflammation is a natural process that occurs after tissue damage, we used the hindpaw plantar incision model. We examined the characteristics of the hindpaw injury using hematoxylin-eosin staining. We found that the incision cut the epidermis and dermis layer without (or minimally) injuring the fascia and muscle tissue, as seen in the representative image obtained 3.5 h after injury, with the presence of an edema in the subcutaneous tissue but minimal immune infiltrate (compare naïve control in the left panels and 3.5 h after injury in the middle panels in Figure 5A). Swelling and inflammation were still present in the dermis and in the subcutaneous tissue 24 h after the injury, with the presence of a substantial number of inflammatory cells infiltrated even in muscle tissue (Figure 5A, right panels). We also quantitatively assessed immune cell recruitment after plantar incision using flow cytometry. We found little neutrophil or macrophage/monocyte recruitment at 3.5 h after injury, but 24 h after incision there was prominent immune infiltration, which was composed mainly by neutrophils with more limited numbers of macrophages/monocytes (Figure 5B and C).

Then, we studied nociception after injury by evaluating the weight bearing ratio between the injured (ipsilateral) and the non-injured (contralateral) hindlimbs. The weight bearing distribution during the basal recording was equal in each lower extremity (the ratio of the values was approximately 1). However, mice developed significant asymmetry in weight bearing at 3.5 h after surgery, manifested as a significant reduction in the ipsilateral/contralateral hindpaw weight bearing ratio (i.e. the weight borne by the injured hindlimb is decreased favoring the use of the non-injured contralateral hindlimb). Weight bearing deficits were short-lived, since they reached values similar to the basal condition as soon as 24 h after surgery (Figure 5D). Mice submitted to the sham procedure did not show any significant change in the weight borne by their hindlimbs at any time-point tested (Figure 5D).

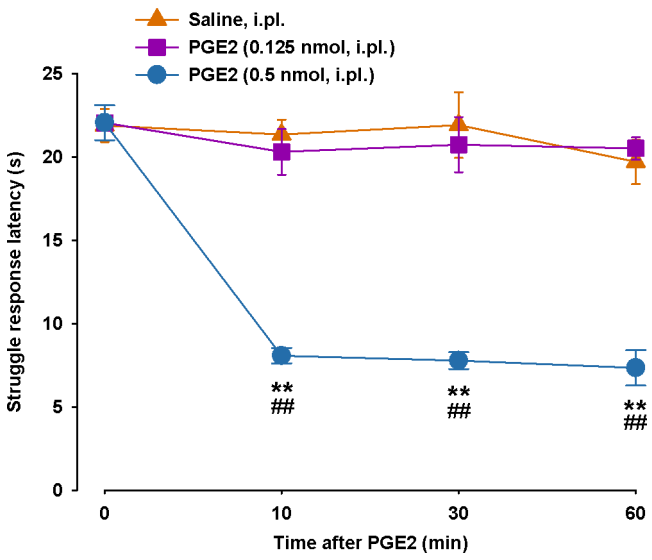

Figure 3. Time course of the effects induced by PGE2 on the behavioral responses to mechanical stimulus. The results represent the latency to struggle response evoked by a mechanical stimulus of 100 g in mice intraplantarly (i.pl.) treated with PGE2 (0.125 or 0.5 nmol) or its solvent, and evaluated at several times (10, 30 and 60 min) after injection. Each point and vertical line represent the mean ± SEM of the values obtained in 8–11 animals. Statistically significant differences between PGE2 and its solvent at the same time after treatment: **P < 0.01, and between untreated animals (time 0) and after PGE2: ##P < 0.01 (two-way ANOVA followed by Student-Newman-Keuls test).

Altogether, our data show that although in our experimental conditions tissue injury and inflammation were still observable 24 h after the surgical procedure, they were not of sufficient intensity to induce an apparent weight bearing asymmetry in the hindlimbs.

We then tested the effects of the administration of the sigma-1 agonists or their solvent after plantar incision. Hindpaw weight bearing asymmetry was obvious at 3.5 h after injury in all groups of mice evaluated (Figure 6A). One day (24 h) after the injury, at time 0 (immediately before the s.c. injection of the drugs tested or their solvent),

there was no observable weight bearing asymmetry, with values of weight bearing ratio between both hindlimbs of approximately 1 (Figure 6A). We then performed the s.c. administration of the non-selective sigma-1 agonist dextromethorphan (16 mg/kg), the prototypical sigma-1 agonist PRE-084 (32 mg/kg) and the selective sigma-1 agonist pridopidine (0.25 mg/kg), at doses that induced sensitization to mechanical stimulation in PGE2-injected mice without inducing mechanical hyperalgesia by themselves (as shown in the previous section). The administration of each sigma-1 agonist tested induced a significant reduction in the ipsilateral/contralateral hindpaw weight bearing ratio from 30 to 90 min post-administration; and then, weight bearing asymmetry fully disappeared 48 h after surgical injury (i.e. 24 h after drug administration) (Figure 6A). Saline (s.c.) administration did not significantly change the distribution of the weight borne by each hindlimb during the 24 h test period (Figure 6A).

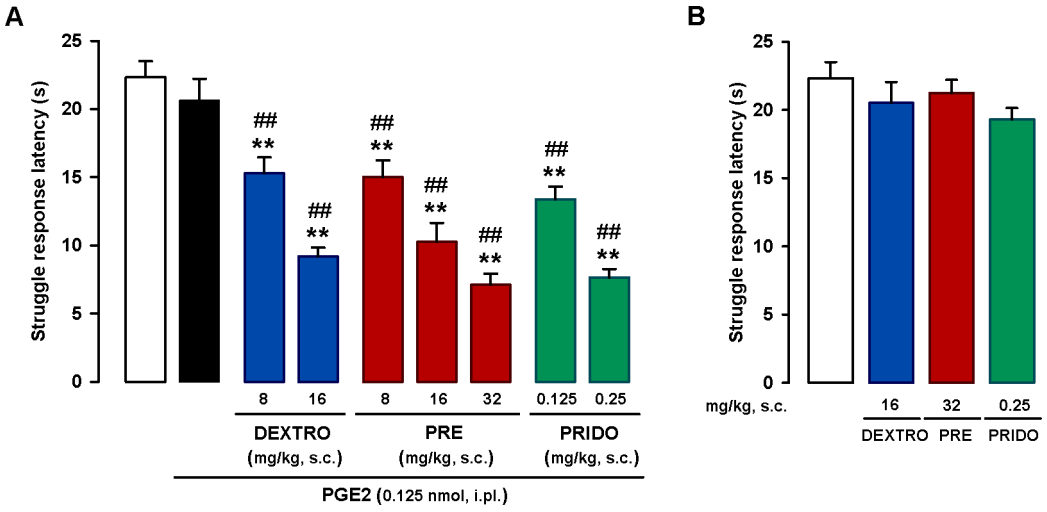

Figure 4. The systemic administration of sigma-1 agonists enhances PGE2-induced mechanical hyperalgesia. The results represent the latency to struggle response evoked by a mechanical stimulus of 100 g in wild-type mice. (A) Effect of the subcutaneous (s.c.) administration of the sigma-1 agonists dextromethorphan (DEXTRO), PRE-084 (PRE), pridopidine (PRIDO) or their solvent (saline), in mice sensitized with the intraplantar (i.pl.) administration of a low dose of PGE2 (0.125 nmol). (B) Absence of effect of the s.c. administration of the sigma-1 agonists in non-sensitized mice (i.e. animals not treated with PGE2 i.pl.). (A and B) Each bar and vertical line represent the mean ± SEM of the values obtained in 8-11 animals. (A) Statistically significant differences between the values obtained in control nonsensitized animals (white bar) and the other experimental groups: **P < 0.01; between the values obtained in sensitized wild-type animals, injected with PGE2, administered with the sigma-1 agonists (blue, red and green bars) or their solvent (black bar): ##P < 0.01 (one-way ANOVA followed by Student-Newman-Keuls test). (B) There were no significant differences between the values obtained in non-sensitized mice treated with the sigma-1 agonists or their solvent (one-way ANOVA followed by Student-Newman-Keuls test).

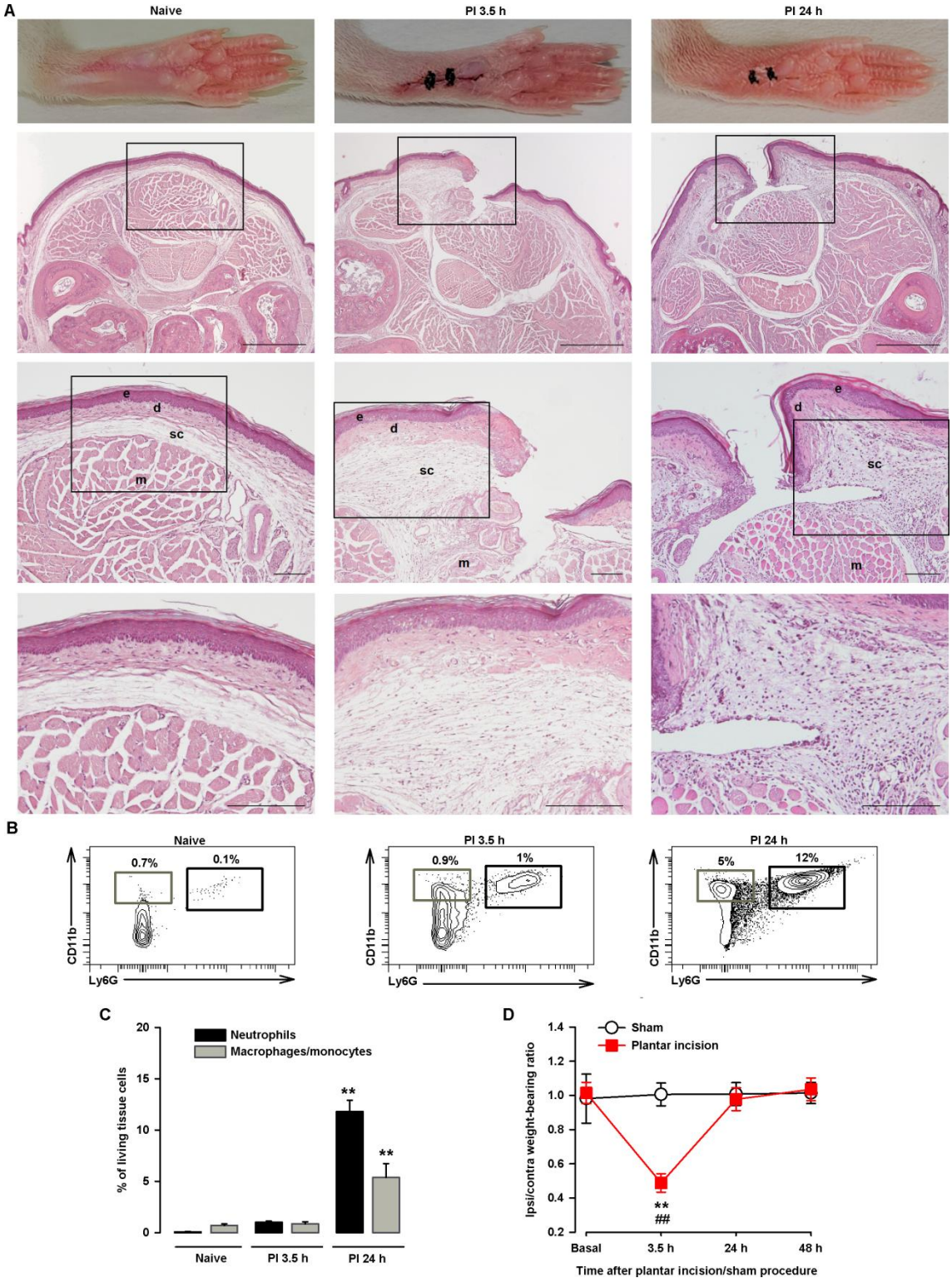

Figure 5. Time course of hindpaw weight bearing distribution, immune cell recruitment and histological changes in the hindpaw after plantar incision. (A) Representative pictures of the paw from control uninjured mice and from mice 3.5 h and 24 h after the incision, and photomicrographs of hematoxylin and eosin-stained paw sections obtained from the mid-plantar region from the same experimental groups, scale bar 500 µm in the upper panels, 100 µm in the middle and 50 µm in the bottom panels. Middle and bottom panels show details of the boxed areas in the top and middle panels, respectively. The relevant structures are labeled in the middle panels for clarity (e: epidermis, d: dermis, sc: subcutaneous tissue, m: muscle tissue). Note the increase in the thickness of d and sc both at 3.5 h

and 24 h after injury, and the presence of the immune cell infiltrate in sc and m at 24 h after incision. (B) Representative FACS diagrams, gated from CD45+ cells, showing that neutrophils (CD11b+Ly6G+ cells), and to a lesser extend macrophages/monocytes (CD11b+Ly6G- cells), increase in the paw 24 h after plantar incision. Gating for neutrophil and macrophages/monocytes quantification is shown as a black rectangle and gray rectangle, respectively, in each FACS diagram. (C) Quantification of neutrophils and macrophages/monocytes with respect to the number of living cells in paw samples from naïve mice and mice with the plantar incision. Each bar and vertical line represent the mean ± SEM of the values obtained in 5-6 animals. Statistically significant differences between the values obtained for each cell type in samples from naïve mice and the other experimental groups: **P < 0.01 (one-way ANOVA followed by Student-Newman-Keuls test). (D) The results represent the ratio between the weight borne by the ipsilateral (ipsi) and the contralateral (contra) paw to the incision, before the surgery and at several times (3.5, 24 and 48 h) after injury (or sham procedure as a control) to wild-type mice. Each point and vertical line represent the mean ± SEM of the values obtained in 8-11 animals. Statistically significant differences between the values obtained in the basal measure and after injury: **P < 0.01; between the values from sham and injured mice, evaluated at the same time-point after the procedure: ##P < 0.01 (two-way repeated-measures ANOVA followed by Student-Newman-Keuls test).

Taking into account that immune cells constitute one of the main sources of PGE2 at the inflamed site (see Introduction for references), and that in our experimental conditions we saw obvious neutrophilic infiltration, we tested the influence of neutrophil depletion (by the administration of an anti-Ly6G) on the proalgesic effect of PRE-084. Mice treated with the anti-Ly6G (10 μg, i.p.), or with a non-reactive isotype antibody as a control, show a similar weight bearing asymmetry at 3.5 h after plantar incision, and both groups returned to values similar to the basal condition 24 h after surgical injury. Then, the administration of PRE-084 (32 mg/kg, s.c.) induced a relapse in weight bearing asymmetry in mice treated with the isotype control antibody (from 30 to 90 min after drug administration), but not in mice treated with the anti-Ly6G (Figure 6B). We also tested the effect of both antibodies on immune cell recruitment after plantar incision. Treatment with the anti-Ly6G induced a 72% decrease in neutrophil infiltration compared to the values seen in isotype control-treated mice, but there was no change in macrophage/monocyte recruitment between mice treated with the anti-Ly6G or the isotype control (Figure 6C and D), which indicates the selectivity of the neutrophil depletion strategy used.

In summary, the sigma-1 agonists dextromethorphan, PRE-084 and pridopidine were able to trigger pain-like behaviors once they apparently resolved, when inflammation and immune cell infiltrate after tissue injury were still present. The presence of

neutrophils at the site of the surgical injury is essential for the proalgesic effect induced by sigma-1 agonism.

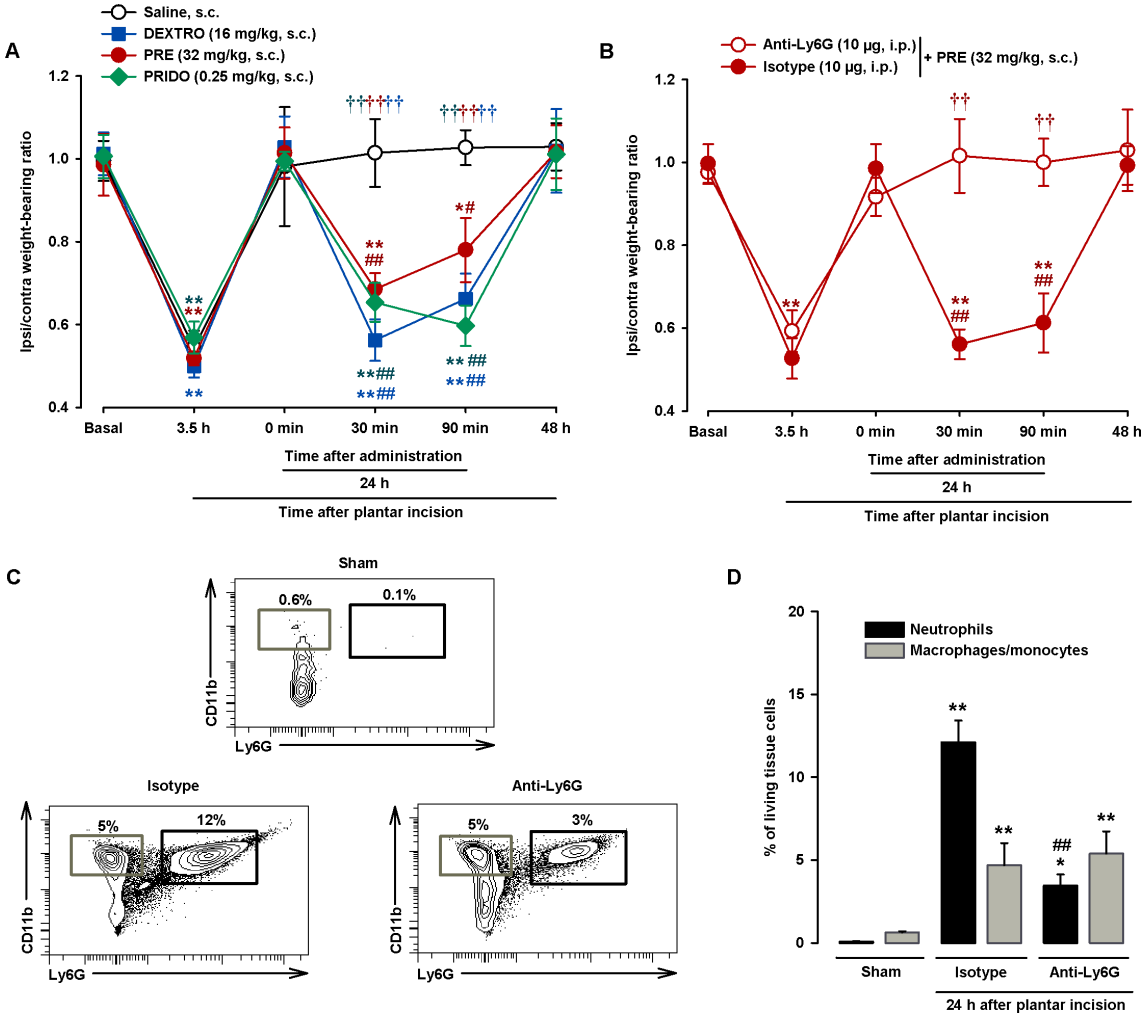

Figure 6. The systemic administration of sigma-1 agonists induces a relapse of hindpaw weight bearing asymmetry after plantar incision in wild-type mice through the actions of neutrophils. (A and B) The results represent the ratio between the weight borne by the ipsilateral (ipsi) and the contralateral (contra) paw to the incision of wild-type mice (A) administered subcutaneously (s.c.) with dextromethorphan (DEXTRO), PRE-084 (PRE), pridopidine (PRIDO) or their solvent, and (B) treated intraperitoneally 24 h before plantar incision with anti-Ly6G (10 µg) or isotype control and administered s.c. 24 h after plantar incision with PRE. DEXTRO, PRE, PRIDO or solvent. Hindpaw weight bearing was recorded immediately before (time 0) and at several times (30 and 90 min and 24 h) after the s.c. injection of sigma-1 agonists. (C) Quantification of neutrophils and macrophages/monocytes with respect to the number of living cells in the paw from naïve mice and 3.5 h or 24 h after the plantar incision in mice treated with the anti-Ly6G or the isotype control. (A and B) Each point and vertical line represent the mean ± SEM of the values obtained in 8-11 animals. Statistically significant differences between the basal measurement and the rest of values: *P < 0.05, **P < 0.01; between the measure previous to drug administration (0 min) and the following measures: #P < 0.05 ## P < 0.01; and between animals treated with the drugs or saline, or animals treated with the anti-Ly6G or the isotype control: ††P < 0.01 (two-way repeated-measures ANOVA followed by Student-Newman-Keuls test). (C) Each bar and vertical line represent the mean ± SEM of the values obtained in 5-6 animals. Statistically significant differences between the number of neutrophils or macrophages/monocytes from sham animals and the other experimental groups: *P < 0.05, **P < 0.01; and between the number of neutrophils from animals treated with the anti-Ly6G or the isotype control: ## P < 0.01. There were no statistical differences

between the number of macrophages/monocytes from mice treated with anti-Ly6G vs. the isotype control (one-way ANOVA followed by Student-Newman-Keuls test).

2.2.4 Selectivity of the pronociceptive effects induced by systemic administration of sigma-1 agonists

We tested for the selectivity of the effects induced by dextromethorphan, PRE-084 and pridopidine on PGE2-induced hyperalgesia and on hindpaw weight bearing asymmetry after surgical injury.

We first evaluated the effects of the association of the s.c. administration of these sigma-1 agonists with the sigma-1 antagonist BD-1063 (32 mg/kg, s.c.) on PGE2-induced hyperalgesia. The administration of the sigma-1 antagonist did not modify the struggle latency to mechanical stimulation in nonsensitized animals (Figure 7A). However, when this dose of BD-1063 was associated with the sigma-1 agonists (dextromethorphan 16 mg/kg, PRE-084 32 mg/kg, or pridopidine 0.25 mg/kg) at s.c. doses which were able to markedly enhance the hyperalgesia induced by a low dose of PGE2 (0.125 nmol), BD-1063 administration was able to fully reverse the sensitizing effect of all three sigma-1 agonists increasing the struggle response latency up to values similar to those found in control non-sensitized animals (Figure 7A).

As an additional test to verify the selectivity of the effect of dextromethorphan, PRE-084 and pridopidine, on PGE2-induced hyperalgesia, we evaluated the effect of these drugs on mice lacking the sigma-1 receptor, the purported target of the three sigma-1 agonists tested. As previously commented, both WT and sigma-1 KO mice showed similar responses to mechanical stimulation in the paw injected with PGE2 0.125 nmol or its solvent (Figure 7B). However, although WT mice given the sigma-1 agonists dextromethorphan (16 mg/kg, s.c.), PRE-084 (32 mg/kg, s.c.) or pridopidine (0.25 mg/kg, s.c.) showed marked potentiation of PGE2-induced hyperalgesia, strongly decreasing the response latency to mechanical stimulation, any of these sigma-1 agonists was able to alter the behavioral response to the sensory stimulus in PGE2-injected sigma-1 KO mice (Figure 7B). The absence of activity of dextromethorphan, PRE-084, and pridopidine in mice lacking sigma-1 receptors suggests that off-target

effects do not contribute to the potentiation of PGE2-induced hyperalgesia by these drugs.

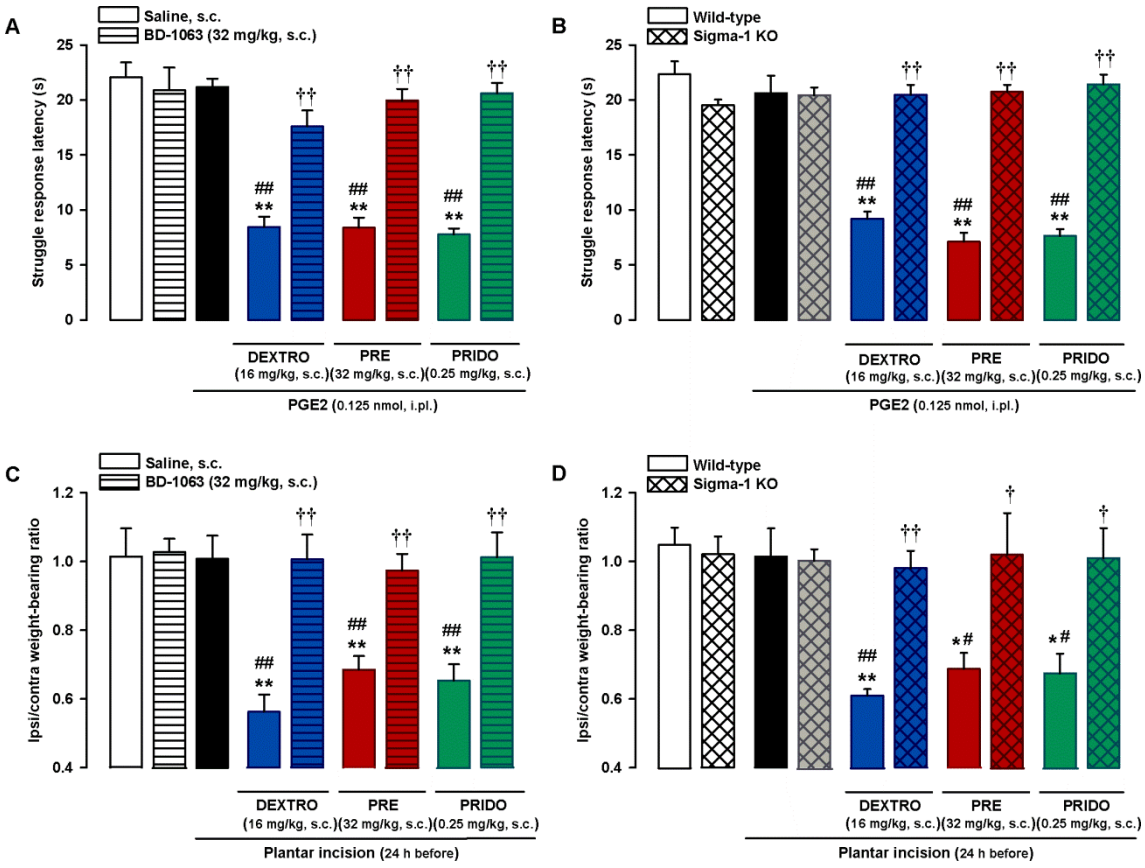

Figure 7. Selectivity of the effects induced by the systemic administration of sigma-1 agonists on PGE2-induced mechanical hyperalgesia and on hindpaw weight bearing asymmetry after plantar incision. (A and C) Reversion of the effects of sigma-1 agonists by the sigma-1 antagonist BD-1063 on (A) mechanical hyperalgesia induced by the intraplantar (i.pl.) injection of PGE2, and on (C) hindpaw weight bearing asymmetry 24 h after plantar incision in wild-type mice. Wild-type mice were subcutaneously (s.c.) treated with BD-1063 (BD) or its solvent alone or associated with dextromethorphan (DEXTRO), PRE-084 (PRE), pridopidine (PRIDO) or their solvent. (B and D) Comparison of the pronociceptive effects of the s.c. administration of the sigma-1 agonists in wild-type (WT) and sigma-1 knockout (KO) mice on (B) PGE2-induced mechanical hyperalgesia and on (D) hindpaw weight bearing asymmetry 24 h after plantar incision. (A-D) Each bar and vertical line represent the mean ± SEM of the values obtained in 8-11 animals. Statistically significant differences between the values obtained in WT non-sensitized control animals (left white bars) and the other experimental groups: *P < 0.05, **P < 0.01. (A and C) Statistically significant differences between the values obtained in sensitized WT animals, injected with PGE2 or with paw incision (black bars), administered with the sigma-1 agonists or their solvent: ##P < 0.01, and between the values obtained in WT sensitized animals administered with the sigma-1 agonist associated with BD or its solvent: ††P < 0.01. (B and D) Statistically significant differences between the values obtained in WT animals sensitized with PGE2 or with paw incision (black bars), administered with the sigma-1 agonists or their solvent: #P < 0.05, ##P < 0.01; and between the effects of sigma-1 agonists administered to WT and sigma-1 KO mice: †P < 0.05; ††P < 0.01 (one-way ANOVA followed by Student-Newman-Keuls test).

We then tested for the selectivity of the effects induced by the sigma-1 agonists on weight bearing asymmetry after plantar incision, using the same strategies that we described above: the association of the administration of the sigma-1 agonists with the sigma-1 antagonist BD-1063 and the comparison of the effects of the sigma-1 agonists in WT and sigma-1 KO mice. Experiments were made 24 h after superficial plantar incision, since as described in the section above, mice apparently recovered a normal weight bearing distribution at this time post-injury, which was approximately equal in the injured and non-injured hindlimb (the ratio of the weight borne by each limb was approximately 1), but s.c. treatment with the sigma-1 agonists dextromethorphan (16 mg/kg), PRE-084 (32 mg/kg) and pridopidine (0.25 mg/kg) were able to exacerbate weight-bearing asymmetry. The s.c. administration of BD-1063 did not modify the weight borne in each hindpaw in non-injured animals but was able to fully reverse the weight bearing asymmetry induced by the sigma-1 agonists (Figure 7C). When we compared WT and sigma-1 KO mice we found that there were no significant differences between the ratio of both hindlimbs in sham mice and those submitted to the plantar incision 24 h before the evaluation, in animals from either genotype. However, although the sigma-1 agonists induced weight bearing asymmetry in WT mice, they were unable to alter the ratio of the weight borne in each hindpaw in sigma-1 KO mice (Figure 7D).

These results support the selectivity of the effects induced by the sigma-1 agonists on both PGE2-induced hyperalgesia and hindpaw weight bearing asymmetry during inflammation-associated tissue damage.

2.2.5 Expression of sigma-1 receptors in mouse and human DRGs

To study the expression of sigma-1 receptors in the DRG, we used an immunohistochemical approach. DRG neurons were identified using the pan-neuronal marker PGP9.5. Sigma-1 receptor immunoreactivity was found in most (if not all) PGP9.5+ DRG cells, indicating that both markers label an overlapping cell population (i.e. DRG neurons). However, the labelling of PGP9.5 and sigma-1 receptor in the neuronal bodies followed different patterns, as there was a rounded area in centred position within most neurons which was completely devoid of sigma-1 staining, but

which retained intense PGP9-5 labelling (Figure 8A, top panels). Higher magnification photomicrographs showed that this particular area in which sigma-1 labelling was absent clearly overlapped with Hoechst 33342 staining (Figure 8A, middle panels). This latter compound labels the cell nuclei, and hence our data indicate that sigma-1 receptors are not present in this location. No sigma-1 receptor immunostaining was detected in DRG sections when the sigma-1 receptor primary antibody was omitted (Figure 8A, bottom panels), supporting the specificity of the sigma-1 receptor antibody used.

Staining for PGP9.5 and sigma-1 receptor in human DRG samples yielded results equivalent to those found in mouse samples: sigma-1 staining was also present in virtually all PGP9.5+ cells and absent in the neuronal nuclei (Figure 8B, top and middle panels). It is interesting to note that human DRG neurons were considerably larger than mouse neurons (compare Figure 8A and B). In contradistinction to the results on mouse samples, the sigma-1 receptor antibody labelled some extraneuronal small-sized particles in the human slices (Figure 8B top and middle panels). When the primary sigma-1 receptor antibody was omitted during the staining procedure, we observed almost an absolute loss of sigma-1-like staining in PGP9.5+ cells, but the extraneuronal staining was preserved (Figure 8B bottom panels). These results support the specificity of the sigma-1 staining in human sensory neurons, and also indicate that the extraneuronal labelling that we detected is due to nonspecific staining during the procedure.

Altogether, our results show that sigma-1 receptors are markedly present in both mouse and human peripheral sensory neurons.

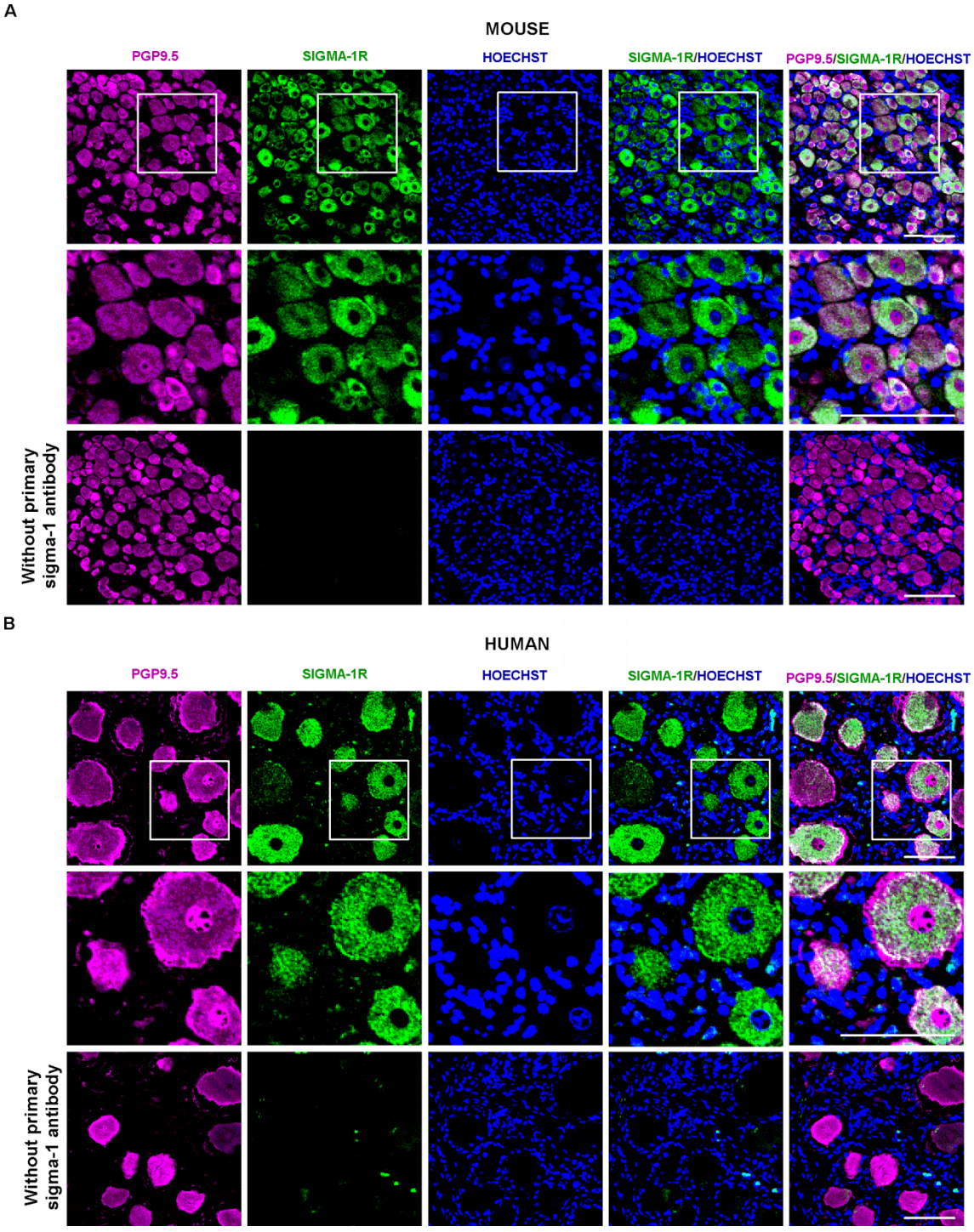

Figure 8. The sigma-1 receptor is selectively present in neurons in mouse or human dorsal root ganglion (DRG). Representative images from the labelling of the pan-neuronal marker PGP9.5 (magenta), sigma-1 receptor (Sigma-1R, green) and Hoechst 33342 (Hoechst) staining (blue) in samples from (A) a L4 DRG from Naïve mice and (B) a human lumbar DRG. Top and bottom panels show low magnification images of experiments performed in the presence (top) or absence (bottom) of the sigma-1 receptor primary antibody. Middle panels show a higher magnification of the area squared in the top panels. Scale bar 100 µm.

2.2.6 Involvement of TRPV1+ nociceptors in the pronociceptive effects of sigma-1 agonism

We aimed to test whether the pronociceptive effects of sigma-1 agonism was mediated by TRPV1+ peripheral sensory neurons. Staining for TRPV1 and IB4 showed no or minimal overlap among DRG neurons from intact mice (see top panels of Figure 9A for representative images). Treatment with the molecular scalpel RTX abolished TRPV1 labeling, but IB4 staining was still readily detectable (Figure 9A, bottom panels), confirming the specificity of the ablation procedure.

We next studied the effects of the *in vivo* ablation of TRPV1-expressing neurons by RTX on the effects of sigma-1 agonists. *In vivo* ablation of TRPV1+ neurons did not affect the responses to mechanical stimulation in mice i.pl. treated with either the low dose of PGE2 (0.125 nmol) or its solvent. However, the s.c. administration of sigma-1 agonists (dextromethorphan 16 mg/kg, PRE-084 32 mg/kg, or pridopidine 0.25 mg/kg) was unable to enhance the sensitization to the mechanical stimulus induced by PGE2 in RTX-treated animals, in contrast to the marked decrease in the struggle response latency in response to the mechanical stimulation seen in PGE2-sensitized mice treated with the solvent of RTX (Figure 9B).

We also explored whether TRPV1+ neurons were responsible for the effects of sigma-1 agonists on weight bearing asymmetry after plantar incision. As in the sections above, experiments were made 24 h after superficial plantar incision, since at this time mice apparently recovered a normal weight bearing distribution which was approximately equal in the injured and non-injured hindlimb, but s.c. treatment with the sigma-1 agonists dextromethorphan (16 mg/kg), PRE-084 (32 mg/kg) and pridopidine (0.25 mg/kg) induced weight-bearing asymmetry. RTX treatment did not alter the hindpaw weight bearing distribution in either mice with plantar incision or with the sham procedure (and treated with the solvent of the drugs), but fully prevented the sensitizing effect of all three sigma-1 agonists on weight bearing asymmetry (Figure 8C).

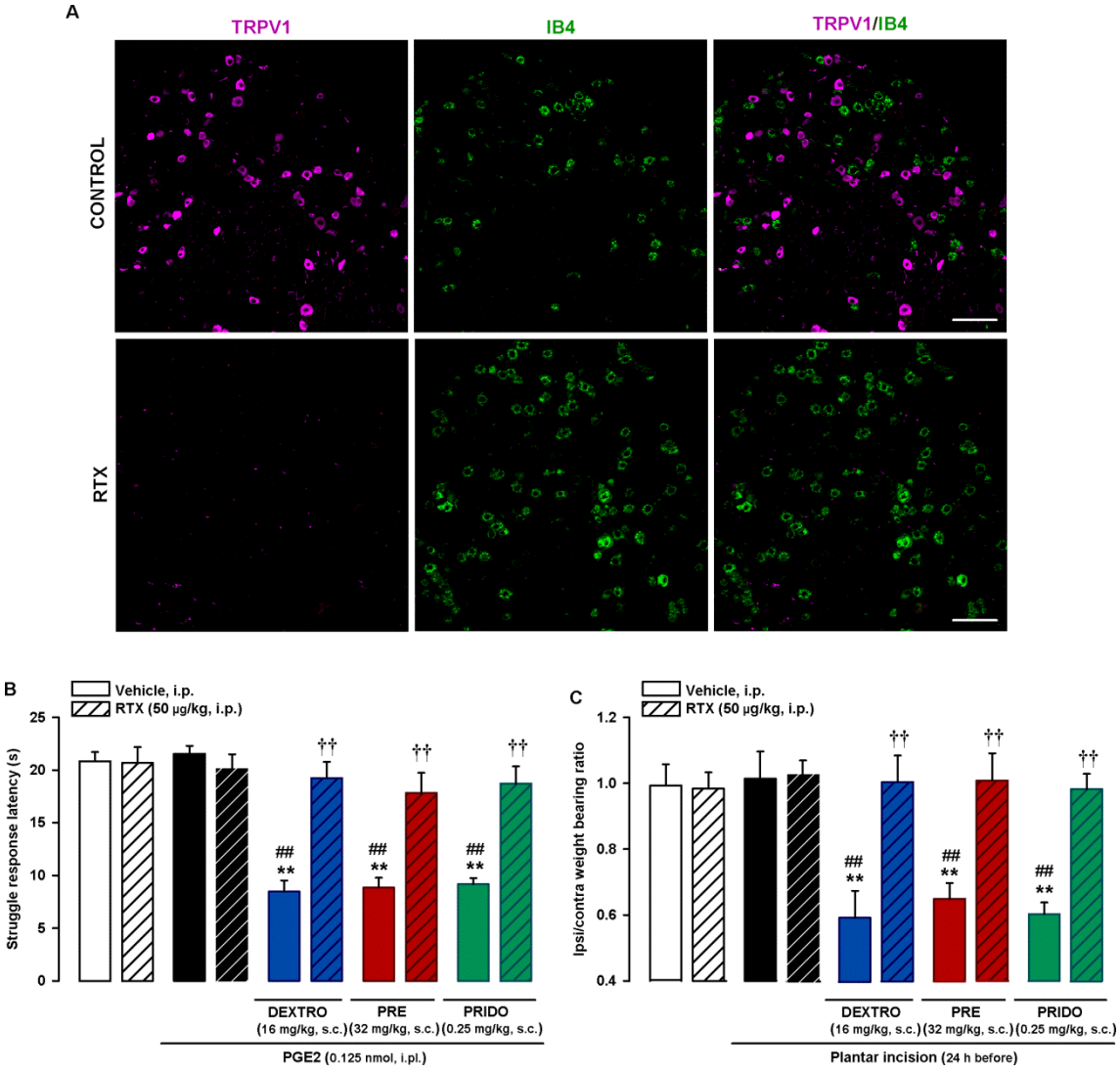

Figure 9. Effect of the *in vivo* ablation of TRPV1-expressing neurons on the effects induced by sigma-1 agonists on PGE2-induced mechanical hyperalgesia and on hindpaw weight bearing asymmetry after plantar incision. Wild-type mice were treated intraperitoneally for two consecutive days with resiniferatoxin (RTX, 25 µg/kg) or its vehicle five days before obtaining samples or performing the behavioral experiments. (A) Double labeling of TRPV1 (magenta) and isolectin B4 (IB4, green) in the L4 dorsal root ganglion (DRG). Top panels: samples from vehicle-treated mice (control). Bottom panels: samples from mice treated with RTX. Scale bar, 100 µm. (B) The results represent the latency to struggle response evoked by a mechanical stimulus of 100 g in mice administered subcutaneously (s.c.) with the sigma-1 agonists dextromethorphan (DEXTRO), PRE-084 (PRE), pridopidine (PRIDO) or their solvent, and injected intraplantarly (i.pl.) with PGE2 (0.125 nmol) or its solvent. (C) The results represent the ratio between the weight borne by the ipsilateral (ipsi) and the contralateral (contra) hindpaw to the incision of wild-type mice administered s.c. with the sigma-1 agonists or their solvent. Behavioral evaluation was performed 24 h after the plantar incision. Values are the mean ± SEM (8-11 animals per group). (B and C) Statistically significant differences between the values obtained in non-sensitized control animals (left white bars) and the other experimental groups: **P < 0.01; between the values obtained in sensitized animals, injected with PGE2 or with paw incision (black bars), administered with the sigma-1 agonists or their solvent: ##P < 0.01; and between sensitized animals administered with the sigma-1 agonists and injected with RTX or its vehicle: ††P < 0.01 (one-way ANOVA followed by Student-Newman-Keuls test).

Therefore, our results suggest that TRPV1+ afferents are needed for the effects of sigma-1 agonists on the potentiation of either PGE2-induced hyperalgesia or hindpaw weight bearing asymmetry after surgical injury.

2.2.7 The effect of sigma-1 agonism is produced at the sensitized site

As the pronociceptive effect of the systemically administered sigma-1 agonists depended on the presence of TRPV1+ neurons, we tested whether the local (intraplantar) administration of the TRP antagonist RR at the sensitized site was enough to reverse the mechanical hyperalgesia resulting from the potentiation of PGE2 effects by sigma-1 agonism. A dose as low as 32 µg of RR, administered at the site injected with PGE2 (0.125 nmol), was able to fully reverse mechanical hyperalgesia in mice s.c. administered with PRE-084 (32 mg/kg). This effect was produced locally at the injection site, since when RR was injected into the paw contralateral to PGE2 injection it was devoid of effect (Figure 10A). These results suggest that TRP activation at the PGE2-sensitized site is needed for the prohyperalgesic effect induced by the systemic administration of PRE-084. We then explored the participation of sigma-1 receptors at the PGE2-sensitized site in the prohyperalgesic effects induced by the systemic administration of PRE-084. We injected the sigma-antagonists BD-1063 (150 µg) or S1RA (200 µg) in the paw treated with PGE2, and we found that local sigma-1 antagonism at the sensitized site was able to abolish the prohyperalgesic effect of systemic sigma-1 agonism, and that this effect was produced locally since sigma-1 antagonists were devoid of effect when administered in the paw contralateral to the PGE2-injected site (Figure 10A). Since these results pointed to a relevant role of sigma-1 receptors at the sensitized site, we tested whether the administration of PRE-084 at the PGE2-injected site was sufficient to potentiate mechanical hyperalgesia. We found that the i.pl. administration of PRE-084 (50-75 µg) at the PGE2-injected site dose-dependently decrease the struggle response latency of mice submitted to the mechanical stimulation, and these effects were mediated locally, since when PRE-084 (75 µg) was injected in the paw contralateral to PGE2 injection, it was devoid of effect (Figure 10B). Altogether, these results suggest that peripheral sigma-1 receptors at the

sensitized site play a relevant role on the potentiation of PGE-induced mechanical hyperalgesia, which also depends on local TRP activation.

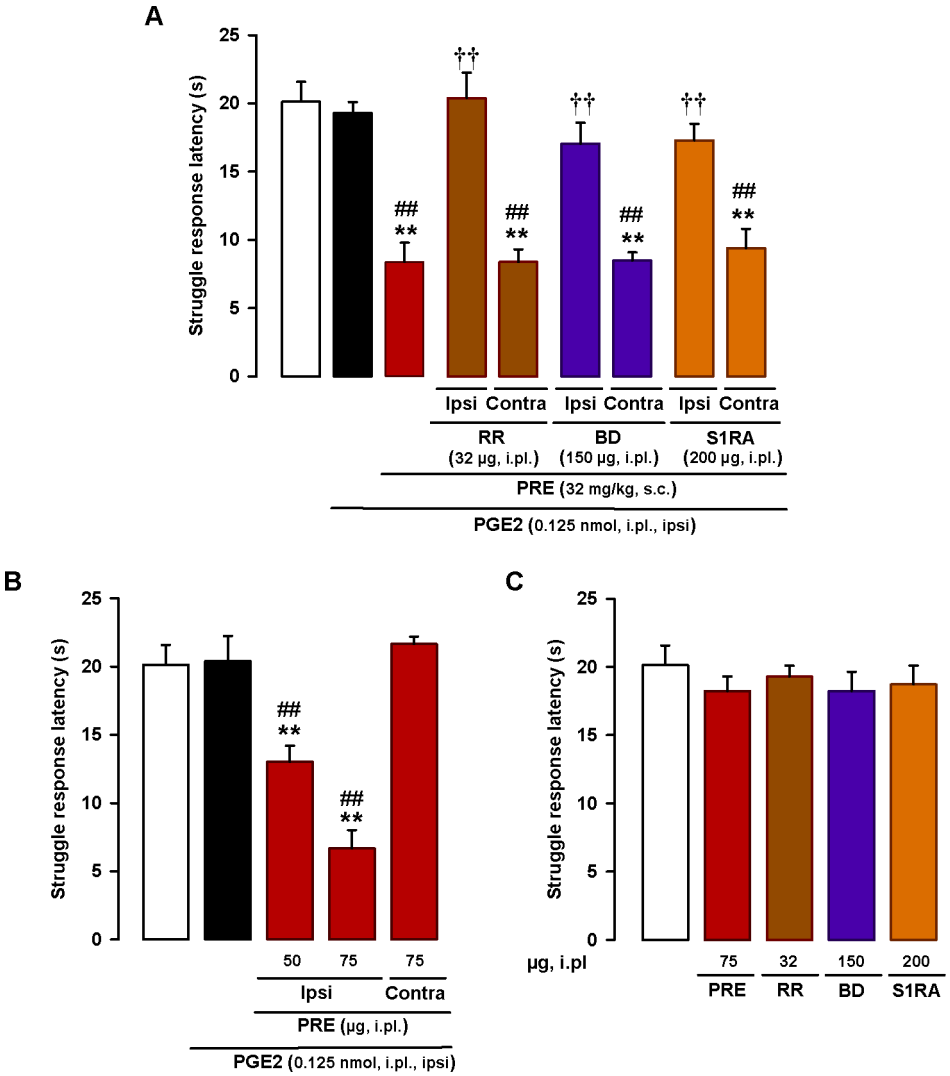

Figure 10. Effects of the local administration of sigma-1 drugs and the TRP antagonist ruthenium red on PGE2-induced mechanical hyperalgesia. The results represent the latency to struggle response evoked by a mechanical stimulus of 100 g in wild-type mice treated intraplantarly (i.pl.) with PGE2 (0.125 nmol) or its solvent. (A) Mice were administered subcutaneously (s.c.) with the sigma-1 agonist PRE-084 (PRE) and i.pl. with the sigma-1 antagonists BD-1063 (BD) or S1RA, or with the TRP antagonist ruthenium red (RR), or their solvents, in the paw ipsilateral (ipsi) or contralateral (contra) to PGE2 administration. Mechanical stimulation was performed in the ipsi paw. (B) Mice were i.pl. administered with PRE in the paw ipsilateral or contralateral to PGE2 injection. Mechanical stimulation was performed in the ipsi paw. (C) Absence of effect of the i.pl. administration of RR, BD, S1RA or PRE in non-sensitized mice. (A and B) Statistically significant differences between the values obtained in control non-sensitized animals (white bar) and the other experimental groups: **P < 0.01; between the values obtained in sensitized wild-type animals, injected with PGE2 (black bars), administered with PRE or its solvent: ##*P* < 0.01. (A) Between PGE2-treated animals administered with PRE alone or associated with BD, S1RA or RR: ††P < 0.01. (C) There were no significant differences between the values obtained in non-sensitized mice with any of the i.pl. treatments tested or their solvent (one-way ANOVA followed by Student-Newman-Keuls test).

Finally, we tested the effect of i.pl. administration of RR (32 µg), BD-1063 (150 µg), S1RA (200 µg) and PRE-084 (75 µg) in non-sensitized mice, and we found that any of these treatments modified the response latency of mice tested with the mechanical stimulus (Figure 10C). Therefore, our results suggest that peripheral TRPs and sigma-1 receptors influence the response to mechanical stimulation only during sensitizing conditions.

2.3 Discussion

In this study, we show that sigma-1 agonism enhances PGE2-induced hyperalgesia and postincisional pain.

The systemic administration of dextromethorphan do not induce per se mechanical hypersensitivity, but increases mechanical hyperalgesia induced by an otherwise inactive low dose of PGE2. The doses used of dextromethorphan in the present study are lower than those with antitussive activity in rodents (e.g. Braga et al., 1994). It is thought that sigma-1 agonism contributes to the antitussive effects of dextromethorphan (Cobos et al., 2008; Nguyen et al., 2016) but this compound has also several additional pharmacological activities (Nguyen et al., 2016), which might potentially influence its antitussive and prohyperalgesic properties. Importantly, the effects of dextromethorphan were replicated by PRE-084 and pridopidine, which are considered to be selective sigma-1 agonists (Motawe et al., 2020; Chen et al., 2021; Jiang et al., 2022).

Mice with a plantar incision changed the weight distribution in their hindpaws in the immediate postoperative period (3.5 h) after the surgical injury, reducing the weight borne by the injured hindlimb and favoring the use of the non-injured contralateral hindlimb. The incision was enough to induce robust behavioral effects without severely injuring deep tissues. In our experimental conditions, weight bearing asymmetry completely disappeared 24 h after surgery, which agrees with the previously described time-course of weight bearing differences after a superficial plantar incision (Lu et al.,

2022). Although weight bearing asymmetry disappeared 24 h after surgical injury, the incision was not fully repaired, as we still detected inflammation and prominent neutrophil recruitment at the incision site. Under this circumstance, systemic administration of any of the three sigma-1 agonists tested, induced a relapse in the pain-like behavior (shifting their body weight toward the non-injured limb) as if it was the immediate postoperative period again. We also show that this pronociceptive effect of sigma-1 agonism was fully dependent on the presence of neutrophils at the injured site, which points to factors released by these immune cells (and not from other possible cellular sources such as epithelia or fibroblasts) as the responsible of weight bearing asymmetry induced by sigma-1 agonism. Importantly, PGE2 is one of the major algogenic chemicals produced by neutrophils (Cunha et al., 2008). Taking into account the enhancement of PGE2-induced hyperalgesia by sigma-1 agonism showed here, the effects of sigma-1 agonists on weight bearing asymmetry could be attributed (at least partially) to the enhancement of the pronociceptive effects of neutrophil-derived PGE2.

While the decrease in the response latency in the paw pressure test used in the experiments with PGE2 clearly relates to hyperalgesia, the significance of weight bearing asymmetry is subject of debate. Weight bearing changes have been suggested as a measure of spontaneous pain or pain evoked by the pressure exerted by the injured limb in contact with the floor, but they might also be consistent with pain avoidance behavior, since it is known that anticipated pain guides motor control, and results in avoidance of activities (such as supporting weight on the injured limb) which could induce or aggravate existing pain (Cobos and Portillo-Salido, 2013; González-Cano et al.,. 2020). In addition, there are important methodological differences for both tests. The experimenter has to hold the mice to perform the paw pressure test, which is a stressor for the rodents. Also, paw pressure stimulation lasts only a few seconds (typically between 10-20 s). In contrast, hindpaw weight bearing is performed in freely-moving mice and assesses tonic postural changes during several minutes. Finally, another obvious difference between our experiments using paw pressure and weight bearing as the pain outcome was that mice were sensitized with an i.pl. injection of a single inflammatory mediator (PGE2) in the experiments on mechanical

hyperalgesia whereas we used a plantar incision (with the subsequent inflammation at the injured site) to induce the postural changes. In spite of the differences in the pain stimulus and the conceptual and methodological differences commented above, we show that dextromethorphan, PRE-084 and pridopidine exert proalgesic effects under both experimental circumstances, which support the robustness of the effects induced by the sigma-1 agonists tested.

Two arguments support that the pronociceptive effects induced by the drugs tested were mediated by sigma-1 receptors, and this is not limited to PRE-084 and pridopidine, which as commented above are considered selective sigma-1 agonists, but also to the non-selective drug dextromethorphan: (1) the effects of the sigma-1 agonists can be reversed by the known sigma-1 antagonist BD-1063. (2) None of the three sigma-1 agonists were able to induce pronociceptive effects in mice lacking sigma-1 receptors (sigma-1 KO mice), their purported pharmacological target.

There is a discrepancy between the pharmacological and genetic inhibition of sigma-1 receptors, as we described that sigma-1 antagonism abolished PGE2-induced hyperalgesia (Ruiz-Cantero et al., 2023), whereas we show here that sigma-1 KO mice exhibited the same PGE2-induced hyperalgesia than WT mice. Indeed, this is not the first time that this type of conflicting results have been reported in sigma-1 receptor research, as it has been shown that the administration of sigma-1 antagonists is able to abolish inflammatory or neuropathic heat hyperalgesia (Romero et al., 2012; Tejada et al., 2014; Bravo-Caparrós et al., 2019) or to potentiate opioid-induced antinociception to heat stimulus (e.g. Mei and Pasternak, 2007; Vidal-Torres et al., 2013), whereas sigma-1 KO mice do not replicate the effect of sigma-1 antagonists and show behavioral responses equivalent to WT mice in all these situations (de la Puente et al., 2009; Vidal-Torres et al., 2013; Tejada et al., 2014; Bravo-Caparrós et al., 2019). Therefore, it has been suggested that compensatory mechanisms might develop in the heat pain pathways of sigma-1 KO mice (Tejada et al., 2014; Bravo-Caparrós et al., 2019). Although in the present study we tested PGE2-induced hyperalgesia to mechanical stimulus, it is relevant to note that this particular form of sensory hypersensitivity is fully dependent on the sensitization of TRPV1-expressing peripheral sensory neurons (Ruiz-Cantero et al., 2023), which although are needed for mechanical

hyperalgesia in this context, normally code for heat stimulus (Cavanaugh et al., 2009). Therefore, it could be hypothesized that this compensatory mechanism might occur on the actions of sigma-1 receptors on TRPV1+ sensory neurons.

Here we show that sigma-1 receptor immunostaining was strikingly similar in mouse and human DRG samples, with the presence of this particular receptor in most (if not all) peripheral sensory neurons. TRPV1 are expressed in the DRG by peptidergic C neurons, which constitute a distinct cellular population in the mouse, with virtually no overlap with non-peptidergic C neurons, which can be labeled with IB4, as reported here and in several other studies (Zwick et al., 2002; Ruiz-Cantero et al., 2023). We show that the *in vivo* ablation of TRPV1+ neurons abolished the effect of sigma-1 agonists on the potentiation of PGE2-induced mechanical hyperalgesia and in the relapse of weight bearing asymmetry after plantar incision. Therefore, these particular sensory neurons are necessary for the pronociceptive effects of sigma-1 agonism on both circumstances. The enhancement of PGE2-induced hyperalgesia induced by the systemic administration of PRE-084 was abolished not only by the administration of the standard TRP antagonist RR in the sensitized paw, but also by the local administration of two different sigma-1 antagonists (BD-1063 and S1RA). Therefore, hyperalgesia was due to simultaneous TRP and sigma-1 activation at the sensitized site. Indeed, the local administration of PRE-084 at the site injected with PGE2 was enough to greatly maximize hyperalgesia. Our results point to a prominent role of peripheral sigma-1 receptors on the pronociceptive actions of sigma-1 agonists. There is only one previous report which describes a peripheral pronociceptive role of a single sigma-1 agonist (PRE-084), which shows that local (intraplantar) administration of the sigma-1 agonist enhances allodynia induced by activation of acid-sensing ion channels (ASICs) and purinergic P2X receptors (Kwon et al., 2016). Interestingly the presence of both of these targets is limited or even absent in mouse TRPV1+ neurons (Zwick et al., 2002; Leffler et al., 2006). We and others have shown that sigma-1 receptors can bind (Cortés-Montero et al., 2019; Ruiz-Cantero et al., 2023) and modulate TRPV1 actions (Ruiz-Cantero et al., 2023), which might explain the dependence on TRPV1 of the effects induced by sigma-1 agonism that we describe here.

Dextromethorphan is a widely used antitussive drug found in most over-the-counter preparations to relieve cough (Nguyen et al., 2016). Taking into account that more than 300 million people undergo a surgical procedure each year worldwide (Rose et al., 2015), it would not be unusual for some of these patients to be taking this antitussive drug. There have been performed some clinical studies to test the influence of dextromethorphan in postsurgical pain during the immediate postoperative period with conflicting results, as while some of them did not find any apparent effect (e.g. McConaghy et al., 1998; Ilkjaer et al., 2000) others reported even analgesic effects of this compound, purportedly attributable to NMDA antagonism (e.g. Helmy and Bali, 2001; Chau-In et al., 2007). To our knowledge, there are no published studies examining the effect of dextromethorphan in the late postoperative recovery phase, when (according to our findings) it might enhance pain due to the presence of the residual inflammation subsequent to tissue injury and repair. It would be interesting to carry out a retrospective study looking at the influence of dextromethorphan treatment on the duration of pain after surgery. We also tested other more selective sigma-1 agonists, specifically PRE-084 and pridopidine. PRE-084 is a prototypical sigma-1 agonist used in most preclinical studies on sigma-1 receptors (e.g. Motawe et al., 2020) but it is far from the clinical setting. However, pridopidine is currently on clinical trials for the treatment of Huntington's disease (Chen et al., 2021) and ALS (Jiang et al., 2022). It is worth pointing out that pain is highly prevalent in Huntington's disease and ALS (Hanisch et al., 2015; Sprenger et al., 2021), and although both are eminently central diseases, it is known that blood from patients with Huntington's disease show an increase of inflammatory markers (such as C-reactive protein and IL-6) indicating the presence of a peripheral inflammation (Chuang and Demontis, 2021), and it has also been described that ALS has a peripheral inflammatory component which affects sensory neurons (Gentile et al., 2019). Therefore, it could be worth to monitor the pain state of patients with these diseases and treated with pridopidine during the clinical trials. A similar recommendation could be made for other sigma-1 agonists, such as blarcamesine (ANAVEX2-73), currently on clinical trials for other neurodegenerative diseases such as Alzheimer's disease, Rett syndrome or Parkinson's disease (Salaciak and Pytka, 2022), as all these diseases have pain as one of the symptoms (Ford, 2010; Monroe et al., 2015; Cappuccio et al., 2019), and are recently described to be

accompanied by a peripheral inflammatory response (Cordone et al., 2022; Princiotta Cariddi et al., 2022; Williams et al., 2022).

2.4 Conclusions

In summary, this study shows that sigma-1 receptor is present in human and mouse DRG neurons, and demonstrates that sigma-1 agonism exacerbates pain-like responses in mice with a mild inflammatory condition. The mechanism of the pronociceptive actions of sigma-1 agonism involves the enhancement of the actions of algogenic chemicals released by immune cells, such as PGE2, able to sensitize TRPV1+ nociceptors (Figure 11A and B). The potentiation of immune-driven pronociceptive effects by sigma-1 agonism seen here in mice, if translated to human patients, might constitute a side effect that has gone unrecognized in patients treated with sigma-1 agonists in current medical practice or clinical trials, and might merit further clinical investigation.

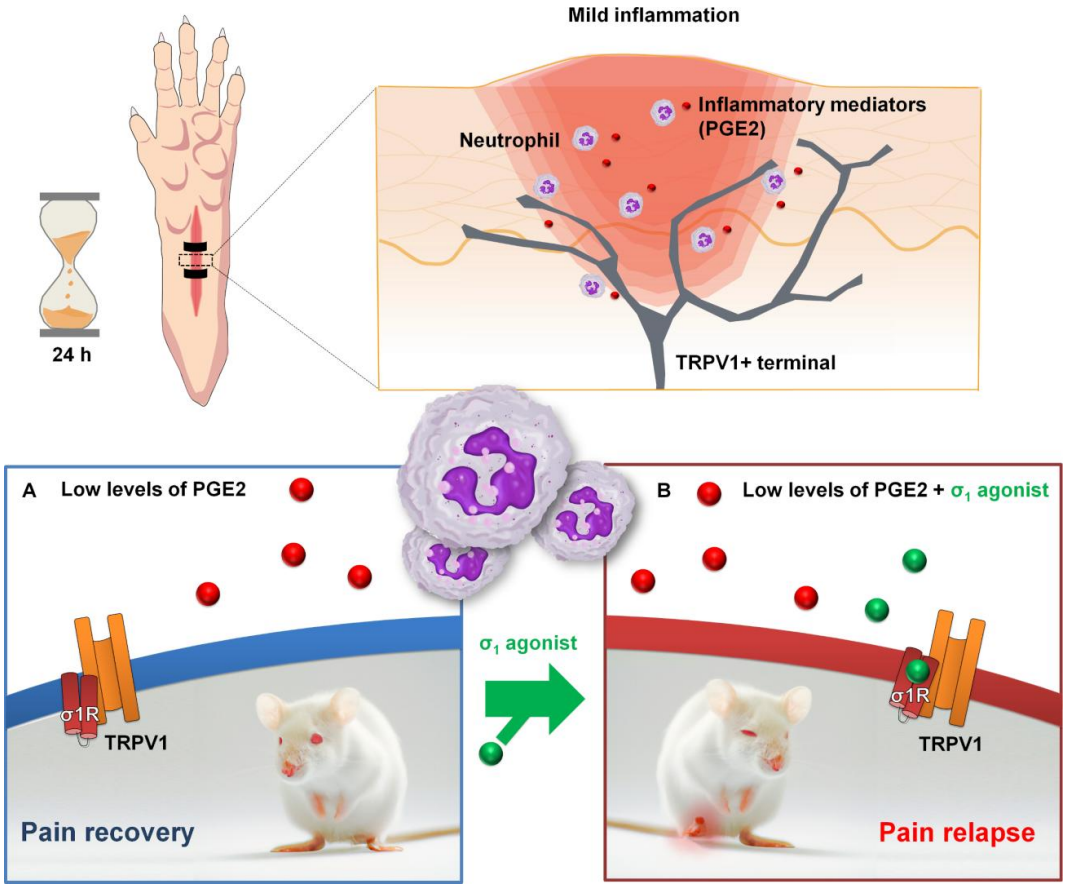

Figure 11. Proposed mechanism for the proalgesic actions of sigma-1 agonism during a mild inflammatory reaction. (Upper panels) Neutrophilic inflammation is present 24 h after plantar incision.

(A) Under normal conditions, the mice apparently recover from the pain induced by the surgical procedure performed 24 h before. (B) However, in the presence of a sigma-1 agonist, mice suffer a relapse in pain-like behavior due to the enhancement of the effects of proalgesic mediators release by immune cells (such as PGE2), which recruit the actions of TRPV1+ peripheral sensory neurons.

3. SIGMA-1 RECEPTORS CONTROL PERIPHERAL NEUROINFLAMMATION AFTER NERVE INJURY: A TRANSCRIPTOMIC STUDY

3.1 Material and methods

3.1.1 Experimental animals

Experiments were done in wild-type (WT) female CD-1 mice (Charles River, Barcelona, Spain) and in sigma-1 receptor knockout (KO) mice (Animal Experimentation Unit - CIC UGR, Granada, Spain), weighing 25-30 g (8 to 11 weeks old). Knockout mice were generated on a CD-1 background as previously described (Entrena et al., 2009), by using a traditional backcrossing breeding strategy with WT progenitors from Charles River for at least 15 generations, which theoretically ensured that the genetic material from the original background is virtually absent (Wong, 2002). Animals were housed in colony cages (10 mice per cage), in a temperature-controlled room (22 ± 2 °C) with an automatic 12-h light/dark cycle (08:00–20:00 h). An igloo and a plastic tunnel were placed in each housing cage for environmental enrichment. Animals were fed a standard laboratory diet and tap water ad libitum until the beginning of the experiments. The behavioral experiments were done during the light phase (from 9:00 a.m. to 3:00 p.m.). The mice were randomized to treatment groups, testing each day a balanced number of animals from several experimental groups, and they were also tested randomly throughout the estrous cycle. Mice were handled in accordance with international standards (European Communities Council directive 2010/63), and the experimental protocols were approved by regional (Junta de Andalucía) and Institutional (Research Ethics Committee of the University of Granada) authorities. To decrease the number of animals in this study, we used the same mice for behavioral studies and immunostaining or fluorescence-activated cell sorting (FACS), when possible.

3.1.2 Spared nerve injury

The spared nerve injury (SNI) was performed as previously described (Decosterd and Woolf, 2000). Briefly, an incision was made in the left thigh skin and through the biceps femoris muscle, at the site of trifurcation of the sciatic nerve, and its three terminal branches (the sural, common peroneal, and tibial nerves) were exposed. The tibial and common peroneal branches were ligated with a silk suture and transected distally, while the sural nerve was left intact. In sham-operated control mice, the sciatic nerve terminal branches were exposed but not ligated. Mice were anesthetized with 4% isoflurane (IsoVet®, B. Braun, Barcelona, Spain) in oxygen. During the surgical procedure, anesthesia was maintained with 2.5% isoflurane delivered via a nose cone. Wounds were closed and the animals returned to their cages. We monitor carefully for signs of distress after surgery. Although mice can move, rise, and get access to food and water normally after surgery, we place some food pellets on the cage floor to facilitate access to them. Autotomy behavior was not observed in any animal following SNI during this study.

3.1.3 Assessment of mechanical allodynia

Mechanical thresholds were tested before surgery (baseline) and 7 days after SNI. Mechanical allodynia was assessed with von Frey filaments according to a previously described method, with slight modifications (Chaplan et al 1994). On each day of evaluation the mice were habituated for 60 minutes in individual transparent plastic chambers (7 × 7 × 13 cm) with a floor made of wire mesh. After the acclimation period, calibrated von Frey monofilaments (Stoelting, Wood Dale, IL, USA) with bending forces that ranged from 0.02 to 1.4 g were applied with the up-down paradigm in the sural nerve territory, starting with the 0.6 g filament, and allowing 10 s between successive applications. The response to the filament was considered positive if immediate flinching, licking/biting or rapid withdrawal of the stimulated paw was observed. In each consecutive test, if there was a positive response, a weaker filament was then used; if there was no response to the filament, a stronger stimulus was then selected. This sequence was repeated 4 times to limit the values of the mechanical threshold.

Behavioral evaluations were performed by an observer blinded to the mouse genotype or pharmacological treatment.

3.1.4 Assessment of cold allodynia

Cold allodynia was tested by gently touching the plantar skin of the hind paw with an acetone drop, as previously described (Nieto et al., 2008). On each day of evaluation the mice were housed and habituated for 30 min in individual transparent plastic enclosures (7 × 7 × 13 cm) with a floor made of wire mesh. Acetone was applied three times to the ipsilateral hind paw at intervals of 30 s, and the duration of biting or licking of the hind paw was recorded with a stopwatch and reported as the cumulative time of biting/licking in all three measurements. A cutoff time of 10 s was used in each of the three trials, because animals rarely licked their hind paw for more than 10 s. During the presurgery baseline evaluation we discarded ≈ 5% of the mice tested due to an exaggerated atypical response to the acetone (> 2 s of cumulative responses to acetone in the three measures).

3.1.5 RNA analysis

3.1.5.1 RNA preparation

The lumbar L3 and L4 dorsal root ganglia (DRGs) and the corresponding lumbar enlargement of the dorsal spinal cord (dSC) were carefully removed from naïve WT and sigma-1 receptor KO mice, and from mice from both genotypes 7 days after SNI surgery. We selected L3 and L4 DRGs because they contain all somas from the common peroneal and tibial branches of the sciatic nerve (Laedermann et al, 2014) which are injured during SNI (see 1.2 for details). We studied DRGs collected in five biological replicates in samples from naïve WT or sigma-1 receptor KO mice, and in four biological replicates from mice with SNI. Each biological replicate was obtained from six mice (twelve ipsilateral L3/4 DRGs or six ipsilateral dSCs). Samples were immediately frozen after dissection in 2 ml eppendorf tubes in contact with dry ice and stored at -80ºC until use. RNA was extracted using the RNeasy Plus Universal Min Kit

(QIAcube / QIAGEN) according to the manufacturer's instructions. Concentration and quality of extracted RNA were measured using the Qubit 4 Fluorometer (Thermo Fisher Scientific, MA, USA) and the 2100 Bioanalyzer Instrument (Agilent Technologies, CA, USA). Sample processing was carried out in the genomics unit of the Pfizer-University of Granada-Junta de Andalucía Center for Genomics and Oncological Research (GENYO).

3.1.5.2 Next-generation transcriptome sequencing (RNA-Seq) for gene expression analysis

Libraries from mRNA were prepared using 1 µg of RNA starting material and the TruSeq Stranded mRNA Library Prep Kit (Illumina, CA, USA) according to the manufacturer's protocol. This protocol captures poly-adenylated RNA by transcription by oligo-dT primer, after which the RNA is fragmented. The sample was back transcribed to generate the cDNA, both in the first and second strands. The 3'ends were adenylated, the adapters and barcodes were ligated, and finally, it was enriched by PCR. Adapters and samples codes (index-barcodes) were added to the libraries to be able to be sequenced simultaneously. mRNA libraries were sequenced on the NextSeq 500 system (Illumina, CA, USA) using the highest output mode and paired-end 75 bp read lengths with a depth of 25-30 million reads for each sample. Sequencing was performed in the genomics unit of GENYO.

Expression data will be submitted to Gene Expression Omnibus (GEO) before publication.

3.1.5.3 Bioinformatics

Fastqs were obtained using Illumina's bcl2fastq software. The quality of the sequences was screened using fastQC, qualimap (Okonechnikov et al., 2016) and multiQC (Ewels et al., 2016). Using the RSEM pipeline (Li et al., 2011), the gene expression were obtained by mappin RNAseq reads with hisat2 aligner (Kim et al., 2019) to the Gencode mouse genome GRCm38 and annotated with the vM25 gtf (Frankish et al., 2021). The differential expression was normalised with NOISeq (Tarazona et al., 2016) following the approach of Trimmed Mean of M values (Gu et al., 2016). The differential

expression analysis was performed with the default recommendations of DESeq2 (Love et al., 2014). Transcripts were considered significantly regulated when the *P* value < 0.01. A threshold fold change of 1.4 was imposed for each transcript to be included in the analysis, similar than in previous transcriptomic studies (Costigan, et al., 2002 and 2010; Yokoyama et al., 2020). To better analyze the differences in WT vs sigma-1 receptor KO mice during the naïve condition and after SNI, we constructed a Weighted Gene Co-expression Network Analysis (WGCNA) using the regulated transcripts in the 4 groups of samples (naïve WT vs naïve KO and SNI WT vs SNI KO) to find groups of genes (modules) with similar expression changes across the experimental conditions tested. Briefly, we computed the absolute Pearson correlation coefficients between each transcript and every other transcript in the expression dataset; these values were used to determine the topological overlap, a measure of connection strength, or 'neighborhood sharing', in the network. This results in modules of co-expressed genes where the members of each network have high topological overlap in their patterns of regulation (Horvath et al., 2006; Oldham et al., 2008; Parikshak et al., 2015; Cobos et al., 2018). WGCNA and the similarity plot of the module eigengenes from each module were done with its corresponding R's package (Langfelder et al., 2008), considering an unsingned network for the topological overlap matrix calculated with a bidweight midcorrelation.

Heat maps were generated using HeatMapImage tool from GenePattern software (v. 3.9.11). To facilitate comparison of transcriptional regulation in the different experimental conditions, the height of heat maps shown maintained the same proportion with the number of regulated transcripts throughout all figures.

To identify the functional categories most prominently represented in the lists of regulated transcripts and in the modules obtained using the WGCNA we made functional Enrichment Analyses analyzing gene lists with Ingenuity Pathway Analysis (IPA) software, version 84978992 (Qiagen, USA). This program can identify the annotations for each gene of a given set in its database, which is constructed from previously published information, and calculates the most over-represented descriptors in the list to return a Benjamini-Hochberg (B-H) adjusted *P* value as a measure of the enrichment in each functional subdivision. As a second method to

determine cellular functions predominant in some gene lists, we used Gene Ontology (GO) enrichment analysis tools (http://geneontology.org).

3.1.6 CFA-induced peripheral inflammation

To compare the immune cell recruitment due to paw inflammation in WT and sigma-1 receptor KO mice, 20 µl of complete Freund's adjuvant (CFA; Sigma-Aldrich) was injected into the right hindpaw of mice from each genotype, using a 1710 TLL Hamilton microsyringe (Hamilton Company, NV, USA) with a 30½-gauge needle. Seven days after the injection, the paws were dissected and the immune cell recruitment was measured by FACS. As a control of the immune cell presence in noninflamed tissue, we used samples from the paw contralateral to the injection, as well as samples from naïve mice.

3.1.7 Fluorescence-activated cell sorting (FACS)

FACS was used to determine the immune cell populations in wild type and sigma-1 receptor KO mice after SNI. Each sample contained the ipsilateral L3 and L4 DRGs from six animals with SNI. The DRGs contralateral to the nerve injury were used as a control. As an additional control, we also tested both left and right L3 and L4 DRGs from 3 naïve animals (12 DRGs in all cases). To study immune cell recruitment after paw inflammation in mice from both genotypes, we tested plantar tissue from animals injected with CFA, using tissue from the paw contralateral to the injection as a control, as well as paw tissue from naïve mice. In all cases, mice were killed by cervical dislocation and DRGs or plantar tissue were dissected and digested with collagenase IV (1 mg/mL, LS004188, Worthington, Lakewood, NJ, USA) and DNAse I (0.1%, LS002007, Worthington) for 1 hour at 37°C with agitation. The digestion was neutralized washing with PBS. Cells of DRGs were gently pipetted up and down, in a PBS with DNAse I solution, to obtain a single cell suspension. In case of plantar tissue, samples were mechanically crushed over a 70 µm filter. Then samples were filtered in a tube with cell strainer cap (pore size 35 µm) and the rat anti-CD32/16 antibody (1:100, 20 minutes, 553141; Biolegend, San Diego, CA) was used to block Fc-γRII (CD32) and Fc-

γRIII (CD16) binding to IgG. Cells were incubated with antibodies recognizing the hematopoietic cell marker CD45 (1:200, 103108, clone 30-F11, Biolegend), the myeloid marker CD11b (1:100, 101227, clone M1/70, Biolegend), the neutrophil-specific marker Ly6G (1:100, 127617, clone 1A8, Biolegend), the B cells CD45R/B220 (1:200, 103239, clone RA3-6B2, Biolegend), the T cells marker TCR β (1:100, 553174, clone H57-597, BD Biosciences, San Jose, CA, USA), the CD4 marker (1:160, 100555, clone RM4-5, Biolegend) and the CD8a marker (1:80, 100752, clone 53-6.7, Biolegend), together with a viability dye (1:1000, 65-0865-14, Thermo Fisher Scientific), for 30 minutes on ice. The populations of macrophages/monocytes (CD45+ CD11b+ Ly6G − cells), neutrophils (CD45+ CD11b+ Ly6G+ cells), B cells (CD45+ CD45R/B220+), T cells (CD45+ TCRβ+), CD4 T cells (CD45+ TCRβ+ CD4+) and CD8 T cells (CD45+ TCRβ+ CD8a+) were determined from the markers indicated above in cells labeled with the viability dye. Before and after incubation with the antibodies, the cells were washed three times in 2% FBS/PBS (FACS buffer). Cells were fixed with paraformaldehyde (2%, 158127, Sigma-Aldrich) for 20 minutes, and on the next day samples were assayed with a BD FACSymphony A5 flow cytometer (BD Biosciences). Compensation beads were used as compensation controls, and fluorescence minus one (FMO) controls were included to determine the level of nonspecific staining and autofluorescence associated with different cell subsets. All data were analyzed with FlowJo 2.0 software (Treestar, Ashland, OR, USA).

3.1.8 Immunohistochemistry

Mice were anesthetized with 4% isoflurane (in oxygen) and perfused transcardially with 0.9% saline solution followed by 4% paraformaldehyde (Sigma-Aldrich). The SC segment innervated by the spinal nerves from the L3-L4 DRGs was dissected and post-fixed for 1 h in the same paraformaldehyde solution. Samples were incubated for 48 h in 30% sucrose (Sigma-Aldrich) at 4ºC to be embedded in O.C.T Tissue-Tek medium (Sakura Finetek, Barcelona, Spain), and frozen and stored at -80º C until the immunohistochemical study. Tissue sections were incubated for 1 h in blocking solution with 5% normal goat serum, 0.3% Triton X-100, and 0.1% Tween 20 in Tris buffer solution. Then, the slides were incubated with the primary antibody rabbit anti-

Allograft Inflammatory Factor 1 (AIF1, 1:200, 019-19741, Wako Chemical, Neuss, Germany) in blocking solution for 1 h at room temperature (RT). AIF1 (also known as ionized calcium-binding adapter molecule 1, IBA-1) is a widely used microglial marker (Jurga et al. 2020). After incubation with the primary antibody, sections were washed again three times for 10 min and incubated with the secondary antibody Alexa Fluor-594 goat anti-rabbit (1:500, A-11012,Thermo Fisher Scientific) and mouse anti-NeuN (neuronal nuclei) Alexa Fluor 488 conjugated (1:500, MAB377X, Merck Millipore). Finally, slides were coverslipped with ProLong Gold Antifade mounting medium (Thermo Fisher Scientific). Images were acquired with a confocal laser-scanning microscope (Model A1, Nikon Instruments Europe BV, Amsterdam, Netherlands).

3.1.9 Maraviroc administration

The day before the SNI, a baseline measurement of the von Frey threshold and the responses to the cold stimulus (acetone) were recorded. Then, the CCR5 antagonist maraviroc was orally administered until day 7 after surgery, when the sensory evaluation took place. Mice were fed with the same diet as the control group, but received 300 mg/L maraviroc (Sigma-Aldrich, Madrid, Spain) in the drinking water (Ochoa-Callejero et al., 2013; Pérez-Martínez et al., 2014 and 2020). The drinking water with the diluted drug was prepared and poured into a 100 ml drinker, which was changed every day to avoid possible degradation of the drug. Control mice received drinking water without any additives.

3.1.10 Data analysis of behavioral and FACS experiments

The data were analyzed with the SigmaPlot 12.0 program (Systat Software Inc., San Jose, CA, USA). For behavioral studies, statistical analysis was carried out with two-way repeated-measures analysis of variance (ANOVA). For the results from FACS assays statistical analysis was performed with two-way ANOVA. The Student-Newman-Keuls post-test was used in all cases. The differences between means were considered significant when the *P* value was below 0.05.

3.2 Results and discussion

3.2.1 Sigma-1 receptor KO mice show a reduced neuropathic pain phenotype after SNI

We compared the response to mechanical and cold stimulation of WT and sigma-1 receptor KO mice before and after SNI. Baseline mechanical threshold in the von Frey test did not significantly differ between both genotypes as WT and sigma-1 receptor KO animals showed a similar mechanical threshold of approximately 1 g (Figure 1A). 7 days after SNI, mechanical thresholds in the paw contralateral to surgery were similar to the baseline values in both WT and sigma-1 receptor KO animals (Figure 1A). However, WT mice developed mechanical allodynia in the injured limb, manifested as a significant reduction in the mechanical threshold in the paw ipsilateral to the SNI. Sigma-1 receptor KO mice also showed mechanical hypersensitivity after SNI although it was significantly less pronounced than WT mice (Figure 1A).

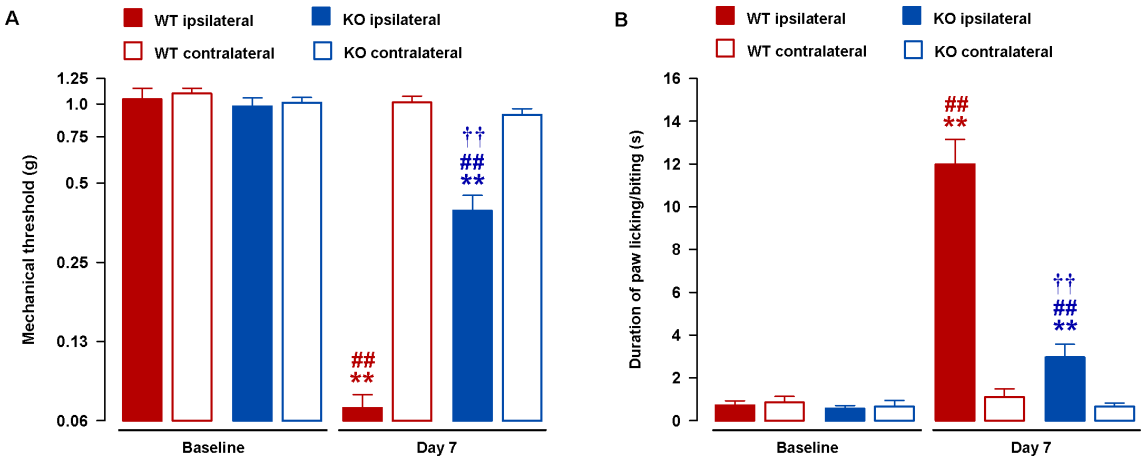

Figure 1. Comparison of spared nerve injury (SNI)-induced neuropathic pain behaviors in wild-type (WT) and sigma-1 receptor knockout (KO) mice. The von Frey threshold (A) and duration of hind paw licking or biting in the acetone test (B) were recorded before the injury (baseline) and 7 days after SNI in the paws ipsilateral and contralateral to the site of surgery. Each bar and vertical line represent the mean ± SEM of the values obtained in 10–12 animals. Statistically significant differences between the values obtained in the ipsilateral paw on the baseline and day 7 after SNI: $^{**}P < 0.01$; between the ipsilateral and contralateral measurements: $^{\#\#}P < 0.01$; and between WT and KO groups stimulated in the paw ipsilateral to SNI: $^{\dagger\dagger}P < 0.01$ (two-way repeated measures ANOVA followed by Student-Newman-Keuls).

Baseline sensitivity to a light cold stimulation (an acetone drop) was equal in WT and sigma-1 receptor KO mice as mice from ether genotype showed a hardly detectable response (licking/biting the paw) to this sensory stimulation (Figure 1B). 7 days after

SNI, the responses to cold stimulation remained unchanged in the paw contralateral to the nerve injury in WT or sigma-1 receptor KO mice (Figure 1B). WT mice developed marked cold allodynia in the injured limb, with values of duration of paw licking/biting of about 12 s. In contrast, sigma-1 receptor KO mice had a minimal cold hypersensitivity, showing only a very modest increase (2.4 s) in the behavioral response (Figure 1B).

In summary, SNI induced robust mechanical and cold hypersensitivity in the paw ipsilateral to the nerve injury in WT mice. Sigma-1 receptor KO mice showed no sensory alterations in basal conditions, but showed reduced neuropathic mechanical and cold allodynia. These results are in agreement with previous reports which show that pain behaviors after SNI are attenuated in either mice or rats during sigma-1 receptor inhibition (Bravo-Caparrós et al., 2019 and 2020; Shin et al., 2022). Finally, the absence of sensory hypersensitivity in the limb contralateral to the surgery also agrees with previous reports using this neuropathic pain model (Richner et al., 2011; Bravo-Caparrós et al., 2019), and indicates that sensory changes after this type of nerve injury are not widespread but limited to the injured limb.

3.2.2 Regulation of the transcriptome in the injured DRG after SNI in WT mice

We then investigated the transcriptional profile of the injured DRGs from WT mice. We evaluated global gene expression by RNAseq in naïve WT mice and 7 days post-SNI, in the ipsilateral L3 and L4 DRG. We obtained 1498 regulated transcripts in the injured DRG compared to the naïve condition. A heat map of the regulated transcripts, where the intensity of the color is used to represent changes (not absolute values) of gene expression, is shown in Figure 2A. The majority of the transcripts regulated in the injured DRG increase their expression after SNI (925 transcripts which go in the heat map from light to dark red after injury), although a significant portion of the transcripts were regulated in the opposite direction (573 transcripts which go in the heat map from dark to light red after injury).

We then made a functional enrichment analysis with the list of all regulated transcripts, using IPA software. The biological functions most significantly associated to the list of transcripts regulated in the DRG after SNI were related to the inflammatory process, such as "Leukocyte migration" and "Inflammation", with B-H *P* values in the range of 10^{-30} (Fig 2B). Other immune-related functions such as "chemotaxis" also showed a very significant B-H *P* value (close to 10^{-18}) (Fig 2B). Importantly, in addition to immune functions, the gene list contained some robust neuronal-related functions such as "Development of neurons" or "Neurotransmission", with B-H *P* values of 10^{-22} - 10^{-18}. All these functions were very populated, containing 104-225 transcripts. It is relevant to note that "Development of neurons", the most significant neuronal-related annotated function in the list also includes an immune component, as it contains some immune genes such as chemokine receptors and structural markers of immune cells such as ITGAM (which encodes for CD11b), among others. It is not surprising that genes involved in this particular function have a mixed origin, since the immune system is well known to play a role in the correct development of nervous tissue. The other neuronal function, "Neurotransmission", showed a much cleaner neuronal component. Finally, IPA also identified "Transport of ion" as a prominent function associated to the gene list containing 100 ion channels, most of them with a clear role in neuronal function (such as TRP channels, or voltage-dependent ion channels). See Table S1 in Appendix or the content of genes in each annotated function. The association of both immune and neuronal functions to the list of genes regulated in the DRG after SNI fully agrees with previous studies (Griffin et al., 2007; Costigan et al., 2010; Cobos et al., 2018).

Some example immune genes regulated in the DRG after SNI are shown in Table 1. These include cathepsins, chemokines, chemokine receptors, and other well-known immune markers. Cathepsin S (CTSS) is robustly upregulated in our dataset, and it is known to activate fractalkine (Montague-Cardoso et al., 2020). CX3CR1, the fractalkine receptor, is also upregulated in our list and it is very important in the recruitment of macrophages (AIF1+ cells) to the DRG (Huang et al., 2014). Other chemokines that have been previously reported to be upregulated after nerve injury and that are also present in our data set include CCL2, which has potent chemotactic activity, and

together with fractalkine, is involved in macrophage recruitment (Huang et al., 2014; Kwon et al., 2015). These proinflammatory macrophages that arrive to the DRG after nerve injury are the primary source of some chemokines such as IL6 (Kwon et al., 2015; Bravo-Caparrós et al., 2020; Kummer et al., 2021), which is also upregulated in our gene list. In addition to transcripts related to macrophage recruitment, we also found some transcripts related to other immune cells. Specifically, we found an upregulation in the transcript for CD4 which is a well-known marker of "helper" T cells. As previously described, these T cells are attracted by macrophages to the injured DRG (Raoof et al., 2018), and both macrophages and T cells play a very important role in the development of neuropathic pain (Cobos et al., 2018). Therefore, our transcriptomic data of the DRG from WT mice after SNI agrees with the previous knowledge on the immune response in the DRG after nerve injury.

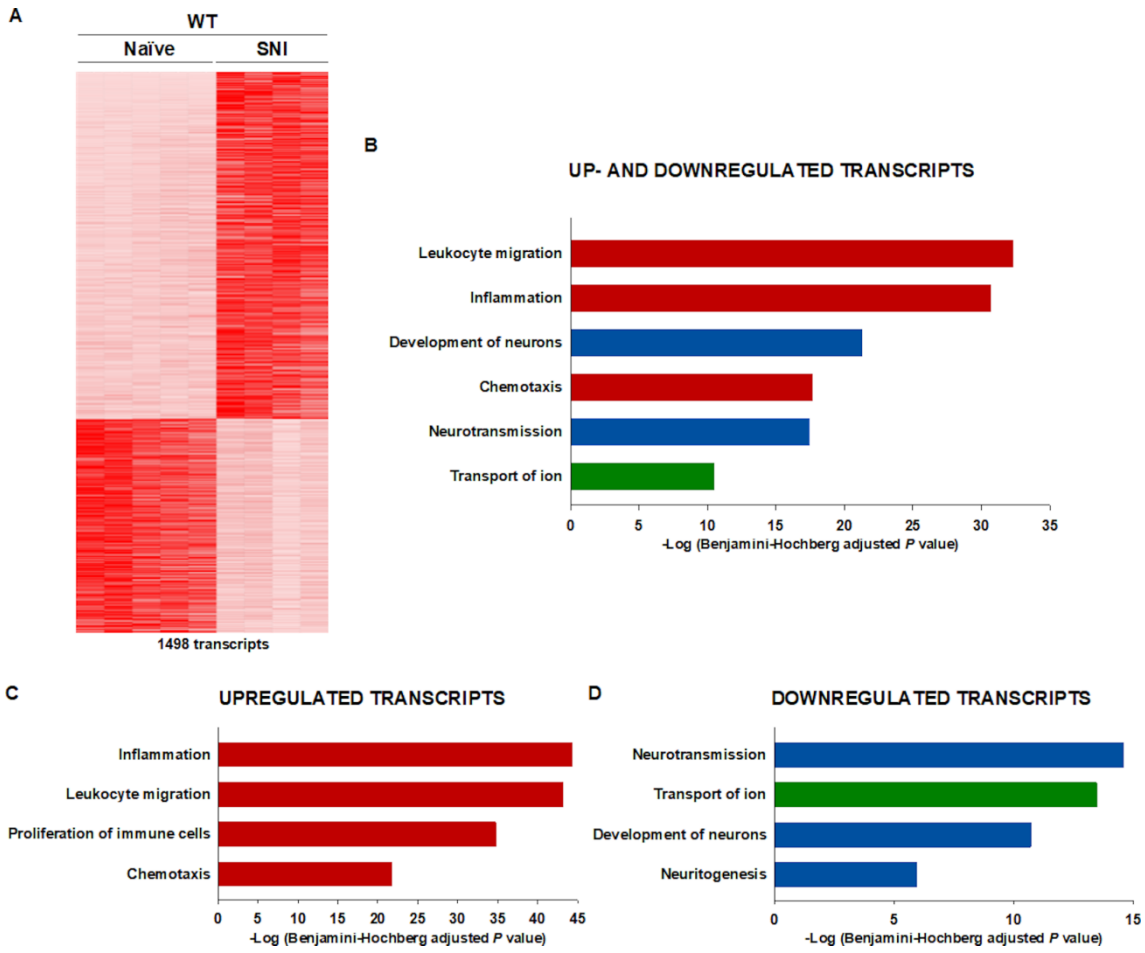

Figure 2. Transcriptional profile of the injured dorsal root ganglia (DRG) from wild-type (WT) mice after spared nerve injury (SNI). (A) Heatmap of the relative expression of the transcripts regulated ($P <$ 0.01 and fold change 1.4) in the L3-L4 DRG 7 days after SNI compared to naïve mice. Light red represents low-level expression and dark red high-level expression. The total number of regulated transcripts is indicated. (B) Representative functional characteristics sorted by the strength of statistical significance (-

log of Benjamini-Hochberg adjusted *P*-value) that IPA software ascribed the function given, using all regulated transcripts, and also splitting the list into the transcripts (C) upregulated or (D) downregulated by nerve injury.

Table 1. Some example immune genes regulated in the injured (L3-L4) DRG after SNI in wild-type mice. Fold change represents the ratio of the expression in SNI/naïve.

GENE ID	GENE NAME	FOLD CHANGE	REGULATION	FUNCTION
ENSMUSG00000030560.17	CTSC	1.87	Upregulated	Cathepsins
ENSMUSG00000038642.10	CTSS	3.14	Upregulated	
ENSMUSG00000018920.11	CXCL16	1.78	Upregulated	Chemokines
ENSMUSG00000035385.5	CCL2	1.78	Upregulated	
ENSMUSG00000035373.2	CCL7	1.82	Upregulated	
ENSMUSG00000009185.2	CCL8	14.97	Upregulated	
ENSMUSG00000019122.8	CCL9	2.26	Upregulated	
ENSMUSG00000035352.3	CCL12	3.95	Upregulated	
ENSMUSG00000014599.10	CSF1	7.87	Upregulated	
ENSMUSG00000025746.11	IL6	4.07	Upregulated	
ENSMUSG00000052336.7	CX3CR1	2.65	Upregulated	Chemokine receptors
ENSMUSG00000032089.16	IL10RA	1.61	Upregulated	
ENSMUSG00000002897.5	IL17RA	2.94	Upregulated	
ENSMUSG00000026072.12	IL1R1	2.58	Upregulated	
ENSMUSG00000030745.9	IL21R	2.84	Upregulated	
ENSMUSG00000030748.9	IL4R	2.38	Upregulated	
ENSMUSG00000027947.11	IL6R	1.69	Upregulated	
ENSMUSG00000024621.16	CSF1R	2.66	Upregulated	
ENSMUSG00000071713.6	CSF2RB	1.86	Upregulated	
ENSMUSG00000025804.5	CCR1	3.62	Upregulated	
ENSMUSG00000049103.14	CCR2	1.94	Upregulated	
ENSMUSG00000079227.10	CCR5	2.87	Upregulated	
ENSMUSG00000023905.15	TNFRSF12A	3.77	Upregulated	
ENSMUSG00000030341.17	TNFRSF1A	1.44	Upregulated	
ENSMUSG00000028599.10	TNFRSF1B	2.22	Upregulated	
ENSMUSG00000024397.14	AIF1	1.74	Upregulated	Other immune markers
ENSMUSG00000051439.7	CD14	2.30	Upregulated	
ENSMUSG00000023274.14	CD4	2.39	Upregulated	
ENSMUSG00000040747.9	CD53	2.11	Upregulated	
ENSMUSG00000022901.13	CD86	2.16	Upregulated	
ENSMUSG00000030786.18	ITGAM	2.35	Upregulated	
ENSMUSG00000075602.10	LY6A	3.53	Upregulated	
ENSMUSG00000025779.10	LY96	1.60	Upregulated	
ENSMUSG00000069516.8	LYZ	2.07	Upregulated	
ENSMUSG00000023992.14	TREM2	3.34	Upregulated	
ENSMUSG00000030579.10	TYROBP	2.29	Upregulated	

Table 2. Some example neuronal genes regulated in the (L3-L4) DRG after SNI in wild-type mice. Fold change represents the ratio of the expression in SNI/naïve.

GENE ID	GENE NAME	FOLD CHANGE	REGULATION	FUNCTION	
ENSMUSG00000045613.9	CHRM2	0.50	Downregulated	Cholinergic receptors	GPCRs
ENSMUSG00000046159.16	CHRM3	1.59	Upregulated		
ENSMUSG00000027107.3	CHRNA1	1.94	Upregulated		
ENSMUSG00000032303.8	CHRNA3	2.08	Upregulated		
ENSMUSG00000035594.10	CHRNA5	6.99	Upregulated		
ENSMUSG00000030525.8	CHRNA7	0.58	Downregulated		
ENSMUSG00000026322.9	HTR4	0.49	Downregulated	Serotonin receptors	
ENSMUSG00000049511.5	HTR1B	0.63	Downregulated		
ENSMUSG00000000766.18	OPRM1	0.55	Downregulated	Opioid receptors	
ENSMUSG00000025905.14	OPRK1	0.54	Downregulated		
ENSMUSG00000050511.1	OPRD1	0.39	Downregulated		
ENSMUSG00000010803.13	GABRA1	0.54	Downregulated	GABA receptors	Ionotropic receptors
ENSMUSG00000031343.13	GABRA3	0.62	Downregulated		
ENSMUSG00000007653.12	GABRB2	0.54	Downregulated		
ENSMUSG00000001260.10	GABRG1	0.60	Downregulated		
ENSMUSG00000020436.17	GABRG2	0.60	Downregulated		
ENSMUSG00000026959.13	GRIN1	0.68	Downregulated	Glutamate receptor	
ENSMUSG00000032269.8	HTR3A	0.43	Downregulated	Serotonin receptor	
ENSMUSG00000040724.5	KCNA2	0.59	Downregulated	Potassium channels	Votage-gated ion channels
ENSMUSG00000027827.17	KCNAB1	0.71	Downregulated		
ENSMUSG00000062785.14	KCNC3	0.66	Downregulated		
ENSMUSG00000036760.7	KCNK9	0.45	Downregulated		
ENSMUSG00000054934.10	KCNMB4	1.71	Upregulated		
ENSMUSG00000002908.17	KCNN1	0.66	Downregulated		
ENSMUSG00000058740.14	KCNT1	0.60	Downregulated		
ENSMUSG00000000794.9	KCNN3	0.58	Downregulated		
ENSMUSG00000064329.13	SCN1A	0.52	Downregulated	Sodium channels	
ENSMUSG00000075316.11	SCN9A	0.70	Downregulated		
ENSMUSG00000014158.12	TRPV4	1.64	Upregulated	Transient receptor potential channels	Other ion channels
ENSMUSG00000032769.5	TRPA1	0.59	Downregulated		
ENSMUSG00000026628.13	ATF3	60.67	Upregulated	Transcription factor	Other neuronal injury marker

It is worth noting that the chemokine with the highest regulation among the transcripts in our dataset is CCL8. To our knowledge there are no previous reports that

describe the role of CCL8 in the DRG after nerve injury. This chemokine has chemoattractant effects for both myeloid and T cells (Zaidi et al., 2011; Heng et al., 2022), and taking into account that both immune cell types participate on pain development (as previously commented), it seems possible that CCL8 might play a role on the immune response leading to neuropathic pain.

Among the neuronal genes regulated in WT mice in the DRG after SNI, we found transcripts of very diverse molecular nature, such as G-protein-coupled receptors (GPCRs - which include several cholinergic, serotonin and opioid receptors), ionotropic receptors (such as subunits of the $GABA_A$ receptor), voltage-gated ion channels (including transcripts encoding for both potassium and sodium channels), and some transient receptor potential (TRP) channels (such as TRPV4 and TRPA1), among other neuronal genes (see Table 2 for details of some regulated neuronal genes).

The decrease in the expression of opioid receptors in the DRG is well documented, in particular with the μ opioid receptor (OPRM1), as it is thought that it is partially responsible of the reduced effectiveness of opioid drugs in neuropathic pain patients (Zhang et al., 1998; Rashid et al., 2004). Another neural downregulated gene is TRPA1 (Transient Receptor Potential Vanilloid 1), which acts as a major sensor for noxious cold (Karashima et al. 2009) and it is known to downregulate after SNI (Staaf et al., 2009). Several receptors for neurotransmitters have an altered expression after nerve injury. For instance, it is known that the subunits of the $GABA_A$ receptor are downregulated during neuropathic pain (Wang et al., 2021). In addition, there are also apparent changes in voltage-gated ion channels. The downregulation of expression of the majority of potassium channels is one of the characteristic features of the neuropathic remodeling within the injured peripheral afferents (Du and Gamper, 2013). Sodium channels are also prominently downregulated after nerve injury (Laedermann et al., 2014). All these previously reported transcriptional changes fully agree with our results (Table 2). Of course there are many other neuronal transcripts which are regulated after nerve injury and that are not mentioned here (see Table 2 and Table S1 in Appendix). It is worth noting that we detected an upregulation in ATF3 (activating transcription factor 3), which is robustly increased after nerve injury (60.67 fold-increase in comparison to naïve samples in our dataset) (Table 2) and it is

considered to be a standard marker of injured neurons (Tsujino et al., 2000; Laedermann et al., 2014; Bravo-Caparrós et al., 2020). This robust increase in ATF3 clearly indicates that our transcriptomic data reflect the changes which occur in the injured DRG.

We noticed that most immune transcripts appear to be upregulated after SNI, whereas most neuronal markers appear to be downregulated (see Tables 1 and 2). We therefore conducted a functional enrichment analysis using exclusively the transcripts up- or downregulated after SNI. When testing the upregulated transcripts we found a marked increase in the enrichment for the annotation of immune functions, in comparison to the analysis using the full list of regulated transcripts, with B-H *P* values close to 10^{-45} (Figure 2C). The description of the content of the functional annotations of the upregulated transcripts is shown in Table S2 in Appendix. When the functional enrichment analysis was carried out using the list of downregulated genes, we found that neuronal functions, such as "Neurotransmission", or "Transport of ion" showed still a highly significant B-H *P* values in the range of 10^{-14} - 10^{-15} (Figure 2D), similar to the significance found when analysing the complete list of genes. The description of the content of the functional annotations of the downregulated transcripts is shown in Table S3 in Appendix. The enrichment in neuronal-related functions in the list of transcripts downregulated after nerve injury is consistent with previously reported datasets using microarrays to determine gene expression after SNI (Costigan et al., 2010), and might contribute or might be a consequence of the sensitization processes of sensory neurons.

In summary, the transcriptomic changes that occur in the injured DRG of WT mice after SNI, under our experimental conditions, agree with the previous literature, and whereas immune-related genes clearly upregulate after nerve injury, a significant portion of neuronal-related transcripts decrease their expression.

3.2.3 Differences in the transcriptional profile of the DRG between uninjured WT and sigma-1 receptor KO mice

We made an initial analysis comparing the transcriptional profile of the L3 and L4 DRG from naïve WT and sigma-1 receptor KO mice. We found significant differences in the expression of 1156 transcripts between genotypes, where 547 of them were upregulated in the sigma-1 receptor KO mice (light blue in the WT and dark blue in the KO) and 609 transcript were downregulated in the sigma-1 receptor KO mice (dark blue in the WT mice and light blue in the mutant animals), as shown in the corresponding heat map in Figure 3A.

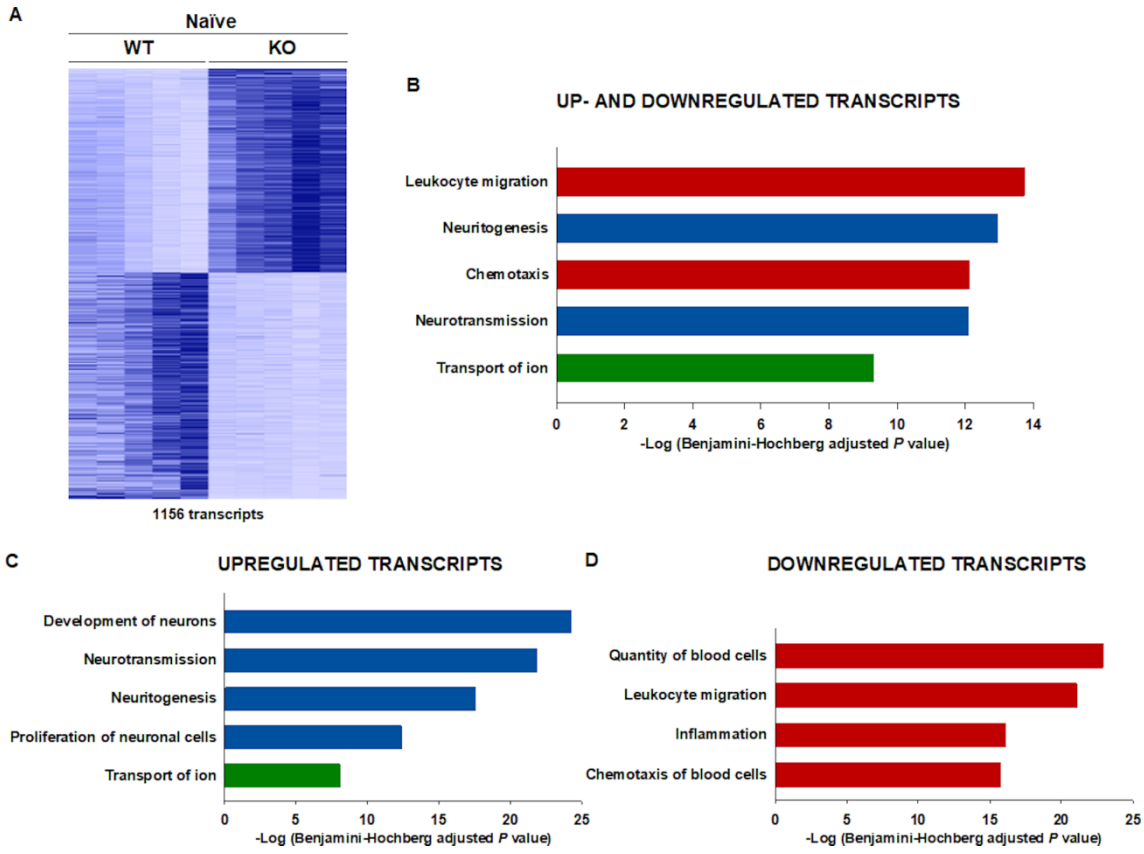

Figure 3. Comparison of the transcriptional profile of the dorsal root ganglia (DRG) from naïve wild-type (WT) and sigma-1 receptor knockout (KO) mice. (A) Heatmap of the relative expression of the transcripts from the L3-L4 DRG with significant differences ($P < 0.01$ and fold change 1.4) between naïve WT and KO mice. Light blue represents low-level expression and dark blue high-level expression. The total number of regulated transcripts is indicated. (B) Representative functional characteristics sorted by the strength of statistical significance (-log of Benjamini-Hochberg adjusted *P*-value) that IPA software ascribed the function given, using all regulated transcripts, and also splitting the list into the transcripts (C) upregulated or (D) downregulated by the knockout of sigma-1 receptor gene.

We then performed a functional enrichment analysis with all DRG transcripts that show differential expression between both genotypes. We found a mix of immune and neuronal functions, as shown in Figure 3B. “Leukocyte migration” and “Chemotaxis” were strongly associated to the gene list, with B-H *P* values of 10^{-13} – 10^{-14}, and include transcripts encoding for cathepsins, several chemokines, chemokine receptors and diverse immune markers. See some example immune genes in Table 3. “Neuritogenesis”, “Neurotransmission”, and “Transport of ion” were also significantly associated to the list of transcripts (B-H *P* value of 10^{-9}-10^{-13}), and this includes receptors for several neurotransmitters, voltage-gated ion channels (both potassium and sodium channels) and other channels, such as TRPA1 or ASIC1. See some example immune genes in Table 4. All these functions were correctly populated with a number of transcripts ranging between 78 and 145. The full content of each functional annotation is shown in Table S4 in Appendix.

Table 3. Some example immune genes whose expression in the DRG (L3-L4) differ between naïve wild-type (WT) and sigma-1 receptor knockout mice (KO). Fold change represents the ratio of the expression in naïve KO/WT.

GENE ID	GENE NAME	FOLD CHANGE	REGULATION	FUNCTION
ENSMUSG00000030560.17	CTSC	0.71	Downregulated	Cathepsins
ENSMUSG00000038642.10	CTSS	0.57	Downregulated	
ENSMUSG00000034855.13	CXCL10	0.47	Downregulated	Chemokines
ENSMUSG00000061353.11	CXCL12	0.70	Downregulated	
ENSMUSG00000035385.5	CCL2	0.5	Downregulated	
ENSMUSG00000035373.2	CCL7	0.37	Downregulated	
ENSMUSG00000020676.2	CCL11	0.46	Downregulated	
ENSMUSG00000035352.3	CCL12	0.51	Downregulated	
ENSMUSG00000071005.7	CCL19	0.09	Downregulated	
ENSMUSG00000004814.10	CCL24	0.26	Downregulated	
ENSMUSG00000044071.9	TAFA2	1.41	Upregulated	
ENSMUSG00000078735.4	IL11RA2	0.03	Downregulated	
ENSMUSG00000024810.16	IL33	0.67	Downregulated	
ENSMUSG00000052336.7	CX3CR1	0.57	Downregulated	Chemokine receptors
ENSMUSG00000045382.6	CXCR4	0.67	Downregulated	
ENSMUSG00000028859.14	CSF3R	0.40	Downregulated	
ENSMUSG00000030748.9	IL4R	0.54	Downregulated	
ENSMUSG00000023915.5	TNFRSF21	1.62	Upregulated	
ENSMUSG00000024621.16	CSF1R	0.60	Downregulated	

ENSMUSG00000049103.14	CCR2	0.50	Downregulated	
ENSMUSG00000079227.10	CCR5	0.49	Downregulated	
ENSMUSG00000044811.13	CD300C2	0.48	Downregulated	Other immune markers
ENSMUSG00000018774.13	CD68	0.63	Downregulated	
ENSMUSG00000030786.18	ITGAM	0.48	Downregulated	
ENSMUSG00000055541.17	LAIR1	0.6	Downregulated	
ENSMUSG00000004707.14	LY9	0.60	Downregulated	
ENSMUSG00000069516.8	LYZ	0.50	Downregulated	
ENSMUSG00000030579.10	TYROBP	0.5	Downregulated	

The functions associated to the list of transcripts with different expressions in uninjured WT and sigma-1 receptor KO mice are similar to what we found when comparing WT mice before and after nerve injury, according to the preceding section. However, as seen in Tables 3 and 4, whereas immune transcripts appeared to be downregulated in the KO mice, most neuronal transcripts appeared to be upregulated (i.e. the opposite than in WT mice after nerve injury). We then performed the functional enrichment analysis using the lists of transcripts up- or downregulated in the sigma-1 receptor KO mice in comparison to WT mice.

Table 4. Some example neuronal genes whose expression in the DRG (L3-L4) differ between naïve wild-type (WT) and sigma-1 receptor knockout mice (KO). Fold change represents the ratio of the expression in naïve KO/WT.

GENE ID	GENE NAME	FOLD CHANGE	REGULATION	FUNCTION	
ENSMUSG00000045613.9	CHRM2	1.73	Upregulated	Cholinergic receptors	GPCRs
ENSMUSG00000032303.8	CHRNA3	1.78	Upregulated		
ENSMUSG00000039809.10	GABBR2	1.57	Upregulated	GABA receptor	
ENSMUSG00000026322.9	HTR4	0.52	Downregulated	Serotonin receptor	
ENSMUSG00000000766.18	OPRM1	0.62	Downregulated	Opioid receptor	
ENSMUSG00000026959.13	GRIN1	1.46	Upregulated	Glutamate receptors	Ionotropic receptors
ENSMUSG00000020524.16	GRIA1	0.68	Downregulated		
ENSMUSG00000055078.7	GABRA5	1.46	Upregulated	GABA receptors	
ENSMUSG00000031343.13	GABRA3	0.67	Downregulated		
ENSMUSG00000032269.8	HTR3A	1.60	Upregulated	Serotonin receptors	
ENSMUSG00000008590.4	HTR3B	1.49	Upregulated		
ENSMUSG00000047976.4	KCNA1	1.46	Upregulated	Potassium channels	Votage-gated ion channels
ENSMUSG00000050556.9	KCNB1	1.56	Upregulated		
ENSMUSG00000058975.7	KCNC1	1.70	Upregulated		

ENSMUSG00000027895.10	KCNC4	1.43	Upregulated		
ENSMUSG00000028631.7	KCNQ4	1.49	Upregulated		
ENSMUSG00000019194.15	SCN1B	1.41	Upregulated	Sodium channels	
ENSMUSG00000070304.12	SCN2B	2.37	Upregulated		
ENSMUSG00000046480.6	SCN4B	1.46	Upregulated		
ENSMUSG00000023033.14	SCN8A	1.58	Upregulated		
ENSMUSG00000023017.10	ASIC1	1.55	Upregulated	Acid channel	Other ion channels
ENSMUSG00000032769.5	TRPA1	0.71	Downregulated	Transient receptor potential channel	

When testing the upregulated transcripts we found a marked increase in the enrichment for the annotation of neuronal functions, which include functions such as "Development of neurons", "Neurotransmission", "Neuritogenesis", or "Proliferation of neuronal cells", with B-H *P* values ranging from 10^{-13} to 10^{-25}. "Transport of ion" was also present with a B-H *P* value of 10^{-9} (Figure 3C). The description of the content of the functional annotations of the upregulated transcripts is shown in Table S5 in Appendix. All functions had a high content in neuronal genes, and interestingly, immune functions completely disappeared from the annotations associated with the list of upregulated transcripts. Not every single regulated neuronal gene experienced an increased expression in the KO mice, since some genes such as OPRM1 or TRPA1 were downregulated (see Table 4). These two particular transcripts are interesting, since both are protein partners of the sigma-1 receptor (Kim et al., 2010; Cortés-Montero et al., 2019; Marcotti et al., 2023; Ruiz-Cantero et al., 2023). The decreased expression in the transcript for the μ opioid receptor might explain the known discrepancies between the pharmacological and genetic inhibition of sigma-1 receptors in the modulation of opioid effects, since it has been described that sigma-1 antagonists enhance opioid antinociception to heat stimulus in WT mice, whereas sigma-1 receptor KO mice show opioid effects equivalent to that of WT mice (Vidal-Torres et al., 2013; Montilla-García et al., 2018). Downregulation of TRPA1 could aid to explain the reduction of nociceptive behaviors seen in sigma-1 receptor KO mice after injection of formalin, a known TRPA1 activator, which was the first evidence of the role of sigma-1 receptors on pain modulation apart from the enhancement of opioid antinociception (Cendán et al., 2005).

The analysis of the transcripts which were downregulated in the KO mice yielded completely different results, since all functional annotations retrieved were related with the actions and functioning of the immune system, such as "Quantity of blood cells", "Leukocyte migration", "Inflammation" or "Chemotaxis of blood cells", with B-H *P* value ranging from 10^{-16} to 10^{-23} (Figure 3D). The description of the content of the functional annotations of the downregulated transcripts is shown in Table S6 in Appendix.

Therefore, in broad terms, the basal transcriptional profile found in the DRG of sigma-1 receptor KO mice is opposite to the changes found in the DRG after nerve injury in the WT mice described in the preceding section. If the transcriptional changes which occur in the DRG after SNI in WT mice are a reflection of the sensitized state of the sensory neurons, the basal alterations shown in the KO mice might reflect a state which dampen nociceptive sensitization. In spite of the high number of genes with an altered transcription in DRG of the KO mice shown here, these mutant mice do not have any overt basal sensory alteration, as shown in this study and in numerous previous studies (reviewed in Tsai et al., 2009; Merlos et al., 2017; Ruiz-Cantero et al., 2021). However, under conditions which normally induce a sensitization of the nociceptive system, such as for instance after administration of chemical algogens or in pathological pain models, sigma-1 receptor KO mice show a decreased sensitization (reviewed Tsai et al., 2009; Merlos et al., 2017; Sánchez-Fernández et al., 2017; Ruiz-Cantero et al., 2021).

We and others have previously reported by inmunohistochemical experiments that sigma-1 receptors are exclusively present in sensory neurons within the DRG (Montilla-García et al., 2018; Shin et al., 2020; Bravo-Caparrós et al., 2020; Ruiz-Cantero et al., 2023). Therefore, the alterations in neuronal genes could be explained as a direct consequence of the absence of sigma-1 receptors in the neurons. It is known that neurons are the major source of some chemokines in the DRG, such as CCL2 (Zhu et al., 2014). Here we show that naïve sigma-1 receptor KO mice have a decreased expression in several chemokines, including CCL2 (see Table 3). It could be hypothesized that the absence of sigma-1 receptors in sensory neurons could alter the production of neuronal-derived chemokines, which in turn might have an impact in the

baseline recruitment/activation of resident immune cells which could be detected by the high sensitivity of the RNAseq technique.

We then investigated the transcriptional profile of the injured DRGs of sigma-1 receptor KO mice. We obtained 2134 regulated transcripts in the injured DRG compared to the naïve condition, which is even higher than the regulatory events that we detected in injured WT mice (compare Figure 2A and 4A). The majority of the transcripts regulated in the injured DRG increase their expression after SNI (1233 transcripts which go in the heat map from light to dark purple after injury), although a significant portion of the transcripts were regulated in the opposite direction (901 transcripts which go in the heat map from dark to light purple after injury), similar to WT mice, as shown in the section above.

We made a functional enrichment analysis with the list of all regulated transcripts. Similar to what we found in WT mice, the biological functions most significantly associated to the list of transcripts regulated in the DRG from sigma-1 receptor KO mice after SNI were related to the inflammatory process, but also including some robust neuronal-related functions. All these functions were very populated, containing 155-322 transcripts. See Table S7 in Appendix for the content of genes in each annotated function. As with the injured WT mice, we conducted a functional enrichment analysis separating the lists of transcripts which were up- or downregulated after SNI. Similar to what we described in the preceding section, when testing the upregulated transcripts we found a marked increase in the enrichment for the annotation of immune functions, and when the functional enrichment analysis was carried out using the list of downregulated genes, we found a clear predominance of neuronal functions (Figure 4D). The description of the content of the functional annotations of the up- and downregulated transcripts are shown in Table S8 and S9 in Appendix. The B-H *P* values of all these functions were even more robust than the values seen in WT mice after SNI (compare Figure 2C-D and Figure 4C-D), which could be influenced by the altered transcriptional profile found in naïve sigma-1 receptor KO mice, as the baseline in naïve mice is the opposite of the regulation of immune and neuronal transcripts after the SNI, which might increase the sensitivity of the technique for detecting changes after injury. Therefore, in general terms, the immune

and neuronal transcriptional alterations induced by nerve injury seem to be preserved in the DRG of sigma-1 receptor KO mice.

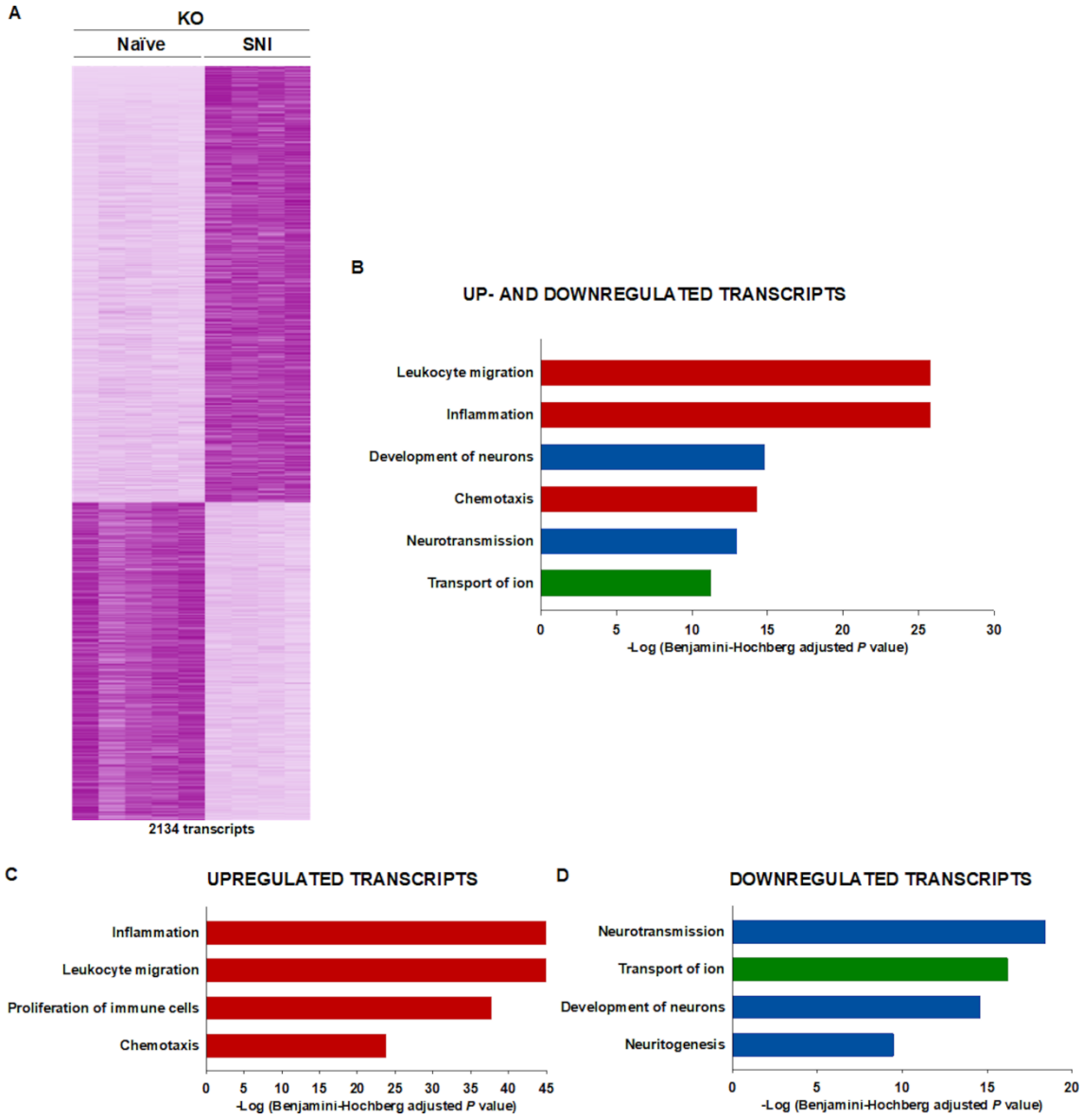

Figure 4. Transcriptional profile of the injured dorsal root ganglia (DRG) from sigma-1 receptor knockout (KO) mice after spared nerve injury (SNI). (A) Heatmap of the relative expression of the transcripts regulated ($P < 0.01$ and fold change 1.4) in the L3-L4 DRG 7 days after SNI compared to naïve mice. Light purple represents low-level expression and dark purple high-level expression. The total number of regulated transcripts is indicated. (B) Representative functional characteristics sorted by the strength of statistical significance (-log of Benjamini-Hochberg adjusted *P*-value) that IPA software ascribed the function given, using all regulated transcripts, and also splitting the list into the transcripts (C) upregulated or (D) downregulated by nerve injury.

3.2.4 Comparison of the transcriptome in the injured DRG after SNI in WT and sigma-1 receptor KO mice

To aid in the search for the mechanisms involved in the amelioration of neuropathic pain in the sigma-1 receptor KO mice, we performed a WGCNA with the transcripts which expressed a differential regulation between both genotypes at either during the naïve condition or after SNI (1259 transcripts), looking for those which are regulated by nerve injury (and hence with chances to be involved in neuropathic pain development) and with an attenuation of the regulation in the mutant mice.

When the WGCNA analysis was carried out, with the exception of 9 transcripts that do not seem to belong to any module (Table S10 in Appendix), all the regulated transcripts were grouped in 4 clusters attending to their topological overlap in their pattern of regulation. The heat maps of these modules are shown in Figure 5A, where light green represents low-level expression and dark green high-level expression. For clarity, the module eigengenes, as the representative of the gene expression profiles in each module, are shown in Figure 5B. The similarities between each module are shown in the heat map in Figure 5C.

It is thought that gene modules are groups of interconnected genes that may participate in a biologically meaningful function (e.g. Horvath et al., 2006; Oldham et al., 2008; Parikshak et al., 2015; Cobos et al., 2018). Therefore we performed a functional enriched analysis for each module. The most significantly associated biological function for each WGCNA module, together with the B-H *P* value and some example genes, is shown in Figure 5A.

Module I is composed by 436 transcripts. The content of this module is enriched in transcripts related with the functioning of the immune system, as “leukocyte migration” (see Figure 5A). All transcripts associated to this function are shown in Table S11 in Appendix. The expression of these genes is already different between WT and sigma-1 receptor KO under naïve conditions, and their expression remained unchanged after SNI in both genotypes (see Figure 5A and B). Therefore, and taking into account that this module is composed of genes not regulated by nerve injury, it does not seem likely that these transcripts are involved in SNI-induced neuropathic

pain or in the attenuation of neuropathic pain seen in sigma-1 receptor KO mice, but just represent stable immune differences in the DRG from WT and sigma-1 receptor KO.

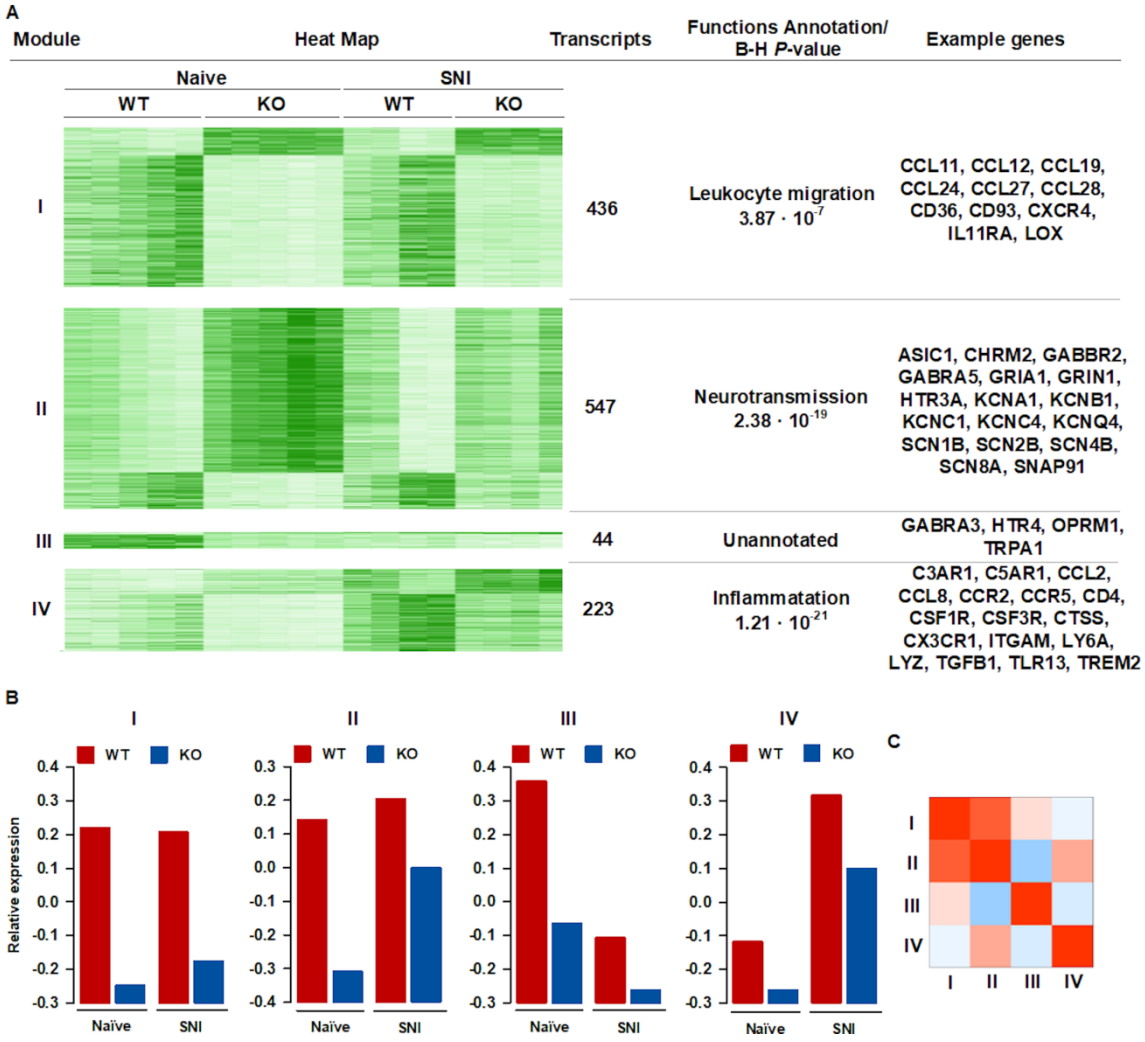

Figure 5. WGCNA of the transcripts in the dorsal root ganglia (DRG) which are differentially expressed between wild-type (WT) and sigma-1 receptor knockout (KO) mice at either naïve or post-SNI conditions. (A) Transcripts from the L3-L4 DRG with significant differences ($P < 0.01$ and fold change 1.4) between WT and KO mice with or without nerve injury were subjected to WGCNA analysis to produce unbiased modules of coregulated transcripts. The first column defines the module number. The second column shows the heatmaps of the relative expression of each transcript in each module. Light green represents low-level expression and dark green high-level expression. The third column shows the number of transcripts for each module. The fourth column gives a brief description of module function as defined by IPA software, indicating the Benjamini-Hochberg *P*-value ascribed to the function given, except for module II which could not be identified within any functional category and remained unannotated. The final column gives example transcripts from each functional subdivision. (B) Representations of the expression of the eigengenes for modules I-IV, with intensity of regulation on the y axis. Each module contains not only genes regulated in the fashion drawn but also reciprocal regulation events. (C) Heatmap of the similarities (adjacencies) in the eigengene network, in which blue color represents low adjacency and red represents high adjacency.

Module II is topologically close to module I (Figure 5C), with a Pearson correlation coefficient between both modules of 0.89. However, according to IPA, and in contradistinction to module I, which was enriched in immune genes (as previously mentioned), module II is very significantly enriched in neuronal genes, as shown in Figure 5A. This result highlights the usefulness of WGCNA to detect subtle differences in the patterns of expression of group of gens with differences in biologically relevant functions. Module II was the most populated among all gene clusters identified by our WGCNA in the DRG, with 547 transcripts. These genes do not suffer changes in expression by SNI in WT mice, similar to the transcripts in module I. Therefore, these transcripts can hardly explain the neuropathic hypersensitivity seen in WT mice. Interestingly, there is an initial robust difference in expression of these transcripts between naïve WT and sigma-1 receptor KO mice (as in module I), but SNI triggers changes in expression of these genes in sigma-1 receptor KO mice, which approach the values of WT mice (Figure 5A and B). Therefore, these transcripts seem unlike to be responsible to the attenuation of neuropathic pain of sigma-1 receptor KO mice. If anything, the normalization in the expression of these genes by nerve injury could be responsible for the sensory gain of the KO in neuropathic pain, as they are not completely immune to neuropathic allodynia.

Module III is the least populated, with only 44 genes (Figure 5A), and shows little overlap in the pattern of expression with the other modules (Figure 5C). There were some genes relevant to neurotransmission inside of this module, such as some receptors for neurotransmitters (GABA and serotonin), and some neuronal genes important for nociception, such as TRPA1 and the OPRM1 (Figure 5A). Most genes contained in this module show a basal expression lower in naïve sigma-1 receptor KO mice than in WT mice. After SNI, WT mice decrease markedly the expression of these transcripts, but gene expression in sigma-1 receptor KO mice tend to follow the exact same direction. In fact, the levels of these transcripts in the mutant animals with nerve injury are much lower than those found in the WT mice (Figure 5A and B). Therefore, if the downregulation of these transcripts in the WT mice after nerve injury would contribute to neuropathic pain, such robust downregulation in the sigma-1 receptor KO mice could not explain the attenuation of the neuropathic pain phenotype of the

mutant mice. An alternative explanation could be that the downregulation of (at least some of) these transcripts could constitute a protective homeostatic response to nerve injury aimed to decrease neuronal excitability, and that this mechanism would be maximized in sigma-1 receptor KO mice contributing to the decreased sensory hypersensitivity. It is difficult to discern a common biological purpose of the content of this module as it is not very populated and our functional enrichment analysis did not conclusively ascribe a robust biological function to this set of transcripts (Figure 5A).

The last module identified by the WGCNA (module IV) was composed by 223 transcripts, and shows a distinct pattern of expression that does not overlap with the other modules (Figure 5C). This group of genes was enriched in immune-related transcripts, being “Inflammation” the most representative function defined by IPA. There were receptors for complement factors, chemokines, chemokine receptors, cathepsins, and several other immune markers (Figure 5A). Sigma-1 receptor KO mice showed a baseline difference in the expression of these transcripts in the naïve condition in comparison to WT mice; then, SNI triggers a prominent regulation of these transcripts in WT mice, which is attenuated in sigma-1 receptor KO mice (Figure 5A and B). The expression of some of these transcripts is shown in Figure 6, to exemplify the similitudes in their pattern or regulation. We included chemokines (CCL2 and CCL8), a cathepsin (CTSS), and cytokine receptors and other immune cell markers (CCR5, CX3CR1, TREM2, LY6A, CD4). Altogether, the transcripts in module IV constitute the specific differences in the SNI-induced neuroinflammatory process in the DRG between WT and sigma-1 receptor KO mice. Taking into account the widely known importance of the neuroinflammatory process in the development of neuropathic pain (reviewed in Austin et al., 2010; Ellis et al., 2013; Fumagalli et al., 2020), the attenuation of the expression of these neuroinflammatory markers in the DRG of sigma-1 receptor KO mice with SNI point to that they might be related to the amelioration of the neuropathic pain phenotype of these mutant animals.

The transcript with the biggest fold difference between WT and sigma-1 receptor KO mice during SNI in module IV is CCL8 (6.93-fold decrease in the sigma-1 receptor KO mice) (see second panel in Figure 6). This cytokine is typically produced by active macrophages (Asano et al., 2015; Halvorsen et al., 2016), although it has been

described that it can also be produced by (at least some types) of neurons (Lu et al., 2017). CCL8 acts as a chemotactic factor to attract macrophages but primarily CD4+ T cells through interaction with CCR5, which is its canonical receptor (Ruffing et al., 1998; Halvorsen et al., 2016; Aldinucci et al., 2020). Interestingly, we found a marked attenuation of the increase of both CCR5 and CD4 in the sigma-1 receptor KO mice (Figure 6). In addition, another transcript with a marked increase after SNI and with a robust attenuation in the sigma-1 receptor KO mice is LY6A (4.97-fold decrease in the sigma-1 receptor KO mice with SNI, see Figure 6), which is also named T-cell-activating-protein (TAP) because of the critical role it plays on T cell activation (Stanford et al., 1997). Therefore, these results suggests that the decrease in some chemokines and other immune cell markers in the injured DRG of sigma-1 receptor KO mice might have a functional repercussion attenuating the recruitment of immune cells.

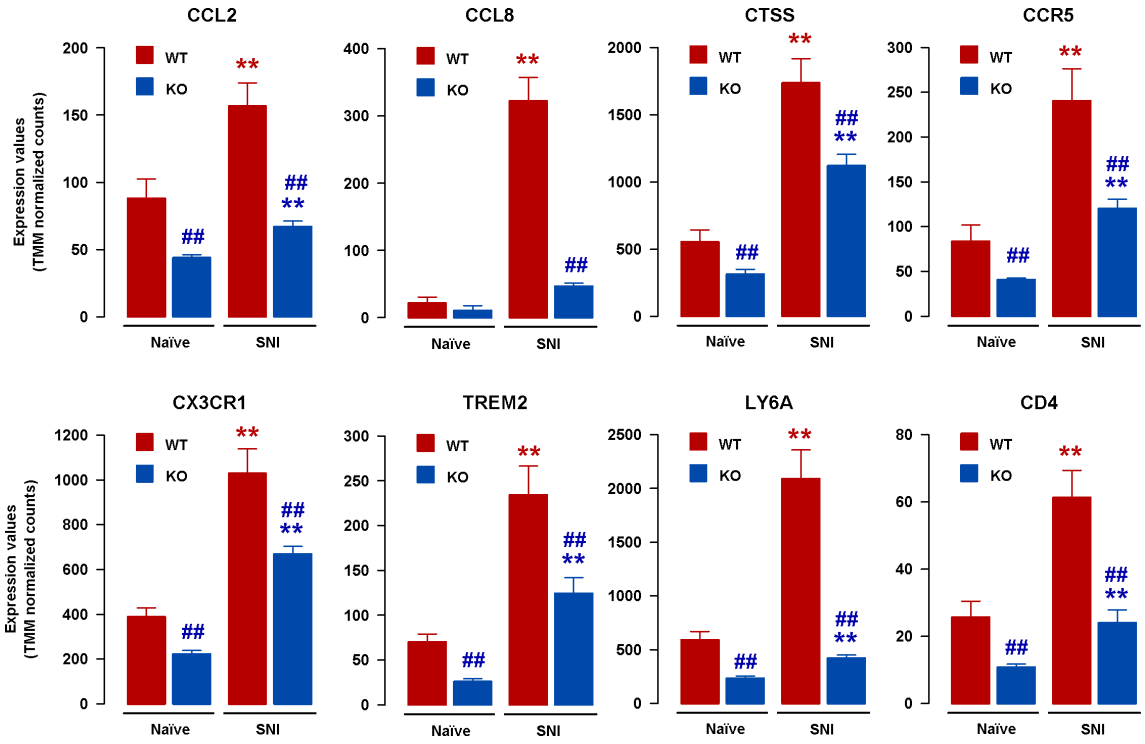

Figure 6. Expression of selected immune markers in the dorsal root ganglia (DRG) from wild-type (WT) and sigma-1 receptor knockout (KO) mice in the naïve condition and after spared nerve injury (SNI). Transcripts were selected from module IV after WGCNA. Expression of CCL2, CCL8, CTSS, CCR5, CX3CR1, TREM2, LY6A and CD4, as trimmed mean of M (TMM) normalized counts in the DRG of WT and KO mice at either naïve or post-SNI conditions. The differential expression analysis was performed with the default recommendations of DESeq2. Statistically significant differences between the values in naïve and SNI groups within samples from the same genotype: $^{**}P < 0.01$; and between the values from WT or KO mice under the same experimental conditions: $^{\#\#}P < 0.01$.

In summary, the analysis of the modules obtained by the expression pattern of the transcripts with a difference between WT and sigma-1 receptor KO mice, point to that a reduced neuroinflammatory process in the DRG of sigma-1 receptor KO mice might be participating in the decreased pain phenotype of these mutant mice.

3.2.5 Infiltration of immune cells in the injured DRG of WT and sigma-1 receptor KO mice after SNI

Taking into account the differences in immune-related transcripts between WT and sigma-1 receptor KO mice previously commented, we studied by FACS the presence of neutrophils (CD45+CD11b+Ly6G+ cells), macrophages/monocytes (CD45+CD11b+Ly6G− cells), B cells (CD45+ CD45R/B220+), and T cells (CD45+ TCRβ+) in DRG from uninjured WT and sigma-1 receptor KO mice, and after SNI.

Although in previous sections we found a lower expression in immune transcripts in naïve sigma-1 receptor KO mice in comparison to naïve WT mice, this did not translate into a decrease in the presence of any of the immune cells tested (see Figure 7A-C), possibly because the sensitivity of FACS to detect changes is lower than that of RNAseq, in particular during the naïve condition, as the number of resident immune cells in the DRG is low.

We then examined whether sigma-1 receptor KO mice had an alteration in the recruitment of immune cells in the DRG after SNI. Neutrophils are not significantly recruited in the ipsi- or contralateral DRG from either WT or sigma-1 receptor KO mice (Figure 7A, left panel). These data agree with previous studies which show that neutrophils do not participate on the neuroinflammatory process after SNI (Lindborg et al., 2018; Bravo-Caparrós et al., 2020). On the other hand, we found a marked increase in the presence of macrophages/monocytes in the injured DRG from WT mice on day 7 after SNI, compared to the values found on the DRG contralateral to the injury or from naïve animals. This increase was partially attenuated in sigma-1 receptor KO mice (Figure 7A, right panel) supporting our previous data where macrophage/monocyte infiltration in the DRG after SNI is decreased by sigma-1

receptor inhibition, purportedly by the decrease in the production of CCL2 (Bravo-Caparrós et al., 2020).

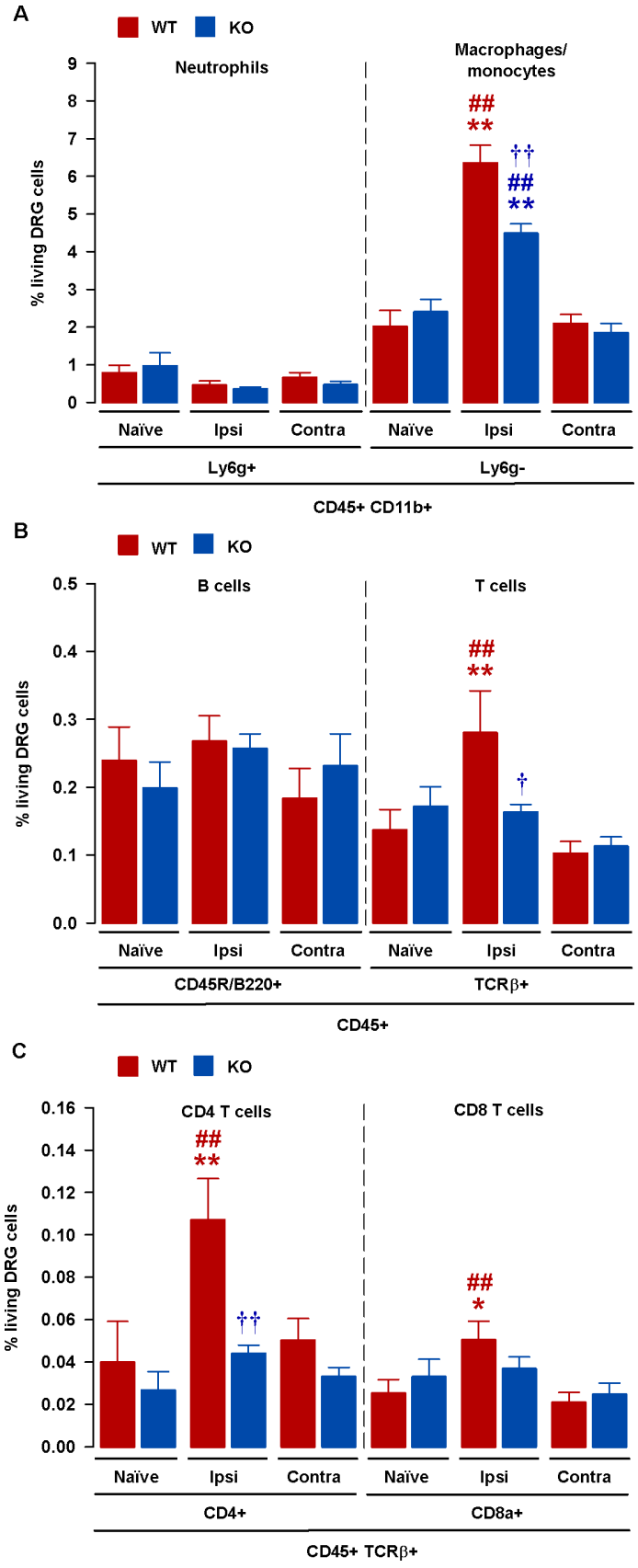

Figure 7. Infiltration of immune cells in the injured dorsal root ganglia (DRG) of wild-type (WT) and sigma-1 receptor knockout (KO) mice after spared nerve injury (SNI). (A) Neutrophils (CD45+ CD11b+ Ly6G+ cells) and macrophages/monocytes (CD45+ CD11b+ Ly6G− cells) , (B) B cells (CD45+ CD45R/B220+) and T cells (CD45+ TCRβ+ cells), (C) CD4 T cells (CD45+ TCRβ +CD4+ cells) and CD8 T cells (CD45+ TCRβ + CD8a+ cells) were determined by FACS in the DRG from naive mice, and ipsilateral and contralateral DRG from mice with SNI 7 days after surgery. For the naïve group, the values from the left and right side were averaged as there were no differences between them. Each bar and vertical line represent the mean ± SEM of the values obtained in 7-10 batches of L3-L4 DRG. Statistically significant differences between the values in naïve and SNI ipsilateral groups within samples from the same genotype: $^{**}P < 0.01$, $^{*}P < 0.05$; between the ipsilateral and contralateral values: $^{\#\#}P < 0.01$; and between DRG ipsilateral to SNI in the WT and KO groups: $^{\dagger\dagger}P < 0.01$, $^{\dagger}P < 0.05$ (two-way ANOVA followed by Student-Newman-Keuls).

We also examined the presence of relevant lymphocyte lineages in the DRG from WT and sigma-1 receptor KO mice before and after nerve injury. B cells did not significantly increase in the ipsi- or contralateral DRG from animals of either genotype (Figure 7B, left panel). Therefore, this immune cell type does not appear to participate on SNI-induced neuropathic pain, as previously reported (Cobos et al., 2018). On the other hand, the number of T cells significantly increased in the DRG ipsilateral to nerve injury of WT mice, compared to the values found on the DRG contralateral to the injury or from naïve animals, and importantly sigma-1 receptor KO mice did not show any apparent increase in the presence of this cell type in the injured DRG (Figure 7B, right panel). We then further explored the contribution of CD4+ and CD8+ subpopulations to the increase in T cells after SNI. We found that the recruitment of CD4+ T cells in the DRG from WT was considerably larger than the increase in CD8+, which was modest (Figure 7C, left and right panel). Sigma-1 receptor KO mice did not show any increase in any of these T cell subpopulations in the injured DRG (Figure 7C, left and right panel). To our knowledge, this is the first report showing that sigma-1 receptor KO mice have an influence on T cell recruitment after nerve injury. As T cells play a pivotal role in the development of neuropathic pain (Costigan et al., 2009; Cobos et al., 2018), it could be hypothesized that the absence in the recruitment of T cells into the DRG of our mutant mice might have an impact in their reduced pain phenotype.

In summary, sigma-1 receptor has a moderate impact in the recruitment of macrophages/monocytes but a marked influence in the recruitment of CD4+ T cells in the DRG after nerve injury. The reduction in the peripheral neuroinflammatory process might account for the amelioration of neuropathic pain in the sigma-1 receptor KO mice.

3.2.6 Infiltration of immune cells in the paw of WT and sigma-1 receptor KO mice after CFA-induced inflammation

Since, as described in the previous sections, sigma-1 receptor KO mice showed a decrease in the recruitment of immune cells in the injured DRG after SNI, we aimed to test whether these mutant mice had a generalized deficit in the recruitment of

immune cells that would account for the decrease in the neuroinflammatory process observed. Therefore, we evaluated immune cell recruitment after paw inflammation induced by CFA.

The number of resident immune cells in the paw tissue from naïve WT or sigma-1 receptor KO was indistinguishable. These include neutrophils (Figure 8A, left panel), macrophages/monocytes (Figure 8A, right panel), B cells (Figure 8B left panel), and T cells (Figure 8B, right panel), including the CD4+ (Figure 8C, left panel) and CD8+ (Figure 8C, right panel) subpopulations.

Seven days after the induction of the inflammation, there was a marked increase in neutrophils (Figure 8A, left panel) and macrophages/monocytes (Figure 8B, left panel) in the CFA-injected paw of both WT and sigma-1 receptor KO mice, in comparison to the values found on the paw contralateral to the injection or from naïve animals. The increase in these immune cells was equally robust in WT or sigma-1 receptor KO mice. We also studied the presence of lymphocyte lineages during CFA-induced inflammation. We did not detect a statistically significant increase in B cells after CFA injection in mice from either genotype (Figure 8B, left panel), but we found a prominent increase in T cell recruitment in the inflamed paw, which was of a similar magnitude in WT and sigma-1 receptor KO mice, and was not detected in the paw contralateral to the CFA-induced inflammation (Figure 8B, right panel). We also studied the CD4+ (Figure 8C, left panel) and CD8+ (Figure 8C, right panel) subpopulations of T cells, and we found that both of them were significantly increased in the inflamed paw, and to a similar extent in both genotypes (even sigma-1 KO mice showed values slightly higher than WT mice for CD4+ T cells) in comparison to the values found on the paw contralateral to the injection or from naïve animals. Therefore, sigma-1 receptor KO mice do not show any apparent deficit in immune cell recruitment in response to paw inflammation.

It can be concluded that the decrease in the neuroinflamatory response in the DRG of sigma-1 receptor KO mice described in the previous sections cannot be explained by an overt deficit in the immune response of these mutant animals.

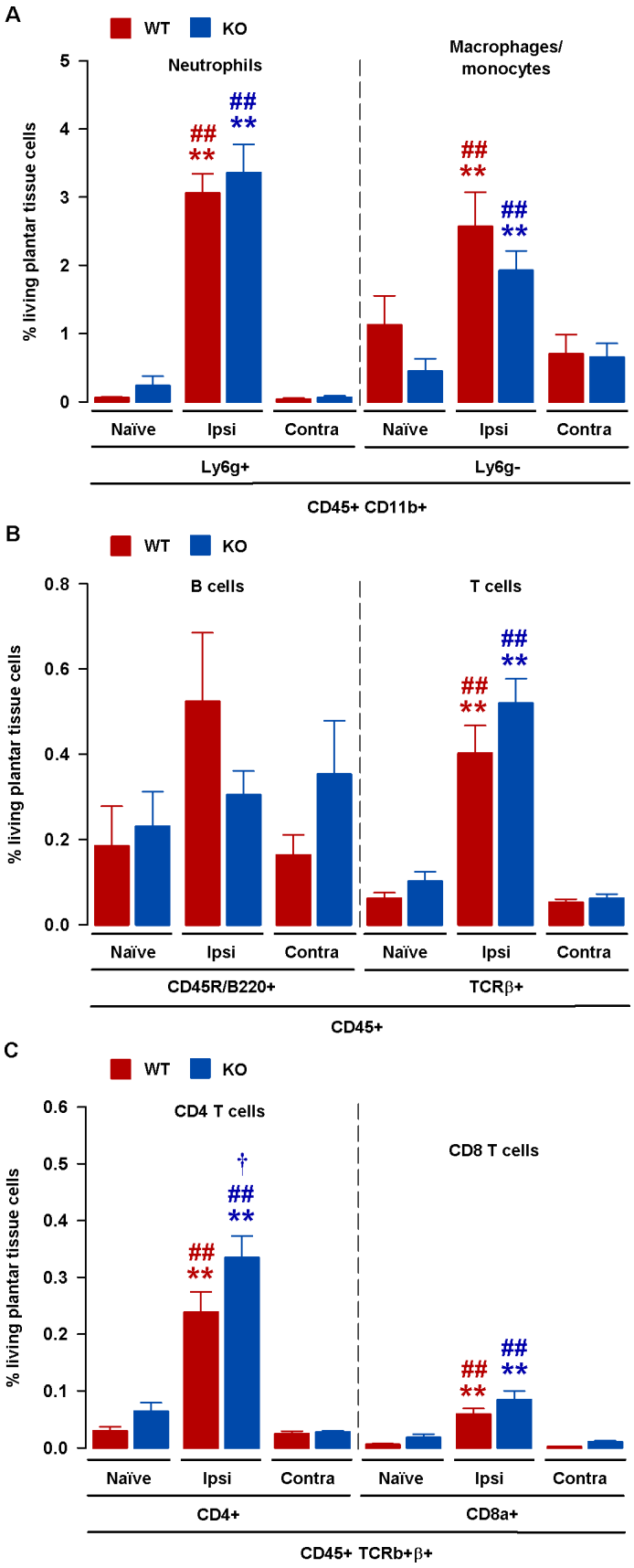

Figure 8. Infiltration of immune cells in the paw of wild-type (WT) and sigma-1 receptor knockout (KO) mice after peripheral inflammation induced by the intraplantar administration of Complete Freund's Adjuvant (CFA). (A) Neutrophils (CD45+ CD11b+ Ly6G+ cells) and macrophages/monocytes (CD45+ CD11b+ Ly6G− cells) , (B) B cells (CD45+ CD45R/B220+) and T cells (CD45+ TCRβ+ cells), (C) CD4 T cells (CD45+ TCRβ +CD4+ cells) and CD8 T cells (CD45+ TCRβ + CD8a+ cells) were determined by FACS in plantar tissue from naive mice, and ipsilateral and contralateral plantar tissue from mice 7 days after with CFA-induced inflammation. For the naïve group, the values from the left and right side were averaged as there were no differences between them. Each bar and vertical line represent the mean ± SEM of the values obtained from 7-10 independent paw samples. Statistically significant differences between the values in naïve and CFA ipsilateral groups within samples from the same genotype: $^{**}P < 0.01$, $^{*}P < 0.05$; between the ipsilateral and contralateral values: $^{\#\#}P < 0.01$; and between the paw ipsilateral to CFA in the WT and KO groups: $^{\dagger\dagger}P < 0.01$, $^{\dagger}P < 0.05$ (two-way ANOVA followed by Student-Newman-Keuls).

3.2.7 Comparison of the transcriptome in the dSC from WT and sigma-1 receptor KO mice

We also studied the transcriptional events in the dSC of WT and sigma-1 receptor KO mice in the naïve condition and after nerve injury. We first compared gene expression in uninjured and SNI WT mice. A heat map of the regulated transcripts is shown in the left panel of Figure 9A. We found 252 transcripts in the dSC regulated by the nerve injury, where the vast majority of transcripts were upregulated (251 transcripts which go in the heat map from light to dark red after injury), and only 1 transcript was downregulated. The number of regulated genes in the dSC is much lower than in the injured DRG (252 vs 1498 transcripts in the dSC vs DRG - compare left panel of Figure 9A with Figure 2A). This is consistent with previous transcriptomic analyses after nerve injury (Griffin et al., 2007; Costigan et al., 2010). We then grouped the genes regulated according to functional class, and found that all major functions ascribed by IPA were of immune nature, and with a very strong B-H *P* value that reached $7.28 \cdot 10^{-54}$ for the most significantly associated function ("Quantity of leukocytes") (Figure 9A, right panel). See Table S12 in Appendix for the content of genes in each annotated function. Some example regulated immune genes were listed in Table 5. The fact that most of the regulated transcripts in the dSC are from immune origin is in full agreement with previous literature, and demonstrates the robustness of the central neuroinflammatory process which occurs after nerve injury (e.g. Griffin et al., 2007).

We then compared the transcriptome of uninjured WT and sigma-1 receptor KO mice. We identified 308 transcripts with a different expression in the naïve WT and sigma-1 receptor KO mice. The heat map of those transcripts is shown in the Figure 9B. There were 128 upregulated genes (which go in the heat map from light to dark blue after injury), and 180 downregulated genes (which go in the heat map from dark to light blue after injury). The number of genes with a difference in the expression between uninjured WT and sigma-1 receptor KO mice is substantially lower in the dSC than in the DRG (308 vs 1156 transcripts in the dSC vs DRG - compare Figure 9B and Figure 3A). The considerably greater impact of the KO of sigma-1 receptors in the DRG than in the dSC points to a more prominent function of these receptors at peripheral than at central level. We performed a functional enrichment analysis with IPA, using the

transcripts that show differential expression between both genotypes in the dSC. However, and in contrast to the robust annotations we found for the DRG analysis (see Section 3.2.3 and Figure 3), IPA was unable to find any robust biological function associated to the list of the transcripts differentially regulated between both genotypes in the dSC. As each software uses its own proprietary database to calculate the functional annotations, we made a second analysis using GO, but it also failed to find a biological function significantly associated to the gene list. Thus, there are not enough genes with a difference in expression between naïve WT and sigma-1 receptor KO mice involved in a single function to be clustered by standard software.

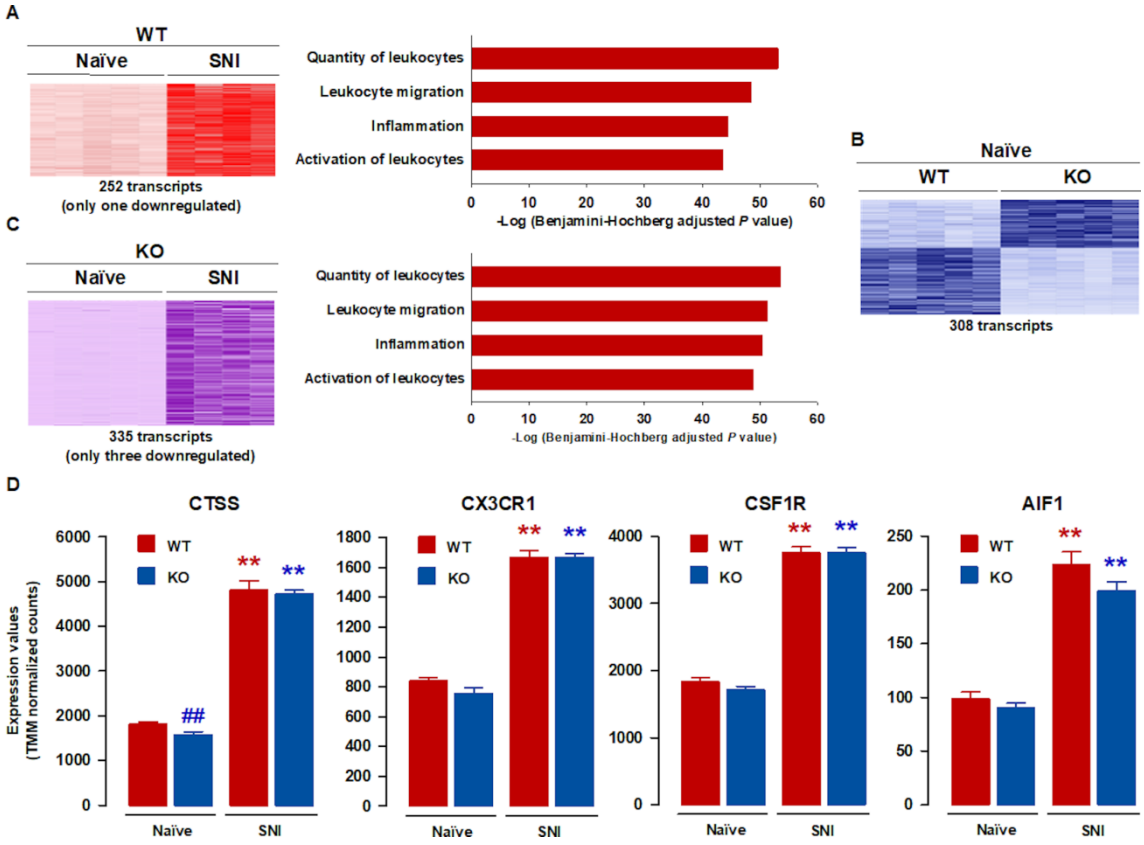

Figure 9. Transcriptional profile of the dorsal spinal cord (dSC) of wild-type (WT) and sigma-1 receptor knockout (KO) mice in the naïve condition and after spared nerve injury (SNI). (A) Left panel shows the heatmap of the relative expression of the transcripts regulated in the dSC from WT mice 7 days after SNI compared to naïve WT mice. Light red represents low-level expression and dark red high-level expression. The total number of regulated transcripts is indicated. Right panel shows representative functional characteristics sorted by the strength of statistical significance (-log of Benjamini-Hochberg adjusted *P*-value) that IPA software ascribed the function given, using all regulated transcripts. (B) Heatmap of the relative expression of the transcripts from the dSC with significant differences between naïve WT and KO mice. Light blue represents low-level expression and dark blue high-level expression. The total number of regulated transcripts is indicated. (C) Left panel shows the heatmap of the relative expression of the transcripts regulated in the dSC from KO mice 7 days after SNI compared to naïve KO mice. Light purple represents low-level expression and dark purple high-level expression. The total

number of regulated transcripts is indicated. Right panel shows representative functional characteristics sorted by the strength of statistical significance (-log of Benjamini-Hochberg adjusted *P*-value) that IPA software ascribed the function given, using all regulated transcripts. (D) Expression of selected immune markers (CCTS, CX3CR1, CSF1R and AIF1), as trimmed mean of M (TMM) normalized counts in the dSC of WT and KO mice at either naïve or post-SNI conditions. The differential expression analysis was performed with the default recommendations of DESeq2. Statistically significant differences between the values in naïve and SNI groups within samples from the same genotype: $^{**}P < 0.01$; and between the values from WT or KO mice under the same experimental conditions: $^{\#\#}P < 0.01$.

We also compared gene expression in uninjured and SNI sigma-1 receptor KO mice. A heat map of the regulated transcripts is shown in the left panel of Figure 9C. The number of regulatory events was slightly larger than in WT mice (compare Figure 9A and C). We found 335 transcripts in the dSC regulated by the nerve injury, where the vast majority of transcripts were upregulated (332 transcripts which go in the heat map from light to dark purple after injury), and only 3 transcripts were downregulated. Similar to WT mice, all major functions ascribed by IPA had a strong immune-related content (Figure 9C, right panel), yielding B-H *P* values comparable to those found in WT mice (compare the right panel of Figure 9A and C). The description of the content of the functional annotations of the transcripts regulated in the dSC from sigma-1 receptor KO mice after SNI is shown in Table S13 in Appendix.

We then selected all transcripts with differences in the expression between WT and sigma-1 receptor KO mice at either naïve conditions or after SNI to perform a WGCNA analysis, as with the analysis of the DRG transcripts (shown in Fig 5). However, among 379 transcripts with differences between WT and KO mice, 332 of them represented genes without obvious regulation induced by injury in either genotype, constituting therefore stable differences in the dSC between WT and KO mice; equivalent to the module I found in the DRG (see section 2.4 and Fig 5). The remaining 47 transcripts did not cluster in modules that could be populated enough to reliably determine a biologically relevant function. This is in contrast to the hundreds of genes which we found in the DRG with a potential role in the effect of sigma-1 receptors on neuropathic pain, and with the marked attenuation of the increase in the immune cell transcripts (and immune cells numbers) in the DRG that we found in the sigma-1 receptor KO mice.

Table 5. Some example immune genes regulated in the dorsal spinal cord after SNI in wild-type mice. Fold change represents the ratio of the expression in SNI/naïve.

GENE ID	GENE NAME	FOLD CHANGE	REGULATION	FUNCTION
ENSMUSG00000038642.10	CTSS	2.65	Upregulated	Cathepsin
ENSMUSG00000052336.7	CX3CR1	1.99	Upregulated	Chemokines
ENSMUSG00000034855.13	CXCL10	4.96	Upregulated	
ENSMUSG00000019122.8	CCL9	2.06	Upregulated	
ENSMUSG00000035373.2	CCL7	11.10	Upregulated	
ENSMUSG00000035385.5	CCL2	3.54	Upregulated	
ENSMUSG00000035352.3	CCL12	4.05	Upregulated	
ENSMUSG00000027399.1	IL1A	2.71	Upregulated	
ENSMUSG00000032089.16	IL10RA	1.92	Upregulated	Chemokine receptors
ENSMUSG00000030748.9	IL4R	1.66	Upregulated	
ENSMUSG00000027947.11	IL6R	1.87	Upregulated	
ENSMUSG00000024621.16	CSF1R	2.04	Upregulated	
ENSMUSG00000071713.6	CSF2RB	2.69	Upregulated	
ENSMUSG00000028859.14	CSF3R	2.59	Upregulated	
ENSMUSG00000025804.5	CCR1	3.62	Upregulated	
ENSMUSG00000079227.10	CCR5	2.87	Upregulated	
ENSMUSG00000010142.12	TNFRSF13B	1.73	Upregulated	
ENSMUSG00000024397.14	AIF1	2.26	Upregulated	Other immune markers
ENSMUSG00000051439.7	CD14	1.51	Upregulated	
ENSMUSG00000044811.13	CD300C2	2.21	Upregulated	
ENSMUSG00000022901.13	CD86	2.14	Upregulated	
ENSMUSG00000030786.18	ITGAM	2.80	Upregulated	
ENSMUSG00000023992.14	TREM2	2.48	Upregulated	
ENSMUSG00000030579.10	TYROBP	1.93	Upregulated	

We have presented in Figure 9D the expression of some selected immune transcripts that are known to play an important role on central neuroinflammation during neuropathic pain, such as CTSS, which is critical for the maintenance of neuropathic pain via cleavage of fractalkine (Clark et al., 2012), the receptors for fractalkine (CX3CR1) and CSF1 (CSF1R), which are both present in activated microglia (Clark et al., 2012; Yu et al., 2021), and AIF1 (also known as IBA-1), which is considered a pan-microglial marker and probably the most standard marker of microglia in pain studies (e.g. Griffin et al., 2007; Costigan et al., 2009). All these transcripts had similar levels in naïve WT and sigma-1 receptor KO mice (or even slightly reduced in the KO mice, as for CTSS), and a nearly identical upregulation after nerve injury in both genotypes. In addition, we also studied the presence of microglia in the dSC by immunostaining.

Figure 10 shows representative images for the double labeling with the neuronal marker NeuN (green) and AIF1 (magenta) in samples of dSC obtained after SNI in WT (top panels) and sigma-1 receptor KO mice (bottom panels). AIF1 staining was more evident in the side ipsilateral to the injury (left side) of samples from either genotype, whereas a much lower intensity of AIF1 staining was detected in the side contralateral to the SNI. Therefore, our results using either transcriptomic analysis or with immunohistochemical experiments point to that the central neuroinflammatory response characteristic of neuropathic pain is preserved in sigma-1 receptor KO mice. Although there are some previous reports showing that sigma-1 inhibition is able to decrease microgliosis in rodent models of osteoarthritis, cancer pain, and central pain (reviewed in Ruiz-Cantero et al., 2021), to our knowledge, this is the first published research exploring the influence of sigma-1 receptors on the microglial response during peripheral neuropathic pain.

It is relevant to mention that it has been described that every single DRG neuron express sigma-1 receptors (Montilla-García et al., 2018; Bravo-Caparrós et al., 2020; Shin et al., 2022), and that the expression levels of this receptor in the DRG are about 6-fold higher than in the dSC (Sánchez-Fernández et al., 2014). Therefore, the prominent effect on the control of the neuroinflammatory process in the DRG seen in sigma-1 receptor KO mice, and the little central effect found in these mutant animals, agree with the anatomical location of sigma-1 receptors.

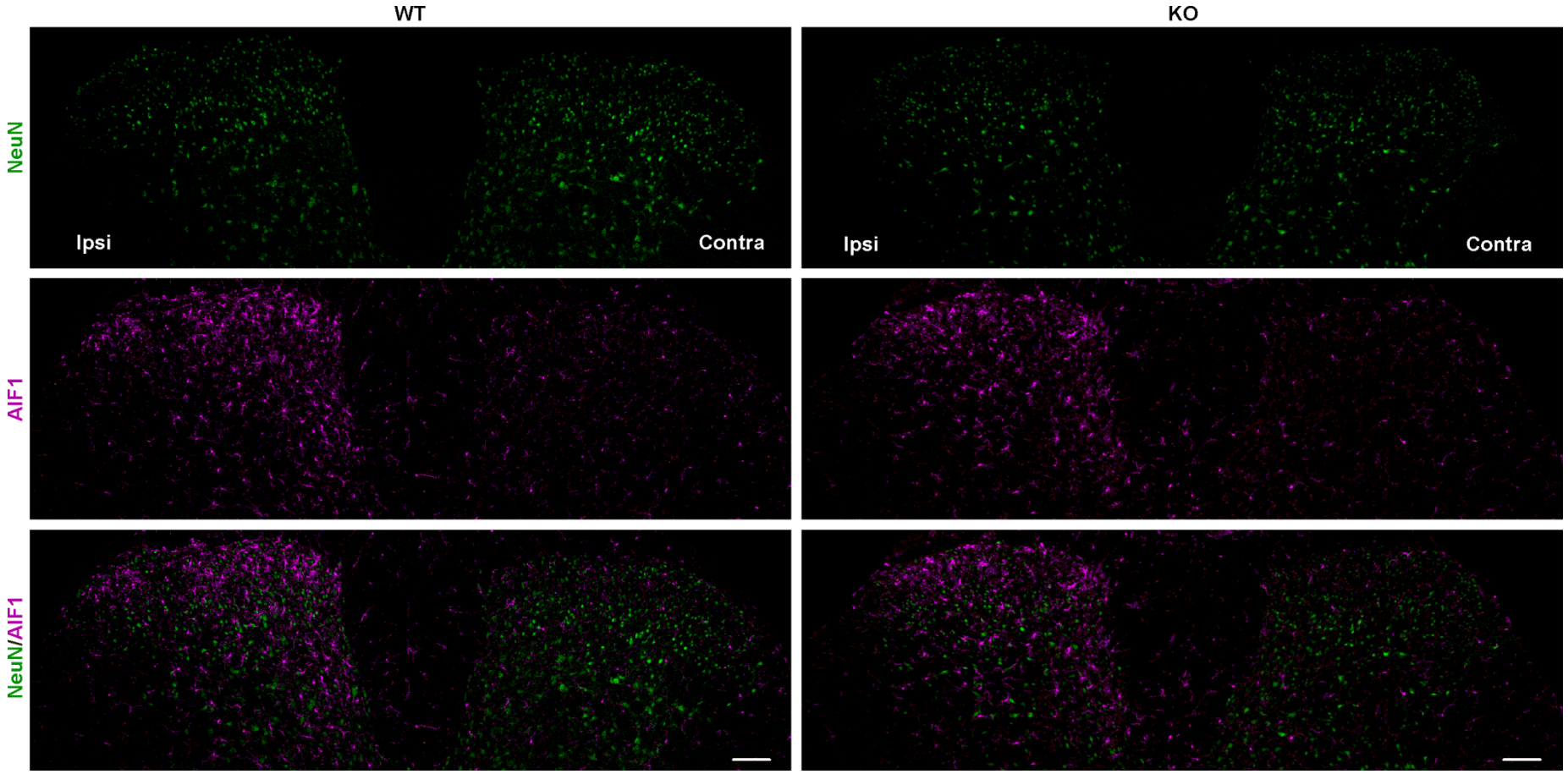

Figure 10. Wild-type (WT) and sigma-1 receptor knockout (KO) mice show an equivalent microglial response in the dorsal spinal cord (dSC) after spared nerve injury (SNI). Representative images of the immunostaining of the pan-neuronal marker NeuN (green) and the pan-microglial marker AIF1 (magenta) in the dSC of WT (left panels) and KO (right panels) mice 7 days after SNI. Scale bar 100 µm.

3.2.8 Effect of maraviroc on mechanical and cold allodynia in WT mice with SNI

As we found that sigma-1 receptor KO mice have attenuated neuropathic hypersensitivity to mechanical and cold stimulus, and that this is accompanied by the reduction in peripheral neuroinflammation, including a full decrease in the recruitment of CD4+ T cells, we attempted to mimic the effect of sigma-1 receptor inhibition by treatment with maraviroc, a CCR5 antagonist which inhibits primarily CD4+ T cells (Rosario et al., 2008).

Mice treated with the solvent of maraviroc showed a marked decrease in the mechanical threshold of the injured paw 7 days after SNI, in comparison to the baseline recording. However, mechanical threshold in the paw contralateral to surgery was similar to the baseline value in these solvent-treated mice (Figure 1A). SNI mice treated during 7 days with maraviroc in the drinking water showed a significant recovery of the mechanical threshold in the paw ipsilateral to the surgery. The effect of maraviroc was restricted to the injured paw, as the mechanical threshold of the contralateral paw was virtually identical to the baseline measure (Figure 11A). The results on cold sensitivity were very different, as treatment with maraviroc was unable to alter the behavioral responses to acetone (licking/biting the paw) in either the injured or the uninjured paw, and mice still showed a marked cold allodynia in the paw ipsilateral to the SNI (Figure 11B).

Maraviroc is used in the treatment of the infection caused by the human immunodeficiency virus (HIV). The dose used in our study in mice was equivalent to the dose used in humans after allometric scaling (Ochoa-Callejero et al., 2013; Pérez-Martínez et al., 2014 and 2020). Therefore, our results would support an additional indication of maraviroc, at doses normally used in therapy, to ameliorate (at least some symptoms associated with) neuropathic pain. There are only two previously published studies which tested the antineuropathic effects of maraviroc, and both studies administered this drug intrathecally (Piotrowska et al., 2016; Kwiatkowski et al., 2016). Here we show that oral administration is enough to induce an effect in tactile allodynia. Taking into account that this drug is known to have a very limited

central permeability (Garvey et al., 2012) it is reasonable to think that its effects are produced peripherally.

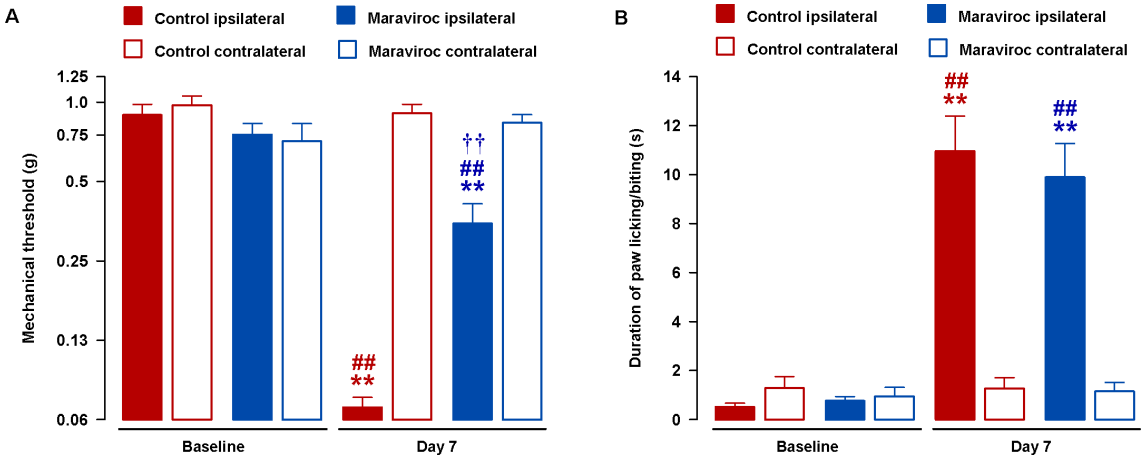

Figure 11. Effect of maraviroc on spared nerve injury (SNI)-induced neuropathic pain behaviors. The von Frey threshold (A) and duration of hind paw licking or biting in the acetone test (B) were recorded before the injury (baseline) and 7 days after SNI in the paws ipsilateral and contralateral to the site of surgery. Maraviroc was dissolved at 300 mg/L in the drinking water and given to the mice from the day before the SNI until the day of the sensory evaluation. Control mice were given drinking water without any additives. Each bar and vertical line represent the mean ± SEM of the values obtained in 10–12 animals. Statistically significant differences between the values obtained in the same paw on the baseline and day 7 after SNI: $^{**}P < 0.01$; between the ipsilateral and contralateral measurements: $^{\#\#}P < 0.01$; and between control and maraviroc treated-mice stimulated in the paw ipsilateral to SNI: $^{\dagger\dagger}P < 0.01$ (two-way repeated measures ANOVA followed by Student-Newman-Keuls).

It is worth mentioning that whereas sigma-1 receptor KO mice had an improvement in both tactile and cold allodynia, the treatment with maraviroc only had an effect on mechanical sensitivity, and therefore it did not fully replicate the effect of sigma-1 inhibition. This is consistent with previously published data where the depletion of macrophages or T cells decreased mechanical allodynia without affecting cold hypersensitivity (Cobos et al., 2018). Therefore, cold allodynia develops from changes in sensory neurons in a manner independent of the participation of immune cells. Whereas the decrease of neuropathic tactile hypersensitivity seen in the sigma-1 receptor KO mice is mirrored by maraviroc treatment and might be attributed to the decreased peripheral neuroinflammation, the robust effect on cold allodynia seen in the mutant animals cannot be attributed to this process but to independent neuronal effects. It has been described that sigma-1 receptor is a modulator of TRPs, including TRPV1 (Cortés-Montero et al., 2019; Ruiz-Cantero et al., 2023), TRPM8 and TRPA1 (Cortés-Montero et al., 2019). In fact, it has recently been shown that TRPA1

modulation by sigma-1 receptor has a strong impact on oxyplatin-induced cold allodynia (Marcotti et al., 2023). Therefore, it is tempting to speculate that the direct modulatory effects of sigma-1 receptors on TRPA1 (maybe in conjunction to other ion channels) might produce the amelioration of SNI-induced cold allodynia in a manner independent of the neuroinflammatory process.

3.3 Conclusions

In summary, our data indicate that peripheral sigma-1 receptors play a pivotal role in the communication between sensory neurons and the immune system after nerve injury. They participate in the production of certain chemokines which have an impact in the recruitment of macrophages/monocytes and CD4+ T cells in the injured DRG. This effect is not due to a broad immunomodulatory effect of sigma-1 receptors, as it is not seen at either the dSC of neuropathic animals or in an inflamed paw. However, although modulation of peripheral neuroinflammation by sigma-1 receptors might explain the amelioration of neuropathic tactile allodynia seen in sigma-1 receptor KO mice, it can hardly explain the effect on cold allodynia. Therefore, sigma-1 receptor inhibition may be potentially effective to decrease neuropathic pain through the inhibition of peripheral neuroinflammation and additional mechanisms.

CONCLUSIONS

CONCLUSIONS

Specific conclusions

1. Sigma-1 receptors are selectively present in every peripheral sensory neuron within the mouse and human DRG.

2. Sigma-1 antagonism reverses hyperalgesia, to heat and mechanical stimuli, induced by sensitizers (PGE2 and NGF) of peptidergic (TRPV1+) C-nociceptors on mice. This antihyperalgesic effect is mediated by the activation of μ opioid receptors by endomorphin-2, which is produced by TRPV1+ neurons.

3. The mechanism of this antihyperalgesic action of sigma-1 antagonists lies in the transfer of sigma-1 receptor from TRPV1 to μ opioid receptor, with the consequent desensitization of TRPV1 and the increase in opioid activity.

4. Sigma-1 antagonism do not reverse hyperalgesia induced by sensitizers (GDNF) of non-peptidergic (IB4+) C-nociceptors, which do not produce endomorphin-2.

5. Sigma-1 agonism enhances PGE2-induced mechanical hyperalgesia and hindpaw weight bearing asymmetry after a mild inflammatory condition induced by a plantar incision. These effects are mediated by TRPV1+ nociceptors.

6. The proalgesic effect induced by sigma-1 agonism on mice with a plantar incision requires the presence of neutrophils at the site of the surgical injury.

7. Spared nerve injury produces neuropathic pain (manifested as mechanical and cold hypersensitivity) on wild-type mice. This is accompanied by marked changes in the DRG, including alterations in the expression of immune- and neuronal-related transcripts as well as infiltration of immune cells (macrophages/monocytes and T cells, particularly CD4 cells). In contrast, the number of transcripts affected by this nerve injury is much lower in the dorsal spinal cord and these transcriptional alterations mainly represent the central neuroinflammatory response.

8. In comparison to wild-type mice, sigma-1 receptor KO mice with spared nerve injury show a decreased sensory hypersensitivity, as well as a reduction in both the

expression of immune-related transcripts and immune cell infiltration in the DRG. However, neuroinflammation in the dorsal spinal cord appears to be preserved in the mutant animals.

General conclusions

1. Sigma-1 receptors are important modulators of the sensitization of TRPV1+ nociceptors at the pain site in mice: whereas sigma-1 antagonists harness neuronally derived endogenous opioids to reduce hyperalgesia induced by inflammatory mediators, sigma-1 agonism exacerbates pain-like behaviors by the enhancement of the actions of algogenic chemicals produced, at least in part, by immune cells.

2. The sigma-1 receptors are also important for the reciprocal cross-talk between peripheral neurons and immune cells in neuropathic pain conditions. Inhibition of sigma-1 receptors ameliorates neuropathic pain, at least in part, by the decrease in the neuroinflammatory response which occurs in the DRG after nerve injury.

3. Sigma-1 antagonists have the potential to be effective analgesics under several circumstances. However, if the pronociceptive effects induced by sigma-1 agonism found here in mice translate to human patients, it might constitute a side effect that has gone unrecognized in patients treated with sigma-1 agonists in current medical practice or in clinical trials.

ABBREVIATIONS

LIST OF ABBREVIATIONS

ANOVA	Analysis of variance
ASIC	Acid-sensing ion channel
ASIC1a	Acid-sensing ion channel of the 1a subtype
ATF3	Activating transcription factor 3
ATP	Adenosine triphosphate
BC	Before Christ
BDNF	Brain-derived neurotrophic factor
BD-1063	1-[2-(3,4-dichlorophenyl)ethyl]-4-methylpiperazine dihydrochloride
CaM	Ca^{2+}-activated calmodulin
cAMP	3′-5′ cyclic adenosine monophosphate
CaMKII	Calmodulin-dependent kinase II
CCL2	Chemokine ligand 2
CCR2	C-C Chemokine Receptor 2
CCR5	C-C Chemokine Receptor 5
CD11b	Cluster of differentiation molecule 11B
CDK5	Cyclin-Dependent Kinase 5
CD45	Cluster of differentiation 45
CD45R/B220	Cluster of differentiation 45R/B cell isoform of 220
CFA	Complete Freud's adjuvant
CGRP	Calcitonin gene related peptide
CNS	Central nervous system
CX3CL1	C-X3-C Motif Chemokine Ligand 1 (Fractalkine)

CX3CR1	C-X3-C Motif Chemokine Receptor 1
Cx43	Connexin 43
DMT	*N,N*-dimethyltryptamine
COX	Cyclooxygenase
DAT	Dopamine transporter
DHEAS	Dehydroepiandrosterone sulfate
DOR	δ-opioid receptor
DRG	Dorsal root ganglion
dSC	Dorsal spinal cord
END2	Endomorphin-2
EP1	Eicosanoid-prostanoid receptors type 1
EP4	Eicosanoid-prostanoid receptors type 4
ER	Endoplasmic Reticulum
ERK	Extracellular-Signal-Regulated Kinase
FACS	Fluorescence-activated cell sorting
FBS	Fetal Bovine Serum
FMO	Fluorescence Minus One
GABA	Gamma-Aminobutyric Acid
GDNF	Glial cell-derived neurotrophic factor
GFRα1	GDNF family receptor α1
GO	Gene Ontology
GPCR	G-protein-coupled receptors
HINT1	Histidine triad nucleotide-binding protein 1

IB4	Isolectin B4
IBA-1	Ionized calcium-binding adapter molecule 1
IL-1β	Interleukin-1 β
IL-6	Interleukin-6
i.p.	Intraperitoneal
IPA	Ingenuity Pathway Analysis
i.pl.	Intraplantar
i.t.	Intrathecal
IP_3	Inositol 1,4,5- trisphosphate
KO	Knockout
Kv	Voltage-gated K+ channels
LPA	Lysophosphatidic acid
LTMRs	Low-threshold mechanoreceptors
Ly6G	Lymphocyte antigen 6 complex locus G6D
MAM	Mitochondria-associated endoplasmic reticulum membrane
MAPK	Mitogen-activated protein kinase
MCP1	Monocyte Chemoattractant Protein-1
MDMA	3,4-methylenedioxymethamphetamine
MOR	μ-opioid receptor
Mrgprd	Mas-related G-protein-coupled receptor D
NeuN	Neuronal nuclei
NF-200	Neurofilament-200
NGF	Nerve Growth Factor

NMDA	*N*-methyl-*D*-aspartate
NMDAR	*N*-methyl-*D*-aspartate receptor
NSAID	Non-steroidal anti-inflammatory drug
Nx	Naloxone
Nx-M	Naloxone methiodide
PBS	Phosphate-Buffered Saline
PCP	Phencyclidine
PGE2	Prostaglandin E2
PI3K	Phosphoinositide 3-kinase
PKA	Protein kinase A
PKC	Protein kinase C
PLCγ	Phospholipase C-γ
p.o.	Orally
PRE-084	[2-(4-morpholinethyl) 1- phenylcyclohexanecarboxylate hydrochloride]
RR	Ruthenium red
RET	Rearranged during transfection
RT	Room Temperature
RTX	Resiniferatoxin
s.c.	Subcutaneous
SC	Spinal cord
SDS-PAGE	Sodium dodecyl sulfate–polyacrylamide gel electrophoresis
SEM	Standard Error of the Mean
SERT	Serotonin transporter

SNI	Spared Nerve Injury
SP	Substance P
S1RA	4-[2-[[5-methyl-1-(2-naphthalenyl)-1H-pyrazol-3-yl]oxy]ethyl] morpholine hydrochloride
TCRβ	T cell receptor beta chain
TNF	Tumor necrosis factor
TrkA	Tropomyosin receptor kinase A
TrkB	Tropomyosin receptor kinase B
TRP	Transient Receptor Potential
TRPA1	Transient Receptor Potential Ankyrin 1
TRPM8	Transient Receptor Potential Melastatin member 8
TRPV1	Transient Receptor Potential Vanilloid type 1
VDCC	Voltage-Dependent Calcium Channels
WGCNA	Weighted Gene Co-expression Network Analysis
WT	Wild-type
σ1	Sigma-1 receptor
σ2	Sigma-2 receptor
5-HT	Serotonin

REFERENCES

REFERENCES

Abadias, M., Escriche, M., Vaqué, A., Sust, M., & Encina, G. (2013). Safety, tolerability and pharmacokinetics of single and multiple doses of a novel sigma-1 receptor antagonist in three randomized phase I studies. *Br. J. Clin. Pharmacol. 75*, 103-117.

Abdo, H., Calvo-Enrique, L., Lopez, J. M., Song, J., Zhang, M. D., Usoskin, D., El, M. A., Adameyko, I., Hjerling-Leffler, J., & Ernfors, P. (2019). Specialized cutaneous Schwann cells initiate pain sensation. *Science 365*, 695-699.

Agard, M., Asakrah, S., & Morici, L. A. (2013). PGE(2) suppression of innate immunity during mucosal bacterial infection. *Front Cell Infect. Microbiol. 3*, 45.

Agha, H. & McCurdy, C. R. (2021). In vitro and in vivo sigma 1 receptor imaging studies in different disease states. *RSC. Med. Chem. 12*, 154-177.

Aishwarya, R., Abdullah, C. S., Morshed, M., Remex, N. S., & Bhuiyan, M. S. (2021). Sigmar1's Molecular, Cellular, and Biological Functions in Regulating Cellular Pathophysiology. *Front Physiol 12*, 705575.

Aldinucci, D., Borghese, C., & Casagrande, N. (2020). The CCL5/CCR5 Axis in Cancer Progression. *Cancers. (Basel) 12.*

Alexander, S. P., Christopoulos, A., Davenport, A. P., Kelly, E., Mathie, A., Peters, J. A., Veale, E. L., Armstrong, J. F., Faccenda, E., Harding, S. D., Pawson, A. J., Southan, C., Davies, J. A., Abbracchio, M. P., Alexander, W., Al-Hosaini, K., Back, M., Barnes, N. M., Bathgate, R., Beaulieu, J. M., Bernstein, K. E., Bettler, B., Birdsall, N. J. M., Blaho, V., Boulay, F., Bousquet, C., Brauner-Osborne, H., Burnstock, G., Calo, G., Castano, J. P., Catt, K. J., Ceruti, S., Chazot, P., Chiang, N., Chini, B., Chun, J., Cianciulli, A., Civelli, O., Clapp, L. H., Couture, R., Csaba, Z., Dahlgren, C., Dent, G., Singh, K. D., Douglas, S. D., Dournaud, P., Eguchi, S., Escher, E., Filardo, E. J., Fong, T., Fumagalli, M., Gainetdinov, R. R., Gasparo, M., Gerard, C., Gershengorn, M., Gobeil, F., Goodfriend, T. L., Goudet, C., Gregory, K. J., Gundlach, A. L., Hamann, J., Hanson, J., Hauger, R. L., Hay, D. L., Heinemann, A., Hollenberg, M. D., Holliday, N. D., Horiuchi, M., Hoyer, D., Hunyady, L., Husain, A., IJzerman, A. P., Inagami, T., Jacobson, K. A., Jensen, R. T., Jockers, R., Jonnalagadda, D., Karnik, S., Kaupmann, K., Kemp, J., Kennedy, C., Kihara, Y., Kitazawa, T., Kozielewicz, P., Kreienkamp, H. J., Kukkonen, J. P., Langenhan, T., Leach, K., Lecca, D., Lee, J. D., Leeman, S. E., Leprince, J., Li, X. X., Williams, T. L., Lolait, S. J., Lupp, A., Macrae, R., Maguire, J., Mazella, J., McArdle, C. A., Melmed, S., Michel, M. C., Miller, L. J., Mitolo, V., Mouillac, B., Muller, C. E., Murphy, P., Nahon, J. L., Ngo, T., Norel, X., Nyimanu, D., O'Carroll, A. M., Offermanns, S., Panaro, M. A., Parmentier, M., Pertwee, R. G., Pin, J. P., Prossnitz, E. R., Quinn, M., Ramachandran, R., Ray, M., Reinscheid, R. K., Rondard, P., Rovati, G. E., Ruzza, C., Sanger, G. J., Schoneberg, T., Schulte, G., Schulz, S., Segaloff, D. L., Serhan, C. N., Stoddart, L. A., Sugimoto, Y., Summers, R., Tan, V. P., Thal, D., Thomas, W. W., Timmermans, P. B. M. W., Tirupula, K., Tulipano, G., Unal, H., Unger, T., Valant, C., Vanderheyden, P., Vaudry, D., Vaudry, H., Vilardaga, J. P., Walker, C. S., Wang, J. M., Ward, D. T., Wester, H. J., Willars, G. B., Woodruff, T. M., Yao, C., & Ye, R. D. (2021). THE CONCISE GUIDE TO PHARMACOLOGY 2021/22: G protein-coupled receptors. *Br. J. Pharmacol. 178 Suppl 1*, S27-S156.

Alexander, S. P. H., Roberts, R. E., Broughton, B. R. S., Sobey, C. G., George, C. H., Stanford, S. C., Cirino, G., Docherty, J. R., Giembycz, M. A., Hoyer, D., Insel, P. A., Izzo, A. A., Ji, Y., MacEwan, D. J., Mangum, J., Wonnacott, S., & Ahluwalia, A. (2018). Goals and practicalities of immunoblotting and immunohistochemistry: A guide for submission to the British Journal of Pharmacology. *Br. J. Pharmacol. 175*, 407-411.

Alon, A., Schmidt, H. R., Wood, M. D., Sahn, J. J., Martin, S. F., & Kruse, A. C. (2017). Identification of the gene that codes for the sigma(2) receptor. *Proc. Natl. Acad. Sci. U. S. A 114*, 7160-7165.

Alonso, G., Phan, V., Guillemain, I., Saunier, M., Legrand, A., Anoal, M., & Maurice, T. (2000).

Immunocytochemical localization of the sigma(1) receptor in the adult rat central nervous system. *Neuroscience 97*, 155-170.

Alvarez, P., Chen, X., Bogen, O., Green, P. G., & Levine, J. D. (2012). IB4(+) nociceptors mediate persistent muscle pain induced by GDNF. *J. Neurophysiol. 108*, 2545-2553.

Apkarian, A. V., Bushnell, M. C., Treede, R. D., & Zubieta, J. K. (2005). Human brain mechanisms of pain perception and regulation in health and disease. *Eur. J. Pain 9*, 463-484.

Asano, K., Takahashi, N., Ushiki, M., Monya, M., Aihara, F., Kuboki, E., Moriyama, S., Iida, M., Kitamura, H., Qiu, C. H., Watanabe, T., & Tanaka, M. (2015). Intestinal CD169(+) macrophages initiate mucosal inflammation by secreting CCL8 that recruits inflammatory monocytes. *Nat. Commun. 6*, 7802.

Austin, P. J. & Moalem-Taylor, G. (2010). The neuro-immune balance in neuropathic pain: involvement of inflammatory immune cells, immune-like glial cells and cytokines. *J. Neuroimmunol. 229*, 26-50.

Azcoitia, I., Sierra, A., Veiga, S., & García-Segura, L. M. (2003). Aromatase expression by reactive astroglia is neuroprotective. *Ann. N. Y. Acad. Sci. 1007*, 298-305.

Baamonde, A., Lastra, A., Juárez, L., García, V., Hidalgo, A., & Menéndez, L. (2005). Effects of the local administration of selective mu-, delta-and kappa-opioid receptor agonists on osteosarcoma-induced hyperalgesia. *Naunyn Schmiedebergs Arch. Pharmacol. 372*, 213-219.

Balasuriya, D., Stewart, A. P., Crottes, D., Borgese, F., Soriani, O., & Edwardson, J. M. (2012). The sigma-1 receptor binds to the Nav1.5 voltage-gated Na+ channel with 4-fold symmetry. *J. Biol. Chem. 287*, 37021-37029.

Bangaru, M. L., Weihrauch, D., Tang, Q. B., Zoga, V., Hogan, Q., & Wu, H. E. (2013). Sigma-1 receptor expression in sensory neurons and the effect of painful peripheral nerve injury. *Mol. Pain 9*, 47.

Barabas, M. E., Kossyreva, E. A., & Stucky, C. L. (2012). TRPA1 is functionally expressed primarily by IB4-binding, non-peptidergic mouse and rat sensory neurons. *PLoS. One. 7*, e47988.

Basbaum, A. I., Bautista, D. M., Scherrer, G., & Julius, D. (2009). Cellular and molecular mechanisms of pain. *Cell 139*, 267-284.

Bastos, L. F., Godin, A. M., Zhang, Y., Jarussophon, S., Ferreira, B. C., Machado, R. R., Maier, S. F., Konishi, Y., de Freitas, R. P., Fiebich, B. L., Watkins, L. R., Coelho, M. M., & Moraes, M. F. (2013). A minocycline derivative reduces nerve injury-induced allodynia, LPS-induced prostaglandin E2 microglial production and signaling via toll-like receptors 2 and 4. *Neurosci. Lett. 543*, 157-162.

Beery, A. K. & Zucker, I. (2011). Sex bias in neuroscience and biomedical research. *Neurosci. Biobehav. Rev. 35*, 565-572.

Beissner, F., Brandau, A., Henke, C., Felden, L., Baumgartner, U., Treede, R. D., Oertel, B. G., & Lotsch, J. (2010). Quick discrimination of A(delta) and C fiber mediated pain based on three verbal descriptors. *PLoS. One. 5*, e12944.

Binshtok, A. M., Wang, H., Zimmermann, K., Amaya, F., Vardeh, D., Shi, L., Brenner, G. J., Ji, R. R., Bean, B. P., Woolf, C. J., & Samad, T. A. (2008). Nociceptors are interleukin-1beta sensors. *J. Neurosci. 28*, 14062-14073.

Blaszczyk, L., Maitre, M., Leste-Lasserre, T., Clark, S., Cota, D., Oliet, S. H. R., & Fenelon, V. S. (2018). Sequential alteration of microglia and astrocytes in the rat thalamus following spinal nerve ligation. *J. Neuroinflammation. 15*, 349.

Bogen, O., Joseph, E. K., Chen, X., & Levine, J. D. (2008). GDNF hyperalgesia is mediated by PLCgamma, MAPK/ERK, PI3K, CDK5 and Src family kinase signaling and dependent on the IB4-binding protein versican. *Eur. J. Neurosci. 28*, 12-19.

Bradbury, E. J., Burnstock, G., & McMahon, S. B. (1998). The expression of P2X3 purinoreceptors in sensory neurons: effects of axotomy and glial-derived neurotrophic factor. *Mol. Cell Neurosci. 12*, 256-268.

Brain, S. D. & Williams, T. J. (1985). Inflammatory oedema induced by synergism between calcitonin gene-related peptide (CGRP) and mediators of increased vascular permeability. *Br. J. Pharmacol. 86*, 855-860.

Bravo-Caparrós, I., Perazzoli, G., Yeste, S., Cikes, D., Baeyens, J. M., Cobos, E. J., & Nieto, F. R. (2019). Sigma-1 Receptor Inhibition Reduces Neuropathic Pain Induced by Partial Sciatic Nerve Transection in Mice by Opioid-Dependent and -Independent Mechanisms. *Front Pharmacol. 10*.

Bravo-Caparrós, I., Ruiz-Cantero, M. C., Perazzoli, G., Cronin, S. J. F., Vela, J. M., Hamed, M. F., Penninger, J. M., Baeyens, J. M., Cobos, E. J., & Nieto, F. R. (2020). Sigma-1 receptors control neuropathic pain and macrophage infiltration into the dorsal root ganglion after peripheral nerve injury. *FASEB J. 34*, 5951-5966.

Brown, M. C., Perry, V. H., Lunn, E. R., Gordon, S., & Heumann, R. (1991). Macrophage dependence of peripheral sensory nerve regeneration: possible involvement of nerve growth factor. *Neuron 6*, 359-370.

Bruna, J. & Velasco, R. (2018). Sigma-1 receptor: a new player in neuroprotection against chemotherapy-induced peripheral neuropathy. *Neural Regen. Res. 13*, 775-778.

Bruna, J., Videla, S., Argyriou, A. A., Velasco, R., Villoria, J., Santos, C., Nadal, C., Cavaletti, G., Alberti, P., Briani, C., Kalofonos, H. P., Cortinovis, D., Sust, M., Vaque, A., Klein, T., & Plata-Salaman, C. (2018). Efficacy of a Novel Sigma-1 Receptor Antagonist for Oxaliplatin-Induced Neuropathy: A Randomized, Double-Blind, Placebo-Controlled Phase IIa Clinical Trial. *Neurotherapeutics. 15*, 178-189.

Bura, A. S., Guegan, T., Zamanillo, D., Vela, J. M., & Maldonado, R. (2013). Operant self-administration of a sigma ligand improves nociceptive and emotional manifestations of neuropathic pain. *Eur. J. Pain 17*, 832-843.

Burnstock, G. (2000). P2X receptors in sensory neurones. *Br. J. Anaesth. 84*, 476-488.

Buvanendran, A., Kroin, J. S., Berger, R. A., Hallab, N. J., Saha, C., Negrescu, C., Moric, M., Caicedo, M. S., & Tuman, K. J. (2006). Upregulation of prostaglandin E2 and interleukins in the central nervous system and peripheral tissue during and after surgery in humans. *Anesthesiology 104*, 403-410.

Canning, B. J. (2009). Central regulation of the cough reflex: therapeutic implications. *Pulm. Pharmacol. Ther. 22*, 75-81.

Cappuccio, G., Bernardo, P., Raiano, E., Pinelli, M., Alagia, M., Esposito, M., Della, C. R., Strisciuglio, P., Brunetti-Pierri, N., & Bravaccio, C. (2019). Pain and sleep disturbances in Rett syndrome and other neurodevelopmental disorders. *Acta Paediatr. 108*, 171-172.

Carcolé, M., Kummer, S., Goncalves, L., Zamanillo, D., Merlos, M., Dickenson, A. H., Fernández-Pastor, B., Cabanero, D., & Maldonado, R. (2019a). Sigma-1 receptor modulates neuroinflammation associated with mechanical hypersensitivity and opioid tolerance in a mouse model of osteoarthritis pain. *Br. J. Pharmacol. 176*, 3939-3955.

Carcolé, M., Zamanillo, D., Merlos, M., Fernández-Pastor, B., Cabanero, D., & Maldonado, R. (2019b). Blockade of the Sigma-1 Receptor Relieves Cognitive and Emotional Impairments Associated to Chronic Osteoarthritis Pain. *Front Pharmacol. 10*, 468.

Carroll, M. C. (2004). The complement system in regulation of adaptive immunity. *Nat. Immunol. 5*, 981-986.

Castany, S., Codony, X., Zamanillo, D., Merlos, M., Verdu, E., & Boadas-Vaello, P. (2019). Repeated Sigma-1 Receptor Antagonist MR309 Administration Modulates Central Neuropathic Pain Development After Spinal Cord Injury in Mice. *Front Pharmacol. 10*, 222.

Castany, S., Gris, G., Vela, J. M., Verdu, E., & Boadas-Vaello, P. (2018). Critical role of sigma-1 receptors in central neuropathic pain-related behaviours after mild spinal cord injury in mice. *Sci. Rep. 8*, 3873.

Cavanaugh, D. J., Lee, H., Lo, L., Shields, S. D., Zylka, M. J., Basbaum, A. I., & Anderson, D. J. (2009). Distinct subsets of unmyelinated primary sensory fibers mediate behavioral responses to noxious thermal and mechanical stimuli. *Proc. Natl. Acad. Sci. U. S. A 106*, 9075-9080.

Cendán, C. M., Pujalte, J. M., Portillo-Salido, E., Montoliu, L., & Baeyens, J. M. (2005). Formalin-induced pain is reduced in sigma(1) receptor knockout mice. *Eur. J. Pharmacol. 511*, 73-74.

Chang, C. T., Jiang, B. Y., & Chen, C. C. (2019). Ion Channels Involved in Substance P-Mediated Nociception and Antinociception. *Int. J. Mol. Sci. 20*.

Chaplan, S. R., Bach, F. W., Pogrel, J. W., Chung, J. M., & Yaksh, T. L. (1994). Quantitative assessment of tactile allodynia in the rat paw. *J. Neurosci. Methods 53*, 55-63.

Chau-In, W., Sukmuan, B., Ngamsangsirisapt, K., & Jirarareungsak, W. (2007). Efficacy of pre- and postoperative oral dextromethorphan for reduction of intra- and 24-hour postoperative morphine consumption for transabdominal hysterectomy. *Pain Med. 8*, 462-467.

Chen, C. C., Akopian, A. N., Sivilotti, L., Colquhoun, D., Burnstock, G., & Wood, J. N. (1995). A P2X purinoceptor expressed by a subset of sensory neurons. *Nature 377*, 428-431.

Chen, S., Liang, T., Xue, T., Xue, S., & Xue, Q. (2021). Pridopidine for the Improvement of Motor Function in Patients With Huntington's Disease: A Systematic Review and Meta-Analysis of Randomized Controlled Trials. *Front Neurol. 12*, 658123.

Chiang, C. C. & Schwedt, T. J. (2020). Calcitonin gene-related peptide (CGRP)-targeted therapies as preventive and acute treatments for migraine-The monoclonal antibodies and gepants. *Prog. Brain Res. 255*, 143-170.

Chien, C. C. & Pasternak, G. W. (1993). Functional antagonism of morphine analgesia by (+)-pentazocine: evidence for an anti-opioid sigma 1 system. *Eur. J. Pharmacol. 250*, R7-R8.

Choi, H. S., Lee, M. J., Choi, S. R., Smeester, B. A., Beitz, A. J., & Lee, J. H. (2018a). Spinal Sigma-1 Receptor-mediated Dephosphorylation of Astrocytic Aromatase Plays a Key Role in Formalin-induced Inflammatory Nociception. *Neuroscience 372*, 181-191.

Choi, H. S., Roh, D. H., Yoon, S. Y., Choi, S. R., Kwon, S. G., Kang, S. Y., Moon, J. Y., Han, H. J., Beitz, A. J., & Lee, J. H. (2018b). Differential involvement of ipsilateral and contralateral spinal cord astrocyte D-serine in carrageenan-induced mirror-image pain: role of sigma1 receptors and astrocyte gap junctions. *Br. J. Pharmacol. 175*, 558-572.

Choi, S. I. & Hwang, S. W. (2018). Depolarizing Effectors of Bradykinin Signaling in Nociceptor Excitation in Pain Perception. *Biomol. Ther. (Seoul.) 26*, 255-267.

Choi, S. R., Moon, J. Y., Roh, D. H., Yoon, S. Y., Kwon, S. G., Choi, H. S., Kang, S. Y., Han, H. J., Beitz, A. J., & Lee, J. H. (2017). Spinal D-Serine Increases PKC-Dependent GluN1 Phosphorylation Contributing to the Sigma-1 Receptor-Induced Development of Mechanical Allodynia in a Mouse Model of Neuropathic Pain. *J. Pain 18*, 415-427.

Choi, S. R., Roh, D. H., Yoon, S. Y., Kwon, S. G., Choi, H. S., Han, H. J., Beitz, A. J., & Lee, J. H. (2016). Astrocyte sigma-1 receptors modulate connexin 43 expression leading to the induction of below-level mechanical allodynia in spinal cord injured mice. *Neuropharmacology 111*, 34-46.

Chu, U. B. & Ruoho, A. E. (2016). Biochemical Pharmacology of the Sigma-1 Receptor. *Mol. Pharmacol. 89*, 142-153.

Chuang, C. L. & Demontis, F. (2021). Systemic manifestation and contribution of peripheral tissues to Huntington's disease pathogenesis. *Ageing Res. Rev. 69*, 101358.

Clark, A. K. & Malcangio, M. (2012). Microglial signalling mechanisms: Cathepsin S and Fractalkine. *Exp. Neurol. 234*, 283-292.

Clark, A. K. & Malcangio, M. (2014). Fractalkine/CX3CR1 signaling during neuropathic pain. *Front Cell Neurosci. 8*, 121.

Cobos, E. J., del, P. E., & Baeyens, J. M. (2007). Irreversible blockade of sigma-1 receptors by haloperidol and its metabolites in guinea pig brain and SH-SY5Y human neuroblastoma cells. *J. Neurochem. 102*, 812-825.

Cobos, E. J., Entrena, J. M., Nieto, F. R., Cendán, C. M., & Del, P. E. (2008). Pharmacology and therapeutic potential of sigma(1) receptor ligands. *Curr. Neuropharmacol. 6*, 344-366.

Cobos, E. J., Nickerson, C. A., Gao, F., Chandran, V., Bravo-Caparrós, I., González-Cano, R., Riva, P., Andrews, N. A., Latremoliere, A., Seehus, C. R., Perazzoli, G., Nieto, F. R., Joller, N., Painter, M. W., Ma, C. H. E., Omura, T., Chesler, E. J., Geschwind, D. H., Coppola, G., Rangachari, M., Woolf, C. J., & Costigan, M. (2018). Mechanistic Differences in Neuropathic Pain Modalities Revealed by Correlating Behavior with Global Expression Profiling. *Cell Rep. 22*, 1301-1312.

Constantin, C. E., Mair, N., Sailer, C. A., Andratsch, M., Xu, Z. Z., Blumer, M. J., Scherbakov, N., Davis, J. B., Bluethmann, H., Ji, R. R., & Kress, M. (2008). Endogenous tumor necrosis factor alpha (TNFalpha) requires TNF receptor type 2 to generate heat hyperalgesia in a mouse cancer model. *J. Neurosci. 28*, 5072-5081.

Cordone, V., Ferrara, F., Pecorelli, A., Guiotto, A., Vitale, A., Amicarelli, F., Cervellati, C., Hayek, J., & Valacchi, G. (2022). The constitutive activation of TLR4-I. *Free Radic. Biol. Med. 181*, 1-13.

Cortés-Montero, E., Sánchez-Blázquez, P., Onetti, Y., Merlos, M., & Garzón, J. (2019). Ligands Exert Biased Activity to Regulate Sigma 1 Receptor Interactions With Cationic TRPA1, TRPV1, and TRPM8 Channels. *Front Pharmacol. 10*, 634.

Costigan, M., Befort, K., Karchewski, L., Griffin, R. S., D'Urso, D., Allchorne, A., Sitarski, J., Mannion, J. W., Pratt, R. E., & Woolf, C. J. (2002). Replicate high-density rat genome oligonucleotide microarrays reveal hundreds of regulated genes in the dorsal root ganglion after peripheral nerve injury. *BMC. Neurosci. 3*, 16.

Costigan, M., Belfer, I., Griffin, R. S., Dai, F., Barrett, L. B., Coppola, G., Wu, T., Kiselycznyk, C., Poddar, M., Lu, Y., Diatchenko, L., Smith, S., Cobos, E. J., Zaykin, D., Allchorne, A., Gershon, E., Livneh, J., Shen, P. H., Nikolajsen, L., Karppinen, J., Mannikko, M., Kelempisioti, A., Goldman, D., Maixner, W., Geschwind, D. H., Max, M. B., Seltzer, Z., & Woolf, C. J. (2010). Multiple chronic pain states are associated with a common amino acid-changing allele in KCNS1. *Brain 133*, 2519-2527.

Costigan, M., Moss, A., Latremoliere, A., Johnston, C., Verma-Gandhu, M., Herbert, T. A., Barrett, L., Brenner, G. J., Vardeh, D., Woolf, C. J., & Fitzgerald, M. (2009). T-cell infiltration and signaling in the adult dorsal spinal cord is a major contributor to neuropathic pain-like hypersensitivity. *J. Neurosci. 29*, 14415-14422.

Cunha, T. M., Verri, W. A., Jr., Silva, J. S., Poole, S., Cunha, F. Q., & Ferreira, S. H. (2005). A cascade of cytokines mediates mechanical inflammatory hypernociception in mice. *Proc. Natl. Acad. Sci. U. S. A 102*, 1755-1760.

Curtis, M. J., Alexander, S. P. H., Cirino, G., George, C. H., Kendall, D. A., Insel, P. A., Izzo, A. A., Ji, Y., Panettieri, R. A., Patel, H. H., Sobey, C. G., Stanford, S. C., Stanley, P., Stefanska, B., Stephens, G. J., Teixeira, M. M., Vergnolle, N., & Ahluwalia, A. (2022). Planning experiments: Updated guidance on experimental design and analysis and their reporting III. *Br. J. Pharmacol. 179*, 3907-3913.

de la Puente, B., Nadal, X., Portillo-Salido, E., Sanchéz-Arroyos, R., Ovalle, S., Palacios, G., Muro, A., Romero, L., Entrena, J. M., Baeyens, J. M., Lopez-Garcia, J. A., Maldonado, R., Zamanillo, D., & Vela, J. M. (2009). Sigma-1 receptors regulate activity-induced spinal sensitization and neuropathic pain after peripheral nerve injury. *Pain 145*, 294-303.

de Yebenes, J. G., Landwehrmeyer, B., Squitieri, F., Reilmann, R., Rosser, A., Barker, R. A., Saft, C., Magnet, M. K., Sword, A., Rembratt, A., & Tedroff, J. (2011). Pridopidine for the treatment of motor function in patients with Huntington's disease (MermaiHD): a phase 3, randomised, double-blind,

placebo-controlled trial. *Lancet Neurol. 10*, 1049-1057.

Decosterd, I. & Woolf, C. J. (2000). Spared nerve injury: an animal model of persistent peripheral neuropathic pain. *Pain 87*, 149-158.

Dhaka, A., Earley, T. J., Watson, J., & Patapoutian, A. (2008). Visualizing cold spots: TRPM8-expressing sensory neurons and their projections. *J. Neurosci. 28*, 566-575.

Du, X. & Gamper, N. (2013). Potassium channels in peripheral pain pathways: expression, function and therapeutic potential. *Curr. Neuropharmacol. 11*, 621-640.

Dubin, A. E. & Patapoutian, A. (2010). Nociceptors: the sensors of the pain pathway. *J. Clin. Invest 120*, 3760-3772.

DuBreuil, D. M., López Soto, E. J., Daste, S., Meir, R., Li, D., Wainger, B., Fleischmann, A., & Lipscombe, D. (2021). Heat But Not Mechanical Hypersensitivity Depends on Voltage-Gated Ca(V)2.2 Calcium Channel Activity in Peripheral Axon Terminals Innervating Skin. *J. Neurosci. 41*, 7546-7560.

Ebbinghaus, M., Uhlig, B., Richter, F., von Banchet, G. S., Gajda, M., Brauer, R., & Schaible, H. G. (2012). The role of interleukin-1beta in arthritic pain: main involvement in thermal, but not mechanical, hyperalgesia in rat antigen-induced arthritis. *Arthritis Rheum. 64*, 3897-3907.

Edwards, D. A. (1968). Mice: fighting by neonatally androgenized females. *Science 161*, 1027-1028.

Ellis, A. & Bennett, D. L. (2013). Neuroinflammation and the generation of neuropathic pain. *Br. J. Anaesth. 111*, 26-37.

Emery, E. C., Luiz, A. P., Sikandar, S., Magnusdottir, R., Dong, X., & Wood, J. N. (2016). In vivo characterization of distinct modality-specific subsets of somatosensory neurons using GCaMP. *Sci. Adv. 2*, e1600990.

Entrena, J. M., Cobos, E. J., Nieto, F. R., Cendán, C. M., Gris, G., Del, P. E., Zamanillo, D., & Baeyens, J. M. (2009). Sigma-1 receptors are essential for capsaicin-induced mechanical hypersensitivity: studies with selective sigma-1 ligands and sigma-1 knockout mice. *Pain 143*, 252-261.

Entrena, J. M., Sánchez-Fernández, C., Nieto, F. R., González-Cano, R., Yeste, S., Cobos, E. J., & Baeyens, J. M. (2016). Sigma-1 Receptor Agonism Promotes Mechanical Allodynia After Priming the Nociceptive System with Capsaicin. *Sci. Rep. 6*, 37835.

Etkin, A., Egner, T., & Kalisch, R. (2011). Emotional processing in anterior cingulate and medial prefrontal cortex. *Trends Cogn Sci. 15*, 85-93.

Ewels, P., Magnusson, M., Lundin, S., & Kaller, M. (2016). MultiQC: summarize analysis results for multiple tools and samples in a single report. *Bioinformatics. 32*, 3047-3048.

Fell, G. L., Robinson, K. C., Mao, J., Woolf, C. J., & Fisher, D. E. (2014). Skin beta-endorphin mediates addiction to UV light. *Cell 157*, 1527-1534.

Fernandes, E. S., Russell, F. A., Spina, D., McDougall, J. J., Graepel, R., Gentry, C., Staniland, A. A., Mountford, D. M., Keeble, J. E., Malcangio, M., Bevan, S., & Brain, S. D. (2011). A distinct role for transient receptor potential ankyrin 1, in addition to transient receptor potential vanilloid 1, in tumor necrosis factor alpha-induced inflammatory hyperalgesia and Freund's complete adjuvant-induced monarthritis. *Arthritis Rheum. 63*, 819-829.

Ferrari, M. D., Klever, R. R., Terwindt, G. M., Ayata, C., & van den Maagdenberg, A. M. (2015). Migraine pathophysiology: lessons from mouse models and human genetics. *Lancet Neurol. 14*, 65-80.

Fichna, J., Janecka, A., Costentin, J., & Do Rego, J. C. (2007). The endomorphin system and its evolving neurophysiological role. *Pharmacol. Rev. 59*, 88-123.

Fiore, N. T. & Austin, P. J. (2016). Are the emergence of affective disturbances in neuropathic pain states contingent on supraspinal neuroinflammation? *Brain Behav. Immun. 56*, 397-411.

Fontanilla, D., Johannessen, M., Hajipour, A. R., Cozzi, N. V., Jackson, M. B., & Ruoho, A. E. (2009). The hallucinogen N,N-dimethyltryptamine (DMT) is an endogenous sigma-1 receptor regulator. *Science 323*, 934-937.

Ford, B. (2010). Pain in Parkinson's disease. *Mov Disord. 25 Suppl 1*, S98-103.

Frankish, A., Diekhans, M., Jungreis, I., Lagarde, J., Loveland, J. E., Mudge, J. M., Sisu, C., Wright, J. C., Armstrong, J., Barnes, I., Berry, A., Bignell, A., Boix, C., Carbonell, S. S., Cunningham, F., Di, D. T., Donaldson, S., Fiddes, I. T., García, G. C., González, J. M., Grego, T., Hardy, M., Hourlier, T., Howe, K. L., Hunt, T., Izuogu, O. G., Johnson, R., Martin, F. J., Martínez, L., Mohanan, S., Muir, P., Navarro, F. C. P., Parker, A., Pei, B., Pozo, F., Riera, F. C., Ruffier, M., Schmitt, B. M., Stapleton, E., Suner, M. M., Sycheva, I., Uszczynska-Ratajczak, B., Wolf, M. Y., Xu, J., Yang, Y. T., Yates, A., Zerbino, D., Zhang, Y., Choudhary, J. S., Gerstein, M., Guigo, R., Hubbard, T. J. P., Kellis, M., Paten, B., Tress, M. L., & Flicek, P. (2021). GENCODE 2021. *Nucleic Acids Res. 49*, D916-D923.

Fumagalli, G., Monza, L., Cavaletti, G., Rigolio, R., & Meregalli, C. (2020). Neuroinflammatory Process Involved in Different Preclinical Models of Chemotherapy-Induced Peripheral Neuropathy. *Front Immunol. 11*, 626687.

Garvey, L., Nelson, M., Latch, N., Erlwein, O. W., Allsop, J. M., Mitchell, A., Kaye, S., Watson, V., Back, D., Taylor-Robinson, S. D., & Winston, A. (2012). CNS effects of a CCR5 inhibitor in HIV-infected subjects: a pharmacokinetic and cerebral metabolite study. *J. Antimicrob. Chemother. 67*, 206-212.

Gentile, F., Scarlino, S., Falzone, Y. M., Lunetta, C., Tremolizzo, L., Quattrini, A., & Riva, N. (2019). The Peripheral Nervous System in Amyotrophic Lateral Sclerosis: Opportunities for Translational Research. *Front Neurosci. 13*, 601.

Ghasemlou, N., Chiu, I. M., Julien, J. P., & Woolf, C. J. (2015). CD11b+Ly6G- myeloid cells mediate mechanical inflammatory pain hypersensitivity. *Proc. Natl. Acad. Sci. U. S. A 112*, E6808-E6817.

Goldberg, D. S. & McGee, S. J. (2011). Pain as a global public health priority. *BMC. Public Health 11*, 770.

González-Cano, R., Montilla-García, Á., Ruiz-Cantero, M. C., Bravo-Caparrós, I., Tejada, M. Á., Nieto, F. R., & Cobos, E. J. (2020). The search for translational pain outcomes to refine analgesic development: Where did we come from and where are we going? *Neurosci. Biobehav. Rev. 113*, 238-261.

Grachev, I. D., Meyer, P. M., Becker, G. A., Bronzel, M., Marsteller, D., Pastino, G., Voges, O., Rabinovich, L., Knebel, H., Zientek, F., Rullmann, M., Sattler, B., Patt, M., Gerhards, T., Strauss, M., Kluge, A., Brust, P., Savola, J. M., Gordon, M. F., Geva, M., Hesse, S., Barthel, H., Hayden, M. R., & Sabri, O. (2021). Sigma-1 and dopamine D2/D3 receptor occupancy of pridopidine in healthy volunteers and patients with Huntington disease: a [(18)F] fluspidine and [(18)F] fallypride PET study. *Eur. J. Nucl. Med. Mol. Imaging 48*, 1103-1115.

Greenspan, J. D., Craft, R. M., LeResche, L., Arendt-Nielsen, L., Berkley, K. J., Fillingim, R. B., Gold, M. S., Holdcroft, A., Lautenbacher, S., Mayer, E. A., Mogil, J. S., Murphy, A. Z., & Traub, R. J. (2007). Studying sex and gender differences in pain and analgesia: a consensus report. *Pain 132 Suppl 1*, S26-S45.

Griffin, R. S., Costigan, M., Brenner, G. J., Ma, C. H., Scholz, J., Moss, A., Allchorne, A. J., Stahl, G. L., & Woolf, C. J. (2007). Complement induction in spinal cord microglia results in anaphylatoxin C5a-mediated pain hypersensitivity. *J. Neurosci. 27*, 8699-8708.

Gris, G., Merlos, M., Vela, J. M., Zamanillo, D., & Portillo-Salido, E. (2014). S1RA, a selective sigma-1 receptor antagonist, inhibits inflammatory pain in the carrageenan and complete Freund's adjuvant models in mice. *Behav. Pharmacol. 25*, 226-235.

Gris, G., Portillo-Salido, E., Aubel, B., Darbaky, Y., Deseure, K., Vela, J. M., Merlos, M., & Zamanillo, D. (2016). The selective sigma-1 receptor antagonist E-52862 attenuates neuropathic pain of different aetiology in rats. *Sci. Rep. 6*, 24591.

Gu, Z., Eils, R., & Schlesner, M. (2016). Complex heatmaps reveal patterns and correlations in multidimensional genomic data. *Bioinformatics. 32*, 2847-2849.

Gudes, S., Barkai, O., Caspi, Y., Katz, B., Lev, S., & Binshtok, A. M. (2015). The role of slow and persistent TTX-resistant sodium currents in acute tumor necrosis factor-alpha-mediated increase in nociceptors excitability. *J. Neurophysiol. 113*, 601-619.

Gusnard, D. A., Akbudak, E., Shulman, G. L., & Raichle, M. E. (2001). Medial prefrontal cortex and self-referential mental activity: relation to a default mode of brain function. *Proc. Natl. Acad. Sci. U. S. A 98*, 4259-4264.

Halvorsen, E. C., Hamilton, M. J., Young, A., Wadsworth, B. J., LePard, N. E., Lee, H. N., Firmino, N., Collier, J. L., & Bennewith, K. L. (2016). Maraviroc decreases CCL8-mediated migration of CCR5(+) regulatory T cells and reduces metastatic tumor growth in the lungs. *Oncoimmunology. 5*, e1150398.

Hanisch, F., Skudlarek, A., Berndt, J., & Kornhuber, M. E. (2015). Characteristics of pain in amyotrophic lateral sclerosis. *Brain Behav. 5*, e00296.

Hanner, M., Moebius, F. F., Flandorfer, A., Knaus, H. G., Striessnig, J., Kempner, E., & Glossmann, H. (1996). Purification, molecular cloning, and expression of the mammalian sigma1-binding site. *Proc. Natl. Acad. Sci. U. S. A 93*, 8072-8077.

Hansen, K. B., Yi, F., Perszyk, R. E., Menniti, F. S., & Traynelis, S. F. (2017). NMDA Receptors in the Central Nervous System. *Methods Mol. Biol. 1677*, 1-80.

Hayashi, T. & Su, T. P. (2007). Sigma-1 receptor chaperones at the ER-mitochondrion interface regulate Ca(2+) signaling and cell survival. *Cell 131*, 596-610.

Helmy, S. A. & Bali, A. (2001a). The effect of the preemptive use of the NMDA receptor antagonist dextromethorphan on postoperative analgesic requirements. *Anesth. Analg. 92*, 739-744.

Helmy, S. A. & Bali, A. (2001b). The effect of the preemptive use of the NMDA receptor antagonist dextromethorphan on postoperative analgesic requirements. *Anesth. Analg. 92*, 739-744.

Hill, R. (2000). NK1 (substance P) receptor antagonists--why are they not analgesic in humans? *Trends Pharmacol. Sci. 21*, 244-246.

Höftberger, R., Kunze, M., Voigtlander, T., Unterberger, U., Regelsberger, G., Bauer, J., Aboul-Enein, F., Garzuly, F., Forss-Petter, S., Bernheimer, H., Berger, J., & Budka, H. (2010). Peroxisomal localization of the proopiomelanocortin-derived peptides beta-lipotropin and beta-endorphin. *Endocrinology 151*, 4801-4810.

Horvath, G. (2000). Endomorphin-1 and endomorphin-2: pharmacology of the selective endogenous mu-opioid receptor agonists. *Pharmacol. Ther. 88*, 437-463.

Horvath, S., Zhang, B., Carlson, M., Lu, K. V., Zhu, S., Felciano, R. M., Laurance, M. F., Zhao, W., Qi, S., Chen, Z., Lee, Y., Scheck, A. C., Liau, L. M., Wu, H., Geschwind, D. H., Febbo, P. G., Kornblum, H. I., Cloughesy, T. F., Nelson, S. F., & Mischel, P. S. (2006). Analysis of oncogenic signaling networks in glioblastoma identifies ASPM as a molecular target. *Proc. Natl. Acad. Sci. U. S. A 103*, 17402-17407.

Hsieh, Y. L., Chiang, H., Tseng, T. J., & Hsieh, S. T. (2008). Enhancement of cutaneous nerve regeneration by 4-methylcatechol in resiniferatoxin-induced neuropathy. *J. Neuropathol. Exp. Neurol. 67*, 93-104.

Huang, Z. Z., Li, D., Liu, C. C., Cui, Y., Zhu, H. Q., Zhang, W. W., Li, Y. Y., & Xin, W. J. (2014). CX3CL1-mediated macrophage activation contributed to paclitaxel-induced DRG neuronal apoptosis and painful peripheral neuropathy. *Brain Behav. Immun. 40*, 155-165.

Hutcheson, D. M., Sánchez-Blázquez, P., Rodríguez-Diaz, M., Garzón, J., Schmidhammer, H., Borsodi, A., Roques, B. P., & Maldonado, R. (1999). Use of selective antagonists and antisense oligonucleotides to evaluate the mechanisms of BUBU antinociception. *Eur. J. Pharmacol. 383*, 29-37.

Ilkjaer, S., Nielsen, P. A., Bach, L. F., Wernberg, M., & Dahl, J. B. (2000). The effect of dextromethorphan, alone or in combination with ibuprofen, on postoperative pain after minor gynaecological surgery. *Acta Anaesthesiol. Scand. 44*, 873-877.

Jeong, Y. C., Son, J. S., & Kwon, Y. B. (2015). The spinal antinociceptive mechanism determined by systemic administration of BD1047 in zymosan-induced hyperalgesia in rats. *Brain Res. Bull. 119*, 93-100.

Ji, R. R., Chamessian, A., & Zhang, Y. Q. (2016). Pain regulation by non-neuronal cells and inflammation. *Science 354*, 572-577.

Ji, R. R., Nackley, A., Huh, Y., Terrando, N., & Maixner, W. (2018). Neuroinflammation and Central Sensitization in Chronic and Widespread Pain. *Anesthesiology 129*, 343-366.

Ji, R. R., Samad, T. A., Jin, S. X., Schmoll, R., & Woolf, C. J. (2002). p38 MAPK activation by NGF in primary sensory neurons after inflammation increases TRPV1 levels and maintains heat hyperalgesia. *Neuron 36*, 57-68.

Ji, R. R., Xu, Z. Z., & Gao, Y. J. (2014). Emerging targets in neuroinflammation-driven chronic pain. *Nat. Rev. Drug Discov. 13*, 533-548.

Jiang, J., Wang, Y., & Deng, M. (2022). New developments and opportunities in drugs being trialed for amyotrophic lateral sclerosis from 2020 to 2022. *Front Pharmacol. 13*, 1054006.

Jin, X. & Gereau, R. W. (2006). Acute p38-mediated modulation of tetrodotoxin-resistant sodium channels in mouse sensory neurons by tumor necrosis factor-alpha. *J. Neurosci. 26*, 246-255.

Johannes, C. B., Le, T. K., Zhou, X., Johnston, J. A., & Dworkin, R. H. (2010). The prevalence of chronic pain in United States adults: results of an Internet-based survey. *J. Pain 11*, 1230-1239.

Johnston, T. H., Geva, M., Steiner, L., Orbach, A., Papapetropoulos, S., Savola, J. M., Reynolds, I. J., Ravenscroft, P., Hill, M., Fox, S. H., Brotchie, J. M., Laufer, R., & Hayden, M. R. (2019). Pridopidine, a clinic-ready compound, reduces 3,4-dihydroxyphenylalanine-induced dyskinesia in Parkinsonian macaques. *Mov Disord. 34*, 708-716.

Jurga, A. M., Paleczna, M., & Kuter, K. Z. (2020). Overview of General and Discriminating Markers of Differential Microglia Phenotypes. *Front Cell Neurosci. 14*, 198.

Kalinski, P. (2012). Regulation of immune responses by prostaglandin E2. *J. Immunol. 188*, 21-28.

Kaliyaperumal, S., Wilson, K., Aeffner, F., & Dean, C., Jr. (2020). Animal Models of Peripheral Pain: Biology Review and Application for Drug Discovery. *Toxicol. Pathol. 48*, 202-219.

Kamei, H., Kameyama, T., & Nabeshima, T. (1998). Effects of sigma receptor ligands on conditioned fear stress. *Methods Find. Exp. Clin. Pharmacol. 20*, 613-618.

Karashima, Y., Talavera, K., Everaerts, W., Janssens, A., Kwan, K. Y., Vennekens, R., Nilius, B., & Voets, T. (2009). TRPA1 acts as a cold sensor in vitro and in vivo. *Proc. Natl. Acad. Sci. U. S. A 106*, 1273-1278.

Kawabata, A. (2011). Prostaglandin E2 and pain--an update. *Biol. Pharm. Bull. 34*, 1170-1173.

Khalilzadeh, E., Azarpey, F., Hazrati, R., & Vafaei, S. G. (2018). Evaluation of different classes of histamine H(1) and H(2) receptor antagonist effects on neuropathic nociceptive behavior following tibial nerve transection in rats. *Eur. J. Pharmacol. 834*, 221-229.

Kim, D., Paggi, J. M., Park, C., Bennett, C., & Salzberg, S. L. (2019). Graph-based genome alignment and genotyping with HISAT2 and HISAT-genotype. *Nat. Biotechnol. 37*, 907-915.

Kim, F. J., Kovalyshyn, I., Burgman, M., Neilan, C., Chien, C. C., & Pasternak, G. W. (2010). Sigma 1 receptor modulation of G-protein-coupled receptor signaling: potentiation of opioid transduction independent from receptor binding. *Mol. Pharmacol. 77*, 695-703.

Kissin, I. (2010). The development of new analgesics over the past 50 years: a lack of real breakthrough drugs. *Anesth. Analg. 110*, 780-789.

Kolls, J. K. & Linden, A. (2004). Interleukin-17 family members and inflammation. *Immunity. 21*, 467-476.

Kotliarova, A. & Sidorova, Y. A. (2021). Glial Cell Line-Derived Neurotrophic Factor Family Ligands, Players at the Interface of Neuroinflammation and Neuroprotection: Focus Onto the Glia. *Front Cell Neurosci. 15*, 679034.

Kourrich, S., Hayashi, T., Chuang, J. Y., Tsai, S. Y., Su, T. P., & Bonci, A. (2013). Dynamic interaction between sigma-1 receptor and Kv1.2 shapes neuronal and behavioral responses to cocaine. *Cell 152*, 236-247.

Kourrich, S., Su, T. P., Fujimoto, M., & Bonci, A. (2012). The sigma-1 receptor: roles in neuronal plasticity and disease. *Trends Neurosci. 35*, 762-771.

Krajewski, J. L. (2020). P2X3-Containing Receptors as Targets for the Treatment of Chronic Pain. *Neurotherapeutics. 17*, 826-838.

Kulkarni, S. K. & Dhir, A. (2009). sigma-1 receptors in major depression and anxiety. *Expert. Rev. Neurother. 9*, 1021-1034.

Kummer, K. K., Zeidler, M., Kalpachidou, T., & Kress, M. (2021). Role of IL-6 in the regulation of neuronal development, survival and function. *Cytokine 144*, 155582.

Kwiatkowski, K., Piotrowska, A., Rojewska, E., Makuch, W., Jurga, A., Slusarczyk, J., Trojan, E., Basta-Kaim, A., & Mika, J. (2016). Beneficial properties of maraviroc on neuropathic pain development and opioid effectiveness in rats. *Prog. Neuropsychopharmacol. Biol. Psychiatry 64*, 68-78.

Kwon, M. J., Kim, J., Shin, H., Jeong, S. R., Kang, Y. M., Choi, J. Y., Hwang, D. H., & Kim, B. G. (2013). Contribution of macrophages to enhanced regenerative capacity of dorsal root ganglia sensory neurons by conditioning injury. *J. Neurosci. 33*, 15095-15108.

Kwon, M. J., Shin, H. Y., Cui, Y., Kim, H., Thi, A. H., Choi, J. Y., Kim, E. Y., Hwang, D. H., & Kim, B. G. (2015). CCL2 Mediates Neuron-Macrophage Interactions to Drive Proregenerative Macrophage Activation Following Preconditioning Injury. *J. Neurosci. 35*, 15934-15947.

Labuz, D., Berger, S., Mousa, S. A., Zollner, C., Rittner, H. L., Shaqura, M. A., Segovia-Silvestre, T., Przewlocka, B., Stein, C., & Machelska, H. (2006). Peripheral antinociceptive effects of exogenous and immune cell-derived endomorphins in prolonged inflammatory pain. *J. Neurosci. 26*, 4350-4358.

Laedermann, C. J., Pertin, M., Suter, M. R., & Decosterd, I. (2014). Voltage-gated sodium channel expression in mouse DRG after SNI leads to re-evaluation of projections of injured fibers. *Mol. Pain 10*, 19.

Langa, F., Codony, X., Tovar, V., Lavado, A., Gimenez, E., Cozar, P., Cantero, M., Dordal, A., Hernandez, E., Perez, R., Monroy, X., Zamanillo, D., Guitart, X., & Montoliu, L. (2003). Generation and phenotypic analysis of sigma receptor type I (sigma 1) knockout mice. *Eur. J. Neurosci. 18*, 2188-2196.

Langfelder, P. & Horvath, S. (2008). WGCNA: an R package for weighted correlation network analysis. *BMC. Bioinformatics. 9*, 559.

Le Pichon, C. E. & Chesler, A. T. (2014). The functional and anatomical dissection of somatosensory subpopulations using mouse genetics. *Front Neuroanat. 8*, 21.

Ledent, C., Vaugeois, J. M., Schiffmann, S. N., Pedrazzini, T., El, Y. M., Vanderhaeghen, J. J., Costentin, J., Heath, J. K., Vassart, G., & Parmentier, M. (1997). Aggressiveness, hypoalgesia and high blood pressure in mice lacking the adenosine A2a receptor. *Nature 388*, 674-678.

Leffler, A., Monter, B., & Koltzenburg, M. (2006). The role of the capsaicin receptor TRPV1 and acid-sensing ion channels (ASICS) in proton sensitivity of subpopulations of primary nociceptive neurons in rats and mice. *Neuroscience 139*, 699-709.

Levine, J. D. & Alessandri-Haber, N. (2007). TRP channels: targets for the relief of pain. *Biochim. Biophys. Acta 1772*, 989-1003.

Lilley, E., Stanford, S. C., Kendall, D. E., Alexander, S. P. H., Cirino, G., Docherty, J. R., George, C. H., Insel, P. A., Izzo, A. A., Ji, Y., Panettieri, R. A., Sobey, C. G., Stefanska, B., Stephens, G., Teixeira, M., & Ahluwalia, A. (2020). ARRIVE 2.0 and the British Journal of Pharmacology: Updated guidance for 2020. *Br. J. Pharmacol. 177*, 3611-3616.

Lindborg, J. A., Niemi, J. P., Howarth, M. A., Liu, K. W., Moore, C. Z., Mahajan, D., & Zigmond, R. E. (2018). Molecular and cellular identification of the immune response in peripheral ganglia following nerve injury. *J. Neuroinflammation. 15*, 192.

Loggia, M. L., Chonde, D. B., Akeju, O., Arabasz, G., Catana, C., Edwards, R. R., Hill, E., Hsu, S., Izquierdo-García, D., Ji, R. R., Riley, M., Wasan, A. D., Zurcher, N. R., Albrecht, D. S., Vangel, M. G., Rosen, B. R., Napadow, V., & Hooker, J. M. (2015). Evidence for brain glial activation in chronic pain patients. *Brain 138*, 604-615.

Love, M. I., Huber, W., & Anders, S. (2014). Moderated estimation of fold change and dispersion for RNA-seq data with DESeq2. *Genome Biol. 15*, 550.

Lu, Y., Jiang, B. C., Cao, D. L., Zhao, L. X., & Zhang, Y. L. (2017). Chemokine CCL8 and its receptor CCR5 in the spinal cord are involved in visceral pain induced by experimental colitis in mice. *Brain Res. Bull. 135*, 170-178.

Lundberg, J. M., Franco-Cereceda, A., Hua, X., Hokfelt, T., & Fischer, J. A. (1985). Co-existence of substance P and calcitonin gene-related peptide-like immunoreactivities in sensory nerves in relation to cardiovascular and bronchoconstrictor effects of capsaicin. *Eur. J. Pharmacol. 108*, 315-319.

Lyden, J. & Binswanger, I. A. (2019). The United States opioid epidemic. *Semin. Perinatol. 43*, 123-131.

Machelska, H. (2011). Control of neuropathic pain by immune cells and opioids. *CNS. Neurol. Disord. Drug Targets. 10*, 559-570.

Magerl, W., Thalacker, E., Vogel, S., Schleip, R., Klein, T., Treede, R. D., & Schilder, A. (2021). Tenderness of the Skin after Chemical Stimulation of Underlying Temporal and Thoracolumbar Fasciae Reveals Somatosensory Crosstalk between Superficial and Deep Tissues. *Life (Basel) 11*.

Mao, J., Gold, M. S., & Backonja, M. M. (2011). Combination drug therapy for chronic pain: a call for more clinical studies. *J. Pain 12*, 157-166.

Marcotti, A., Fernandez-Trillo, J., Gonzalez, A., Vizcaino-Escoto, M., Ros-Arlanzon, P., Romero, L., Vela, J. M., Gomis, A., Viana, F., & de la Pena, E. (2023b). TRPA1 modulation by Sigma-1 receptor prevents oxaliplatin-induced painful peripheral neuropathy. *Brain 146*, 475-491.

Martin, W. R., Eades, C. G., Thompson, J. A., Huppler, R. E., & Gilbert, P. E. (1976). The effects of morphine- and nalorphine- like drugs in the nondependent and morphine-dependent chronic spinal dog. *J. Pharmacol. Exp. Ther. 197*, 517-532.

Massaad, C. A., Safieh-Garabedian, B., Poole, S., Atweh, S. F., Jabbur, S. J., & Saade, N. E. (2004). Involvement of substance P, CGRP and histamine in the hyperalgesia and cytokine upregulation induced by intraplantar injection of capsaicin in rats. *J. Neuroimmunol. 153*, 171-182.

Mathieson, S., Lin, C. C., Underwood, M., & Eldabe, S. (2020). Pregabalin and gabapentin for pain. *BMJ 369*, m1315.

Matsumoto, R. R., Liu, Y., Lerner, M., Howard, E. W., & Brackett, D. J. (2003). Sigma receptors: potential medications development target for anti-cocaine agents. *Eur. J. Pharmacol. 469*, 1-12.

Matthes, H. W., Maldonado, R., Simonin, F., Valverde, O., Slowe, S., Kitchen, I., Befort, K., Dierich, A., Le, M. M., Dolle, P., Tzavara, E., Hanoune, J., Roques, B. P., & Kieffer, B. L. (1996). Loss of morphine-induced analgesia, reward effect and withdrawal symptoms in mice lacking the mu-opioid-receptor gene. *Nature 383*, 819-823.

Maurice, T. & Goguadze, N. (2017). Role of sigma(1) Receptors in Learning and Memory

and Alzheimer's Disease-Type Dementia. *Adv. Exp. Med. Biol. 964*, 213-233.

Maurice, T. & Su, T. P. (2009). The pharmacology of sigma-1 receptors. *Pharmacol. Ther. 124*, 195-206.

Mavlyutov, T. A., Duellman, T., Kim, H. T., Epstein, M. L., Leese, C., Davletov, B. A., & Yang, J. (2016). Sigma-1 receptor expression in the dorsal root ganglion: Reexamination using a highly specific antibody. *Neuroscience 331*, 148-157.

McConaghy, P. M., McSorley, P., McCaughey, W., & Campbell, W. I. (1998). Dextromethorphan and pain after total abdominal hysterectomy. *Br. J. Anaesth. 81*, 731-736.

McCoy, D. D., Knowlton, W. M., & McKemy, D. D. (2011). Scraping through the ice: uncovering the role of TRPM8 in cold transduction. *Am. J. Physiol Regul. Integr. Comp Physiol 300*, R1278-R1287.

Mei, J. & Pasternak, G. W. (2001). Molecular cloning and pharmacological characterization of the rat sigma1 receptor. *Biochem. Pharmacol. 62*, 349-355.

Mei, J. & Pasternak, G. W. (2007). Modulation of brainstem opiate analgesia in the rat by sigma 1 receptors: a microinjection study. *J. Pharmacol. Exp. Ther. 322*, 1278-1285.

Menéndez, L., Lastra, A., Hidalgo, A., & Baamonde, A. (2002). Unilateral hot plate test: a simple and sensitive method for detecting central and peripheral hyperalgesia in mice. *J. Neurosci. Methods 113*, 91-97.

Menéndez, L., Lastra, A., Meana, A., Hidalgo, A., & Baamonde, A. (2005). Analgesic effects of loperamide in bone cancer pain in mice. *Pharmacol. Biochem. Behav. 81*, 114-121.

Merlos, M., Burgueno, J., Portillo-Salido, E., Plata-Salaman, C. R., & Vela, J. M. (2017). Pharmacological Modulation of the Sigma 1 Receptor and the Treatment of Pain. *Adv. Exp. Med. Biol. 964*, 85-107.

Meyer, R.A., Campbell, J.N., Raja, S.N., 2006. Peripheral mechanisms of cutaneous nociception. In: McMahon, K.Me. (Ed.), Wall and Melzack's Textbook of Pain. Elsevier, pp. 3–34 SB.

Miczek, K. A., Thompson, M. L., & Shuster, L. (1982). Opioid-like analgesia in defeated mice. *Science 215*, 1520-1522.

Middleton, S. J., Barry, A. M., Comini, M., Li, Y., Ray, P. R., Shiers, S., Themistocleous, A. C., Uhelski, M. L., Yang, X., Dougherty, P. M., Price, T. J., & Bennett, D. L. (2021). Studying human nociceptors: from fundamentals to clinic. *Brain 144*, 1312-1335.

Minnone, G., De, B. F., & Bracci-Laudiero, L. (2017). NGF and Its Receptors in the Regulation of Inflammatory Response. *Int. J. Mol. Sci. 18*.

Monroe, T. B., Gore, J. C., Chen, L. M., Mion, L. C., & Cowan, R. L. (2012). Pain in people with Alzheimer disease: potential applications for psychophysical and neurophysiological research. *J. Geriatr. Psychiatry Neurol. 25*, 240-255.

Montague-Cardoso, K. & Malcangio, M. (2020). Cathepsin S as a potential therapeutic target for chronic pain. *Med. Drug Discov. 7*, 100047.

Montilla-García, Á., Perazzoli, G., Tejada, M. Á., González-Cano, R., Sánchez-Fernández, C., Cobos, E. J., & Baeyens, J. M. (2018). Modality-specific peripheral antinociceptive effects of mu-opioid agonists on heat and mechanical stimuli: Contribution of sigma-1 receptors. *Neuropharmacology 135*, 328-342.

Montilla-García, Á., Tejada, M. Á., Perazzoli, G., Entrena, J. M., Portillo-Salido, E., Fernández-Segura, E., Canizares, F. J., & Cobos, E. J. (2017). Grip strength in mice with joint inflammation: A rheumatology function test sensitive to pain and analgesia. *Neuropharmacology 125*, 231-242.

Moon, J. Y., Choi, S. R., Roh, D. H., Yoon, S. Y., Kwon, S. G., Choi, H. S., Kang, S. Y., Han, H. J., Kim, H. W., Beitz, A. J., Oh, S. B., & Lee, J. H. (2015). Spinal sigma-1 receptor activation increases the production of D-serine in astrocytes which contributes to the development of mechanical allodynia in a mouse model of neuropathic pain. *Pharmacol. Res. 100*, 353-364.

Moon, J. Y., Roh, D. H., Yoon, S. Y., Choi, S. R., Kwon, S. G., Choi, H. S., Kang, S. Y., Han, H. J., Beitz, A. J., Oh, S. B., & Lee, J. H. (2014). sigma1 receptors activate astrocytes via p38 MAPK phosphorylation leading to the development of mechanical allodynia in a mouse model of neuropathic pain. *Br. J. Pharmacol. 171*, 5881-5897.

Moriyama, T., Higashi, T., Togashi, K., Iida, T., Segi, E., Sugimoto, Y., Tominaga, T., Narumiya, S., & Tominaga, M. (2005). Sensitization of TRPV1 by EP1 and IP reveals peripheral nociceptive mechanism of prostaglandins. *Mol. Pain 1*, 3.

Moro-García, M. A., Mayo, J. C., Sainz, R. M., & Alonso-Arias, R. (2018). Influence of Inflammation in the Process of T Lymphocyte Differentiation: Proliferative, Metabolic, and Oxidative Changes. *Front Immunol. 9*, 339.

Motawe, Z. Y., Abdelmaboud, S. S., Cuevas, J., & Breslin, J. W. (2020). PRE-084 as a tool to uncover potential therapeutic applications for selective sigma-1 receptor activation. *Int. J. Biochem. Cell Biol. 126*, 105803.

Mousa, S. A., Machelska, H., Schafer, M., & Stein, C. (2002). Immunohistochemical localization of endomorphin-1 and endomorphin-2 in immune cells and spinal cord in a model of inflammatory pain. *J. Neuroimmunol. 126*, 5-15.

Nguyen, L., Thomas, K. L., Lucke-Wold, B. P., Cavendish, J. Z., Crowe, M. S., & Matsumoto, R. R. (2016). Dextromethorphan: An update on its utility for neurological and neuropsychiatric disorders. *Pharmacol. Ther. 159*, 1-22.

Nieto, F. R., Cendán, C. M., Canizares, F. J., Cubero, M. A., Vela, J. M., Fernández-Segura, E., & Baeyens, J. M. (2014). Genetic inactivation and pharmacological blockade of sigma-1 receptors prevent paclitaxel-induced sensory-nerve mitochondrial abnormalities and neuropathic pain in mice. *Mol. Pain 10*, 11.

Nieto, F. R., Cendán, C. M., Sánchez-Fernández, C., Cobos, E. J., Entrena, J. M., Tejada, M. Á., Zamanillo, D., Vela, J. M., & Baeyens, J. M. (2012). Role of sigma-1 receptors in paclitaxel-induced neuropathic pain in mice. *J. Pain 13*, 1107-1121.

Nieto, F. R., Entrena, J. M., Cendán, C. M., Del, P. E., Vela, J. M., & Baeyens, J. M. (2008). Tetrodotoxin inhibits the development and expression of neuropathic pain induced by paclitaxel in mice. *Pain 137*, 520-531.

Nikolaev, Y. A., Feketa, V. V., Anderson, E. O., Schneider, E. R., Gracheva, E. O., & Bagriantsev, S. N. (2020). Lamellar cells in Pacinian and Meissner corpuscles are touch sensors. *Sci. Adv. 6*.

Nomura, H., Furuta, A., & Iwaki, T. (2002). Dorsal root rupture injury induces extension of astrocytic processes into the peripheral nervous system and expression of GDNF in astrocytes. *Brain Res. 950*, 21-30.

Numazaki, M., Tominaga, T., Takeuchi, K., Murayama, N., Toyooka, H., & Tominaga, M. (2003). Structural determinant of TRPV1 desensitization interacts with calmodulin. *Proc. Natl. Acad. Sci. U. S. A 100*, 8002-8006.

O'Brien, E. E., Smeester, B. A., Michlitsch, K. S., Lee, J. H., & Beitz, A. J. (2015). Colocalization of aromatase in spinal cord astrocytes: differences in expression and relationship to mechanical and thermal hyperalgesia in murine models of a painful and a non-painful bone tumor. *Neuroscience 301*, 235-245.

Ochoa-Callejero, L., Pérez-Martínez, L., Rubio-Mediavilla, S., Oteo, J. A., Martínez, A., & Blanco, J. R. (2013). Maraviroc, a CCR5 antagonist, prevents development of hepatocellular carcinoma in a mouse model. *PLoS. One. 8*, e53992.

Ohta, T., Ikemi, Y., Murakami, M., Imagawa, T., Otsuguro, K., & Ito, S. (2006). Potentiation of transient receptor potential V1 functions by the activation of metabotropic 5-HT receptors in rat primary sensory neurons. *J. Physiol 576*, 809-822.

Okonechnikov, K., Conesa, A., & García-Alcalde, F. (2016). Qualimap 2: advanced multi-sample quality control for high-throughput sequencing data. *Bioinformatics. 32*, 292-294.

Oldham, M. C., Konopka, G., Iwamoto, K., Langfelder, P., Kato, T., Horvath, S., & Geschwind, D. H. (2008). Functional organization of the transcriptome in human brain. *Nat. Neurosci. 11*, 1271-1282.

Ortega-Roldán, J. L., Ossa, F., & Schnell, J. R. (2013). Characterization of the human sigma-1 receptor chaperone domain structure and binding immunoglobulin protein (BiP) interactions. *J. Biol. Chem. 288*, 21448-21457.

Ortíz-Rentería, M., Juárez-Contreras, R., González-Ramírez, R., Islas, L. D., Sierra-Ramírez, F., Llorente, I., Simón, S. A., Hiriart, M., Rosenbaum, T., & Morales-Lázaro, S. L. (2018). TRPV1 channels and the progesterone receptor Sig-1R interact to regulate pain. *Proc. Natl. Acad. Sci. U. S. A 115*, E1657-E1666.

Palacios, G., Muro, A., Verdu, E., Pumarola, M., & Vela, J. M. (2004). Immunohistochemical localization of the sigma1 receptor in Schwann cells of rat sciatic nerve. *Brain Res. 1007*, 65-70.

Paniagua, N., Giron, R., Goicoechea, C., López-Miranda, V., Vela, J. M., Merlos, M., & Martín, M. I. (2017). Blockade of sigma 1 receptors alleviates sensory signs of diabetic neuropathy in rats. *Eur. J. Pain 21*, 61-72.

Paniagua, N., Goicoechea, C., Abalo, R., López-Miranda, V., Vela, J. M., Merlos, M., Martín, M. I., & Giron, R. (2019). May a sigma-1 antagonist improve neuropathic signs induced by cisplatin and vincristine in rats? *Eur. J. Pain 23*, 603-620.

Parada, C. A., Tambeli, C. H., Cunha, F. Q., & Ferreira, S. H. (2001). The major role of peripheral release of histamine and 5-hydroxytryptamine in formalin-induced nociception. *Neuroscience 102*, 937-944.

Parenti, C., Marrazzo, A., Arico, G., Cantarella, G., Prezzavento, O., Ronsisvalle, S., Scoto, G. M., & Ronsisvalle, G. (2014a). Effects of a selective sigma 1 antagonist compound on inflammatory pain. *Inflammation 37*, 261-266.

Parenti, C., Marrazzo, A., Arico, G., Parenti, R., Pasquinucci, L., Ronsisvalle, S., Ronsisvalle, G., & Scoto, G. M. (2014b). The antagonistic effect of the sigma 1 receptor ligand (+)-MR200 on persistent pain induced by inflammation. *Inflamm. Res. 63*, 231-237.

Parikshak, N. N., Gandal, M. J., & Geschwind, D. H. (2015). Systems biology and gene networks in neurodevelopmental and neurodegenerative disorders. *Nat. Rev. Genet. 16*, 441-458.

Pérez-Martínez, L., Pérez-Matute, P., Aguilera-Lizarraga, J., Rubio-Mediavilla, S., Narro, J., Recio, E., Ochoa-Callejero, L., Oteo, J. A., & Blanco, J. R. (2014). Maraviroc, a CCR5 antagonist, ameliorates the development of hepatic steatosis in a mouse model of non-alcoholic fatty liver disease (NAFLD). *J. Antimicrob. Chemother. 69*, 1903-1910.

Pérez-Martínez, L., Romero, L., Muñoz-Galván, S., Verdugo-Sivianes, E. M., Rubio-Mediavilla, S., Oteo, J. A., Carnero, A., & Blanco, J. R. (2020). Implications of maraviroc and/or rapamycin in a mouse model of fragility. *Aging (Albany. NY) 12*, 8565-8582.

Phelps, E. A., Delgado, M. R., Nearing, K. I., & LeDoux, J. E. (2004). Extinction learning in humans: role of the amygdala and vmPFC. *Neuron 43*, 897-905.

Phillips, S. N., Fernando, R., & Girard, T. (2017). Parenteral opioid analgesia: Does it still have a role? *Best. Pract. Res. Clin. Anaesthesiol. 31*, 3-14.

Pina, L. T. S., Gouveia, D. N., Costa, J. S., Quintans, J. S. S., Quintans-Junior, L. J., Barreto, R. S. S., & Guimaraes, A. G. (2017). New perspectives for chronic pain treatment: a patent review (2010-2016). *Expert. Opin. Ther. Pat 27*, 787-796.

Pinho-Ribeiro, F. A., Verri, W. A., Jr., & Chiu, I. M. (2017). Nociceptor Sensory Neuron-Immune Interactions in Pain and Inflammation. *Trends Immunol. 38*, 5-19.

Piomelli, D., Hohmann, A. G., Seybold, V., & Hammock, B. D. (2014). A lipid gate for the peripheral control of pain. *J. Neurosci. 34*, 15184-15191.

Piotrowska, A., Kwiatkowski, K., Rojewska, E., Makuch, W., & Mika, J. (2016). Maraviroc reduces neuropathic pain through

polarization of microglia and astroglia - Evidence from in vivo and in vitro studies. *Neuropharmacology 108*, 207-219.

Powell, R., Young, V. A., Pryce, K. D., Sheehan, G. D., Bonsu, K., Ahmed, A., & Bhattacharjee, A. (2021). Inhibiting endocytosis in CGRP(+) nociceptors attenuates inflammatory pain-like behavior. *Nat. Commun. 12*, 5812.

Prato, V., Taberner, F. J., Hockley, J. R. F., Callejo, G., Arcourt, A., Tazir, B., Hammer, L., Schad, P., Heppenstall, P. A., Smith, E. S., & Lechner, S. G. (2017). Functional and Molecular Characterization of Mechanoinsensitive "Silent" Nociceptors. *Cell Rep. 21*, 3102-3115.

Priestley, J. V. (2009). Neuropeptides: sensory systems. In M. Malcangio (Eds.), *Synaptic Plasticity in Pain Textbook.* Springer, pp. 935-943.

Princiotta, C. L., Mauri, M., Cosentino, M., Versino, M., & Marino, F. (2022). Alzheimer's Disease: From Immune Homeostasis to Neuroinflammatory Condition. *Int. J. Mol. Sci. 23.*

Przewlocki, R., Hassan, A. H., Lason, W., Epplen, C., Herz, A., & Stein, C. (1992). Gene expression and localization of opioid peptides in immune cells of inflamed tissue: functional role in antinociception. *Neuroscience 48*, 491-500.

Qiu, F., Qiu, C. Y., Liu, Y. Q., Wu, D., Li, J. D., & Hu, W. P. (2012). Potentiation of acid-sensing ion channel activity by the activation of 5-HT(2) receptors in rat dorsal root ganglion neurons. *Neuropharmacology 63*, 494-500.

Raoof, R., Willemen, H. L. D. M., & Eijkelkamp, N. (2018). Divergent roles of immune cells and their mediators in pain. *Rheumatology. (Oxford) 57*, 429-440.

Rashid, M. H., Inoue, M., Toda, K., & Ueda, H. (2004). Loss of peripheral morphine analgesia contributes to the reduced effectiveness of systemic morphine in neuropathic pain. *J. Pharmacol. Exp. Ther. 309*, 380-387.

Reeh, P. W. & Fischer, M. J. M. (2022). Nobel somatosensations and pain. *Pflugers Arch. 474*, 405-420.

Renthal, W., Tochitsky, I., Yang, L., Cheng, Y. C., Li, E., Kawaguchi, R., Geschwind, D. H., & Woolf, C. J. (2020). Transcriptional Reprogramming of Distinct Peripheral Sensory Neuron Subtypes after Axonal Injury. *Neuron 108*, 128-144.

Richner, M., Bjerrum, O. J., Nykjaer, A., & Vaegter, C. B. (2011). The spared nerve injury (SNI) model of induced mechanical allodynia in mice. *J. Vis. Exp.*

Rittner, H. L., Brack, A., Machelska, H., Mousa, S. A., Bauer, M., Schafer, M., & Stein, C. (2001). Opioid peptide-expressing leukocytes: identification, recruitment, and simultaneously increasing inhibition of inflammatory pain. *Anesthesiology 95*, 500-508.

Ro, L. S., Chen, S. T., Tang, L. M., & Jacobs, J. M. (1999). Effect of NGF and anti-NGF on neuropathic pain in rats following chronic constriction injury of the sciatic nerve. *Pain 79*, 265-274.

Roberson, D. P., Gudes, S., Sprague, J. M., Patoski, H. A., Robson, V. K., Blasl, F., Duan, B., Oh, S. B., Bean, B. P., Ma, Q., Binshtok, A. M., & Woolf, C. J. (2013). Activity-dependent silencing reveals functionally distinct itch-generating sensory neurons. *Nat. Neurosci. 16*, 910-918.

Rodríguez-Muñoz, M., Cortés-Montero, E., Pozo-Rodrigálvarez, A., Sánchez-Blázquez, P., & Garzón-Niño, J. (2015a). The ON:OFF switch, sigma1R-HINT1 protein, controls GPCR-NMDA receptor cross-regulation: implications in neurological disorders. *Oncotarget. 6*, 35458-35477.

Rodríguez-Muñoz, M., Sánchez-Blázquez, P., Herrero-Labrador, R., Martínez-Murillo, R., Merlos, M., Vela, J. M., & Garzón, J. (2015b). The sigma1 receptor engages the redox-regulated HINT1 protein to bring opioid analgesia under NMDA receptor negative control. *Antioxid. Redox. Signal. 22*, 799-818.

Roh, D. H., Choi, S. R., Yoon, S. Y., Kang, S. Y., Moon, J. Y., Kwon, S. G., Han, H. J., Beitz, A.

J., & Lee, J. H. (2011). Spinal neuronal NOS activation mediates sigma-1 receptor-induced mechanical and thermal hypersensitivity in mice: involvement of PKC-dependent GluN1 phosphorylation. *Br. J. Pharmacol. 163*, 1707-1720.

Roh, D. H., Kim, H. W., Yoon, S. Y., Seo, H. S., Kwon, Y. B., Kim, K. W., Han, H. J., Beitz, A. J., & Lee, J. H. (2008). Intrathecal administration of sigma-1 receptor agonists facilitates nociception: involvement of a protein kinase C-dependent pathway. *J. Neurosci. Res. 86*, 3644-3654.

Romero, L., Zamanillo, D., Nadal, X., Sánchez-Arroyos, R., Rivera-Arconada, I., Dordal, A., Montero, A., Muro, A., Bura, A., Segales, C., Laloya, M., Hernández, E., Portillo-Salido, E., Escriche, M., Codony, X., Encina, G., Burgueno, J., Merlos, M., Baeyens, J. M., Giraldo, J., López-García, J. A., Maldonado, R., Plata-Salaman, C. R., & Vela, J. M. (2012). Pharmacological properties of S1RA, a new sigma-1 receptor antagonist that inhibits neuropathic pain and activity-induced spinal sensitization. *Br. J. Pharmacol. 166*, 2289-2306.

Rosario, M. C., Jacqmin, P., Dorr, P., James, I., Jenkins, T. M., Abel, S., & van der Ryst, E. (2008a). Population pharmacokinetic/pharmacodynamic analysis of CCR5 receptor occupancy by maraviroc in healthy subjects and HIV-positive patients. *Br. J. Clin. Pharmacol. 65 Suppl 1*, 86-94.

Rose, J., Weiser, T. G., Hider, P., Wilson, L., Gruen, R. L., & Bickler, S. W. (2015). Estimated need for surgery worldwide based on prevalence of diseases: a modelling strategy for the WHO Global Health Estimate. *Lancet Glob. Health 3 Suppl 2*, S13-S20.

Ruffing, N., Sullivan, N., Sharmeen, L., Sodroski, J., & Wu, L. (1998). CCR5 has an expanded ligand-binding repertoire and is the primary receptor used by MCP-2 on activated T cells. *Cell Immunol. 189*, 160-168.

Ruiz-Cantero, M. C., Cortés-Montero, E., Jain, A., Montilla-García, Á., Bravo-Caparrós, I., Shim, J., Sánchez-Blázquez, P., Woolf, C. J., Baeyens, J. M., & Cobos, E. J. (2023). The sigma-1 receptor curtails endogenous opioid analgesia during sensitization of TRPV1 nociceptors. *Br. J. Pharmacol. 180*, 1148-1167.

Ruiz-Cantero, M. C., González-Cano, R., Tejada, M. Á., Santos-Caballero, M., Perazzoli, G., Nieto, F. R., & Cobos, E. J. (2021). Sigma-1 receptor: A drug target for the modulation of neuroimmune and neuroglial interactions during chronic pain. *Pharmacol. Res. 163*, 105339.

Ruoho, A. E., Chu, U. B., Ramachandran, S., Fontanilla, D., Mavlyutov, T., & Hajipour, A. R. (2012). The ligand binding region of the sigma-1 receptor: studies utilizing photoaffinity probes, sphingosine and N-alkylamines. *Curr. Pharm. Des 18*, 920-929.

Russell, F. A., King, R., Smillie, S. J., Kodji, X., & Brain, S. D. (2014). Calcitonin gene-related peptide: physiology and pathophysiology. *Physiol Rev. 94*, 1099-1142.

Sa, K. N., Moreira, L., Baptista, A. F., Yeng, L. T., Teixeira, M. J., Galhardoni, R., & de Andrade, D. C. (2019). Prevalence of chronic pain in developing countries: systematic review and meta-analysis. *Pain Rep. 4*, e779.

Salaciak, K. & Pytka, K. (2022). Revisiting the sigma-1 receptor as a biological target to treat affective and cognitive disorders. *Neurosci. Biobehav. Rev. 132*, 1114-1136.

Sánchez-Blázquez, P., Rodríguez-Muñoz, M., Herrero-Labrador, R., Burgueno, J., Zamanillo, D., & Garzón, J. (2014). The calcium-sensitive Sigma-1 receptor prevents cannabinoids from provoking glutamate NMDA receptor hypofunction: implications in antinociception and psychotic diseases. *Int. J. Neuropsychopharmacol. 17*, 1943-1955.

Sánchez-Fernández, C., Entrena, J. M., Baeyens, J. M., & Cobos, E. J. (2017). Sigma-1 Receptor Antagonists: A New Class of Neuromodulatory Analgesics. *Adv. Exp. Med. Biol. 964*, 109-132.

Sánchez-Fernández, C., Montilla-García, Á., González-Cano, R., Nieto, F. R., Romero, L., Artacho-Cordón, A., Montes, R., Fernández-Pastor, B., Merlos, M., Baeyens, J. M., Entrena, J. M., & Cobos, E. J. (2014). Modulation of peripheral mu-opioid

analgesia by sigma1 receptors. *J. Pharmacol. Exp. Ther. 348*, 32-45.

Sánchez-Fernández, C., Nieto, F. R., González-Cano, R., Artacho-Cordón, A., Romero, L., Montilla-García, Á., Zamanillo, D., Baeyens, J. M., Entrena, J. M., & Cobos, E. J. (2013). Potentiation of morphine-induced mechanical antinociception by sigma(1) receptor inhibition: role of peripheral sigma(1) receptors. *Neuropharmacology 70*, 348-358.

Sanderson, N. K., Skinner, K., Julius, D., & Basbaum, A. I. (2004). Co-localization of endomorphin-2 and substance P in primary afferent nociceptors and effects of injury: a light and electron microscopic study in the rat. *Eur. J. Neurosci. 19*, 1789-1799.

Scanlin, H. L., Carroll, E. A., Jenkins, V. K., & Balkowiec, A. (2008). Endomorphin-2 is released from newborn rat primary sensory neurons in a frequency- and calcium-dependent manner. *Eur. J. Neurosci. 27*, 2629-2642.

Scherrer, G., Imamachi, N., Cao, Y. Q., Contet, C., Mennicken, F., O'Donnell, D., Kieffer, B. L., & Basbaum, A. I. (2009). Dissociation of the opioid receptor mechanisms that control mechanical and heat pain. *Cell 137*, 1148-1159.

Schmidt, H. R., Zheng, S., Gurpinar, E., Koehl, A., Manglik, A., & Kruse, A. C. (2016). Crystal structure of the human sigma1 receptor. *Nature 532*, 527-530.

Scholz, J. & Woolf, C. J. (2007). The neuropathic pain triad: neurons, immune cells and glia. *Nat. Neurosci. 10*, 1361-1368.

Schwarz, S., Pohl, P., & Zhou, G. Z. (1989). Steroid binding at sigma-"opioid" receptors. *Science 246*, 1635-1638.

Shah, S., Carver, C. M., Mullen, P., Milne, S., Lukacs, V., Shapiro, M. S., & Gamper, N. (2020). Local Ca(2+) signals couple activation of TRPV1 and ANO1 sensory ion channels. *Sci. Signal. 13*.

Sheehan, K., Lee, J., Chong, J., Zavala, K., Sharma, M., Philipsen, S., Maruyama, T., Xu, Z., Guan, Z., Eilers, H., Kawamata, T., & Schumacher, M. (2019). Transcription factor Sp4 is required for hyperalgesic state persistence. *PLoS. One. 14*, e0211349.

Shen, B., Behera, D., James, M. L., Reyes, S. T., Andrews, L., Cipriano, P. W., Klukinov, M., Lutz, A. B., Mavlyutov, T., Rosenberg, J., Ruoho, A. E., McCurdy, C. R., Gambhir, S. S., Yeomans, D. C., Biswal, S., & Chin, F. T. (2017). Visualizing Nerve Injury in a Neuropathic Pain Model with [(18)F]FTC-146 PET/MRI. *Theranostics. 7*, 2794-2805.

Shin, S. M., Wang, F., Qiu, C., Itson-Zoske, B., Hogan, Q. H., & Yu, H. (2022). Sigma-1 receptor activity in primary sensory neurons is a critical driver of neuropathic pain. *Gene Ther. 29*, 1-15.

Sikandar, S., Minett, M. S., Millet, Q., Santana-Varela, S., Lau, J., Wood, J. N., & Zhao, J. (2018). Brain-derived neurotrophic factor derived from sensory neurons plays a critical role in chronic pain. *Brain 141*, 1028-1039.

Silva, R. & Malcangio, M. (2021). Fractalkine/CX(3)CR(1) Pathway in Neuropathic Pain: An Update. *Front Pain Res. (Lausanne) 2*, 684684.

Sisignano, M., Baron, R., Scholich, K., & Geisslinger, G. (2014). Mechanism-based treatment for chemotherapy-induced peripheral neuropathic pain. *Nat. Rev. Neurol. 10*, 694-707.

Sorge, R. E., Mapplebeck, J. C., Rosen, S., Beggs, S., Taves, S., Alexander, J. K., Martin, L. J., Austin, J. S., Sotocinal, S. G., Chen, D., Yang, M., Shi, X. Q., Huang, H., Pillon, N. J., Bilan, P. J., Tu, Y., Klip, A., Ji, R. R., Zhang, J., Salter, M. W., & Mogil, J. S. (2015). Different immune cells mediate mechanical pain hypersensitivity in male and female mice. *Nat. Neurosci. 18*, 1081-1083.

Souza, G. R., Cunha, T. M., Silva, R. L., Lotufo, C. M., Verri, W. A., Jr., Funez, M. I., Villarreal, C. F., Talbot, J., Sousa, L. P., Parada, C. A., Cunha, F. Q., & Ferreira, S. H. (2015). Involvement of nuclear factor kappa B in the maintenance of persistent inflammatory hypernociception. *Pharmacol. Biochem. Behav. 134*, 49-56.

Souza, G. R., Talbot, J., Lotufo, C. M., Cunha, F. Q., Cunha, T. M., & Ferreira, S. H. (2013).

Fractalkine mediates inflammatory pain through activation of satellite glial cells. *Proc. Natl. Acad. Sci. U. S. A 110*, 11193-11198.

Sprenger, G. P., Roos, R. A. C., van, Z. E., Reijntjes, R. H., Achterberg, W. P., & de Bot, S. T. (2021). The prevalence of pain in Huntington's disease in a large worldwide cohort. *Parkinsonism. Relat Disord. 89*, 73-78.

Staaf, S., Oerther, S., Lucas, G., Mattsson, J. P., & Ernfors, P. (2009). Differential regulation of TRP channels in a rat model of neuropathic pain. *Pain 144*, 187-199.

Stanford, W. L., Haque, S., Alexander, R., Liu, X., Latour, A. M., Snodgrass, H. R., Koller, B. H., & Flood, P. M. (1997). Altered proliferative response by T lymphocytes of Ly-6A (Sca-1) null mice. *J. Exp. Med. 186*, 705-717.

Su, T. P., Hayashi, T., Maurice, T., Buch, S., & Ruoho, A. E. (2010). The sigma-1 receptor chaperone as an inter-organelle signaling modulator. *Trends Pharmacol. Sci. 31*, 557-566.

Su, T. P., Su, T. C., Nakamura, Y., & Tsai, S. Y. (2016). The Sigma-1 Receptor as a Pluripotent Modulator in Living Systems. *Trends Pharmacol. Sci. 37*, 262-278.

Takano, S., Uchida, K., Inoue, G., Miyagi, M., Aikawa, J., Iwase, D., Iwabuchi, K., Matsumoto, T., Satoh, M., Mukai, M., Minatani, A., & Takaso, M. (2017). Nerve growth factor regulation and production by macrophages in osteoarthritic synovium. *Clin. Exp. Immunol. 190*, 235-243.

Talavera, K., Startek, J. B., Alvarez-Collazo, J., Boonen, B., Alpizar, Y. A., Sánchez, A., Naert, R., & Nilius, B. (2020). Mammalian Transient Receptor Potential TRPA1 Channels: From Structure to Disease. *Physiol Rev. 100*, 725-803.

Tan, A. M., Samad, O. A., Dib-Hajj, S. D., & Waxman, S. G. (2015). Virus-Mediated Knockdown of Nav1.3 in Dorsal Root Ganglia of STZ-Induced Diabetic Rats Alleviates Tactile Allodynia. *Mol. Med. 21*, 544-552.

Tanaka, T., Narazaki, M., & Kishimoto, T. (2014). IL-6 in inflammation, immunity, and disease. *Cold Spring Harb. Perspect. Biol. 6*, a016295.

Tarazona, S., García-Alcalde, F., Dopazo, J., Ferrer, A., & Conesa, A. (2011). Differential expression in RNA-seq: a matter of depth. *Genome Res. 21*, 2213-2223.

Tchedre, K. T., Huang, R. Q., Dibas, A., Krishnamoorthy, R. R., Dillon, G. H., & Yorio, T. (2008). Sigma-1 receptor regulation of voltage-gated calcium channels involves a direct interaction. *Invest Ophthalmol. Vis. Sci. 49*, 4993-5002.

Tejada, M. Á., Montilla-García, Á., Cronin, S. J., Cikes, D., Sánchez-Fernández, C., González-Cano, R., Ruiz-Cantero, M. C., Penninger, J. M., Vela, J. M., Baeyens, J. M., & Cobos, E. J. (2017). Sigma-1 receptors control immune-driven peripheral opioid analgesia during inflammation in mice. *Proc. Natl. Acad. Sci. U. S. A 114*, 8396-8401.

Tejada, M. Á., Montilla-Garcia, Á., Sánchez-Fernández, C., Entrena, J. M., Perazzoli, G., Baeyens, J. M., & Cobos, E. J. (2014). Sigma-1 receptor inhibition reverses acute inflammatory hyperalgesia in mice: role of peripheral sigma-1 receptors. *Psychopharmacology (Berl) 231*, 3855-3869.

Tsai, S. Y., Hayashi, T., Mori, T., & Su, T. P. (2009). Sigma-1 receptor chaperones and diseases. *Cent. Nerv. Syst. Agents Med. Chem. 9*, 184-189.

Tsujino, H., Kondo, E., Fukuoka, T., Dai, Y., Tokunaga, A., Miki, K., Yonenobu, K., Ochi, T., & Noguchi, K. (2000). Activating transcription factor 3 (ATF3) induction by axotomy in sensory and motoneurons: A novel neuronal marker of nerve injury. *Mol. Cell Neurosci. 15*, 170-182.

Vega-Avelaira, D., Geranton, S. M., & Fitzgerald, M. (2009). Differential regulation of immune responses and macrophage/neuron interactions in the dorsal root ganglion in young and adult rats following nerve injury. *Mol. Pain 5*, 70.

Vela, J. M., Merlos, M., & Almansa, C. (2015). Investigational sigma-1 receptor antagonists for the treatment of pain. *Expert. Opin. Investig. Drugs 24*, 883-896.

Verri, W. A., Jr., Cunha, T. M., Parada, C. A., Poole, S., Cunha, F. Q., & Ferreira, S. H. (2006). Hypernociceptive role of cytokines and chemokines: targets for analgesic drug development? *Pharmacol. Ther. 112*, 116-138.

Vidal-Torres, A., de la Puente, B., Rocasalbas, M., Tourino, C., Bura, S. A., Fernández-Pastor, B., Romero, L., Codony, X., Zamanillo, D., Buschmann, H., Merlos, M., Baeyens, J. M., Maldonado, R., & Vela, J. M. (2013). Sigma-1 receptor antagonism as opioid adjuvant strategy: enhancement of opioid antinociception without increasing adverse effects. *Eur. J. Pharmacol. 711*, 63-72.

Villard, V., Espallergues, J., Keller, E., Vamvakides, A., & Maurice, T. (2011). Anti-amnesic and neuroprotective potentials of the mixed muscarinic receptor/sigma 1 (sigma1) ligand ANAVEX2-73, a novel aminotetrahydrofuran derivative. *J. Psychopharmacol. 25*, 1101-1117.

Wagner, K. M., Gomes, A., McReynolds, C. B., & Hammock, B. D. (2020). Soluble Epoxide Hydrolase Regulation of Lipid Mediators Limits Pain. *Neurotherapeutics. 17*, 900-916.

Wainger, B. J., Buttermore, E. D., Oliveira, J. T., Mellin, C., Lee, S., Saber, W. A., Wang, A. J., Ichida, J. K., Chiu, I. M., Barrett, L., Huebner, E. A., Bilgin, C., Tsujimoto, N., Brenneis, C., Kapur, K., Rubin, L. L., Eggan, K., & Woolf, C. J. (2015). Modeling pain in vitro using nociceptor neurons reprogrammed from fibroblasts. *Nat. Neurosci. 18*, 17-24.

Wang, C., Hao, H., He, K., An, Y., Pu, Z., Gamper, N., Zhang, H., & Du, X. (2021). Neuropathic Injury-Induced Plasticity of GABAergic System in Peripheral Sensory Ganglia. *Front Pharmacol. 12*, 702218.

Wei, Z., Fei, Y., Su, W., & Chen, G. (2019). Emerging Role of Schwann Cells in Neuropathic Pain: Receptors, Glial Mediators and Myelination. *Front Cell Neurosci. 13*, 116.

Williams, G. P., Schonhoff, A. M., Sette, A., & Lindestam Arlehamn, C. S. (2022). Central and Peripheral Inflammation: Connecting the Immune Responses of Parkinson's Disease. *J. Parkinsons. Dis. 12*, S129-S136.

Wong, G. T. (2002). Speed congenics: applications for transgenic and knock-out mouse strains. *Neuropeptides 36*, 230-236.

Woodbury, C. J., Zwick, M., Wang, S., Lawson, J. J., Caterina, M. J., Koltzenburg, M., Albers, K. M., Koerber, H. R., & Davis, B. M. (2004). Nociceptors lacking TRPV1 and TRPV2 have normal heat responses. *J. Neurosci. 24*, 6410-6415.

Woolf, C. J. & Ma, Q. (2007). Nociceptors--noxious stimulus detectors. *Neuron 55*, 353-364.

Woolf, C. J., Safieh-Garabedian, B., Ma, Q. P., Crilly, P., & Winter, J. (1994). Nerve growth factor contributes to the generation of inflammatory sensory hypersensitivity. *Neuroscience 62*, 327-331.

Xing, L., Yang, T., Cui, S., & Chen, G. (2019). Connexin Hemichannels in Astrocytes: Role in CNS Disorders. *Front Mol. Neurosci. 12*, 23.

Yaksh, T. L., Woller, S. A., Ramachandran, R., & Sorkin, L. S. (2015). The search for novel analgesics: targets and mechanisms. *F1000Prime. Rep. 7*, 56.

Yan, Y. Y., Li, C. Y., Zhou, L., Ao, L. Y., Fang, W. R., & Li, Y. M. (2017). Research progress of mechanisms and drug therapy for neuropathic pain. *Life Sci. 190*, 68-77.

Yao, C. & Narumiya, S. (2019). Prostaglandin-cytokine crosstalk in chronic inflammation. *Br. J. Pharmacol. 176*, 337-354.

Yokoyama, H., Hirai, T., Nagata, T., Enomoto, M., Kaburagi, H., Leiyo, L., Motoyoshi, T., Yoshii, T., Okawa, A., & Yokota, T. (2020). DNA Microarray Analysis of Differential Gene Expression in the Dorsal Root Ganglia of Four Different Neuropathic Pain Mouse Models. *J. Pain Res. 13*, 3031-3043.

Yu, X., Basbaum, A., & Guan, Z. (2021). Contribution of colony-stimulating factor 1 to neuropathic pain. *Pain Rep. 6*, e883.

Yue, J. X., Wang, R. R., Yu, J., Tang, Y. Y., Hou, W. W., Lou, G. D., Zhang, S. H., & Chen, Z. (2014). Histamine upregulates Nav1.8 expression in primary afferent neurons via

H2 receptors: involvement in neuropathic pain. *CNS. Neurosci. Ther. 20*, 883-892.

Zaidi, M. R., Davis, S., Noonan, F. P., Graff-Cherry, C., Hawley, T. S., Walker, R. L., Feigenbaum, L., Fuchs, E., Lyakh, L., Young, H. A., Hornyak, T. J., Arnheiter, H., Trinchieri, G., Meltzer, P. S., De Fabo, E. C., & Merlino, G. (2011). Interferon-gamma links ultraviolet radiation to melanomagenesis in mice. *Nature 469*, 548-553.

Zamanillo, D., Romero, L., Merlos, M., & Vela, J. M. (2013). Sigma 1 receptor: a new therapeutic target for pain. *Eur. J. Pharmacol. 716*, 78-93.

Zhang, H., Ma, S. B., Gao, Y. J., Xing, J. L., Xian, H., Li, Z. Z., Shen, S. N., Wu, S. X., Luo, C., & Xie, R. G. (2020). Spinal CCL2 Promotes Pain Sensitization by Rapid Enhancement of NMDA-Induced Currents Through the ERK-GluN2B Pathway in Mouse Lamina II Neurons. *Neurosci. Bull. 36*, 1344-1354.

Zhang, J., Cavanaugh, D. J., Nemenov, M. I., & Basbaum, A. I. (2013). The modality-specific contribution of peptidergic and non-peptidergic nociceptors is manifest at the level of dorsal horn nociresponsive neurons. *J. Physiol 591*, 1097-1110.

Zhang, X., Bao, L., Shi, T. J., Ju, G., Elde, R., & Hokfelt, T. (1998). Down-regulation of mu-opioid receptors in rat and monkey dorsal root ganglion neurons and spinal cord after peripheral axotomy. *Neuroscience 82*, 223-240.

Zhang, X., Huang, J., & McNaughton, P. A. (2005). NGF rapidly increases membrane expression of TRPV1 heat-gated ion channels. *EMBO J. 24*, 4211-4223.

Zhao, R. & Tsang, S. Y. (2017). Versatile Roles of Intracellularly Located TRPV1 Channel. *J. Cell Physiol 232*, 1957-1965.

Zhu, S., Wang, C., Han, Y., Song, C., Hu, X., & Liu, Y. (2015). Sigma-1 Receptor Antagonist BD1047 Reduces Mechanical Allodynia in a Rat Model of Bone Cancer Pain through the Inhibition of Spinal NR1 Phosphorylation and Microglia Activation. *Mediators. Inflamm. 2015*, 265056.

Zhu, W., Frost, E. E., Begum, F., Vora, P., Au, K., Gong, Y., MacNeil, B., Pillai, P., & Namaka, M. (2012). The role of dorsal root ganglia activation and brain-derived neurotrophic factor in multiple sclerosis. *J. Cell Mol. Med. 16*, 1856-1865.

Zhu, X., Cao, S., Zhu, M. D., Liu, J. Q., Chen, J. J., & Gao, Y. J. (2014). Contribution of chemokine CCL2/CCR2 signaling in the dorsal root ganglion and spinal cord to the maintenance of neuropathic pain in a rat model of lumbar disc herniation. *J. Pain 15*, 516-526.

Zwick, M., Davis, B. M., Woodbury, C. J., Burkett, J. N., Koerber, H. R., Simpson, J. F., & Albers, K. M. (2002). Glial cell line-derived neurotrophic factor is a survival factor for isolectin B4-positive, but not vanilloid receptor 1-positive, neurons in the mouse. *J. Neurosci. 22*, 4057-4065.

PUBLISHED ARTICLES

ARTICLES FROM THIS PHD THESIS

Ruiz-Cantero, M. C., Cortés-Montero, E., Jain, A., Montilla-García, A., Bravo-Caparrós, I., Shim, J., Sánchez-Blázquez, P., Woolf, C., Baeyens, J. M., & Cobos, E. J. (2023) Sigma-1 receptor curtails endogenous opioid analgesia during sensitization of TRPV1 nociceptors. *Br J Pharmacol. 180 (8)*, 1148-1167. https://doi.org/10.1111/bph.16003.

Ruiz-Cantero, M. C., González-Cano, R., Tejada, M. Á., Santos-Caballero, M., Perazzoli, G., Nieto, F. R., Cobos, & E. J. (2021) Sigma-1 receptor: A drug target for the modulation of neuroimmune and neuroglial interactions during chronic pain. *Pharmacol Res. 163*, 105339. https://doi.org/10.1016/j.phrs.2020.105339.

Ruiz-Cantero, M. C.*, Huerta, M. Á.*, Tejada, M. Á., Santos-Caballero, M., Fernández-Segura, E., Cañizares, F.J., Entrena, J. M., Baeyens, J. M., & Cobos, E.J. Sigma-1 receptor agonism exacerbates immune-driven nociception: role of TRPV1+ nociceptors. (*Equal contribution). To be submitted.

Ruiz-Cantero, M. C., González-Cano, R., Entrena, J. M., Artacho-Cordón, A., Huerta, M. Á., Portillo-Salido, E., Nieto, F.R., Costigan, M., Baeyens, J. M., & Cobos, E. J. Sigma-1 receptors control peripheral neuroinflammation after nerve injury: a transcriptomic study. To be submitted.

OTHER ARTICLES

Jain, A., Gyori, B. M., Hakim, S., Bunga, S., Taub, D. G., **Ruiz-Cantero, M. C.**, Tong-Li, C., Andrews, N., Sorger, P. K., & Woolf, C. J. (2023). Nociceptor neuroimmune interactomes reveal cell type- and injury-specific inflammatory pain pathways. *bioRxiv*,2023.02.01.526526. https://doi.org/10.1101/2023.02.01.526526. Preprint.

Szczepańska, K., Podlewska, S., Dichiara, M., Gentile, D., Patamia, V., Rosier, N., Mönnich, D., **Ruiz-Cantero, M. C.**, Karcz, T., Łażewska, D., Siwek, A., Pockes, S., Cobos, E. J., Marrazzo, A., Stark, H., Rescifina, A., Bojarski, A. J., Amata, E., & Kieć-Kononowicz, K. (2022). Structural and Molecular Insight into Piperazine and Piperidine Derivatives as Histamine H3 and Sigma-1 Receptor Antagonists with Promising Antinociceptive Properties. *ACS Chem Neurosci.13(1),* 1-15, https://doi.org/10.1021/acschemneuro.1c00435

González-Cano, R., **Ruiz-Cantero, M. C.**, Santos-Caballero, M., Gómez-Navas, C., Tejada, M. Á., & Nieto, F. R. (2021). Tetrodotoxin, a Potential Drug for Neuropathic and Cancer Pain Relief?. *Toxins (Basel). 13(7)*, 483, https://doi.org/10.3390/toxins13070483.

Cortés-Montero, E., Rodríguez-Muñoz, M., **Ruiz-Cantero, M. C.**, Cobos, E. J., Sánchez-Blázquez, P., & Garzón-Niño, J. (2020). Calmodulin Supports TRPA1 Channel Association with Opioid Receptors and Glutamate NMDA Receptors in the Nervous Tissue. *Int J Mol Sci. 22 (1),* 229, https://doi.org/10.3390/ijms22010229.

Bravo-Caparrós, I.*, **Ruiz-Cantero, M. C.***, Perazzoli, G.*, Cronin, S. J. F., Vela, J. M., Hamed, M. F., Penninger, J. M., Baeyens, J. M., Cobos, E. J, & Nieto, F. R. (2020). Sigma-1 receptors control neuropathic pain and macrophage infiltration into the dorsal root ganglion after peripheral nerve injury. *FASEB J. 34(4)*, 5951-596, https://doi.org/10.1096/fj.201901921R. (*Equal contribution)

González-Cano, R., Montilla-Garcíaa, Á., **Ruiz-Cantero, M. C.**, Bravo-Caparrós, I., Tejada, M. Á., Nieto, F. R., & Cobos, E. J. (2020). The search for translational pain outcomes to refine analgesic development: where did we come from and where are we going?. *Neurosci Biobehav Rev.* 113, 238-261, https://doi.org/10.1016/j.neubiorev.2020.03.004.

Pasquinucci, L., Parenti, C., **Ruiz-Cantero, M. C.**, Georgoussi, Z., Pallaki, P., Cobos, E. J., Amata, E., Marrazzo, A., Prezzavento, O., Arena, E., Dichiara, M., Salerno, L., & Turnaturi, R. (2020). Novel N-substituted benzomorphan-based compounds: from MOR-agonist/DOR-antagonist to biased/unbiased MOR agonists. *ACS Medicinal Chemistry Letters.* 11(5), 678-685, https://doi.org/10.1021/acsmedchemlett.9b00549.

Montilla-García, Á., Tejada, M. Á., **Ruiz-Cantero, M. C.**, Bravo-Caparrós, I., Yeste, S., Zamanillo, D., & Cobos, E. J. (2019). Modulation by Sigma-1 Receptor of Morphine Analgesia and Tolerance: Nociceptive Pain, Tactile Allodynia and Grip Strength Deficits During Joint Inflammation. *Front Pharmacol. 22*, 10:136, https://doi.org/10.3389/fphar.2019.00136.

Tejada, M. Á., Montilla-García, Á., González-Cano, R., Bravo-Caparrós, I., **Ruiz-Cantero, M. C.**, Nieto, F. R, & Cobos, E. J. (2018). Targeting immune-driven opioid analgesia by sigma-1 receptors: Opening the door to novel perspectives for the analgesic use of sigma-1 antagonists. *Pharmacol Res. 131*, 224-230, https://doi.org/10.1016/j.phrs.2018.02.008.

Tejada, M. Á., Montilla-García, Á., Cronin, S. J., Cikes, D., Sánchez-Fernández, C., González-Cano, R., **Ruiz-Cantero, M.C.**, Penninger, J. M., Vela, J. M., Baeyens, J. M., & Cobos, E. J. (2017). Sigma-1 receptors control immune-driven peripheral opioid analgesia during inflammation in mice*. Proc. Natl. Acad. Sci. U. S. A 114*, 8396-8401, https://doi.org/10.1073/pnas.1620068114.

Szczepańska, K., Karcz, T., Dichiara, M., Mogilski, S., Kalinowska-Tłuścik, J., Pilarski, B., Leniak, A., Pietruś, W., Podlewska, S., Popiołek-Barczyk, K., Humphrys, L., **Ruiz-Cantero, M. C.**, Reiner-Link, D., Leitzbach, L., Łażewska, D., Pockes, S., Calmels, T., Cobos, E. J., Marrazzo, A., Stark, H., Bojarski, A., & Kiec-Kononowicz, K. Dual piperidine-based histamine H3 and sigma-1 receptor ligands in the treatment of nociceptive and neuropathic pain. *J. Med. Chem*. Submitted.

APPENDIX

APPENDIX

Table S1 (Related to Figure 2 of the transcriptome study). Functional enrichment analysis using Ingenuity Pathway Analysis (IPA) software of the up- and downregulated genes in the injured (L3-L4) DRG after SNI in wild-type mice. Table shows selected functional annotations, their Benjamini-Hochberg (B-H) adjusted *P* value, and their gene content. Analysis was performed on transcripts with a *P* value < 0.01 and a fold change of 1.4.

Category	Function	Function Annotation	B-H *P* value	Number of genes	Genes
Cellular Movement	Migration	Leukocyte migration	$4.79 \cdot 10^{-33}$	225	ABCA1, ABCB4, ACKR1, ADAM8, ADCYAP1, AIF1, AIM2, ALOX5AP, ANGPTL2, ANXA1, AQP9, AR, ARHGEF2, ARRB1, BACH2, BATF3, BCL3, BCL6, C3, C3AR1, C4A/C4B, C5AR1, C6, CAMK1, CCL2, CCL7, CCL9, CCR1, CCR2, CCR5, CD14, CD1D, CD207, CD38, CD4, CD53, CD55, CD59A, CD63, CD72, CD86, CDCP1, CDKN1A, CEBPA, CH25H, CHRNA7, CHST1, CHST2, CITED2, CLEC10A, COL4A3, CR2, CRH, CRLF2, CSF1, CSF1R, CSF2RB, CTSC, CTSS, CTTN, CX3CR1, CXCL16, CYP1B1, CYP26A1, CYSLTR1, CYSLTR2, DAPK2, DOCK11, DOCK8, DRD2, DUSP1, EPHA2, EPS8, F13A1, F2R, FCER1G, FCGR2A, FCGR2B, FERMT3, FGF3, FGL2, FLNA, FOS, FOSL2, FYB1, GC, GFAP, GGT5, GPR183, GPR34, GPR65, GPRC5A, GPSM1, GRK6, GRN, GRP, HAO1, HDAC6, HDC, HEBP1, HGF, HPGDS, HPSE, HRH3, HSD3B7, HSPB1, IGFBP3, IL10RA, IL17RA, IL1R1, IL1RN, IL21R, IL4R, IL6, IL6R, INPP5D, IRF6, ITGAM, JUN, KLF6, KLK5, KNG1, LAMA5, LGALS1, LGALS3, LILRB3, LRRK2, LTC4S, LY6A (INCLUDES OTHERS), LY96, LYZ, MAPK14, MARCHF1, MC4R, MCOLN2, MS4A4A, MSR1, MSTN, MYADM, NCKAP1L, NFIL3, NFKBIZ, NLRP12, NLRP3, NOD2, NOG, NPY, OPRD1, OPRM1, OR51E2, P2RY1, P2RY12, P2RY6, PBLD, PDE4D, PENK, PER1, PGF, PIK3CG, PIK3R5, PKP3, PLA2G2D, PLAT, PLAU, PLAUR, PLCB3, PODXL, POMC, PPBP, PRDM1, PRKCQ, PRKG1, PROCR, PTGDR, PTPN1, PTPRJ, PTPRO, PTX3, RASGRP1, RCAN1, RIPK3, RTN4, S100A10, S1PR2, SAA1, SAMSN1, SCN9A, SDC1, SEMA3E, SERPINA3, SERPINB1, SERPINE1, SGPL1, SH2D1A, SH3KBP1, SOCS3, SOX11, SPI1, SST, STAB1, STAT5A, STAT5B, STING1, TAC1, TGFBR2, TIMP1, TLN1, TLR2, TLR7, TMSB4X (INCLUDES OTHERS), TNFAIP6, TNFAIP8L2, TNFRSF1A, TNFRSF1B, TNR, TREM2, TRPA1, TRPC6, TRPV4, TYROBP, UNC5B, VAV1, VAV3, WFDC17, XDH
Inflammation	Inflammation	Inflammation	$2.22 \cdot 10^{-31}$	201	ABCD2, ACKR1, ADAM8, AGTR1B, AIF1, ALOX5AP, ANGPTL2, ANXA1, AOAH, AQP9, ATF3, BCL2A1, BCL2L11, BCL6, BLNK, C1QA, C3, C3AR1, C4A/C4B, C5AR1, C6, CASP3, CCL2, CCL7,

					CCL8, CCN4, CCR1, CCR2, CCR5, CD14, CD163, CD1D, CD33, CD38, CD4, CD63, CD72, CD84, CDCP1, CDKN1A, CEBPA, CEBPD, CERS6, CH25H, CHRNA7, CLCF1, CLEC4A, CNTNAP2, CR2, CRH, CRLF2, CSF1, CSF1R, CTLA2A/CTLA2B, CTSS, CX3CR1, CXCL16, CYP4F16/CYP4F37, CYSLTR1, DAGLB, DAPK2, DNASE1, DOCK11, DUSP1, EPHA2, F2R, FCER1G, FCGR1A, FCGR2A, FCGR2B, FGF2, FNDC4, FOS, GADD45A, GAL, GC, GGT5, GPR183, GPSM1, GRK6, GRN, GRP, HAVCR2, HEBP1, HGF, HPGDS, HPSE, HRH3, HSD3B7, HSPB1, IL10RA, IL17RA, IL1R1, IL1RN, IL4R, IL6, IL6R, INPP5D, IRAK3, IRF6, ISL1, ITGAM, JUN, KNG1, LGALS1, LGALS3, LILRB3, LOXL2, LRRK2, LTBP1, LY96, LYZ, MAPK14, METRNL, MFGE8, MMP19, MS4A2, MSR1, MSTN, NAIP, NCKAP1L, NFIL3, NFKBIZ, NLRC3, NLRP12, NLRP3, NOD2, NPY, NPY1R, NRROS, NTS, ODC1, OPRD1, OPRM1, P2RY6, PDE4D, PDE6B, PENK, PIK3AP1, PIK3CG, PIK3R5, PLA2G2D, PLAT, PLAU, PLAUR, PLIN2, POMC, PRDM1, PRKCG, PRKG1, PROCR, PROS1, PTGDR, PTPRJ, PTPRO, PTX3, RIPK3, SAA1, SASH3, SBNO2, SCN9A, SDC1, SERPINA3, SERPINB1, SERPINE1, SETD4, SLC6A4, SOCS3, SPI1, SST, STAT5A, STAT5B, STING1, SYT7, TAC1, TBXAS1, TGFBR2, TLR13, TLR2, TLR7, TLR8, TMEM106A, TNFAIP6, TNFAIP8L2, TNFRSF1A, TNFRSF1B, TNIP2, TREM2, TREX1, TRPC6, TRPV4, TSPAN2, TUBA1A, TUBB2A, TUBB3, TYROBP, ULBP1, VAV1, VAV3, VSIR, ZFP36
Nervous System Development and Function	Development	Development of neurons	$5.15 \cdot 10^{-22}$	202	ADAMTS1, ADAMTS3, ADAMTS4, ADCYAP1, AKAP5, ALKAL2, AR, ARHGEF15, ATF3, BASP1, BEX1, BTBD8, BTG2, C1QL2, C3, C4A/C4B, CACNA2D2, CACNB2, CACNB4, CADPS2, CAMK1, CAMK1G, CAMK2B, CASP3, CBLN2, CCKAR, CD38, CDH9, CDKN1A, CHL1, CHODL, CHRNA1, CHRNA3, CHRNA7, CNTN1, CNTN4, CNTNAP2, CPNE5, CRH, CRMP1, CSF1, CSMD3, CTTN, CUX2, CX3CR1, DAB2, DAGLB, DGKG, DRAXIN, DRD2, DTNBP1, ECEL1, EHD1, EIF4EBP1, EPHA3, EPHA7, EPHA8, EPHB2, EPS8, F2R, FAT3, FCGR2B, FES, FEZ1, FGF13, FGF2, FLNA, FLRT3, FOS, FUT9, GABRA1, GABRB2, GABRG2, GALNS, GAP43, GFAP, GFRA1, GFRA3, GPC2, GPRASP2, GPRIN1, GPRIN3, GRN, HDAC6, HERC1, HES5, HGF, HSPB1, HTR4, ID2, IGSF21, IGSF9, IGSF9B, IL1R1, IL1RAPL1, IL6, INPP5J, ITGAM, ITPR1, JUN, KIAA0319, KIF23, KIRREL3, KNDC1, LGALS1, LINGO2, LINGO4, LNX1, LRRK2, LRRN1, LRRTM3, LST1, MAFB, MAPK6, MDGA1, MICALL1, MINAR1, MTSS1, MYO10, NEGR1, NGB, NLGN2, NOG, NRG2, NRN1, NRXN3, NSG1, NTNG1, OLFM3, ONECUT1, OPRM1, PALLD, PIP5K1B, PLAT, PLAU, PLPPR4, PLXNA4, POMC, POU4F2, POU4F3, PRAG1, PRDM1, PRKCG, PRKG1, PRSS12, PSD, PTPN5, PTPRJ, PTPRK, PTPRO, PVALB, RAB33A, RBPJ, REM2, RHOG, RHOQ, RIMS2, RIT2, RND1, RORB, RTN4, S1PR2, SCN1A, SDK1, SEMA3C, SEMA3E, SEMA6A, SEZ6L, SHANK1, SLC5A7, SLC9A5, SLITRK3, SLITRK4, SMAD1, SNAP25, SOX11, SRPX2, SRRM4, STMN2, SYT17, SYT3, SYT4, TGIF1, TH, THRB, TLR2, TLR7, TMEM108, TNFRSF1B, TNIK, TNR, TPBG, TREM2, TRPC3, TRPC6, TRPV4, TSPAN2, UCN, VAMP1, VASH2, VGF, ZNF804A

Cellular Movement	Chemotaxis	Chemotaxis	$2.37 \cdot 10^{-18}$	123	ACKR1, ADAM8, AIF1, AKAP12, ANGPTL2, ANXA1, AQP9, ARRB1, BDKRB2, C3, C3AR1, C4A/C4B, C5AR1, CCL2, CCL7, CCL9, CCR1, CCR2, CCR5, CD38, CD4, CD72, CDCP1, CDKN1A, CH25H, COL4A3, CSF1, CSF1R, CTH, CTTN, CX3CR1, CXCL16, CYSLTR1, DAPK2, DOCK11, DRD2, DUSP1, EPHA2, EPHB2, F2R, FCER1G, FCGR2A, FGF2, GFRA1, GPR183, GPSM1, GRK6, GRN, GRP, HDAC6, HEBP1, HGF, HOMER3, HOXB9, HPSE, HRH3, HSD3B7, HSPB1, IL17RA, IL1R1, IL4R, IL6, IL6R, INPP5D, ITGAM, JUN, KNG1, LGALS1, LGALS3, LILRB3, LRRK2, MAPK14, MSTN, MT2, MTSS1, NCKAP1L, NLRP12, NOD2, NPY, OPRD1, OPRM1, P2RY12, PDE4D, PENK, PGF, PIK3CG, PIK3R5, PLAT, PLAU, PLAUR, PLXNA4, PRKCG, PRKCQ, PRKG1, PTGDR, PTPRJ, PTPRO, RGS10, RHOG, RTN4, RXFP1, S1PR2, SAA1, SCN9A, SEMA3E, SERPINA3, SERPINB1, SERPINE1, SNAI2, SOCS3, SPI1, TAC1, TGFA, TLR2, TNFAIP6, TNFRSF1A, TNR, TPBG, TREM2, TRPC6, TRPV4, VAV1, VAV3
Nervous System Development and Function	Neurotransmission	Neurotransmission	$4.05 \cdot 10^{-18}$	104	ADARB1, AKAP12, AKAP5, ANKS1B, APBA2, BCHE, CA8, CACNB2, CACNB4, CAMKV, CBLN2, CCKBR, CCL2, CD86, CDH8, CHRM2, CHRM3, CHRNA1, CHRNA3, CHRNA5, CHRNA7, CLTB, CNTNAP2, CRH, CTH, CX3CR1, DGKB, DRD2, ELFN2, EPHA7, EPHB2, EPS8, F2R, FGF12, GABRA1, GABRA3, GABRB2, GABRG1, GABRG2, GAL, GPRASP2, GRIA2, GRIA4, GRIK1, GRM8, HCRTR2, HTR1B, HTR3A, HTR4, ITPR1, KCNA2, KCNAB1, KCNC3, KCNK9, KCNMB4, KCNN1, KCNN3, KCNT1, KNG1, LYPD1, MC4R, NETO1, NLGN2, NPY, NPY2R, NRXN3, NTNG1, OPRK1, OPRM1, PLAT, PLAU, PLPPR4, POMC, PRKAR2B, PRKCG, PRMT8, PTX3, RAB11FIP5, RIMS2, RIT2, RPS6KA1, RTN4, SCN1A, SCN9A, SHANK1, SHISA9, SLC17A8, SLC1A1, SLC4A8, SLC5A7, SLC6A4, SNAP25, SST, SV2B, SYT10, TH, TNFRSF12A, TNFRSF1A, TNFRSF1B, TNR, TSPOAP1, TUBB2B, UNC119, XDH
Molecular Transport	Transport	Transport of ion	$3.52 \cdot 10^{-11}$	100	ABCC3, ACTN2, AKAP5, AKT3, ANO1, ANO3, ANO7, AQP9, ATP13A4, ATP2B3, CACNA1E, CACNA2D1, CACNA2D2, CACNB2, CACNB4, CALB1, CAMK2B, CASP3, CCR1, CCR5, CDH23, CHRNA1, CHRNA7, CLIC1, CLIC4, CNTN1, CYB5R1, CYSLTR1, DRD2, EPM2A, F2R, FGF12, FGF13, FGF2, FXYD2, GABRA1, GABRA3, GABRB2, GABRG2, GRIA4, HTR3A, HTR3B, ITPR1, KCNA2, KCNA4, KCNAB1, KCNB2, KCNC3, KCNG4, KCNH4, KCNH6, KCNH7, KCNIP2, KCNJ3, KCNK1, KCNK16, KCNK18, KCNK9, KCNMB4, KCNN1, KCNN3, KCNS3, KCNT1, KCNV1, MCOLN2, NALCN, P2RX6, P2RY1, P2RY12, P2RY6

Table S2 (Related to Figure 2 of the transcriptome study). Functional enrichment analysis using Ingenuity Pathway Analysis (IPA) software of the upregulated genes in the injured (L3-L4) DRG after SNI in wild-type mice. Table shows selected functional annotations, their Benjamini-Hochberg (B-H) adjusted *P* value, and their gene content. Analysis was performed on transcripts with a *P* value < 0.01 and a fold change of 1.4.

Category	Function	Function Annotation	B-H *P* value	Number of genes	Genes
Inflammation	Inflammation	Inflammation	$5.51 \cdot 10^{-45}$	174	ACKR1, ADAM8, AIF1, ALOX5AP, ANGPTL2, ANXA1, AOAH, AQP9, ATF3, BCL2A1, BCL2L11, BCL6, BLNK, C1QA, C3, C3AR1, C4A/C4B, C5AR1, C6, CASP3, CCL2, CCL7, CCL8, CCN4, CCR1, CCR2, CCR5, CD14, CD163, CD1D, CD33, CD38, CD4, CD63, CD72, CD84, CDCP1, CDKN1A, CEBPA, CEBPD, CERS6, CH25H, CLCF1, CLEC4A, CR2, CRH, CRLF2, CSF1, CSF1R, CTLA2A/CTLA2B, CTSS, CX3CR1, CXCL16, CYP4F16/CYP4F37, CYSLTR1, DAGLB, DUSP1, EPHA2, FCER1G, FCGR1A, FCGR2A, FCGR2B, FGF2, FNDC4, FOS, GADD45A, GAL, GC, GGT5, GPR183, GPSM1, GRK6, GRN, GRP, HAVCR2, HEBP1, HPGDS, HSD3B7, HSPB1, IL10RA, IL17RA, IL1R1, IL1RN, IL4R, IL6, IL6R, INPP5D, IRAK3, ITGAM, JUN, KNG1, LGALS1, LGALS3, LILRB3, LOXL2, LTBP1, LY96, LYZ, MAPK14, METRNL, MFGE8, MMP19, MSR1, MSTN, NAIP, NCKAP1L, NFIL3, NFKBIZ, NLRC3, NLRP12, NLRP3, NOD2, NPY, NPY1R, NRROS, NTS, ODC1, P2RY6, PDE6B, PENK, PIK3AP1, PIK3CG, PIK3R5, PLA2G2D, PLAT, PLAU, PLAUR, PLIN2, POMC, PRDM1, PRKCG, PROCR, PROS1, PTPRJ, PTPRO, PTX3, RIPK3, SAA1, SASH3, SBNO2, SDC1, SERPINA3, SERPINB1, SERPINE1, SETD4, SLC6A4, SOCS3, SPI1, STAT5A, STAT5B, STING1, TBXAS1, TGFBR2, TLR13, TLR2, TLR7, TLR8, TMEM106A, TNFAIP6, TNFAIP8L2, TNFRSF1A, TNFRSF1B, TNIP2, TREM2, TREX1, TRPV4, TUBA1A, TUBB2A, TUBB3, TYROBP, ULBP1, VAV1, VSIR, ZFP36
Cellular Movement	Migration	Leukocyte migration	$7.30 \cdot 10^{-44}$	186	ABCA1, ACKR1, ADAM8, ADCYAP1, AIF1, AIM2, ALOX5AP, ANGPTL2, ANXA1, AQP9, ARHGEF2, ARRB1, BATF3, BCL3, BCL6, C3, C3AR1, C4A/C4B, C5AR1, C6, CAMK1, CCL2, CCL7, CCL8, CCL9, CCR1, CCR2, CCR5, CD14, CD1D, CD207, CD38, CD4, CD53, CD59A, CD63, CD72, CD86, CDCP1, CDKN1A, CEBPA, CH25H, CHST1, CHST2, CITED2, CLEC10A, CR2, CRH, CRLF2, CSF1, CSF1R, CSF2RB, CTSC, CTSS, CTTN, CX3CR1, CXCL16, CYP1B1, CYP26A1, CYSLTR1, DOCK8, DRD2, DUSP1, EPHA2, EPS8, F13A1, FCER1G, FCGR2A, FCGR2B, FERMT3, FGF3, FGL2, FLNA, FOS, FOSL2, FYB1, GC, GFAP, GGT5, GPR183, GPR34, GPR65, GPRC5A, GPSM1, GRK6, GRN, GRP, HAO1, HDAC6, HDC, HEBP1, HPGDS, HSD3B7, HSPB1, IGFBP3, IL10RA, IL17RA, IL1R1, IL1RN, IL21R, IL4R, IL6, IL6R, INPP5D, ITGAM, JUN, KLF6, KNG1, LAMA5, LGALS1, LGALS3, LILRB3, LTC4S, LY6A (INCLUDES

					OTHERS), LY96, LYZ, MAPK14, MARCHF1, MC4R, MCOLN2, MS4A4A, MSR1, MSTN, MYADM, NCKAP1L, NFIL3, NFKBIZ, NLRP12, NLRP3, NOD2, NPY, OR51E2, P2RY12, P2RY6, PBLD, PENK, PER1, PIK3CG, PIK3R5, PKP3, PLA2G2D, PLAT, PLAU, PLAUR, PODXL, POMC, PRDM1, PROCR, PTPN1, PTPRJ, PTPRO, PTX3, RCAN1, RIPK3, RTN4, S100A10, S1PR2, SAA1, SDC1, SERPINA3, SERPINB1, SERPINE1, SGPL1, SOCS3, SOX11, SPI1, STAB1, STAT5A, STAT5B, STING1, TGFBR2, TIMP1, TLN1, TLR2, TLR7, TMSB4X (INCLUDES OTHERS), TNFAIP6, TNFAIP8L2, TNFRSF1A, TNFRSF1B, TREM2, TRPV4, TYROBP, VAV1, WFDC17, XDH
Hematological System Development and Function	Proliferation	Proliferation of immune cells	$1.77 \cdot 10^{-35}$	153	ADCYAP1, AIF1, ANXA1, ARG2, BCL2A1, BCL2L11, BCL3, BCL6, BHLHE41, BLNK, C3, C5AR1, CASP3, CCL2, CCR2, CCR5, CD14, CD1D, CD244, CD300C, CD38, CD4, CD59A, CD72, CD84, CD86, CDKN1A, CEBPA, CFP, CHRNA1, CLCF1, CLEC10A, CLEC4A, CR2, CRH, CRLF2, CSF1, CSF1R, CSF2RB, CTH, CXCL16, CYSLTR1, DOCK8, DRD2, DUSP1, DUSP14, EHD1, EHD4, EPHA2, EPHB2, ETS2, FCER1G, FCGR2A, FCGR2B, FGL2, FOS, FYB1, GADD45A, GAL, GCH1, GPNMB, GPR183, HAO1, HAVCR2, HPGDS, HR, IL10RA, IL13RA1, IL1R1, IL1RN, IL21R, IL2RG, IL4R, IL6, IL6R, INPP5D, IRS2, ITGAM, ITPR1, JUN, KLRB1, LAPTM5, LGALS1, LGALS3, LILRB3, LTBP1, LY6A (INCLUDES OTHERS), LY96, MAFB, MAPK14, MBL2, MMP19, MTHFD2, MVP, NABP1, NBEAL2, NCKAP1L, NFIL3, NPY, NPY1R, OTULINL, P2RY6, PENK, PIK3AP1, PIK3CG, PIM1, PLA2G2D, PLAU, PLAUR, PNP, POMC, PRDM1, PTPRJ, PTPRN, RASGRF2, RBPJ, RCAN1, RHOG, RHOQ, RIPK3, RPS6KA1, S1PR2, SASH3, SERPINA3G (INCLUDES OTHERS), SERPINE1, SH3BP2, SH3KBP1, SIGLEC1, SLC7A5, SOCS3, SOX11, SPI1, STAT5A, STAT5B, STING1, TALDO1, TGFBR2, TICAM2, TIFA, TLN1, TLR2, TLR7, TNFRSF1A, TNFRSF1B, TREM2, TYR, TYROBP, ULBP1, UNC93B1, VAV1, VSIR, WT1, XDH
Cellular Movement	Chemotaxis	Chemotaxis	$1.71 \cdot 10^{-22}$	100	ACKR1, ADAM8, AIF1, AKAP12, ANGPTL2, ANXA1, AQP9, ARRB1, BDKRB2, C3, C3AR1, C4A/C4B, C5AR1, CCL2, CCL7, CCL8, CCL9, CCR1, CCR2, CCR5, CD38, CD4, CD72, CDCP1, CDKN1A, CH25H, CSF1, CSF1R, CTH, CTTN, CX3CR1, CXCL16, CYSLTR1, DRD2, DUSP1, EPHA2, EPHB2, FCER1G, FCGR2A, FGF2, GFRA1, GPR183, GPSM1, GRK6, GRN, GRP, HDAC6, HEBP1, HOMER3, HSD3B7, HSPB1, IL17RA, IL1R1, IL4R, IL6, IL6R, INPP5D, ITGAM, JUN, KNG1, LGALS1, LGALS3, LILRB3, MAPK14, MSTN, MT2, MTSS1, NCKAP1L, NLRP12, NOD2, NPY, P2RY12, PENK, PIK3CG, PIK3R5, PLAT, PLAU, PLAUR, PLXNA4, PRKCG, PTPRJ, PTPRO, RHOG, RTN4, S1PR2, SAA1, SERPINA3, SERPINB1, SERPINE1, SNAI2, SOCS3, SPI1, TGFA, TLR2, TNFAIP6, TNFRSF1A, TPBG, TREM2, TRPV4, VAV1

Table S3 (Related to Figure 2 of the transcriptome study). Functional enrichment analysis using Ingenuity Pathway Analysis (IPA) software of the downregulated genes in the injured (L3-L4) DRG after SNI in wild-type mice. Table shows selected functional annotations, their Benjamini-Hochberg (B-H) adjusted *P* value, and their gene content. Analysis was performed on transcripts with a *P* value < 0.01 and a fold change of 1.4.

Category	Function	Function Annotation	B-H *P* value	Number of genes	Genes
Nervous System Development and Function	Neurotransmission	Neurotransmission	$2.72 \cdot 10^{-15}$	56	AKAP5, BCHE, CA8, CACNB2, CACNB4, CAMKV, CDH8, CHRM2, CHRNA7, CNTNAP2, DGKB, EPHA7, F2R, FGF12, GABRA1, GABRA3, GABRB2, GABRG2, GPRASP2, GRIA2, GRIA4, GRIK1, GRM8, HCRTR2, HTR1B, HTR3A, HTR4, KCNA2, KCNAB1, KCNC3, KCNK9, KCNN1, KCNN3, KCNT1, LYPD1, NRXN3, NTNG1, OPRK1, OPRM1, PRKAR2B, PRMT8, RIMS2, RIT2, SCN1A, SCN9A, SHANK1, SLC17A8, SLC1A1, SNAP25, SST, SV2B, SYT10, TH, TNR, TSPOAP1, UNC119
Molecular Transport	Transport	Transport of ion	$3.59 \cdot 10^{-14}$	60	AKAP5, AKT3, ANO3, ATP2B3, CACNA1E, CACNA2D2, CACNB2, CACNB4, CALB1, CAMK2B, CHRNA7, CNTN1, EPM2A, F2R, FGF12, FGF13, FXYD2, GABRA1, GABRA3, GABRB2, GABRG2, GRIA4, HTR3A, HTR3B, KCNA2, KCNA4, KCNAB1, KCNB2, KCNC3, KCNG4, KCNH6, KCNH7, KCNIP2, KCNJ3, KCNK1, KCNK18, KCNK9, KCNN1, KCNN3, KCNS3, KCNT1, KCNV1, NALCN, P2RX6, P2RY1, PLCB3, PRLR, SCN10A, SCN1A, SCN9A, SLC17A8, SLC1A1, SLC22A18, SLC24A4, SLC34A2, SLC9A5, TRPA1, TRPC3, TRPC6, TRPM8
Nervous System Development and Function	Development	Development of neurons	$1.95 \cdot 10^{-11}$	86	ADAMTS3, AKAP5, AR, BEX1, CACNA2D2, CACNB2, CACNB4, CADPS2, CAMK1G, CAMK2B, CDH9, CHODL, CHRNA7, CNTN1, CNTN4, CNTNAP2, CSMD3, CUX2, DGKG, EPHA7, EPHA8, F2R, FAT3, FEZ1, FGF13, GABRA1, GABRB2, GABRG2, GPRASP2, GPRIN3, HERC1, HES5, HGF, HTR4, ID2, IGSF21, IGSF9, IL1RAPL1, INPP5J, KIAA0319, KIF23, KIRREL3, KNDC1, LINGO2, LINGO4, LNX1, LRRK2, LRRN1, MINAR1, NEGR1, NGB, NOG, NRG2, NRN1, NRXN3, NTNG1, OLFM3, ONECUT1, OPRM1, POU4F2, POU4F3, PRKG1, PSD, PTPRK, PVALB, REM2, RIMS2, RIT2, RORB, SCN1A, SEMA3E, SHANK1, SLC9A5, SLITRK3, SLITRK4, SNAP25, SYT3, TH, THRB, TMEM108, TNR, TRPC3, TRPC6, TSPAN2, VAMP1, ZNF804A
Nervous System Development and Function	Neuritogenesis	Neuritogenesis	$1.16 \cdot 10^{-6}$	61	ADAMTS3, AKAP5, AR, BEX1, CAMK1G, CAMK2B, CHODL, CHRNA7, CNTN1, CNTN4, CNTNAP2, CSMD3, CUX2, DGKG, EPHA7, EPHA8, FAT3, FEZ1, FGF13, GPRASP2, GPRIN3, HERC1, HGF, IGSF9, IL1RAPL1, INPP5J, KIAA0319, KIF23,

					KIRREL3, KNDC1, LNX1, LRRK2, MINAR1, NEGR1, NGB, NRN1, NTNG1, OPRM1, POU4F2, POU4F3, PRKG1, PSD, PTPRK, PVALB, REM2, RIMS2, RIT2, SCN1A, SEMA3E, SHANK1, SLC9A5, SLITRK3, SLITRK4, SNAP25, SYT3, TMEM108, TNR, TRPC3, TRPC6, TSPAN2, ZNF804A

Table S4 (Related to Figure 3 of the transcriptome study). Functional enrichment analysis using Ingenuity Pathway Analysis (IPA) software of the up- and downregulated genes in the DRG (L3-L4) of naïve sigma-1 receptor knockout mice (KO) compared to wild-type (WT). Table shows selected functional annotations, their Benjamini-Hochberg (B-H) adjusted *P* value, and their gene content. Analysis was performed on transcripts with a *P* value < 0.01 and a fold change of 1.4.

Category	Function	Function Annotation	B-H *P* value	Number of genes	Genes
Cellular Movement, Immune Cell	Migration	Leukocyte migration	$1.87 \cdot 10^{-14}$	145	ABCB1B, ACKR1, APOD, ARAP3, BCL11B, C3AR1, C5AR1, CAMP, CCL11, CCL19, CCL12, CCL24, CCL27, CCL28, CCL7, CCR2, CCR5, CD177, CD276, CD300LB, CD34, CD36, CD53, CD55, CD93, CDH3, CHI3L1, CHST1, CLEC10A, CNN2, CSF1R, CSF3R, CTSC, CTSK, CTSS, CX3CR1, CXCL10, CXCL12, CXCR4, CYBB, CYSLTR2, DCN, DDIT4, DYSF, EAR2 (INCLUDES OTHERS), EDN3, EGR2, ELMO1, ESR2, F2R, FASN, FERMT3, FOXJ1, GBF1, GLO1, GPC3, GPR183, GPR34, GPR65, GPSM3, HCLS1, HEBP1, HSPB1, ICAM2, IL11RA, IL33, IL36G, IL4R, ITGAM, ITGB2, ITK, KCNIP3, KIT, LCN2, LCP2, LDLR, LGALS1, LGALS3, LILRB3, LOX, LTF, LUM, LY6A (INCLUDES OTHERS), LYZ, MAP4K1, MC4R, MIA3, MMP2, MMP9, MPO, MSR1, MTOR, MYD88, MYO1F, NAAA, NCF4, NCKAP1L, NFIC, OPRM1, PADI4, PARP1, PDK4, PDPN, PER1, PILRA, PKP3, PLAUR, PPBP, PTAFR, PTGIR, PTK2B, PTPN6, PTPRC, RAC2, RASGRP4, RPL13A, RRM2, S100A4, S100A8, S100A9, SELPLG, SERPINA3, SGK1, SGPP2, SIGMAR1, SLFN12L, SPI1, SPN, SPP1, SST, TAFA4, TGFB1, THBS4, TIMP2, TLR9, TMSB4X (INCLUDES OTHERS), TNFAIP8, TNFRSF21, TNFSF10, TREM2, TRPA1, TSPAN33, TYROBP, VCAN, XDH
Nervous System Development and Function	Neuritogenesis	Neuritogenesis	$1.12 \cdot 10^{-13}$	123	A2M, ADCY3, ALK, APBB1, ARHGAP44, ATP8A2, BCL11B, BMP5, CAMK2G, CAMK4, CCL19, CDK5R1, CHRNA3, CLSTN1, CNTN2, CNTNAP1, CPEB3, CPNE5, CPNE6, CRIP1, CX3CR1, CXCL12, CXCR4, CYBB, CYFIP2, DAB2, DCX, DNER, DNM3, DPYSL5, EDN3, ELFN1, ELMO1, EPHA8, FAM107A, FASN, FBXO31, FES, FGF2, GDA, GRIN1, HMGB2, HSPB1, IL11RA, IL33, INPP5J, IQSEC1, ITGAM, KIF1A, KIF20B, KIF23, KIF3C, KNDC1, L1CAM, LCN2, LGALS1, LOX, MAP1B, MAPK8IP2, MFN2, MTOR, MYD88, MYH10, MYH7B, MYO5B, NCDN, NDRG4, NEFH, NEFM, NEGR1, NGEF, NGFR, NME2, NTRK1, NYAP2, OPRM1, PIP5K1B, PLXNA4, POU4F3, PRKCE, PTK2B, RAB3IL1, RAB6B, RAP1GAP2, RIMS3, RIMS4, RNF157, ROBO1, ROR1, RPS14, RPS6, RTN4RL1, S100A9, SCN1B, SCN4B, SEMA7A, SEZ6, SGK1, SH3GL2, SHOX2, SKOR2,

					SLC9A1, SLITRK1, SLITRK6, SNAP91, SPOCK1, SPTBN2, STK38L, SV2A, SYT17, SYT2, SYT3, TGFB1, THBS4, TMEM108, TNFRSF21, TREM2, TTL, UST, VASH2, WASF1, XLR3C (INCLUDES OTHERS), XLR4C (INCLUDES OTHERS)
Cellular Movement	Chemotaxis	Chemotaxis	$7.51 \cdot 10^{-13}$	92	A2M, ACKR1, APLNR, ARAP3, ARHGEF16, BAIAP2L1, BDKRB2, BIN2, C3AR1, C5AR1, CAMP, CCL11, CCL19, CCL12, CCL24, CCL27, CCL28, CCL7, CCR2, CCR5, CD36, CSF1R, CSF3R, CX3CR1, CXCL10, CXCL12, CXCR4, CYBB, DYSF, EAR2 (INCLUDES OTHERS), EDN3, ELMO1, F2R, FGF2, GBF1, GPR183, GPSM3, HCLS1, HEBP1, HMGB2, HSPB1, IL33, IL4R, ITGAM, ITGB2, KIT, L1CAM, LCN2, LDLR, LGALS1, LGALS3, LILRB3, LOX, MMP2, MMP9, MT2, MTOR, MYD88, MYH10, MYO1F, MYO5B, NCKAP1L, NPTX1, OPRM1, PLAUR, PLXNA4, PTAFR, PTK2B, PTPN6, PTPRC, RAC2, RASGRP4, ROBO1, RPL13A, RXFP1, S100A4, S100A8, S100A9, SCN1B, SCN2B, SELPLG, SERPINA3, SPI1, SPN, SPP1, TAFA4, TEK, TGFB1, THBS4, TLR9, TREM2, WARS1
Nervous System Development and Function	Neurotransmission	Neurotransmission	$8.29 \cdot 10^{-13}$	78	ADCY3, ALK, ARHGAP44, ASIC1, CAMK4, CCL12, CHRM2, CHRNA3, CLSTN1, CLSTN2, CLSTN3, CPLX1, CPLX2, CX3CR1, DNM1, ELFN1, ESR2, F2R, GABBR2, GABRA3, GABRA5, GRIA1, GRIN1, HCN2, HCRTR1, HTR3A, HTR4, JPH3, KCNA1, KCNB1, KCNC1, KCNC4, KCNQ4, KIF5A, L1CAM, LYNX1, LYPD1, MAOB, MAPK8IP2, MC4R, MTOR, MYH10, MYH14, MYO5B, NCAN, NGFR, NPTX1, NRXN2, NSF, OPRM1, PCDH17, PCDH8, PCDHB5, PCDHB6, PRKACA, PTK2B, RAB11FIP5, SCN1B, SCN2B, SCN4B, SCN8A, SEZ6, SH3GL2, SLC17A7, SLC17A8, SLC8A3, SNAP91, SSH1, SST, STX1B, STXBP1, SV2A, SV2C, SYN1, SYN2, TH, WASF1, XDH
Molecular Transport	Transport	Transport of ion	$5.15 \cdot 10^{-10}$	81	ABCB1B, ABCB8, ASIC1, ATP1A1, ATP1A3, ATP1B1, ATP2A2, ATP2A3, ATP2B2, ATP2B3, ATP5E, CALB1, CAMK2G, CCR5, CXCL10, CXCL12, EDN3, F2R, FGF2, FXYD2, FXYD7, GABRA3, GRIA1, GRIN1, HCN2, HTR3A, HTR3B, ITPR2, KCNA1, KCNB1, KCNC1, KCNC4, KCNG3, KCNG4, KCNH1, KCNH7, KCNIP3, KCNJ16, KCNJ8, KCNQ4, KCNS1, KEL, LRRC55, LRRC8A, LRRC8D, NSF, P2RX5, PACS1, PER1, PKD2, SCARA5, SCN1B, SCN2B, SCN4B, SCN8A, SCNN1A, SGK1, SLC10A2, SLC12A3, SLC15A2, SLC17A7, SLC17A8, SLC22A7, SLC24A3, SLC24A4, SLC36A1, SLC37A2, SLC40A1, SLC4A1, SLC4A2, SLC7A5, SLC8A3, SLC9A1, SLC9A3, SLCO2B1, STEAP4, TF, TGFB1, TRPA1, TRPM6, TSPO

Table S5 (Related to Figure 3 of the transcriptome study). Functional enrichment analysis using Ingenuity Pathway Analysis (IPA) software of the upregulated genes in the DRG (L3-L4) of naïve sigma-1 receptor knockout mice (KO) compared to wild-type (WT). Table shows selected functional annotations, their Benjamini-Hochberg (B-H) adjusted *P* value, and their gene content. Analysis was performed on transcripts with a *P* value < 0.01 and a fold change of 1.4.

Category	Function	Function Annotation	B-H *P* value	Number of genes	Genes
Nervous System Development and Function	Development	Development of neurons	$5.90 \cdot 10^{-25}$	112	ADCY3, ADGRL1, ALK, APBB1, ARHGAP44, ATP8A2, BCAN, BCL11B, CAMK2G, CDHR1, CDK5R1, CHRNA3, CLSTN1, CLSTN2, CLSTN3, CNTN2, CNTNAP1, CPEB3, CPNE6, CYFIP2, DCTN1, DNER, DNM3, DPYSL5, EGR2, ELFN1, ELMO1, F2R, FAIM2, FAM107A, FASN, FBXO31, FGF2, GABRA5, GRIN1, HAPLN4, HSPB1, INPP5J, IQSEC1, KIF1A, KIF3C, KNDC1, L1CAM, LGI2, LHFPL4, LOX, MAP1B, MAPK8IP2, MDGA1, MFN2, MTOR, MYH10, MYH7B, MYO5B, NCAN, NCDN, NDRG4, NEFH, NEFM, NEGR1, NGEF, NGFR, NRXN2, NTRK1, NYAP2, PCDH8, PCDHB5, PCDHB6, PIP5K1B, PLXNA4, POU4F3, PRKCE, PTK2B, RAB6B, RAP1GAP2, RHO, RIMS3, RIMS4, RNF157, ROBO1, RTN4RL1, SCN1B, SCN4B, SEMA7A, SEZ6, SEZ6L, SEZ6L2, SGK1, SH3GL2, SHOX2, SKOR2, SLC17A7, SLC9A1, SLITRK1, SLITRK6, SNAP91, SPOCK1, SPTBN2, STK38L, SV2A, SYN1, SYN2, SYT17, SYT2, SYT3, TMEM108, TNFRSF21, TTL, UST, VASH2, WASF1, YWHAG
Nervous System Development and Function	Neurotransmission	Neurotransmission	$1.47 \cdot 10^{-22}$	66	ADCY3, ALK, ARHGAP44, ASIC1, CHRM2, CHRNA3, CLSTN1, CLSTN2, CLSTN3, CPLX1, CPLX2, DNM1, ELFN1, ESR2, F2R, GABBR2, GABRA5, GRIN1, HCN2, HCRTR1, HTR3A, JPH3, KCNA1, KCNB1, KCNC1, KCNC4, KCNQ4, KIF5A, L1CAM, LYNX1, MAPK8IP2, MC4R, MTOR, MYH10, MYH14, MYO5B, NCAN, NGFR, NPTX1, NRXN2, NSF, PCDH17, PCDH8, PCDHB5, PCDHB6, PRKACA, PTK2B, RAB11FIP5, SCN1B, SCN2B, SCN4B, SCN8A, SEZ6, SH3GL2, SLC17A7, SLC8A3, SNAP91, SSH1, STX1B, STXBP1, SV2A, SV2C, SYN1, SYN2, WASF1, XDH
Nervous System Development and Function	Neuritogenesis	Neuritogenesis	$3.04 \cdot 10^{-18}$	86	ADCY3, ALK, APBB1, ARHGAP44, ATP8A2, BCL11B, CAMK2G, CDK5R1, CHRNA3, CLSTN1, CNTN2, CNTNAP1, CPEB3, CPNE6, CYFIP2, DNER, DNM3, DPYSL5, ELFN1, ELMO1, FAM107A, FASN, FBXO31, FGF2, GRIN1, HSPB1,

					INPP5J, IQSEC1, KIF1A, KIF3C, KNDC1, L1CAM, LOX, MAP1B, MAPK8IP2, MFN2, MTOR, MYH10, MYH7B, MYO5B, NCDN, NDRG4, NEFH, NEFM, NEGR1, NGEF, NGFR, NTRK1, NYAP2, PIP5K1B, PLXNA4, POU4F3, PRKCE, PTK2B, RAB6B, RAP1GAP2, RIMS3, RIMS4, RNF157, ROBO1, RTN4RL1, SCN1B, SCN4B, SEMA7A, SEZ6, SGK1, SH3GL2, SHOX2, SKOR2, SLC9A1, SLITRK1, SLITRK6, SNAP91, SPOCK1, SPTBN2, STK38L, SV2A, SYT17, SYT2, SYT3, TMEM108, TNFRSF21, TTL, UST, VASH2, WASF1
Nervous System Development and Function	Proliferation	Proliferation of neuronal cells	$4.48 \cdot 10^{-13}$	59	ALK, APBB1, ARHGEF11, BCAN, CALB1, CDK5R1, CNTN2, DHCR24, DNER, DPYSL5, ESR2, FAM107A, FGF1, FGF2, FKBP5, FZD8, ISLR2, KCNA1, KIF3C, KIT, KNDC1, L1CAM, MAP1B, MMP24, MTOR, MYH10, NCAN, NCDN, NEFH, NEFM, NEGR1, NGEF, NGFR, NPTX1, NTRK1, PACS1, PARP1, PLXNA4, POU4F3, PRKACA, PROKR2, PTK2B, RIMS3, RIMS4, ROBO1, RTN1, SCN1B, SCN4B, SEMA7A, SGK1, SGPP2, SKOR2, SLC9A1, SPOCK2, STK38L, SYN1, SYNGR1, TESK1, TIMP2
Molecular Transport	Transport	Transport of ion	$8.83 \cdot 10^{-9}$	49	ABCB8, ASIC1, ATP1A1, ATP1A3, ATP1B1, ATP2A2, ATP2B2, ATP2B3, CALB1, CAMK2G, F2R, FGF2, FXYD7, GRIN1, HCN2, HTR3A, HTR3B, KCNA1, KCNB1, KCNC1, KCNC4, KCNG4, KCNH1, KCNIP3, KCNQ4, KCNS1, LRRC55, LRRC8A, LRRC8D, NSF, P2RX5, PACS1, PER1, SCN1B, SCN2B, SCN4B, SCN8A, SCNN1A, SGK1, SLC15A2, SLC17A7, SLC22A7, SLC24A3, SLC36A1, SLC4A2, SLC7A5, SLC8A3, SLC9A1, SLC9A3

Table S6 (Related to Figure 3 of the transcriptome study). Functional enrichment analysis using Ingenuity Pathway Analysis (IPA) software of the downregulated genes in the DRG (L3-L4) of naïve sigma-1 receptor knockout mice (KO) compared to wild-type (WT). Table shows selected functional annotations, their Benjamini-Hochberg (B-H) adjusted *P* value, and their gene content. Analysis was performed on transcripts with a *P* value < 0.01 and a fold change of 1.4.

Category	Function	Function Annotation	B-H *P* value	Number of genes	Genes
Hematological System Development and Function	Quantity	Quantity of blood cells	$1.22 \cdot 10^{-23}$	124	ABCB1B, ADAMTS12, APEX2, APOBEC1, ATM, BANK1, BCL6B, BRCA1, BUB1, C3AR1, C5AR1, CAMK4, CAMP, CARD11, CCL11, CCL19, CCL12, CCL24, CCL7, CCR2, CCR5, CD300C, CD33, CD34, CD36, CDKN2C, CENPX, CHI3L1, CLEC10A, CLEC4A, CNN2, CSF1R, CSF3R, CTSK, CTSS, CX3CR1, CXCL10, CXCL12, CXCR4, CYBB, DCN, E2F2, EPB42, FANCD2, FCGR1A, FERMT3, FES, GLI3, GPC3, GPR183, GSTP1, HBA1/HBA2, HBB, HCLS1, HTR4, IL11RA, IL33, IL4R, ITGAM, ITGB2, ITPR2, KEL, KLHL6, LAIR1, LAMA3, LCN2, LCP2, LGALS1, LGALS3, LILRB3, LIPG, LUM, LY6A (INCLUDES OTHERS), LY9, LYL1, MAD2L1, MFAP2, MLF1, MMP9, MPO, MYD88, NCKAP1L, NFE2, OPRM1, PCLAF, PILRA, PTAFR, PTPN6, PTPRC, PTTG1, PURA, RAC2, RIOX2, RPL22L1, RPS6, S100A8, S100A9, SELPLG, SHCBP1, SLC14A1, SLC40A1, SLC4A1, SLFN12L, SPI1, SPN, SPP1, SPTA1, SST, STEAP4, STK17B, TAL1, TEC, TEK, TF, TGFB1, TGFBI, TLR9, TNFSF10, TREM2, TRPA1, TSPAN33, TSPO, TYROBP, VCAN
Cellular Movement	Migration	Leukocyte migration	$8.64 \cdot 10^{-22}$	109	ABCB1B, APOD, ARAP3, C3AR1, C5AR1, CAMP, CCL11, CCL19, CCL12, CCL24, CCL27, CCL7, CCR2, CCR5, CD177, CD276, CD300LB, CD34, CD36, CD53, CD55, CD93, CHI3L1, CLEC10A, CNN2, CSF1R, CSF3R, CTSC, CTSK, CTSS, CX3CR1, CXCL10, CXCL12, CXCR4, CYBB, CYSLTR2, DCN, EAR2 (INCLUDES OTHERS), EDN3, FERMT3, GLO1, GPC3, GPR183, GPR34, GPR65, GPSM3, HCLS1, HEBP1, ICAM2, IL11RA, IL33, IL4R, ITGAM, ITGB2, LCN2, LCP2, LGALS1, LGALS3, LILRB3, LTF, LUM, LY6A (INCLUDES OTHERS), LYZ, MAP4K1, MMP2, MMP9, MPO, MSR1, MYD88, MYO1F, NAAA, NCF4, NCKAP1L, OPRM1, PADI4, PDPN, PILRA, PKP3, PLAUR, PPBP, PTAFR, PTPN6, PTPRC, RAC2, RASGRP4, RPL13A, RRM2, S100A4, S100A8, S100A9, SELPLG, SIGMAR1, SLFN12L, SPI1, SPN, SPP1, SST, TAFA4, TGFB1, THBS4, TLR9, TMSB4X (INCLUDES OTHERS), TNFAIP8, TNFSF10, TREM2, TRPA1, TSPAN33, TYROBP, VCAN
Inflammation	Inflammation	Inflammation	$8.01 \cdot 10^{-17}$	90	ADAMTS12, ARAP3, ATM, C3AR1, C5AR1, CAMP, CASP4, CCL11, CCL19, CCL12, CCL24, CCL27, CCL7, CCR2, CCR5, CD276, CD33, CD36, CHI3L1, CLEC12A, CLEC4A, CSF1R, CSF3R, CTSS, CX3CR1, CXCL10, CXCL12, CXCR4, CYBA, CYBB, E2F2, EAR2 (INCLUDES OTHERS),

					EDN3, FANCD2, FCGR1A, GPR183, GPSM3, GPX1, HEBP1, IL1RL2, IL33, IL4R, ITGAM, ITGB2, LCN2, LGALS1, LGALS3, LILRB3, LTBP1, LTF, LUM, LYZ, MAOB, MMP2, MMP9, MPO, MSR1, MT-ND3, MYD88, MYO1F, NCKAP1L, OPRM1, PBK, PLAUR, PTAFR, PTGIS, PTPN6, RAC2, RASGRP4, RIOX2, RPL13A, S100A4, S100A8, S100A9, SELPLG, SPI1, SPP1, SST, TAFA4, TEK, TGFB1, THBS4, TLR13, TLR9, TMEM106A, TNIP2, TREM2, TYROBP, ULBP1, VSIR
Cellular Movement	Chemotaxis	Chemotaxis of blood cells	$1.78 \cdot 10^{-16}$	53	ARAP3, C3AR1, C5AR1, CAMP, CCL11, CCL19, CCL12, CCL24, CCL27, CCL7, CCR2, CCR5, CSF1R, CSF3R, CX3CR1, CXCL10, CXCL12, CXCR4, CYBB, EAR2 (INCLUDES OTHERS), EDN3, GPR183, GPSM3, HEBP1, IL33, IL4R, ITGAM, ITGB2, LCN2, LGALS1, LGALS3, LILRB3, MMP2, MMP9, MYD88, MYO1F, NCKAP1L, OPRM1, PLAUR, PTPN6, PTPRC, RAC2, RASGRP4, RPL13A, S100A4, S100A8, S100A9, SELPLG, SPI1, SPP1, TAFA4, TGFB1, THBS4

Table S7 (Related to Figure 4 of the transcriptome study). Functional enrichment analysis using Ingenuity Pathway Analysis (IPA) software of the up- and downregulated genes in the injured (L3-L4) DRG after SNI in sigma-1 receptor knockout mice. Table shows selected functional annotations, their Benjamini-Hochberg (B-H) adjusted *P* value, and their gene content. Analysis was performed on transcripts with a *P* value < 0.01 and a fold change of 1.4.

Category	Function	Function Annotation	B-H *P* value	Number of genes	Genes
Cellular Movement	Migration	Leukocyte migration	$1.76 \cdot 10^{-25}$	322	ABCA1, ABCB1B, ABCG1, ADA, ADAM19, ADAM8, ADCYAP1, ADRB2, AGT, AHR, AIF1, AIM2, ALOX5, ALOX5AP, ANGPT1, ANGPTL2, ANXA1, APBB1IP, APOD, AQP9, AR, AREG, ARHGEF2, ARRB1, BATF3, BCL11B, BCL2, BCL3, BTK, C3, C3AR1, C4A/C4B, C5AR1, C6, CAMK1, CAMK2N2, CARD14, CARD9, CASP8, CASR, CCL11, CCL12, CCL2, CCL21, CCL6, CCL7, CCL9, CCN3, CCR1, CCR2, CCR5, CD14, CD1D, CD200R1, CD207, CD300A, CD300LB, CD300LF, CD302, CD37, CD38, CD4, CD44, CD48, CD53, CD55, CD59A, CD63, CD72, CD74, CD86, CDCP1, CDH3, CDKN1A, CEBPA, CFB, CH25H, CHGA, CHRNA7, CHST2, CITED2, CLEC10A, CLEC4M, CLEC5A, CMKLR1, CNR2, COL4A3, CR2, CRH, CSF1, CSF1R, CSF2RB, CSF3R, CTSC, CTSE, CTSS, CTTN, CX3CR1, CXADR, CXCL14, CXCL16, CXCR2, CYBB, CYP1B1, CYP26A1, CYSLTR1, DAPK2, DDR2, DOCK2, DOCK8, DRD2, DUSP1, ECM1, EEF1A2, EGFR, ELF4, ELMO1, EPHA2, EPS8, F13A1, F2R, FABP5, FCER1G, FCGR2A, FCGR2B, FERMT3, FGF3, FGL2, FLNA, FOS, FOSL2, FOXJ1, FOXM1, FYB1, GATA2, GCNT1, GFAP, GGT5, GNAO1, GPR183, GPR34, GPR65, GPRC5A, GPSM3, GRP, GSDMD, HAO1, HCK, HCLS1, HDC, HGF, HLA-DQB1, HPGDS, HPSE, HRH3, HSD3B7, HSPB1, ID1, IFITM3, IGFBP3, IL10RA, IL17RA, IL1R1, IL1RN, IL21R, IL4R, IL6R, IL7, INPP5D, ITGAE, ITGAM, ITGB1, ITGB2, JUN, KCNIP3, KLF6, KNG1, LAMA5, LCP1, LGALS1, LGALS3, LILRB3, LILRB4, LPAR3, LSP1, LTC4S, LUM, LY6A (INCLUDES OTHERS), LY96, LYN, LYST, LYZ, MAPK10, MAPK14, MARCHF1, MC4R, MCOLN2, MET, MMP2, MS4A4A, MSR1, MSTN, MYADM, MYD88, MYO1E, MYO1F, MYO1G, NCF1, NCF4, NCKAP1L, NDST1, NEDD4L, NFATC2, NFIC, NFIL3, NFKBIZ, NLRC4, NLRP12, NLRP3, NOD2, NOG, NOS1, NPY, OLFM4, OPRD1, OR51E2, P2RY1, P2RY12, P2RY6, PBLD, PCSK9, PDE4B, PDE4D, PDK2, PENK, PF4, PIK3CG, PKP3, PLA2G2D, PLAT, PLAU, PLAUR, PLCB2, PLCB3, PLTP, PODXL, POMC, PPARG, PRDM1, PRKCA, PRKCB, PRKCQ, PROCR, PTAFR, PTGDR, PTPN1, PTPN6, PTPRC, PTPRO, PTX3, PYCARD, RAC2, RAP1GAP, RASGRP1, RASGRP4, RASSF5, RCAN1, RGS3, RIPK2, RIPK3, RTN4, RUNX3, S100A10, S1PR2, SAG, SAMSN1, SATB1, SCG2, SDC1, SELPLG, SEMA3E, SEMA4A, SERPINA3, SERPINB1, SERPINE1, SGPP2, SH2D1A, SH3KBP1, SKAP1,

					SLAMF1, SLAMF9, SOCS3, SOX11, SPI1, STAB1, STAT5A, STAT5B, STING1, SYK, TAC1, TGFB1, TGFBR1, TGFBR2, TIMP1, TLR2, TLR7, TLR9, TMSB4X (INCLUDES OTHERS), TNFAIP6, TNFAIP8, TNFAIP8L2, TNFRSF1B, TNR, TREM2, TRPV4, TYROBP, UNC5B, VAV1, VDR, WAS, WFDC17, XDH
Inflammation	Inflammation	Inflammation	$1.76 \cdot 10^{-26}$	275	ABCD2, ACHE, ADA, ADAM8, ADAMTS12, ADRB2, AGT, AGTR1B, AHR, AIF1, AKNA, ALOX5, ALOX5AP, ANGPT1, ANGPTL2, ANXA1, AOAH, AQP9, ATF3, BCL2A1, BIRC3, BLNK, BTK, C1QA, C3, C3AR1, C4A/C4B, C5AR1, C6, CASP3, CASP4, CASP8, CASR, CCL11, CCL12, CCL2, CCL21, CCL7, CCN3, CCN4, CCR1, CCR2, CCR5, CD14, CD163, CD1D, CD300A, CD33, CD37, CD38, CD4, CD44, CD63, CD72, CD74, CD84, CDCP1, CDKN1A, CEBPA, CEBPD, CELA1, CERS6, CH25H, CHGA, CHRNA7, CLCA1, CLCF1, CLEC12A, CLEC4A, CLEC4M, CLEC5A, CMKLR1, CNR2, CNTNAP2, CR2, CRH, CSF1, CSF1R, CSF3R, CTLA2A/CTLA2B, CTSE, CTSS, CX3CR1, CXADR, CXCL14, CXCL16, CXCR2, CYBA, CYBB, CYP4F16/CYP4F37, CYSLTR1, DAGLB, DAPK2, DOCK2, DUSP1, ECM1, EGFR, ELF4, ELMO1, EPHA2, F2R, FCER1G, FCGR1A, FCGR2A, FCGR2B, FGF1, FNDC4, FOS, GADD45A, GAL, GCNT1, GGT5, GNAO1, GPR183, GPSM3, GRP, HAVCR2, HCK, HGF, HPGDS, HPSE, HRH3, HSD3B7, HSPB1, IGF1, IL10RA, IL17RA, IL1R1, IL1RL2, IL1RN, IL4R, IL6R, IL7, INPP5D, IRAK3, ITGAM, ITGB1, ITGB2, JUN, KNG1, LCP1, LGALS1, LGALS3, LILRA5, LILRB3, LILRB4, LOXL2, LSP1, LTBP1, LUM, LY96, LYN, LYST, LYZ, MAPK14, METRNL, MFGE8, MMP19, MMP2, MSR1, MSTN, MYD88, MYO1E, MYO1F, NAIP, NAIP1 (INCLUDES OTHERS), NCF1, NCKAP1L, NFATC2, NFIL3, NFKBIZ, NLRC3, NLRC4, NLRP1, NLRP12, NLRP3, NOD2, NOS1, NPY, NPY1R, NRROS, NTS, ODC1, OPRD1, P2RY6, PBK, PDE4B, PDE4D, PDE6B, PDK2, PENK, PF4, PIK3AP1, PIK3CG, PLA2G2D, PLAT, PLAU, PLAUR, PLIN2, POMC, PPARG, PRDM1, PRKCA, PRKCB, PRKCE, PRKCG, PROCR, PROS1, PTAFR, PTGDR, PTGS1, PTPN6, PTPRO, PTX3, PYCARD, RAC2, RAP1GAP, RASGRP4, RIOX2, RIPK2, RIPK3, SASH3, SBNO2, SCG2, SCN11A, SCYL3, SDC1, SELPLG, SEMA7A, SERPINA3, SERPINB1, SERPINE1, SERPINI1, SETD4, SLAMF1, SLC11A1, SLC6A4, SOCS3, SPI1, STAT5A, STAT5B, STING1, SYK, SYT7, TAC1, TBXAS1, TGFB1, TGFBR2, TLR13, TLR2, TLR7, TLR8, TLR9, TMEM106A, TMEM229B, TNFAIP6, TNFAIP8L2, TNFRSF1B, TNIP2, TREM2, TREX1, TRPV4, TSPAN2, TUBA1A, TUBA1C, TUBA4A, TUBB2A, TUBB3, TUBG2, TYROBP, ULBP1, UNC13D, VAV1, VSIR, WAS
Nervous System Development and Function	Development	Development of neurons	$1.72 \cdot 10^{-15}$	314	ACHE, ADAM19, ADAMTS1, ADAMTS3, ADAMTS4, ADCY1, ADCYAP1, ADRB2, AGAP2, AGT, AHR, ALKAL2, AMIGO2, AMIGO3, ANGPT1, AR, ARC, AREG, ARHGAP33, ARHGEF15, ASAP1, ATF3, BCAN, BCL11B, BCL2, BTBD8, BTG2, C1QL2, C21ORF91, C3, C4A/C4B, CACNA2D2, CACNB2, CACNG2, CADPS2, CAMK1, CAMK1G, CAMK2B, CAMK4, CASP3, CASP6, CBLN2, CCKAR, CCL21, CCN5, CD38, CD44, CDK5R2, CDKN1A, CHL1, CHODL, CHRNA1, CHRNA3, CHRNA7, CLSTN1, CNTN1, CNTN4, CNTNAP1, CNTNAP2, COBL, COLQ, CPEB3, CPNE5,

					CPNE9, CRH, CSF1, CTTN, CUX2, CX3CR1, CYBB, DAB1, DAB2, DAGLB, DCX, DDAH1, DGKG, DLG4, DLGAP3, DOK7, DRAXIN, DRD2, DSCAM, DTNBP1, DYNLT1, ECEL1, EFEMP1, EFNA3, EGFR, EIF4EBP1, ELMO1, EN1, EPB41L3, EPHA3, EPHA8, EPHB2, EPOR, EPS8, F2R, FAIM2, FBXO31, FCGR2B, FES, FEZ1, FGF13, FGF5, FGF9, FLNA, FLRT1, FLRT2, FLRT3, FOS, FRMD7, FSTL4, FUT9, GABRA1, GABRB2, GABRG2, GALNS, GAP43, GFAP, GFRA1, GFRA2, GFRA3, GNAO1, GPC2, GPR37, GPRASP2, GPRIN3, GRIN1, GRM4, HAPLN4, HGF, HMGB2, HSPB1, HTR4, HTR7, ID1, IGF1, IGSF21, IGSF9, IGSF9B, IL1R1, INPP5J, IQSEC1, ISL2, ITGAM, ITGB1, ITGB2, ITPR1, JUN, KIAA0319, KIRREL3, KLHL1, KNDC1, LGALS1, LGI2, LHFPL4, LINGO1, LINGO2, LINGO4, LRAT, LRRN1, LRRTM3, LST1, LYN, LZTS1, MAFB, MAPK6, MCF2, MDGA1, MET, MINAR1, MTSS1, MYD88, MYH7B, MYO10, MYO5B, MYOC, NCDN, NCK2, NDRG4, NEDD4L, NEFH, NEFL, NEFM, NEGR1, NME2, NOG, NOS1, NRG1, NRG2, NRG3, NRN1, NRXN3, NSG1, NTM, NTNG1, NTRK1, NUAK1, NYAP2, OLFM3, ONECUT1, PACSIN1, PARD6B, PCDH10, PCYT1B, PF4, PLAT, PLAU, PLPPR4, PLXNA4, POMC, POU4F1, POU4F2, POU4F3, PPFIA2, PRDM1, PRICKLE2, PRKCA, PRKCE, PRKCG, PRRXL1, PRSS12, PSD, PTK7, PTPN5, PTPRO, PVALB, RAB33A, RAB3A, RAB3IL1, REG1A, REM2, RHO, RHOG, RHOQ, RIMS1, RIMS2, RIMS3, RIT2, RND1, RNF157, ROBO1, RTN4, RTN4RL1, RUNX3, S1PR2, SCN11A, SCN1A, SCN1B, SCN4B, SCYL3, SDK1, SEMA3C, SEMA3E, SEMA3F, SEMA4A, SEMA6A, SEMA7A, SEPTIN4, SERPINI1, SEZ6L, SH3GL2, SHANK1, SHOX2, SIX4, SKOR2, SLC17A7, SLC5A7, SLC9A5, SLITRK3, SLITRK4, SMAD1, SNAP25, SOX11, SPOCK1, SRPX2, SRRM4, ST8SIA1, STMN2, SV2A, SYN2, SYT17, SYT2, SYT3, TBX6, TGFB1, TGFBR1, TGIF1, TH, TLR2, TLR7, TLX3, TMEM108, TNFRSF1B, TNIK, TNR, TPBG, TREM2, TRPC3, TRPC4, TRPV4, TSKU, TSPAN2, UCN, UGDH, UST, VAMP1, VASH2, VGF, WAS, WEE1, ZNF365, ZNF804A
Cellular Movement	Chemotaxis	Chemotaxis	$5.44 \cdot 10^{-15}$	173	ADAM8, AGT, AIF1, AKAP12, ALOX5, ANGPT1, ANGPTL2, ANXA1, AQP9, ARRB1, BDKRB2, BIN2, C3, C3AR1, C4A/C4B, C5AR1, CASR, CCL11, CCL2, CCL2, CCL21, CCL6, CCL7, CCL9, CCN3, CCR1, CCR2, CCR5, CD37, CD38, CD4, CD44, CD72, CD74, CDCP1, CDKN1A, CH25H, CHGA, CMKLR1, CNR2, COL4A3, CSF1, CSF1R, CSF3R, CTH, CTSE, CTTN, CX3CR1, CXADR, CXCL14, CXCL16, CXCR2, CYBB, CYSLTR1, DAPK2, DOCK2, DRD2, DUSP1, EGFR, ELMO1, EPHA2, EPHB2, F2R, FCER1G, FCGR2A, GFRA1, GNAO1, GPR183, GPSM3, GRP, HCK, HCLS1, HGF, HMGB2, HPSE, HRH3, HSD3B7, HSPB1, IGF1, IL17RA, IL1R1, IL4R, IL6R, IL7, INPP5D, ITGAM, ITGB1, ITGB2, JAG2, JUN, KNG1, LCP1, LGALS1, LGALS3, LILRB3, LPAR3, LSP1, LYN, LYST, MAPK14, MET, MMP2, MSTN, MT2, MTSS1, MYD88, MYO1E, MYO1F, MYO5B, NCK2, NCKAP1L, NDST1, NLRP12, NOD2, NPTX1, NPY, OPRD1, P2RY12, PDE4B, PDE4D, PENK, PF4, PIK3CG, PLAT, PLAU, PLAUR, PLXNA4, PPARG, PRKCA, PRKCB, PRKCG, PRKCQ, PTAFR, PTGDR, PTPN6, PTPRC, PTPRO, RAC2, RAP1GAP, RASGRP4, RGS10, RGS3, RHOG, ROBO1,

					RTN4, S1PR2, SCG2, SCN1B, SCN2B, SELPLG, SEMA3E, SEMA3F, SERPINA3, SERPINB1, SERPINE1, SLAMF1, SNAI2, SOCS3, SPI1, SYK, TAC1, TGFA, TGFB1, TGFBR1, TLR2, TLR9, TNFAIP6, TNR, TPBG, TREM2, TRPV4, VAV1, WAS
Nervous System Development and Function	Neurotransmission	Neurotransmission	$1.10 \cdot 10^{-13}$	155	ADARB1, ADCY1, ADRB2, AKAP12, AMPH, ANKS1B, APBA2, ARC, ASIC1, BCHE, CA8, CACNA1I, CACNA2D3, CACNB2, CACNG2, CAMK4, CAMKV, CASR, CBLN2, CCKBR, CCL12, CCL2, CD44, CD86, CDH8, CHRM2, CHRM3, CHRNA1, CHRNA3, CHRNA4, CHRNA5, CHRNA7, CLSTN1, CNTNAP2, CNTNAP4, CPLX2, CRH, CTH, CX3CR1, DLG4, DLGAP3, DNM1, DPP6, DRD2, EPHB2, EPS8, F2R, FGF12, FSTL1, GABBR2, GABRA1, GABRB2, GABRG1, GABRG2, GAL, GNAO1, GPRASP2, GRIA2, GRIA4, GRIK1, GRIK4, GRIN1, GRM4, GRM8, HCN2, HCRTR2, HTR1A, HTR1B, HTR3A, HTR4, IGF1, ITGB1, ITPR1, JPH3, JPH4, KCNA2, KCNB1, KCNC1, KCNC3, KCNC4, KCND1, KCND2, KCNH2, KCNJ11, KCNK9, KCNMB1, KCNMB4, KCNN1, KCNN2, KCNN3, KCNT1, KCTD12, KNG1, LPAR3, LZTS1, MC4R, MET, MYO5B, NETO1, NPTX1, NPY, NPY2R, NRG1, NRG3, NRXN3, NTNG1, OPRK1, PLAT, PLAU, PLPPR4, PNKD, POMC, PRKAR2B, PRKCA, PRKCB, PRKCG, PRMT8, PTX3, RAB11FIP5, RAB3A, RASD2, RIMS1, RIMS2, RIT2, RPS6KA1, RTN4, SCN11A, SCN1A, SCN1B, SCN2B, SCN4B, SCN5A, SCN8A, SH3GL2, SHANK1, SHISA9, SLC17A7, SLC1A1, SLC1A6, SLC4A8, SLC5A7, SLC6A4, SLC9A9, SNAP25, SV2A, SV2B, SYN2, TH, TNFRSF12A, TNFRSF1B, TNR, TSPOAP1, TUBB2B, UNC119, XDH
Molecular Transport	Transport	Transport of ion	$5.44 \cdot 10^{-12}$	156	ABCB1B, ABCC3, ABCC8, ACTN2, ADA, ADRB2, AGT, AKT3, ANO3, ANO7, AQP9, ASIC1, ASIC3, ATP1A1, ATP1B1, ATP2B2, ATP2B3, ATP8B1, BCL2, CACNA1I, CACNA2D1, CACNA2D2, CACNA2D3, CACNB2, CALB1, CAMK2B, CASP3, CASR, CCR1, CCR5, CDH23, CHRNA1, CHRNA4, CHRNA7, CLCA1, CLIC1, CLIC4, CNTN1, CYB5R2, CYSLTR1, DPP6, DRD2, F2R, FGF12, FGF13, FKBP4, GABRA1, GABRB1, GABRB2, GABRG2, GRIA4, GRIK4, GRIN1, HCN2, HTR3A, HTR3B, IGF1, ITPR1, KCNA2, KCNA4, KCNB1, KCNB2, KCNC1, KCNC3, KCNC4, KCND2, KCND3, KCNF1, KCNG1, KCNG4, KCNH2, KCNH4, KCNH7, KCNIP2, KCNIP3, KCNJ11, KCNJ12, KCNJ3, KCNJ4, KCNK1, KCNK16, KCNK18, KCNK6, KCNK9, KCNMB1, KCNMB4, KCNN1, KCNN2, KCNN3, KCNQ5, KCNS1, KCNS2, KCNS3, KCNT1, KCNV1, MCOLN2, NALCN, NEDD4L, NOS1, P2RX6, P2RY1, P2RY12, P2RY6, PACC1, PIEZO1, PKD2L1, PLCB2, PLCB3, PLP2, PPARG, PRKCB, PRLR, PTHLH, SCN10A, SCN11A, SCN1A, SCN1B, SCN2B, SCN4A, SCN4B, SCN5A, SCN8A, SLC11A1, SLC12A3, SLC15A3, SLC17A7, SLC1A1, SLC1A6, SLC1A7, SLC24A4, SLC25A18, SLC26A4, SLC34A2, SLC36A1, SLC37A1, SLC37A2, SLC39A2, SLC4A8, SLC5A7, SLC6A7, SLC8A2, SLC9A5, SLC9A9, SLCO2B1, STEAP3, STEAP4, SYK, TF, TGFB1, TMEM63C, TRPC3, TRPC4, TRPM8, TRPV4, TSPO, VDR

Table S8 (Related to Figure 4 of the transcriptome study). Functional enrichment analysis using Ingenuity Pathway Analysis (IPA) software of the upregulated genes in the injured (L3-L4) DRG after SNI in sigma-1 receptor knockout mice. Table shows selected functional annotations, their Benjamini-Hochberg (B-H) adjusted *P* value, and their gene content. Analysis was performed on transcripts with a *P* value < 0.01 and a fold change of 1.4.

Category	Function	Function Annotation	B-H *P* value	Number of genes	Genes
Inflammation	Inflammation	Inflammation	$2.45 \cdot 10^{-52}$	237	ADA, ADAM8, ADAMTS12, ADRB2, AHR, AIF1, AKNA, ALOX5, ALOX5AP, ANGPTL2, ANXA1, AOAH, AQP9, ATF3, BCL2A1, BIRC3, BLNK, BTK, C1QA, C3, C3AR1, C4A/C4B, C5AR1, C6, CASP3, CASP4, CASP8, CCL11, CCL12, CCL2, CCL21, CCL7, CCN3, CCN4, CCR1, CCR2, CCR5, CD14, CD163, CD1D, CD300A, CD33, CD37, CD38, CD4, CD44, CD63, CD72, CD74, CD84, CDCP1, CDKN1A, CEBPA, CEBPD, CELA1, CERS6, CH25H, CLCA1, CLCF1, CLEC12A, CLEC4A, CLEC4M, CLEC5A, CMKLR1, CNR2, CR2, CRH, CSF1, CSF1R, CSF3R, CTLA2A/CTLA2B, CTSE, CTSS, CX3CR1, CXADR, CXCL14, CXCL16, CXCR2, CYBA, CYBB, CYP4F16/CYP4F37, CYSLTR1, DAGLB, DOCK2, DUSP1, ECM1, EGFR, ELF4, EPHA2, FCER1G, FCGR1A, FCGR2A, FCGR2B, FNDC4, FOS, GADD45A, GAL, GCNT1, GGT5, GPR183, GPSM3, GRP, HAVCR2, HCK, HPGDS, HSD3B7, HSPB1, IGF1, IL10RA, IL17RA, IL1R1, IL1RL2, IL1RN, IL4R, IL6R, IL7, INPP5D, IRAK3, ITGAM, ITGB1, ITGB2, JUN, KNG1, LGALS1, LGALS3, LILRA5, LILRB3, LILRB4, LOXL2, LSP1, LTBP1, LUM, LY96, LYN, LYST, LYZ, MAPK14, METRNL, MFGE8, MMP19, MMP2, MSR1, MSTN, MYD88, MYO1F, NAIP, NAIP1 (INCLUDES OTHERS), NCF1, NCKAP1L, NFATC2, NFIL3, NFKBIZ, NLRC3, NLRC4, NLRP1, NLRP12, NLRP3, NOD2, NPY, NPY1R, NRROS, NTS, ODC1, P2RY6, PBK, PDE4B, PDE6B, PENK, PF4, PIK3AP1, PIK3CG, PLA2G2D, PLAT, PLAU, PLAUR, PLIN2, POMC, PPARG, PRDM1, PRKCG, PROCR, PROS1, PTAFR, PTGS1, PTPN6, PTPRO, PTX3, PYCARD, RAC2, RASGRP4, RIOX2, RIPK2, RIPK3, SASH3, SBNO2, SCYL3, SDC1, SELPLG, SERPINA3, SERPINB1, SERPINE1, SETD4, SLAMF1, SLC11A1, SLC6A4, SOCS3, SPI1, STAT5A, STAT5B, STING1, SYK, TBXAS1, TGFB1, TGFBR2, TLR13, TLR2, TLR7, TLR8, TLR9, TMEM106A, TNFAIP6, TNFAIP8L2, TNFRSF1B, TNIP2, TREM2, TREX1, TRPV4, TUBA1A, TUBA1C, TUBB2A, TUBB3, TYROBP, ULBP1, UNC13D, VAV1, VSIR, WAS
Cellular Movement	Migration	Leukocyte migration	$7.04 \cdot 10^{-50}$	263	ABCA1, ABCB1B, ADA, ADAM19, ADAM8, ADCYAP1, ADRB2, AHR, AIF1, AIM2, ALOX5, ALOX5AP, ANGPTL2, ANXA1, APBB1IP, APOD, AQP9, AREG, ARHGEF2, ARRB1, BATF3,

					BCL3, BTK, C3, C3AR1, C4A/C4B, C5AR1, C6, CAMK1, CARD14, CARD9, CASP8, CCL11, CCL12, CCL2, CCL21, CCL6, CCL7, CCL9, CCN3, CCR1, CCR2, CCR5, CD14, CD1D, CD200R1, CD207, CD300A, CD300LB, CD300LF, CD302, CD37, CD38, CD4, CD44, CD48, CD53, CD59A, CD63, CD72, CD74, CD86, CDCP1, CDKN1A, CEBPA, CFB, CH25H, CHST2, CITED2, CLEC10A, CLEC4M, CLEC5A, CMKLR1, CNR2, CR2, CRH, CSF1, CSF1R, CSF2RB, CSF3R, CTSC, CTSE, CTSS, CTTN, CX3CR1, CXADR, CXCL14, CXCL16, CXCR2, CYBB, CYP1B1, CYP26A1, CYSLTR1, DDR2, DOCK2, DOCK8, DRD2, DUSP1, ECM1, EGFR, ELF4, EPHA2, EPS8, F13A1, FABP5, FCER1G, FCGR2A, FCGR2B, FERMT3, FGF3, FGL2, FLNA, FOS, FOSL2, FOXM1, FYB1, GATA2, GCNT1, GFAP, GGT5, GPR183, GPR34, GPR65, GPRC5A, GPSM3, GRP, GSDMD, HAO1, HCK, HCLS1, HDC, HLA-DQB1, HPGDS, HSD3B7, HSPB1, IFITM3, IGFBP3, IL10RA, IL17RA, IL1R1, IL1RN, IL21R, IL4R, IL6R, IL7, INPP5D, ITGAE, ITGAM, ITGB1, ITGB2, JUN, KLF6, KNG1, LAMA5, LGALS1, LGALS3, LILRB3, LILRB4, LSP1, LTC4S, LUM, LY6A (INCLUDES OTHERS), LY96, LYN, LYST, LYZ, MAPK14, MARCHF1, MC4R, MCOLN2, MET, MMP2, MS4A4A, MSR1, MSTN, MYADM, MYD88, MYO1F, MYO1G, NCF1, NCF4, NCKAP1L, NDST1, NFATC2, NFIL3, NFKBIZ, NLRC4, NLRP12, NLRP3, NOD2, NPY, OLFM4, OR51E2, P2RY12, P2RY6, PBLD, PDE4B, PENK, PF4, PIK3CG, PKP3, PLA2G2D, PLAT, PLAU, PLAUR, PLCB2, PLTP, PODXL, POMC, PPARG, PRDM1, PROCR, PTAFR, PTPN1, PTPN6, PTPRC, PTPRO, PTX3, PYCARD, RAC2, RASGRP4, RCAN1, RIPK2, RIPK3, RTN4, S100A10, S1PR2, SAG, SDC1, SELPLG, SEMA4A, SERPINA3, SERPINB1, SERPINE1, SLAMF1, SLAMF9, SOCS3, SOX11, SPI1, STAB1, STAT5A, STAT5B, STING1, SYK, TGFB1, TGFBR1, TGFBR2, TIMP1, TLR2, TLR7, TLR9, TMSB4X (INCLUDES OTHERS), TNFAIP6, TNFAIP8, TNFAIP8L2, TNFRSF1B, TREM2, TRPV4, TYROBP, VAV1, WAS, WFDC17, XDH
Hematological System Development and Function	Proliferation	Proliferation of immune cells	$1.89 \cdot 10^{-38}$	212	ADA, ADCYAP1, ADRB2, AHCY, AHR, AIF1, ANXA1, ARG2, ARHGDIB, BCL2A1, BCL3, BHLHE41, BIRC3, BLNK, BTK, BTNL2, C3, C5AR1, CASP3, CASP8, CCDC88B, CCL12, CCL2, CCL21, CCR2, CCR5, CD14, CD180, CD1D, CD200R1, CD244, CD300A, CD300C, CD37, CD38, CD4, CD44, CD48, CD59A, CD72, CD74, CD84, CD86, CDKN1A, CDKN2A, CEBPA, CFB, CFP, CHRNA1, CISH, CLCF1, CLEC10A, CLEC2D (INCLUDES OTHERS), CLEC4A, CLEC4M, CMTM7, CNR2, CR2, CRH, CSF1, CSF1R, CSF2RB, CSF3R, CTH, CXCL14, CXCL16, CYBB, CYSLTR1, DAPP1, DOCK2, DOCK8, DRD2, DUSP1, ELF4, EPHA2, EPHB2, ETS2, FCER1G, FCGR2A, FCGR2B, FGL2, FOS, FYB1, GADD45A, GAL, GATA2, GCH1, GCNT1, GPR183, GRAP, HAO1, HAVCR2, HCK, HCLS1, HLA-DQB1, HLA-E, HPGDS, HR, IGF1, IKZF1, IL10RA, IL13RA1, IL1R1, IL1RN, IL21R, IL2RB, IL2RG, IL31RA, IL4R, IL6R, IL7, INPP5D, IRF8, IRS2, ISG20, ITGAM, ITGB1, ITGB2, ITPR1, JUN, KLRB1, LAPTM5, LAT2, LGALS1, LGALS3,

					LILRB3, LILRB4, LTBP1, LY6A (INCLUDES OTHERS), LY86, LY96, LYN, MAFB, MAPK14, MBL2, MET, MMP19, MTHFD2, MVP, MYD88, NABP1, NBEAL2, NCK2, NCKAP1L, NFATC2, NFIL3, NPY, NPY1R, P2RY6, PENK, PIEZO1, PIK3AP1, PIK3CG, PLA2G2D, PLAU, PLAUR, PLCB2, PNP, POMC, PPARG, PRDM1, PTPN6, PTPRC, PYCARD, RAC2, RASGRF2, RCAN1, RHOG, RHOH, RHOQ, RIPK2, RIPK3, RPS6KA1, S1PR2, SASH3, SERPINA3G (INCLUDES OTHERS), SERPINE1, SH3BP2, SH3KBP1, SIGLEC1, SLAMF1, SOCS3, SOX11, SOX5, SPI1, STAT5A, STAT5B, STING1, STK17B, SYK, TALDO1, TGFB1, TGFBR1, TGFBR2, TICAM2, TIFA, TLR2, TLR7, TLR9, TNFRSF13B, TNFRSF1B, TREM2, TRIM30A/TRIM30D, TYR, TYROBP, ULBP1, UNC93B1, VAV1, VSIR, WAS, WT1, XDH
Cellular Movement	Chemotaxis	Chemotaxis	$1.61 \cdot 10^{-24}$	138	ADAM8, AIF1, AKAP12, ALOX5, ANGPTL2, ANXA1, AQP9, ARRB1, BDKRB2, BIN2, C3, C3AR1, C4A/C4B, C5AR1, CCL11, CCL12, CCL2, CCL21, CCL6, CCL7, CCL9, CCN3, CCR1, CCR2, CCR5, CD37, CD38, CD4, CD44, CD72, CD74, CDCP1, CDKN1A, CH25H, CMKLR1, CNR2, CSF1, CSF1R, CSF3R, CTH, CTSE, CTTN, CX3CR1, CXADR, CXCL14, CXCL16, CXCR2, CYBB, CYSLTR1, DOCK2, DRD2, DUSP1, EGFR, EPHA2, EPHB2, FCER1G, FCGR2A, GFRA1, GPR183, GPSM3, GRP, HCK, HCLS1, HMGB2, HSD3B7, HSPB1, IGF1, IL17RA, IL1R1, IL4R, IL6R, IL7, INPP5D, ITGAM, ITGB1, ITGB2, JUN, KNG1, LGALS1, LGALS3, LILRB3, LSP1, LYN, LYST, MAPK14, MET, MMP2, MSTN, MT2, MTSS1, MYD88, MYO1F, NCK2, NCKAP1L, NDST1, NLRP12, NOD2, NPY, P2RY12, PDE4B, PENK, PF4, PIK3CG, PLAT, PLAU, PLAUR, PLXNA4, PPARG, PRKCG, PTAFR, PTPN6, PTPRC, PTPRO, RAC2, RASGRP4, RHOG, RTN4, S1PR2, SELPLG, SERPINA3, SERPINB1, SERPINE1, SLAMF1, SNAI2, SOCS3, SPI1, SYK, TGFA, TGFB1, TGFBR1, TLR2, TLR9, TNFAIP6, TPBG, TREM2, TRPV4, VAV1, WAS

Table S9 (Related to Figure 4 of the transcriptome study). Functional enrichment analysis using Ingenuity Pathway Analysis (IPA) software of the downregulated genes in the injured (L3-L4) DRG after SNI in sigma-1 receptor knockout mice. Table shows selected functional annotations, their Benjamini-Hochberg (B-H) adjusted *P* value, and their gene content. Analysis was performed on transcripts with a *P* value < 0.01 and a fold change of 1.4.

Category	Function	Function Annotation	B-H *P* value	Number of genes	Genes
Nervous System Development and Function	Neurotransmission	Neurotransmission	$3.71 \cdot 10^{-19}$	102	ADCY1,AMPH,ASIC1,BCHE,CA8,CACNA1I,CACNA2D3,CACNB2,CACNG2,CAMKV,CASR,CDH8,CHRM2,CHRNA4,CHRNA7,CLSTN1,CNTNAP2,CNTNAP4,CPLX2,DLG4,DLGAP3,DNM1,DPP6,F2R,FGF12,FSTL1,GABBR2,GABRA1,GABRB2,GABRG2,GNAO1,Gprasp2,GRIA2,GRIA4,GRIK1,GRIK4,GRIN1,GRM4,GRM8,HCN2,HCRTR2,HTR1A,HTR1B,HTR3A,HTR4,JPH3,JPH4,KCNA2,KCNB1,KCNC1,KCNC3,KCNC4,KCND1,KCND2,KCNH2,KCNJ11,KCNK9,KCNMB1,KCNN1,Kcnn2,KCNN3,KCNT1,LPAR3,LZTS1,MYO5B,NPTX1,Nrg1,NRG3,Nrxn3,NTNG1,OPRK1,PNKD,PRKAR2B,PRKCA,PRKCB,PRMT8,RAB3A,RASD2,RIMS1,RIMS2,RIT2,SCN11A,SCN1A,SCN1B,SCN2B,SCN4B,SCN5A,SCN8A,SH3GL2,SHANK1,SLC17A7,SLC1A1,SLC1A6,SLC9A9,SNAP25,SV2A,SV2B,SYN2,TH,TNR,TSPOAP1,UNC119
Molecular Transport	Transport	Transport of ion	$6.52 \cdot 10^{-17}$	100	ABCC8,AGT,AKT3,ANO3,ASIC1,ASIC3,ATP1A1,ATP1B1,ATP2B2,ATP2B3,BCL2,CACNA1I,CACNA2D2,CACNA2D3,CACNB2,CALB1,CAMK2B,CASR,CHRNA4,CHRNA7,CNTN1,DPP6,F2R,FGF12,FGF13,FKBP4,GABRA1,GABRB2,GABRG2,GRIA4,GRIK4,GRIN1,HCN2,HTR3A,HTR3B,KCNA2,KCNA4,KCNB1,KCNB2,KCNC1,KCNC3,KCNC4,KCND2,KCND3,KCNF1,KCNG1,KCNG4,KCNH2,KCNH7,KCNIP2,KCNIP3,KCNJ11,KCNJ12,KCNJ3,KCNJ4,KCNK1,KCNK18,KCNK9,KCNMB1,KCNN1,Kcnn2,KCNN3,KCNQ5,KCNS1,KCNS2,KCNS3,KCNT1,KCNV1,NALCN,NEDD4L,NOS1,P2RX6,P2RY1,PLCB3,PRKCB,PRLR,SCN10A,SCN11A,SCN1A,SCN1B,SCN2B,SCN4A,SCN4B,SCN5A,SCN8A,SLC17A7,SLC1A1,SLC1A6,SLC24A4,SLC25A18,SLC34A2,SLC36A1,SLC6A7,SLC8A2,SLC9A5,SLC9A9,TRPC3,TRPC4,TRPM8,VDR
Nervous System Development and	Development	Development of neurons	$2.58 \cdot 10^{-15}$	168	ACHE,ADAMTS3,ADCY1,AGAP2,AGT,AMIGO2,AMIGO3,ANGPT1,AR,ASAP1,BCAN,BCL11B,BCL2,CACNA2D2,CACNB2,CACNG2,CADPS2,CAMK1G,CAMK2B,

Function					CDK5R2,CHODL,CHRNA7,CLSTN1,CNTN1,CNTN4,CNTNAP1,CNTNAP2,COBL,COLQ,CPEB3,CPNE9,CUX2,DAB1,DGKG,DLG4,DLGAP3,DOK7,DSCAM,EFNA3,ELMO1,EPB41L3,EPHA8,F2R,FAIM2,FBXO31,FEZ1,FGF13,FGF5,FGF9,FLRT1,FRMD7,FSTL4,GABRA1,GABRB2,GABRG2,GFRA2,GNAO1,GPR37,Gprasp2,GPRIN3,GRIN1,GRM4,HAPLN4,HGF,HTR4,HTR7,ID1,IGSF21,IGSF9,INPP5J,IQSEC1,ISL2,KIAA0319,KIRREL3,KNDC1,LGI2,LHFPL4,LINGO1,LINGO2,LINGO4,LRRN1,LZTS1,MCF2,MINAR1,MYH7B,MYO5B,NCDN,NDRG4,NEDD4L,NEFH,NEFL,Nefm,NEGR1,NOG,NOS1,Nrg1,NRG2,NRG3,NRN1,Nrxn3,NTM,NTNG1,NTRK1,NUAK1,NYAP2,OLFM3,ONECUT1,PACSIN1,PCDH10,PCYT1B,POU4F1,POU4F2,POU4F3,PRICKLE2,PRKCA,PRKCE,Prrxl1,PSD,PTK7,PVALB,RAB3A,REM2,RHO,RIMS1,RIMS2,RIMS3,RIT2,RNF157,ROBO1,RTN4RL1,RUNX3,SCN11A,SCN1A,SCN1B,SCN4B,SEMA3E,SEMA3F,SEMA7A,SEPTIN4,SERPINI1,SH3GL2,SHANK1,SHOX2,SIX4,SKOR2,SLC17A7,SLC9A5,SLITRK3,SLITRK4,SNAP25,SPOCK1,ST8SIA1,SV2A,SYN2,SYT2,SYT3,TH,TLX3,TMEM108,TNR,TRPC3,TRPC4,TSPAN2,UST,VAMP1,WEE1,ZNF365,ZNF804A
Nervous System Development and Function	Neuritogenesis	Neuritogenesis	$3.38 \cdot 10^{-10}$	130	ACHE,ADAMTS3,ADCY1,AGAP2,AGT,AMIGO3,ANGPT1,AR,ASAP1,BCL11B,BCL2,CAMK1G,CAMK2B,CDK5R2,CHODL,CHRNA7,CLSTN1,CNTN1,CNTN4,CNTNAP1,CNTNAP2,COBL,CPEB3,CPNE9,CUX2,DAB1,DGKG,DLG4,DSCAM,EFNA3,ELMO1,EPB41L3,EPHA8,FBXO31,FEZ1,FGF13,FGF5,FLRT1,FRMD7,FSTL4,GFRA2,GNAO1,GPR37,Gprasp2,GPRIN3,GRIN1,GRM4,HGF,HTR7,ID1,IGSF9,INPP5J,IQSEC1,KIAA0319,KIRREL3,KNDC1,LINGO1,LZTS1,MCF2,MINAR1,MYH7B,MYO5B,NCDN,NDRG4,NEDD4L,NEFH,NEFL,Nefm,NEGR1,NOS1,Nrg1,NRN1,NTM,NTNG1,NTRK1,NUAK1,NYAP2,PACSIN1,PCYT1B,POU4F1,POU4F2,POU4F3,PRICKLE2,PRKCA,PRKCE,Prrxl1,PSD,PTK7,PVALB,RAB3A,REM2,RIMS1,RIMS2,RIMS3,RIT2,RNF157,ROBO1,RTN4RL1,RUNX3,SCN11A,SCN1A,SCN1B,SCN4B,SEMA3E,SEMA3F,SEMA7A,SEPTIN4,SERPINI1,SH3GL2,SHANK1,SHOX2,SKOR2,SLC9A5,SLITRK3,SLITRK4,SNAP25,SPOCK1,ST8SIA1,SV2A,SYT2,SYT3,TMEM108,TNR,TRPC3,TRPC4,TSPAN2,UST,WEE1,ZNF365,ZNF804A

Table S10 of the transcriptome study. DRG transcripts not included in any module by the WGCNA using all regulated genes in the DRG (L3-L4) of sigma-1 receptor knockout mice (KO) compared to wild-type (WT) in the naïve condition or after SNI. Significantly regulated transcripts (*P* value < 0.01 and fold change of 1.4, n=1250) were subject to WGCNA to produce clusters of co-regulated transcripts, with no preconceived structure.

Gene ID	Gene name
ENSMUSG00000028228.5	CPNE3
ENSMUSG00000033826.10	DNAH8
ENSMUSG00000030703.8	GDPD3
ENSMUSG00000094036.1	GM6465
ENSMUSG00000096732.7	GM8897
ENSMUSG00000021303.14	GNG4
ENSMUSG00000050138.8	KCNK12
ENSMUSG00000018362.14	KPNA2
ENSMUSG00000058153.15	SEZ6L

Table S11 (Related to Figure 5 of the transcriptome study). WGCNA and functional enrichment analysis using Ingenuity Pathway Analysis (IPA) software of all regulated genes in the DRG (L3-L4) of sigma-1 receptor knockout mice (KO) compared to wild-type (WT) in the naïve condition or after SNI. Significantly regulated transcripts (*P* value < 0.01 and fold change of 1.4) were subject to WGCNA to produce clusters of co-regulated transcripts, with no preconceived structure. Table shows selected functional annotations, their Benjamini-Hochberg (B-H) adjusted *P* value, and their gene content.

Module	Category	Function	Function Annotation	B-H *P* value	Number of genes	Genes
I	Cellular Movement	Migration	Leukocyte migration	$3.87 \cdot 10^{-7}$	62	ABCB1B, C5AR2, CAMP, CARD14, CCL11, CCL19, CCL12, CCL24, CCL27, CCL28, CCL7, CD177, CD276, CD300LB, CD34, CD36, CD55, CD93, CH25H, CNN2, CNR1, CTSK, CXCL10, CXCR4, DEPTOR, EAR2 (INCLUDES OTHERS), ESR2, F2RL1, GLO1, IL11RA, IL1RN, IL36G, ITK, KIT, LCN2, LCP2, LOX, LTF, MAP4K1, MMP2, MMP9, MPO, MYD88, NAAA, PADI4, PDPN, PILRA, PPBP, RPL13A, RRM2, S100A4, S100A8, S100A9, SIGMAR1, SLFN12L, SPN, SPP1, TAFA4, TMSB4X (INCLUDES OTHERS), TSPAN33
II	Nervous System Development and Function	Neurotransmission	Neurotransmission	$2.38 \cdot 10^{-19}$	61	ADCY3, ALK, ARHGAP44, ASIC1, CHRM2, CLSTN1, CLSTN2, CLSTN3, CPLX1, CPLX2, DNM1, ELFN1, F2R, GABBR2, GABRA5, GRIA1, GRIN1, HCN2, HCRTR1, HTR3A, JPH3, KCNA1, KCNB1, KCNC1, KCNC4, KCNQ4, KIF5A, L1CAM, LYNX1, MAOB, MAPK8IP2, MTOR, MYH10, MYH14, MYO5B, NCAN, NGFR, NPTX1, NRXN2, NSF, PCDH17, PCDH8, PCDHB6, PRKACA, PTK2B, SCN1B, SCN2B, SCN4B, SCN8A, SEZ6, SH3GL2, SLC17A7, SLC8A3, SNAP91, SSH1, STX1B, STXBP1, SV2A, SYN1, SYN2, WASF1
III	Unannotated				44	A3GALT2, ADAMTS9, BCL6B, CARD11, CDH9, CYP2J13, CYSLTR2, DGKI, DYRK4, EFCAB10, EPHA8, FXYD2, GABRA3, GM49027, H2AC19, H3C4, HTR4, KCNG3, KCTD16, KIF23, LRRC31, LYPD1, MLF1, MPP7, OBSCN, OPRM1, PAQR5, PDGFC, PLCXD3, PSTPIP1, RARRES1, RXFP1, SLC17A8, SLC24A4, SLC51A, SNAPC5, SST, ST6GALNAC3, SYNPR, TH, TMEM266, TRPA1, VMN1R85, ZFP804B

IV	Inflammation	Inflammation	Inflammation	$1.21 \cdot 10^{-21}$	60	ADAMTS12, BCL2A1, C1QTNF12, C3AR1, C5AR1, CASP4, CCL2, CCL8, CCR2, CCR5, CD1D, CD33, CD4, CDCP1, CLEC4A, CR2, CSF1R, CSF3R, CTSS, CX3CR1, CYBA, CYBB, FCGR1A, GAL, GPR183, HEBP1, HSPB1, IL1RL2, IL4R, ITGAM, ITGB2, LGALS1, LGALS3, LILRB3, LTBP1, LY6A, LYZ, MSR1, MYO1F, NCKAP1L, NOD2, NPY1R, NTS, PBK, PLAUR, PRDM1, PTAFR, PTPN6, RAC2, RASGRP4, SELPLG, SERPINA3, SLC6A4, SPI1, TGFB1, TLR13, TMEM106A, TNIP2, TREM2, TUBA1C, TYROBP, VSIR

Table S12 (Related to Figure 9 of the transcriptome study). Functional enrichment analysis using Ingenuity Pathway Analysis (IPA) software of the regulated genes in the ipsilateral dorsal spinal cord after SNI in wild-type mice. Table shows selected functional annotations, their Benjamini-Hochberg (B-H) adjusted *P* value, and their gene content. Analysis was performed on transcripts with a *P* value < 0.01 and a fold change of 1.4.

Category	Function	Function Annotation	B-H *P* value	Number of genes	Genes
Hematological System Development and Function	Quantity	Quantity of leukocytes	$7.28 \cdot 10^{-54}$	116	ABCA1, ADAM8, ADORA3, APBB1IP, ARHGDIB, ATF3, BLNK, BST2, BTK, C1QA, C3AR1, C4A/C4B, CCL12, CCL2, CCL7, CCL9, CCR1, CCR5, CD180, CD24A, CD300C, CD34, CD44, CD84, CD86, CEBPA, CSF1R, CSF2RB, CSF3R, CTLA2A/CTLA2B, CTSS, CX3CR1, CXCL10, DOCK2, DOCK8, ELF4, FCER1G, FCGR1A, FCGR2A, FCRLS, FERMT3, FES, FLI1, FYB1, GADD45A, GCNT1, GCNT2, GRN, HAVCR2, HCAR2, HCK, HCLS1, HEXB, HLA-A, HVCN1, IKZF1, IL10RA, IL1A, IL4R, IL6R, INPP5D, IRF5, IRF8, ITGAM, ITGB2, ITGB5, KLHL6, LAG3, LAIR1, LCP2, LTC4S, LYN, MERTK, MFNG, NABP1, NCKAP1L, NLRC5, NPY, PIK3AP1, PIK3CG, PIK3R5, PLCG2, PLD4, PMAIP1, PSMB8, PTPN6, PTPRC, PYCARD, RAC2, RASAL3, RHOH, RIGI, RUNX1, SAMSN1, SASH3, SELPLG, SIGLEC8, SLA, SOCS3, SPI1, STING1, SYK, TGFB1, TLR2, TLR7, TLR9, TNFAIP8L2, TNFRSF13B, TRAF3IP3, TREM2, TRIM30A/TRIM30D, TYROBP, UNC93B1, VAV1, WAS, WDFY4
Cellular Movement	Migration	Leukocyte migration	$3.88 \cdot 10^{-49}$	107	ABCA1, ADAM8, ADORA3, AIF1, ALOX5AP, ANGPTL2, APBB1IP, ARAP3, ARHGAP25, BTK, C3AR1, C4A/C4B, CARD9, CCL12, CCL2, CCL7, CCL9, CCR1, CCR5, CD14, CD34, CD37, CD44, CD53, CD86, CEBPA, COCH, CSF1R, CSF2RB, CSF3R, CTSS, CX3CR1, CXCL10, CYP1B1, DOCK2, DOCK8, ELF4, F11R, FCER1G, FCGR2A, FERMT3, FYB1, GCNT1, GFAP, GGT5, GPR34, GRN, HCAR2, HCK, HCLS1, HLA-A, HPGDS, IL10RA, IL1A, IL4R, IL6R, INPP5D, IRF5, IRF7, ITGAM, ITGAX, ITGB2, LAG3, LCP2, LTC4S, LYN, MERTK, MYO1F, NCF1, NCF4, NCKAP1L, NPY, P2RY12, P2RY6, PIK3CG, PIK3R5, PLCB2, PLCG2, PROCR, PSMB8, PTPN6, PTPRC, PYCARD, RAC2, RIGI, RUNX1, S100A10, SAMSN1, SCN9A, SELPLG, SERPINA3, SIGLEC8, SLAMF8, SOCS3, SPI1, STING1, SYK, TGFB1, TLR2, TLR7, TLR9, TNFAIP8L2, TRAF3IP3, TREM2, TYROBP, VAV1, WAS

Inflammation	Inflammation	Inflammation	$3.52 \cdot 10^{-45}$	94	ADAM8, ADORA3, AIF1, AKNA, ALOX5AP, ANGPTL2, ARAP3, ARHGAP25, ATF3, BLNK, BTK, C1QA, C3AR1, C4A/C4B, CCL12, CCL2, CCL7, CCR1, CCR5, CD14, CD33, CD37, CD44, CD84, CEBPA, CSF1R, CSF3R, CTLA2A/CTLA2B, CTSS, CX3CR1, CXCL10, DOCK2, ELF4, F11R, FCER1G, FCGR1A, FCGR2A, GADD45A, GAL, GCNT1, GGT5, GRN, HAVCR2, HCAR2, HCK, HLA-A, HPGDS, IL10RA, IL1A, IL4R, IL6R, INPP5D, IRF5, ITGAM, ITGB2, LGALS3BP, LYN, MYO1F, NAIP, NAIP1 (INCLUDES OTHERS), NCF1, NCKAP1L, NPY, P2RY6, PIK3AP1, PIK3CG, PIK3R5, PLCG2, PROCR, PTPN6, PYCARD, RAC2, SASH3, SCN9A, SELPLG, SERPINA3, SLAMF8, SLC11A1, SOCS3, SPI1, STING1, SYK, TGFB1, TLR13, TLR2, TLR7, TLR9, TNFAIP8L2, TREM2, TYROBP, USP18, VAV1, VSIR, WAS
Hematological System Development and Function	Activation	Activation of leukocytes	$2.60 \cdot 10^{-44}$	86	ATF3, BLNK, BTK, C1QA, C3AR1, C4A/C4B, CARD9, CCL2, CCL2, CCR5, CD14, CD180, CD24A, CD37, CD44, CD84, CD86, CEBPA, CSF1R, CSF2RB, CTSS, CX3CR1, CXCL10, DOCK2, FCER1G, FCGR1A, FCGR2A, GADD45A, GPR34, GRN, HAVCR2, HCK, HLA-A, HVCN1, IL1A, IL4R, IL6R, INPP5D, IRF5, IRF8, ITGAM, ITGB2, LAG3, LAIR1, LAPTM5, LAT2, LCP2, LGALS3BP, LTC4S, LYN, MERTK, MFNG, NCF1, NPY, P2RY6, PIK3CG, PLCG2, PSMB8, PTPN6, PTPRC, PYCARD, RHOH, RIGI, RSAD2, RUNX1, SAMSN1, SASH3, SCN9A, SIGLEC8, SLC11A1, STING1, SYK, TGFB1, TLR2, TLR7, TLR9, TNFAIP8L2, TNFRSF13B, TREM2, TYROBP, UNC93B1, USP18, VAV1, VSIR, WAS, WDFY4

Table S13 (Related to Figure 9 of the transcriptome study). Functional enrichment analysis using Ingenuity Pathway Analysis (IPA) software of the regulated genes in the ipsilateral dorsal spinal cord after SNI in sigma-1 receptor knockout mice. Table shows selected functional annotations, their Benjamini-Hochberg (B-H) adjusted *P* value, and their gene content. Analysis was performed on transcripts with a *P* value < 0.01 and a fold change of 1.4.

Category	Function	Function Annotation	B-H *P* value	Number of genes	Genes
Hematological System Development and Function	Quantity	Quantity of leukocytes	$2.94 \cdot 10^{-54}$	135	ABCA1, ADAM8, ADORA3, APBB1IP, ARHGDIB, ATF3, B2M, BLNK, BTK, C1QA, C3, C3AR1, C4A/C4B, CCL2, CCR5, CCR6, CD180, CD24A, CD300A, CD300C, CD300LF, CD34, CD44, CD84, CD86, CEBPA, CLEC4A, CSF1, CSF1R, CSF2RB, CSF3R, CTLA2A/CTLA2B, CTSD, CTSE, CTSS, CX3CR1, DAPP1, DOCK2, DOCK8, EGR3, ELF4, FCER1G, FCGR1A, FCGR2A, FCGR2B, FCRLS, FERMT3, FES, FYB1, GADD45A, GCNT1, GCNT2, GRN, HAVCR2, HCAR2, HCK, HCLS1, HEXB, HVCN1, ICOSLG/LOC102723996, IKZF1, IL10RA, IL1A, IL21R, IL4R, IL6R, IL7R, INPP5D, IRF5, IRF8, ITGAM, ITGB2, ITGB5, KLHL6, LAG3, LAIR1, LCP2, LGALS1, LGALS3, LYL1, LYN, MFNG, MSN, NABP1, NCKAP1L, NPY, PIK3AP1, PIK3CG, PIK3R5, PLCG2, PLD4, PMAIP1, POU2F2, PSMB8, PTAFR, PTPN6, PTPRC, PYCARD, RAC2, RASAL3, RHOH, RORC, RPS6KA1, RUNX1, SAMSN1, SASH3, SELPLG, SERPINB1, SERPINB6, SIGLEC8, SLA, SOCS3, SPI1, STING1, SYK, TAP1, TGFB1, TGFBR1, TIMP1, TLR2, TLR7, TLR9, TNFAIP8L2, TNFRSF13B, TNFRSF1A, TNFRSF1B, TREM2, TRIM30A/TRIM30D, TSPO, TYROBP, UNC93B1, VAV1, VIP, WAS, WDFY4
Cellular Movement	Migration	Leukocyte migration	$4.55 \cdot 10^{-52}$	107	ANXA2, ATF3, B2M, BLNK, BTK, C1QA, C3, C3AR1, C4A/C4B, CARD9, CCDC88B, CCL2, CCR5, CCR6, CD14, CD180, CD24A, CD300A, CD300LF, CD37, CD44, CD84, CD86, CEBPA, CLEC4A, CLEC5A, CSF1, CSF1R, CSF2RB, CTSH, CTSS, CX3CR1, DAPP1, DOCK2, DYSF, EGR3, FCER1G, FCGR1A, FCGR2A, FCGR2B, GADD45A, GPR34, GRN, HAVCR2, HCK, HSPB8, HVCN1, ICOSLG/LOC102723996, IL1A, IL21R, IL4R, IL6R, INPP5D, IRF5, IRF8, ITGAM, ITGB2, LAG3, LAIR1, LAPTM5, LCP2, LGALS1, LGALS3, LGALS3BP, LYN, MFNG, NCF1, NPY, P2RY6, PDE6B, PIK3CG, PLCG2, POU2F2, PSMB8, PTGS1, PTPN6, PTPRC, PYCARD, RET, RHOH, RUNX1, SAMSN1, SASH3, SCN9A, SIGLEC8, SLC11A1, STING1, SYK, TGFB1, THEMIS2, TLR1, TLR2, TLR7, TLR9, TNFAIP8L2, TNFRSF13B, TNFRSF1A, TNFRSF1B, TREM2, TYROBP,

					UNC93B1, USP18, VAV1, VIP, VSIR, WAS, WDFY4
Inflammation	Inflammation	Inflammation	$3.85 \cdot 10^{-51}$	115	ADAM8, ADORA3, AIF1, AKNA, ALOX5AP, ANGPTL2, ANXA2, ARHGAP25, ATF3, BLNK, BTK, C1QA, C3, C3AR1, C4A/C4B, CALCB, CCL2, CCR5, CCR6, CD14, CD300A, CD33, CD37, CD44, CD84, CEBPA, CLEC4A, CLEC5A, CSF1, CSF1R, CSF3R, CTLA2A/CTLA2B, CTSE, CTSS, CX3CR1, CYBA, DOCK2, DYSF, ELF4, F11R, FCER1G, FCGR1A, FCGR2A, FCGR2B, GADD45A, GAL, GCNT1, GGT5, GRN, HAVCR2, HCAR2, HCK, HPGDS, HSPB1, ICOSLG/LOC102723996, IL10RA, IL1A, IL4R, IL6R, INPP5D, IRF5, ITGAM, ITGB2, LACC1, LGALS1, LGALS3, LGALS3BP, LYN, MYO1F, NAIP, NAIP1 (INCLUDES OTHERS), NCF1, NCKAP1L, NPY, P2RY6, PDE6B, PIK3AP1, PIK3CG, PIK3R5, PLCG2, PLIN2, PROCR, PTAFR, PTGS1, PTPN6, PYCARD, RAC2, SASH3, SCN9A, SELPLG, SERPINA3, SERPINB1, SLAMF8, SLC11A1, SOCS3, SPI1, STING1, SYK, TBXAS1, TGFB1, TLR1, TLR13, TLR2, TLR7, TLR9, TNFAIP8L2, TNFRSF1A, TNFRSF1B, TREM2, TYROBP, USP18, VAV1, VIP, VSIR, WAS
Hematological System Development and Function	Activation	Activation of leukocytes	$1.66 \cdot 10^{-49}$	124	ABCA1, ADAM8, ADORA3, AIF1, ALOX5AP, ANGPTL2, ANXA2, APBB1IP, ARHGAP25, BTK, C3, C3AR1, C4A/C4B, CALCB, CARD9, CCL2, CCR5, CCR6, CD14, CD300A, CD300LF, CD34, CD37, CD44, CD53, CD86, CEBPA, CLEC5A, COCH, CSF1, CSF1R, CSF2RB, CSF3R, CTSC, CTSE, CTSS, CTSZ, CX3CR1, CYP1B1, DOCK2, DOCK8, DYSF, ELF4, F11R, FCER1G, FCGR2A, FCGR2B, FERMT3, FYB1, GCNT1, GFAP, GGT5, GPR34, GRN, HCAR2, HCK, HCLS1, HPGDS, HSPB1, IL10RA, IL1A, IL21R, IL4R, IL6R, IL7R, INPP5D, IRF5, ITGAM, ITGAX, ITGB2, LAG3, LAYN, LCP2, LGALS1, LGALS3, LYN, MSN, MYO1F, NCF1, NCF4, NCKAP1L, NPY, P2RY12, P2RY6, PIK3CG, PIK3R5, PLCB2, PLCG2, PROCR, PSMB8, PTAFR, PTPN6, PTPRC, PYCARD, RAC2, RORC, RUNX1, S100A10, SAMSN1, SCN9A, SELPLG, SERPINA3, SERPINB1, SIGLEC8, SLAMF8, SOCS3, SPI1, STING1, SYK, TGFB1, TGFBR1, TIMP1, TLR2, TLR7, TLR9, TNFAIP8L2, TNFRSF1A, TNFRSF1B, TREM2, TYROBP, UCP2, VAV1, VIP, WAS